MATHEMATICAL MODELS FOR PREDICTING SOLAR RADIATION AND CAPACITY OF SOLAR DRIVEN REFRIGERATION SYSTEM FOR MILK COOLING

PATRICK MBUTHIA WAINAINA

A Thesis Submitted to the Graduate School in Partial Fulfillment of the Requirements for the Doctor of Philosophy Degree in Agricultural Engineering of Egerton University

EGERTON UNIVERSITY

JUNE 2022

DECLARATION AND RECOMMENDATION

Declaration

This thesis is my original work and has not been presented in this university or any other for the award of a degree.

Signature 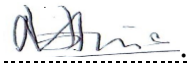 Date: May 26th, 2022

Patrick M. Wainaina

BD11/0429/14

Recommendations

This thesis has been submitted with our approval as university supervisors.

Signature 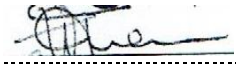 Date; May 28, 2022

Dr. Musa R. Njue

Department of Agricultural Engineering

Egerton University

Signature  Date; May 29, 2022

Prof. Michael W. Okoth

Department of Food Science, Nutritional and Technology

University of Nairobi

Signature  Date: May 26nd, 2022

Dr. George O. Owino

Department of Industrial and Energy Engineering

Egerton University

COPYRIGHT

DEDICATION

This research work is dedicated to my late parents, John Wainaina and Alice Wainaina, for their tireless effort, encouragement and words of wisdom, which I cherish and honour in my daily walk of life. They supported me throughout my life; when challenged at various levels of my education, they have prayed for God's Blessings in my endeavors. They cared and natured good character and a positive attitude in persistence which is paramount to any successful journey. In addition, they also sacrificed immensely in numerous ways to ensure that I pursued education to the great altitude of success. To my dear wife Salome Mbuthia, who has been a source of encouragement and inspiration during challenging times of my academic programme. I appreciate her prayers, understanding and support during my study and research period.

To my lovely children, Ian Wainaina and Jane Wangari, for continuous support during this research period. I also dedicate this research thesis to my numerous friends, course mates and church members who have supported me throughout my research period. I appreciate all they have done, especially their prayers and advice needed to overcome challenges encountered during this research process.

In a special way, this thesis is dedicated to all my trainers of goodwill; the primary and secondary school teachers and University lecturers, especially my supervisors, Dr. Njue, Dr. Owino and Prof. Okoth. They not only supervised my work during this research period but also immensely contributed to my success in my academic exploration.

Finally, this thesis is dedicated to all those farmers and milk producers who are willing to use this refrigeration system. Thank you all for the patience and support you accorded me during this research period. May God Almighty Bless you mightily.

ACKNOWLEDGEMENTS

I thank God Almighty for not only the provision of life but good health and zeal that has enabled me to complete this research. Special thanks to Egerton University, which provided a conducive environment and opportunity for my mentorship during my research training period.

Through the Federal Ministry of Education and Research in the framework of Global E initiative, I also thank the German Government for funding my research under the Reduction of post-harvest losses RELOAD Project at Egerton University. I acknowledge Mr. Michael Hesse of the University of Kassel and Prof. Joseph Matofari of Egerton University for the facilitation of funds, equipment and research travels during the research.

I appreciate my Supervisors, Dr. Musa Njue, Dr. George Owino and Prof. Michael W. Okoth, who have dedicated their intellect, time, guidance, suggestions and valuable contributions. From their commitment and sacrifice, I have been exposed to a higher level of critical thinking and analysis in the world of research, which I would not have achieved without them. Special appreciation to Dr. Njue for allowing this research to be set up and conducted in his research and fabrication facility at Nakuru. Thank you, and God bless you.

ABSTRACT

The solar energy needed to drive solar-driven milk refrigeration systems is only abundant in the mid hours. It is completely unavailable in the early and late hours of the day. The mismatch between solar energy availability and the milk cooling load energy demands and intermittent availability of solar energy negates the application of solar-driven milk cooling refrigeration systems. It is prudent to harness and store solar energy during peak periods of high solar energy for milk cooling during low or insufficient solar energy availability. This study has analyzed solar energy predicting models from literature reviews and annual solar energy trends from different sites and selected a solar radiation prediction model for predicting mean daily solar radiation levels. The input parameters considered are readily available in most meteorological stations in remote regions. The performance of four mean daily solar radiation prediction models namely; Gadiwala (MI), Seme (M2), Sendanayake (M3) and Samani (M4) when compared with measured data in Nakuru indicated a strong correlation of coefficient R^2 of 0.826, 0.735, 0.810 and 0.760 respectively. Three refrigeration systems with AC reciprocating compressor capacities of; 200 W, 250 W and 350 W were investigated for maximum cooling loads under varying mean daily solar radiations. Equal amounts of water stored in milk cans were surrounded by an ice layer, followed by an outer brine solution, which was then insulated by a polystyrene jacket. In each system, water in the milk can was cooled by an evaporator submerged in the brine solution, forming a layer of ice surrounding the milk cans. Four PV panels, each of 200 Wp, connected via an inverter provided the power required to operate the compressors in each refrigeration system. Temperature variation of the water in the milk cans and the amount of ice formed were used to determine the solar driven refrigeration system with maximum cooling load, based on solar radiation available. The cooling curve obtained in each refrigeration system provided nonlinear regression mathematical models for predicting maximum cooling loads for the solar-driven refrigeration systems. The coefficient of correlation R^2 between the actual and predicted maximum cooling loads for the 200W, 250W and the 350W solar refrigeration systems were 0.8647, 0.9413 and 0.956 respectively. An accurate model for predicting the solar-driven refrigeration capacity of a milk cooling system with the provision of sensible thermal energy storage for matching solar energy availability and milk cooling load energy demands at any site could be a useful tool for optimization in the design and application of solar-driven milk cooling refrigeration systems. Designer and manufacturer of solar-powered milk cooling systems for large, medium and small businesses would find the solar driven refrigeration maximum cooling models load a suitable tool.

TABLE OF CONTENTS

LIST OF FIGURES

LIST OF TABLES

LIST OF SYMBOLS

C_p Specific heat capacity

G Global radiation over a period of time

G_{dh} Daily global radiation on a horizontal surface

H Incoming daily solar radiation

h Specific Enthalpy

I_{SC} Solar constant

L_d Astronomical day length

$\dot{m}$ Mass flow rate

n Brightness sunshine hours

P_r Rated PV power output

P_o PV cell power output

Q_L Refrigeration cooling load

T_C Temperature coefficient of a PV cell

T_{bi} Inlet refrigerant temperature at evaporator

T_{bo} Outlet refrigerant temperature at evaporator

T_{con} Condenser refrigerant inlet temperature

U Overall heat transfer coefficient

ϕ Latitude

δ_S Solar inclination angle

α Heat transfer coefficient of a liquid

ρ_V Density of saturated vapour

ρ_L Density of saturated liquid

η Efficiency

ω Angular velocity

ω_s Sunset hoursP_s

S_R Power supply kWh

Annual mean daily solar radiation W/m^2

LIST OF ABBREVIATIONS AND ACRONYMS

AAR	Ammonia Absorption Refrigeration
AC	Alternating Current
Ambnt	Ambient
ANN	Artificial Neural Network
CHP	Cogeneration of Heat and Power
CHX	A combustor heat exchanger duplex
COC	Coefficient Of Correlation
Com	Compressor
COP	Coefficient of Performance
COPr	Coefficient of Performance of the Refrigerator
CSP	Concentrating solar power
CSR	Climatological Solar Radiation
CTAR	Constant Temperature Adsorption Refrigeration
CVC	Conventional Vapor Compression Cycle
DC	Direct Current
DNI	Direct Normal Irradiance
FAO	Food and Agriculture Organization
FESR.	Fuel Energy Savings Ratio
GA	General Algorithm
GHI	Global Horizontal Irradiance
GW	Gigawatts
HRSG	Heat Recovery Steam Generator
IB	Ice Bank
IC.	Incremental Conductance
ITS	Ice Thermal Storage
KC	Kalina Cycle
KLACC.	Kalina Lithium Bromide Absorption Chiller Cycle
KPCC	Kalina Power-Cooling Cycle
LM	Levenberg-Marquardt
LMTD	Logarithmic Mean Temperature Difference

MABE	Mean Average Bias Error
MAE	Mean Absolute Error
MBD	Mean Bias Difference
MBE	Mean Bias Error
MEHD	Multi-Effect Humidification and Dehumidification
MPE	Mean Percentage Error
MPPT	Maximum Power Point Tracking
MSE	Root mean-square error
NASA	National Aeronautics and Space Administration
ORC	Organic Rankine Cycle
P&O.	Perturb and Observe
PCM	Phase Change Material
PLC	Programmable Logical Control
PPG	Photoplethysmogram
Pr	Prandtl Number
PSO	Particle Swarm Optimization
PTC	Parabolic Trough Collector
PV	Photo Voltaic
PVT	Hybrid Photovoltaic/thermal
RMSE	Root Mean Square Error
SAAC	Solar Ammonia Absorption Cycle
SAR	Solar adsorption refrigeration
SCS	Solar systems
SMEs	Small and Medium Enterprises
SMEs	Small and Medium-Sized Enterprises
SNGDAC	Solar or Natural Gas-Powered Absorption Chillers
STC	Standard Test Condition
SUPG	Solar Updraft power generator
SVCAIRSPC	Solar Vapour Compressional Absorption Integrated Refrigeration Systems
TD	Temperatures Difference
TEG	Thermoelectric Generator

TIT	Turbine Inlet Temperature
TR.	Ton of Refrigeration
UTC	Coordinated universal time
VAR	Vapour Absorption Refrigeration System
VCR	Vapour Compression Refrigeration System
VTEJ	Variable Throat Ejector
Wp	Watt Power

CHAPTER ONE
INTRODUCTION

1.1 Background of The Study

A Quick Overview of Radiant Cooling's History Residents in the Northern Hemisphere heated the interiors of their underground shelters by drawing smoke from fires via stone-covered, floor-cut ditches during the Neolithic period (Teitelbaum et al., 2019). Despite the exceedingly harsh outside temperatures, the heated stones would transmit heat from the floor into the living rooms, creating extremely comfortable interior settings. The widespread use of radiant heating systems driven by water has occurred in Europe over the last century. Warm water is transported back and forth between these systems via a network of pipe loops constructed into the concrete floor slab. The slab's temperature can be adjusted, allowing for hitherto unattainable comfort levels. This is accomplished by altering the water temperature. A radiant slab may also transmit energy far more effectively than a forced-air system since the capacity of water to carry heat is significantly larger than that of air (Shu et al., 2020). For many years, embedded copper tubes were the preferred for cooling the vast majority of new installations (Gupta & Sharma, 2021). Copper was thought to be a material that was both easy to work with and inexpensive at the time. However, it was beset by issues like kinks during installation, corrosion, pitting, and material buildup, all of which contributed to the system's efficacy gradually deteriorating and a shorter overall lifespan.

According to Do et al. (2022), the three primary categories into which radiant systems are grouped in the REHVA manual on radiant systems are radiant cooling panels (RCP), water-based embedded surface cooling systems (ESCS), and thermally activated building systems. RCPs are metal panels that hang from the ceiling and contain pipes. The temperature of the heat transmission medium is usually between the room and ambient temperatures: cement screed, gypsum board, or plaster cover ESCS pipes. Thermal insulation separates these pipes from the main building construction (the floor, the walls, and the ceiling). They can be found in a wide range of structures and cool by reacting with heat carriers at relatively high temperatures. Last but not least, "systems with pipes embedded in the building structure (slab, walls)," also known as TABS, take advantage of the building structure's thermal storage capacity and operate at heat carrier temperatures close to ambient. These systems serve a variety of applications due to their different thermal and control features; as a result, their design and scaling approaches are as diverse.

One of the most notable advantages of radiant cooling systems is their ability to utilise less energy than conventional cooling systems (Teitelbaum et al., 2020). Radiant cooling has

been demonstrated to significantly reduce energy consumption, with potential savings varying depending on the local temperature. Berkeley National Laboratory in California conducted this research. (Tang et al., 2021). According to their findings, the average savings in the United States compared to traditional systems is thirty percent. There is a 17 percent chance of saving in hot and humid places, whereas there is a 42 percent chance of keeping in hot and dry regions.

Several factors contribute to lower energy use, the majority of which are related to the benefits of hydroponics in general and the unique qualities of radiant heat transmission (Rapisarda et al., 2022). Pumping water is much easier than blowing air to transport the same amount of British thermal units. A pump uses significantly less electricity than a fan. Furthermore, the air handling component of a radiant cooling system is far smaller than that of traditional cooling systems, resulting in decreased electrical energy usage. Significant, incredible surfaces act as heat sinks in radiant cooling systems, drawing heat away from our bodies and into the system (Li & Fan, 2019). The overall amount of heat that must be transmitted through convection is minimized because the majority of heat is lost through radiation. This allows customers to set a greater air temperature without sacrificing comfort. As a result, energy consumption is reduced, and general comfort is improved. In systems with a significant mass, radiant cooling provides an extra alternative for energy savings. This cooling technology allows a portion of the cooling load to be shifted to off-peak, less expensive nighttime hours.

Another significant benefit of radiant cooling system is that they provide comfort to the people who use the room (Radzai et al., 2022). Because of its cooling effect, the excellent massive surface acts as a heat sink, drawing heat away from our bodies and providing an extraordinarily comfortable and stable interior climate. The volume of forced airflow is considerably reduced compared to traditional air conditioning systems. This eliminates chilly draughts and eliminates the potential of allergens and dust flowing. Due to the absence of a great reduction of noise produced by fans or blowers, radiant cooling systems have a deficient background noise level (Nardell, 2021).

Biological causes account for the bulk of food spoilage and losses and physical and chemical contamination. The biological reasons are influenced by environmental elements like as temperature, relative humidity, and air velocity (Yahaya & Mardiyya, 2019). It is critical to creating novel food processing and storage methods to reduce the influence of biological factors, prevent post-harvest contamination, and limit post-harvest losses.

According to Zavala-Nacul and Revoredo-Giha (2022), in the majority of developing economies in rural areas such as Kenya, a shortage of chilling milk technology is directly linked

to the inconsistent availability and price fluctuations of the national grid electricity power. According to Girma (2020), the problem of electrification in remote rural and pre-urban areas can be handled by deploying autonomous electrical power systems that are solely powered by environmentally benign energy sources like solar power. Solar energy is a viable energy source since it is readily available in most emerging economies, particularly in tropical countries where vast quantities may be produced. The technologies are efficient, low-maintenance, and highly dependable (Ahmadi et al., 2018).

One of the most common disadvantages associated with the usage of solar energy technology is its unpredictability, which is entirely reliant on the current weather conditions, the time of year, and the geographic location. As a result, the load may be rejected, resulting in poor solar energy refrigeration system performance and efficiency (Selvaraj & Victor, 2021). Energy markets, like fossil-based energy, rely on exploration and proven reserves for economic support. The evaluation of solar radiation resources is required to design and sell energy technology in the renewable energy industry (Benedek et al., 2018). Solar radiation is used as the primary energy source in a variety of solar-based renewable energy technologies, including photovoltaic conversion systems. Nwaigwe et al. (2019) discovered a linear link between the degrees of uncertainty in solar photovoltaic (PV) system life cycle savings and the degrees of uncertainty in the sun resource or radiation.

System performance and characterization can be improved when reliability, mismatch in solar energy availability, and solar energy demands are considered during a solar-powered milk chilling system, resulting in more efficient, dependable, and cost-effective systems (Panchal et al., 2020). Large, medium and small businesses have attempted to design and manufacture solar-powered milk cooling systems. A range of strategies has been developed to reduce the amount of energy required by dairy processing enterprises, according to Singh et al. (2019). Heat and power cogeneration are one of these technologies (CHP). The majority of today's solar systems store solar energy in batteries. This improves the dependability of equipment like solar cooling and raises disposal issues once the batteries' useful life has passed.

The main impediment to using solar technology to cool milk is the lack of sufficient equipment to store solar energy during periods of low solar radiation or when solar energy is absent. This is the primary challenge that solar technology applications encounter. Ice, molten salts, phase change materials (PCM), and undercooled secondary refrigerants have been researched as alternate thermal energy storage mediums. The trouble with milk chilling was caused, according to Orwa et al. (2021) by the short time required to cool the milk to 4 degrees Celsius, which was less than three hours. As a result, the slowest and least effective

refrigeration technologies have very limited application in the milk cooling industry. According to a study conducted by Sidney et al. (2022) an off-grid system consisting of photovoltaic panels and a refrigerated compressor is the most cost-effective way to cool milk. Suppose the design and development of the technologies are flawed. In that case, solar milk cooling refrigeration systems on medium and minor scales may be inefficient, uneconomical, and out of reach for the bulk of dairy applications in emerging countries.

A model that predicts the cooling load energy generated by a solar-driven milk cooling refrigeration system based on solar energy availability in a specific geographic location would make the system affordable and available to the majority of small and medium-sized enterprises (SMEs) in rural settings in developing economies. All of these advantages would improve rural dwellers' quality of life. It would be possible to offer milk cooling energy even when solar energy is in insufficient supply by collecting and storing excess solar energy available during peak periods and converting the excess solar energy into sensible thermal energy. The milk would be chilled consistently and reliably as a result of this method.

1.2 Statement of the Problem

Solar radiation energy is the most direct, abundant, and steady source of energy on Earth because of nuclear fusion in the sun. Solar radiation data for different locations are needed for a variety of purposes, such as determining power levels in photovoltaic (PV) modules, calculating cooling loads in buildings, and calculating water budgets. Solar technologies' capacity and performance are determined by the amount of solar radiation available in the area where they will be deployed. Precision data and knowledge of available global solar radiation in the region of interest are required to construct solar energy application systems with precision. This makes it possible to create more efficient systems. For a variety of reasons, including economic and historical ones, few weather stations in developing countries, particularly those in rural areas, are less equipped to measure solar radiation.

The amount of solar radiation that reaches the earth surface is dependent on local meteorological variables. Studying solar radiation under local meteorological conditions is critical. In areas where meteorological data is lacking, solar radiation can be estimated using models and empirical correlations based on available data. In these places, solar radiation can thus be approximated. Several different models have been examined in order to generate an accurate estimate of solar radiation from current weather data.

However, most models require astronomical and physical data, the vast majority of which are unavailable in developing countries like Kenya. The bulk of artificial neural network

models have limited uses in developing nations because of a lack of data on astronomical factors such as sky transmittance, albedo, relative air pressure, clearness index, and cloudiness index. The variable levels of solar radiation throughout the year and at different times of the day makes solar technology ineffective and unreliable due to lack of an accurate design tools for predicting the capacity of solar milk cooling system based on the solar radiation of a specific location. As a result, the amount of accessible solar energy on daily and seasonal milk cooling loads are out of sync. The load on the system may be rejected at some time, resulting in poor performance of the self-contained solar energy refrigeration system. Hence, this study sought to develop a mathematical model for predicting the solar driven refrigeration system capacity for milk cooling based on the mean daily solar radiation available at a specific location.

A model that predicts the cooling load energy generated by a solar-driven milk cooling refrigeration system based on solar energy availability in a specific geographic location would reduce design inaccuracy, improve efficiency, and make the system more affordable and available to the majority of small and medium-sized enterprises (SMEs) in rural settings in developing economies. All of these advantages would improve rural dwellers' quality of life.

This study aimed to develop mathematical models based on actual cooling loads that might be met by available sun radiation in a given region. The built models should be able to predict the maximum cooling demand that solar radiation can meet and the quantity of solar-powered refrigeration capacity that is appropriate for the location. As a result, the models would calculate the amount of cooling load available at a given area based on the available mean daily solar radiation

1.3 Objectives

1.3.1 Broad Objective

To develop a mathematical model for predicting the solar-driven refrigeration system capacity for milk cooling.

1.3.2 Specific Objectives

i. To establish the best fitting models(s) for predicting solar radiation at various sites in Nakuru county
ii. To determine the capacity of a solar-driven refrigeration system that provide maximum cooling load energy based on available. Solar energy
iii. To develop and validate mathematical models for predicting the optimum solar driven refrigeration cooling loads for a solar driven refrigeration system

1.4 Research Questions

i. Which model from the literature review and solar energy availability trends would predict daily mean solar availability in various site within Nakuru county?

ii. What capacity of a solar-driven refrigeration system would provide maximum cooling energy loads from solar energy available in various sites in Nakuru county?

iii. Which mathematical model would predict the solar-driven refrigeration system with maximum cooling load capacity based on the solar and how accurate is the mathematical models compared to the prototype solar-driven refrigeration system?

1.5 Justification of the study

Before starting the design and construction of any solar energy system, it must be determined that the system will be able to meet the projected demand and do so at a cost that is affordable over the system's entire life cycle. Milk cooling capacity and component specifications must be carefully assessed when manufacturing solar-powered refrigeration systems for milk cooling, based on the amount of available solar energy and the amount of energy required to meet the milk cooling loads' energy demands. This is particularly critical in order to ensure that the systems are constructed efficiently and economically.

Energy demand and supply compatibility must be maximized when building a solar refrigeration system for milk cooling. This can be accomplished by collecting and storing solar energy for use when solar energy is scarce. It would be helpful to have a method for estimating a solar-driven refrigeration system's maximum solar driven refrigeration capacity so that enough solar energy can be captured and stored as sensible thermal energy for use during periods of low solar energy. This would help close the gap between the amount of solar energy available and the amount of milk cooling load energy needed. An accurate model for predicting the solar-driven refrigeration capacity of a milk cooling system with sensible thermal energy storage (TES), for matching solar energy availability and milk cooling load energy requirements at any geographical location, will be a valuable tool for optimizing the design and application of solar-driven milk cooling refrigeration systems. In any region, this model will be able to match solar energy availability with milk cooling load energy needs.

Solar energy can be stored in a variety of ways, the most common of which are alkaline batteries, ice banks, and low-temperature secondary refrigerants. The use of ice banks and low-temperature secondary refrigerants necessitates precise refrigeration system sizing, which must be proportional to the amount of readily available solar energy at a given location.

This project aims to develop mathematical models for forecasting the cooling loads of solar-driven refrigeration systems based on the amount of solar radiation available in a given region. This research aims to close the gap between the highest available energy supply and the lowest available energy demand.

1.6 Scope and Limitations

1.6.1 Scope

Only vapour compression refrigeration systems with reciprocating AC compressors and R134a refrigerant were investigated for milk refrigeration in this research. The cooling process involves a rapid rate of cooling to significantly reduce the levels of microorganisms present in the milk in less than three hours. The vapour compression refrigeration system is the most effective for this application compared to other refrigeration systems. The mathematical modelling is based on nonlinear regression models created from cooling curves shown against the best performing system based on the material utilized and solar radiation levels measured at the site. This was necessary due to the intricacy of the designs utilized in refrigeration components and equipment from many manufacturers.

1.6.2 Limitations

The analysis of the performance was carried out using water in place of milk.

CHAPTER TWO
LITERATURE REVIEW

2.1 Introduction

Reviews of relevant prior research to the question we were trying to address in this study section. Previous authors' opinions on the process of constructing a mathematical model for evaluating the milk-cooling performance of solar-powered refrigeration systems were investigated in this work. Several theoretical techniques for developing mathematical models for prediction were investigated. Graphics depicting the relationships between the several researched components presented the conceptual framework.

2.2 Solar Energy

Throughout this historical period, the continuous delivery of electric power is critical to the ever-increasing rate of innovation in all fields. Fossil fuels are required for the production of reliable and consistent energy. Still, they are costly, are known to generate dangerous emissions, and are subject to changes in the worldwide price of oil. On the other hand, solar power is a plentiful, cost-effective, and environmentally friendly source of energy that can be produced in any country. It is dependable is limited due to its dependency on weather conditions. Solar power prediction helps to provide a steady supply by compensating for volatility of the source (Yin et al., 2020).

Because fossil fuels are becoming increasingly scarce, research into alternative energy sources has exploded (Safari et al., 2019). Photovoltaic cells are currently the most common way of generating solar energy, and the most important renewable energy source. Solar energy is appealing for various reasons, including its environmental friendliness, independence from volatile markets like oil prices, and less reliance on imported commodities and other external sources of supply (Hojjatian et al., 2021). Solar cells are expected to contribute to future energy production significantly, yet their low return on investment and high initial cost prevent widespread use. There is insufficient supply that can be expected, in part due to the unpredictability of the weather. Because photovoltaic cells generate electricity by converting solar energy into electric current, the daily solar energy output is essential when sizing a photovoltaic system (Hayat et al., 2019). As a result, the amount of energy produced is determined by the amount of solar irradiance present on any particular day, influenced by various factors such as location, time, and weather. The power received from the Sun in the form of electromagnetic radiation that falls within the wavelength range of the solar cell in use is referred to as solar irradiance.

Bad weather has a major impact on the amount of electricity generated by solar power plants, according to Nishiyama et al. (2021). As a result, a power supply firm must obtain the remaining energy from various power-producing companies that use more expensive fossil fuels in order to meet demand. This step is being taken to meet the energy demands. Both the amount of power sought and the urgency of the order are taken into account when determining the electricity expenses paid by businesses. According to Fan et al. (2019), placing orders with electrical firms on time helps achieve the stated power supply targets and helps save money. As a result, having historical data on the amount of energy generated is critical for maintaining service levels and cutting costs. By researching both historical and current data on the relationship between irradiance and meteorological conditions, it is feasible to develop reasonable projections of future solar energy production (lvarez-Alvarado et al., 2021).

Solar radiation is the most direct source of permanent solar energy available on Earth, with approximately a hundred thousand million Watts of this renewable energy reaching the surface. Zhu et al. (2021) used an artificial neural network of 30 neurons in the first layer, ten neurons in the second layer, and one neuron in the third layer with five inputs and one output to forecast the daily distribution of global solar irradiance for clear days. They claimed that for clear days, the daily distribution of global solar irradiance is appropriate and that solar radiation data is helpful to engineers in selecting the number of solar modules for solar power plants.

Elmi (2018) claims that the sun is a 1.39109 m diameter sphere of highly heated gaseous stuff. It has a temperature of 5,777 K and is 1500 million kilometers from Earth. In the form of X-rays and gamma rays, solar energy is radiated to the earth's surface. Solar radiation is deflected, dispersed, and reflected as it passes through the atmosphere, losing the majority of its energy. Bailek et al. (2020) estimated monthly mean solar radiation over Turkey using several regression analyses. They concluded that the sun's energy that reaches the earth's surface is a constant of 1.367 kW/m^2.

The three components of solar radiation are beam, diffuse, and total radiation. Direct sun energy reaches the earth's surface without being scattered by the atmosphere, whereas diffuse solar radiation does after being spread by the particles in the atmosphere. The sum of the beam and diffuse solar radiation that enters the earth's atmosphere is known as total solar radiation (Apell & McNeill, 2019).

The geographical location of the earth's surface relative to the sun and the climatic condition of a region are important factors in determining the intensity of solar radiation. The following words related to solar energy were defined by Guasp et al. (2020). Solar insolation is measured in kW/m^2 and is the amount of solar energy incident on a unit surface. Solar

insolation is a constant with 1.367 kW/m^2 known as the solar constant. On a given day, the peak solar insolation on the terrestrial surface is around 1 kW/m^2 due to air factors. Insolation can be achieved using a variety of wave lengths, including ultraviolet (magnetic), visible light, and infrared thermal wave lengths. However, according to Yang et al. (2019), 50 percent of solar energy is thermal, and just about a quarter of that is UV. Solar radiation changes dramatically with the number of days in the year, according to Modenese et al. (2018). The months of October, November, December, January, and February have the highest solar radiation levels, while May, June, and July have the lowest.

2.2.1 Solar Energy Technology

According to the National Aeronautics and Space Administration (NASA) (Sharafati et al., 2019), solar radiation is the most potent energy source on the planet. Due to the rapid depletion of convectional energy sources, extensive research into new, more efficient, and environmentally friendly energy sources has been promoted. According to G.K. (2011), generating electricity in remote places at a fair cost and scaling the power system are significant factors, and photovoltaics and other renewable energy systems are ideal possibilities for medium and small power equipment. Solar energy technology has made important contributions to solving some of the world's most critical energy issues (Shahsavari & Akbari, 2018).

According to Alsayah et al. (2019), the fundamental attraction of solar PV systems is that they produce electrical power without affecting the environment by directly converting a free and abundant source of energy, solar energy, into electrical energy. Fashina et al. (2018), demonstrated many key benefits and applications derived from solar energy technologies, including direct use of heat for absorption refrigeration systems, direct conversion of light to electricity without moving parts, rapid response in output to changes in input radiation, and high power to weight ratio, which is essential in space applications. The energy is time cyclic and highly dependent on weather and season. Thus, the necessity for energy storage to provide power in the absence of irradiation is one of the primary limiting constraints in the deployment of solar technology (Karunathilake et al., 2019).

According to Hafez et al. (2020), only two widely recognised technologies for converting solar energy into electricity are addressed in The Future of Solar Energy: photovoltaics (PV) and concentrated solar power (CSP), often known as solar thermal. These technologies are studied in their existing and potential future forms. Because energy supply infrastructure lasts several decades typically, these technologies will continue to dominate

solar-powered generation until 2050, and we have no plans to look further forward. We, too, do not make any predictions, in contrast to several previous research on the future, for two reasons. For starters, a significant expansion of the solar business beyond its current, relatively tiny size could result in changes that we can't even predict. Second, we acknowledge that future solar energy deployment will be greatly reliant on the unpredictability of future market conditions and government policies, including but not limited to activities targeted at minimizing the adverse effects of global climate change.

Solar energy is now the most abundant and environmentally friendly renewable energy source (Baloch et al.,2022). The United States of America has some of the most productive solar resources. Today's technology allows us to harvest this resource in various ways, allowing individuals and businesses to take advantage of the Sun's light and heat in a variety of ways. Three fundamental technologies are frequently used to gather solar energy, according to Ahmadi et al. (2018). Photovoltaics (PV) convert light directly to electricity; concentrating solar power (CSP) uses the Sun's heat (thermal energy) to power large-scale electric turbines, and heating and cooling systems collect thermal energy to provide hot water and air conditioning. One method for implementing solar energy is distributed generation, in which the necessary equipment is installed on rooftops or ground-mounted arrays near the point of consumption. Some technologies have the potential to be scaled up to utility-scale applications, allowing them to generate energy similarly to a central power plant.

Photovoltaic (PV) systems convert solar energy directly into electricity (Nazari et al., 2018). When sunlight strikes a semiconductor-based photovoltaic (PV) module, the atomic bonds that retain electrons are broken. An electric current is created when electrons move through a circuit. Solar photovoltaic modules have at least thirty years and require little maintenance. Photovoltaic (PV) electricity production peaks in the middle of the day, when the Sun is at its highest point. This time of day corresponds to the height of daily demand. Homeowners can cut or eliminate their monthly electricity expenses by installing a few dozen photovoltaic (PV) panels. At the same time, utilities can build enormous "farms" of PV panels to supply pollution-free electricity to their consumers (Sreenath et al., 2022). The vast majority of electrical items, such as computer chips, audio amplifiers, temperature sensors, and solar cells, are made of semiconducting materials. PV modules have traditionally been made from a variety of silicon varieties; however, an increasing number of companies are also making PV modules using alternative semiconductor materials. Each photovoltaic (PV) technology has its own distinct cost and performance characteristics that set it apart, stimulating industry

competitiveness. A photovoltaic (PV) system's application and configuration may have different effects on its cost and performance.

Concentrating Mirrors are used in concentrating solar power plants, commonly known as CSP plants, to concentrate the Sun's heat and power a traditional steam turbine that creates energy (Elbeh & Sleiti, 2021). Regardless of demand, the thermal energy concentrated in a CSP plant can be stored and used to generate electricity at any time of day. According to Ding and Bauer (2021), around 1,400 megawatts of concentrated solar power (CSP) facilities are already operational in the United States, with another 340 megawatts expected to be operational within the following year. The two commercially available technologies for concentrating solar power are Power Towers and Parabolic Troughs (CSP). The Compact Linear Fresnel Reflector (CLFR) and the Dish Engine are further examples of CSP technology. To generate power, CSP requires exact circumstances, such as areas with a high concentration of direct sunlight (such as the southwestern United States) and large, contiguous stretches of dry, level terrain.

2.2.2 Solar PV energy technology application

Solar photovoltaics (PV) has a number of societal advantages, including the elimination of pollutants from energy production, the use of very little water, the availability of abundant resources, the lack of audible operations, a long lifespan and low maintenance (Tazvinga et al., 2020). However, integrating solar photovoltaics (PV) into electric grids has many issues, the most serious of which is variable power generation, which can lead to increased system stress. The necessity for additional reserves on the electric grid to compensate for swings in power output due to the variable nature of solar photovoltaics (PV) may limit future deployment or reduce the potential for lowering carbon emissions.

The process of evaluating the power generation of solar PV systems typically consists of the two steps listed below, according to Kim et al. (2019). The solar irradiance and the temperature of the solar PV cell are fed into a power modelling method after meteorological data, and an estimate of solar irradiance is collected. According to Zeng et al. (2021), solar irradiance can be estimated for the past (hindcasting), present (analysis), and future (forecasting). The approaches used to compute the power output are, for the most part, the same after establishing the solar irradiation. The method proposed in this paper uses historical data and runs the algorithms as if they were current to provide an analysis.

Regardless of how precise the power algorithm is, if the solar irradiance used as an input for photovoltaic power modelling is erroneous, the power output will be incorrect (Manoharan et al., 2020). Solar irradiance forecasts are frequently classified into two types.

First, short-term forecasting uses a variety of cutting-edge approaches, including neural networks (Korkmaz et al., 2021). Solar irradiance can also be calculated using satellite data as a proxy, the most used method (Vaishnav et al., 2018). Simple numerical weather prediction (NWP) models or ground-collected data are used in the methodologies mentioned above. The National Weather Service provided satellite data and hydrometeor assimilation data for this story. Because there is no model output for solar irradiance at time zero for the model in use, the solar irradiance field from the NWP assimilation model is not used. Shortwave and longwave radiation are both included in this field.

Furthermore, at this moment, specific NWP assimilation models do not produce direct-normal or diffuse radiation output fields. The amount of radiation received per unit area by a plane perpendicular to the Sun's rays is known as direct-normal radiation output. The diffuse radiation output is the quantity of radiation per unit area that does not come straight from the Sun.

Inderwildi et al. (2020). After extensive research, solar energy components were divided into two kernel subsystems, namely solar collectors and solar thermal energy storage applications. The solar thermal subsystem required superb optical performance to release the necessary at rapid speed above 200m/s, while the thermal storage subsystem required high thermal storage density and excellent heat transfer rate. PVT (photovoltaic/thermal) hybrid collectors have been designed to convert solar energy into both electricity and heat. The PVT system, which consists of a PV module and an absorber plate, takes heat from the PV module and lowers its temperature, increasing the PV module's efficiency by 5 to 20%. This design works well in low-temperature applications like residential hot water heating and adsorption refrigeration systems (Lima et al., 2020).

The development of a SCADA based solar-powered irrigation system was identified as being quite helpful in areas where there was plenty of sunshine. Still, insufficient water to carry out farming activities, such as rubber plantations, strawberry plantations, or any other plantation that requires frequent watering (Adenugba et al., 2019). The system was powered by a solar system, which is a renewable energy source that converts sunlight into electricity using solar panel modules. Creating and installing an automated SCADA controlled system using a PLC as a controller was critical for agriculture, oil and gas monitoring and control. Furthermore, the system was fueled by an intelligent solar system with solar panels that target the Sun's energy. Aside from that, the solar system lowered both energy costs and pollutants. Four input sensors were used in the system: two soil moisture and two-level detecting sensors. The soil moisture sensor detects the amount of water in the tank, while the level detection

sensors sense the humidity of the soil. Two solenoid valves control the output sides, controlled by two moisture sensors each.

According to Imran et al. (2020), one of the most significant fixed expenditures in agriculture is energy, which is especially true for greenhouse growers. Traditional energy sources, such as fossil fuels, have negative environmental and agricultural consequences. As a result, using solar energy for agricultural purposes might save money while benefiting the environment.

Solar photovoltaic (PV) water pumps are helpful in most areas when electricity is unavailable. Furthermore, these systems deliver water to areas that are geographically isolated. Simple photovoltaic (PV) systems are frequently constructed to operate only when the sun shines and give water wherever required. Farmers do not employ solar storage batteries in these situations since the water is kept in containers or pumped straight to the crops. Tracking mounts, storage channels, and inverters can be used in more extensive systems. Because the power is consistent throughout the system, a large-scale photovoltaic system requires minimal maintenance from the farmer. Irrigation, cow watering, and pond aeration are just a few of the applications for these systems.

Unreliable electrical supply has a significant impact on agriculture. As a result, several farmers have faced serious financial difficulties. Solar energy is less expensive than traditional electricity sources for powering agricultural operations (Zhao et al., 2019). Solar energy for farming uses can also help mitigate the effects of drought-related problems. One solution to the problem is to use solar energy in water-scarce areas, particularly for water pumping and irrigation. Technological innovation may help farmers as the agriculture sector becomes more sensitive to new ideas and practices.

Solar energy solves another problem associated with unpredictable power sources (Ulsrud, 2020). The farmer will always have access to electricity because of solar energy and effective energy storage technologies. One of the most important things to consider in agricultural productivity is energy. Farmers are the group most vulnerable to the consequences of global warming (Babu et al., 2021). As a result, they must play a critical role in executing long-term energy expansion. Solar energy provides a wide range of agricultural output options.

In terms of solar energy for industrial use, Mariya et al. (2020) researched solar-powered reverse trash vending machines. The project was carried out to construct a Solar Powered Reverse Trash Vendo Machine that would encourage people to recycle and reduce the Philippines' practice of inappropriate waste disposal. The device's main processing module was a Gizduino X ATMega 1281, with a Gizduino 644 microcontroller board and a GSM

Shield module for connectivity. The Gizduino boards were programmed using the Arduino1.6 IDE. The gadget was powered by a 15V rechargeable battery charged by a solar panel mounted on the device's roof to promote energy conservation and green engineering concepts in the study's development. The machine was used to process empty plastic bottles (500 ml. max with a base diameter of 3.5 inches and aluminium cans). These recyclable materials were scanned, crushed, and deposited in a bin after being placed into the machine.

Chickens must be fed on a regular basis to be productive, so the manner of providing them must be examined. Radwan et al. (2020) investigated solar energy utilization to heat chicken houses. The traditional way of chicken feeding and warming is to provide food continuously. The feeder is aware of the food remaining in cages and feeding the chickens at the appropriate moment to avoid a productivity drop. Chicken growers also struggle to successfully manage their operations since they must periodically visit the cages to oversee the fowl. To feed the chickens at a consistent time, precision and timing are essential. The planned feeder was deemed to benefit the business owner in terms of time and effort. Another benefit of the technique was the cost reduction for the poultry business owner. This device was created to automatically feed hens at predetermined intervals and alert users when feed supplies were running low. Solar panels were used to gather power from the sun for this prototype, which was then stored in a normal car battery. The feeds were stored in a container and evenly dispensed to the chicken feeding basin using a conveyor. It would be more efficient than the traditional manual feeding method because less work would be required, and fewer feeds would be wasted. Furthermore, the stored energy can be used for lighting reasons by growers to save energy and money.

Microbial fuel cells have been developed as a result of recent solar energy research. The solar-powered microbial fuel cell is a new method for generating electricity using electrochemically active microorganisms fueled by solar energy via photosynthesized metabolites from algae, cyanobacteria, or living higher plants in situ (Yu et al., 2018).

The pH membrane gradient, which affects cell voltage and power generation, is a common issue with microbial fuel cells. Acid production at the anode, alkaline creation at the cathode, and nonspecific proton exchange through the membrane contribute to this problem. The invention of a reversible bio electrode capable of both bios catalyzed anodic and cathodic electron transfer was reported in the study as a solution for a new type of solar energy powered microbial fuel cell. The cathodic reduction reaction, which held the formation of a pH membrane gradient, utilized anodic generated protons. Depending on aeration or solar energy exposure, the microbial fuel cell generated power continuously and repeatedly reversed

polarity. Algae, (cyano) bacteria and protozoa were found in the bio catalytic biofilm of the reversible bio electrode. These findings support the use of solar-powered microbial fuel cells.

The company designed and documented a solar-powered, wireless, wrist-worn platform to continuously monitor physiological and environmental data throughout daily activities (De Fazio et al., 2022). This platform was shown to be capable of producing photoplethysmogram (PPG) signals in the investigation. A 574 nm green light source was utilized to get the PPG from the radial artery with little signal conditioning in order to stick to a low power budget for solar powering. Two monocrystalline solar cells were used to charge the inbuilt 20 mAh lithium polymer battery. The device was tethered to a smartphone using Bluetooth Low Energy (BLE), which turns the phone into an access point to a dedicated server for long-term data storage. Depending on the availability of solar energy, two power management strategies were proposed. If the battery is low in low-light circumstances, the gadget obtains a 5-second PPG waveform per minute, consuming 0.57 mW on average. The device was designed to enter its typical 30 Hz acquisition mode, consuming roughly 13.7 mW in instances when the battery was at a sustainable voltage. The research also shows how we're working to improve the charge storage capacity of our onboard supercapacitor.

Increased solar power generation necessitates automated forecasting systems to reduce power loss, cost, and environmental impact for houses and companies that create and consume power (Nwaigwe et al., 2019). Based on machine learning, image processing, and audio classification approaches, Al-Hajj et al. (2021) conducted a study on methods of solar power forecasting for people and small enterprises. To develop reliable ANN projections, these new energy market participants and prosumers required new artificial neural network ANN performance tuning methodologies.

Input masking, a neural network (ANN) tuning approach initially developed for acoustic signal classification and image edge recognition, was applied to prosumer solar data to increase prediction accuracy over typical macro grid ANN performance tuning techniques. Based on error clustering in the time domain, ANN inputs customize time-of-day masking. The R2 value improved prediction to target correlation, cutting sample prediction inaccuracy by 14.4%, with matching reductions in a mean average error of 5.37 percent and root mean squared error of 6.83 percent.

Apart from photovoltaic solar energy applications, vast amounts of solar thermal energy have been used in numerous technologies, as detailed below, particularly in power plants using solar concentrators.

2.2.3 Concentrating Solar Power Plants

Concentrating solar power, or CSP is a new technique with a lot of potential for countries with abundant sunshine and clean skies (Hernández et al., 2021). Its electrical output is ideally matched to the fluctuating daily electricity demand in areas where air conditioning systems are becoming more prevalent. It provided services such as electricity that could be dispatched as needed, allowing it to be used for the base, shoulder, and peak loads when backed up by thermal storage facilities and combustible fuel. It will be able to compete with coal facilities that emit far more CO^2 than CSP within one to two decades. The sunniest places, such as North Africa, may be able to export excess solar electricity to nearby regions, such as Europe, where renewable energy demand is high. Concentrating solar plants can also produce hydrogen, which can be mixed with natural gas to produce low-carbon liquid fuels for transportation and other end uses in the medium to long term. For CSP to claim its share of the approaching energy revolution, scientists, industry, governments, financial institutions, and the general public must work together during the next ten years. This road map is meant to aid in the advancement of these critical advancements.

A study on heat transport phenomena in concentrating solar power systems was undertaken by Palacios et al. (2020). Solar thermal energy is used to drive a thermal power cycle for the generation of electricity in concentrated solar power (CSP). CSP systems are designed as big, centralized power plants, such as power towers and trough systems, to benefit from economies of scale through dispatchable thermal energy storage, a key advantage over alternative energy generation methods. Compared to other solar-fossil hybrid power plants, the combination of large solar concentration ratios and high solar conversion efficiencies provides a strong opportunity for specific power cycles like the Brayton gas cycle, which uses supercritical fluids like supercritical carbon dioxide CO_2. This study of numerous heat transport processes seen in CSP technologies provides a detailed thermal-fluids evaluation. Receivers, heat transfer fluids (HTFs), thermal storage media and system designs, thermodynamic power block systems/components, and high-temperature materials are among the sub-systems and heat transfer fundamental phenomena visible inside CSP systems. This research includes literature reviews, trade studies, and phenomenological comparisons of heat transfer medium (HTM), components, and systems, all aiming to promote high-performance and efficient CSP systems. Furthermore, more research is being done to develop sophisticated heat transfer modelling methodologies for gas-particle receiver systems and performance and efficiency enhancement recommendations, notably for solarized supercritical power systems.

Mehellou et al. (2018) created solar concentrators for solar-pumped solid-state lasers to boost both efficiency and laser output power. A primary concentrator with a 2 m by 2 m Fresnel lens captured natural sunlight, which was restricted by a cone-shaped hybrid concentrator. A cylinder with coolant encircling and a liquid light-guide lens was used to couple solar power to a laser rod (LLGL). The cylindrical LLGL's performance was studied both theoretically and empirically. Since the diameter is 14 mm, LLGL produces effective and consistent pumping along a rod with a diameter of 6 mm and a length of 100 mm, with a 120 W laser output and a slope efficiency of 4.3 percent. The collecting efficiency was measured at 30.0 W/m^2, 1.5 times higher than the previous measurement. The entire conversion efficiency was more significant than 3.2 percent, comparable to that of a commercial lamp-pumped solid-state laser. The concept of the light guiding lens was recommended for concentrator photovoltaics and other solar energy optics.

Similarly, Belgasim et al. (2018) used geographic information systems to conduct a study on the potential of concentrating solar power in all provinces of South Africa, with a good prospect for the development of large-scale concentrating solar power facilities. The regions were deemed viable provided they received enough sunlight, were close enough to transmission lines, were flat enough, had no threatened vegetation, and had an excellent land-use profile. The solar resource, slope, places with 'least threatened' vegetation, proximity to transmission lines, and areas ideal for the development of big concentrating solar power plants were all depicted on various maps. It was discovered that the selected appropriate locations could host plants with a nominal capacity of 510.3 GW in the Northern Cape, 25.3 GW in the Free State, 10.5 GW in the Western Cape, and 1.6 GW in the Eastern Cape, giving a total potential nominal capacity of 547.6 GW for the country.

A concentrated solar power (CSP) system must include thermal energy storage (TES). It allows plant operators to generate electricity outside of daylight hours and feed it into the grid to fulfil peak demand (Pelay et al., 2017). Molten salts are used as both the heat transport fluid and the heat storage medium in current CSP sensible heat storage systems. The maximum operating temperature for these systems is roughly 400 ^{O}C. Future TES systems are projected to run at temperatures ranging from 600 to 1000 degrees Celsius to achieve improved thermal efficiency and lower electricity costs. A TES idea based on thermochemical cycles (TCs) based on multivalent solid oxides was presented to suit future operating temperature and electricity cost requirements. The system uses a pair of reduction and oxidation (REDOX) reactions to store and release heat. Hot air from the solar receiver is utilised to lower the oxidation state of an oxide cation, such as Fe3+, to Fe2+ in the storage step. As a result, heat energy is retained

in chemical bonds, and the oxide becomes charged. The reduced oxide is re-oxidized in the air, producing heat to liberate the stored energy.

There is no need for fluid storage because air is employed as both the heat transfer fluid and the reactant. The research looked into the technical and financial viability of the suggested TES concept. The DOE's storage cost and LCOE targets are $15/kWh and $0.09/kWh. Thermodynamic simulations and bibliographic information were used to identify sixteen pure oxide cycles. The kinetics of re-oxidation of various oxides was found to be a significant hurdle to adopting the proposed approach. A down selection was made based on operating temperature, material costs, and preliminary laboratory data. Cobalt oxide, manganese oxide, and barium oxide were chosen for development research to increase REDOX reaction kinetics.

A novel strategy based on mixed oxides was proposed to improve the REDOX kinetics of the selected oxides. Some of the primary oxide cations are partially replaced with secondary cations. This generates a charge imbalance in the lattice, increasing the anion vacancy density. These vacancies improve ionic mass transfer and speed up re-oxidation. The inclusion of a secondary oxide enhanced the re-oxidation fractions of Mn_3O_4 to Mn_2O_3 and CaO to CO_3O_4 by up to 16 times. In barium-based mixed oxides, however, there was no improvement. Mixed oxides were found to assist in stabilizing or improving the TES properties following long-term thermal cycling and improving short-term re-oxidation kinetics. A reduction in particle size in the mixed oxides could account for some of this improvement. Manganese-iron, cobalt-aluminium, and cobalt iron mixed oxides have been recommended for future engineering scale demonstrations based on the measurement results. We were able to demonstrate the charge and discharge of the TES media in both a bench top fixed bed and a rotating kiln-moving bed reactor using cobalt and manganese mixed oxides. The fixed bed arrangement is simple, but charging requires a high mass flow rate and a higher fluid temperature (Pelay et al., 2017).

The rotating kiln allows for direct solar irradiation and vastly improved heat transmission; however, designs for transporting the TES oxide into and out of the reactor must be established. The CSP plant's economics will determine the final reactor and system architecture. A materials compatibility analysis was also carried out. Inconel 625 was discovered as a promising high-temperature engineering material for building a reactor that could store either cobalt or manganese mixed oxides. A packed bed reactor model was used as a baseline to examine the economics of such a CSP facility. The model was used to apply measured cobalt-aluminium oxide reaction kinetics, and the effects of bed characteristics and process parameters on the overall system design were studied. A network of eight fixed bed reactors with charge and discharge temperatures between 1200^{o}C and 600^{o}C, providing a

constant output temperature of 900°C, was found to be the best TES system design. The charge and discharge times are both eight hours. This design was incorporated into a CSP plant's process flowsheet, and the system's economics were calculated using Aspen Plus and the National Renewable Energy Laboratory's Solar Advisory Model. Storage costs are highly dependent on material costs and were estimated to be roughly $40/kWh for cobalt-based mixed oxide. Because of lower materials costs on a large scale, it could drop to $10/kWh. The calculated LCOE was between $0.22 and $0.30 per kW-h. The high LCOE in this first concept is due to the high charging temperature required and the expensive cost of cobalt oxide. A manganese oxide-based moving bed reactor is projected to enhance the proposed concept's economics significantly (Pelay et al., 2017).

Electricity generated by concentrated solar power (CSP) systems is said to be a future energy source. Islam et al. (2018) discussed previous experiments (including the French Thermis project) and the various strategies now in use. He pointed to the areas that appeared to be the best candidates for this procedure. The three primary systems were given in the study: parabolic cylinder, tower, and Stirling cycle installations. The study proposed a pricing assessment and its evolution and the investments made in various installations (in Italy, Spain, Germany and Portugal). The study studied the case of hybrid installations (sun and gas), evoking the Desertic project, a collection of hybrid installations presented by the German industry. According to the findings, there has been no major technological advancement in this technique.

2.2.4 Solar Water Heater using Refrigerant R134a

An experimental investigation was conducted on a heat pipe solar water heater prototype that used the refrigerant R134a as a transfer fluid (Sitepu et al., 2018). The study's goal was to learn more about the prototype's attributes and performance. The refrigerant R134a was utilized as a transfer medium to transfer heat from the collector to the heated fluid effectively. The initial pressure inside the heat pipe was changed in the trials. For three days of the experiment, the prototype was subjected to solar irradiation near Medan city. The system's efficiency was determined by measuring solar collector temperatures, solar radiation, water temperature, and ambient temperature. The findings revealed that when the initial pressure of the working fluid increases, the temperature of the hot water rises. However, the rise was not linear, implying an optimal beginning pressure existed. The maximum hot water temperature and maximum thermal efficiency were 45.36°C and 53.23 percent, respectively, when the

refrigerant pressure was 110 psi. The key conclusion was that solar water heaters employing R134a should be run at a pressure of 110 psi.

Refrigeration and heating systems use a lot of energy all over the world (Waite et al., 2017). However, because of the thermal capacity, the system had the potential to store "coldness" or heat. This feature enabled various load shifting and shedding tactics to reduce energy consumption while maintaining the original cooling and indoor climate quality. They looked into the possibilities of such a method and its capacity to drastically reduce the cost of operating systems like supermarket refrigeration and heat pumps for residential homes in this study. They used weather forecasts and predictions of varying electricity prices to apply more load to the system when the thermodynamic cycle was most efficient and consume larger shares of the electricity when demand and thus prices were low, using modern Economic Model Predictive Control (MPC) methods. The capacity to regulate power use in response to power grid demands was a popular feature in a future Smart Grid. The efficient use of more renewable energy necessitates ways to control power consumption such that it increases when there is an energy surplus and lowers when there is a shortage. This should happen almost quickly to handle intermittent energy sources such as wind turbines. They hoped that their power management method would allow thermal storage devices to be used for flexible power consumption. The combination of numerous units would greatly contribute to the reduction of total electricity demand.

Elsayed et al. (2022) conducted an experimental investigation and performance tests on a thermal bubble pump to lift the refrigerant absorbent solution from the generator to the separator in a 100 percent solar-powered diffusion absorption refrigerator (DAR), leaving gravity circulation to complete the refrigeration cycle. The system included a Methanol-charged experimental apparatus for testing the performance of various bubble pump topologies utilizing solar energy gathered by two modules of flat plate solar collectors, each with a $1m^2$ aperture cross-sectional area. Temperatures and flow rates the measurements were made at operating vacuum pressures, and the results were examined. Experiments revealed that a riser with an 8mm diameter, 0.2 submergence ratio, and an 800 mm head provided the best solution delivery. The DAR was designed to keep vaccinations, fruits, and vegetables fresh in farms and rural areas where regular electricity was sparse or unreliable. The findings of this study showed that the pump tube diameter of 8mm, pump lift of 0.8m, and submergence ratio of 0.2 is the best parameters for better solution circulation and subsequent adaption to the diffusion and absorption refrigeration system.

2.2.5 Refrigerant Operated Solar Thermal Plants

A feasibility study was conducted on a system that combines a solar collector-thermal storage system with a primary Rankine cycle power generator using R123 refrigerant and a heat transfer fluid (Khatoon et al., 2021). Mineral oil was heated in solar collectors with evacuated tubes before being transferred to a thermal storage tank. A heat exchanger generates a superheated refrigerant vapour that alternates between mineral oil and refrigerant and powers a radial turbo generator. Due to supplemental natural gas fire, the system delivered a continuous output of 50 kW while maintaining a consistent temperature in the thermal storage independent of available solar energy. The system's performance was simulated for sunshine conditions in southern California during the hottest summer day and the coldest winter day. A thorough economic analysis was also carried out. The selection of essential permanent evacuated tube collectors, which are less prone to breakage in harsh desert environments, was vital to the system's competitive advantage over more modern solar thermal power plants. Furthermore, because fossil fuels fueled the power plant, it could run continuously even when there was little sunlight or when night fell.

2.2.6 Power and Refrigeration Cogeneration Plants

Jiang et al. (2017) designed and investigated a cascading cycle for electricity and refrigeration cogeneration. The revolutionary cascading cycle Pumpless Organic Rankine Cycle (ORC) operated as the initial stage, and the refrigerant R245fa was chosen as the working fluid. The second stage of the sorption refrigeration cycle was the development of a silica gel and LiCl composite sorbent for better sorption characteristics. The experimental system was set up, and several hot water inlet temperatures ranging from 75 to 95 degrees Celsius were investigated for the study of cogeneration performance. Under the conditions of 95°C hot water inlet temperature, 25°C cooling water temperature, and ten °C chilled water outlet temperature, the peak power and refrigeration output were able to reach 232 W and 4.94 kW, respectively. The cascading system's total energy and exergy efficiency ranged from 0.236 to 0.277 and 0.101 to 0.132 for various working situations. When the hot water inlet temperature is 95°C, the exergy efficiency of heat utilization varies from 30.1 percent to 41.8 percent, which is 144 percent and 60 percent greater than pumpless ORC and sorption chiller, respectively.

A resorption system for electricity and refrigeration cogeneration was the subject of an experimental investigation (Surrya et al., 2019). By then, energy conversion technologies, particularly for power generation and refrigeration powered by low-temperature heat, had gained traction. Because there is no ammonia liquid in the system, reabsorption refrigeration

is considered safer and more straightforward construction than adsorption refrigeration. Three HTS (high-temperature salt) unit beds, three LTS (low-temperature salts) unit beds, one expander, three ammonia valves, two oil valves, four water valves, and connection pipes made up the cogeneration system. $MnCl_2$, $CaCl_2$, and NH_3 solutions were chosen as a chemical working pair. The scroll expander was selected for the expansion process because it is ideal for small type power generation systems. The cogeneration system was filled with 4.8 kg $MnCl_2$ and 3.9 kg $CaCl_2$ impregnated in expanded natural graphite treated with the sulfuric acid type (ENG-TSA). The maximum cooling power of 2.98 kW was achieved in the experiments. In contrast, full-shaft power was around 253 W with an average value of 82.3 W. When the heat source temperature is less than 170°C, the cogeneration system can be used. Total energy efficiency rises to 0.417 percent before falling to 0.407 percent, while exergy efficiency rises to 0.16 percent.

The impact of various refrigerants on the performance of binary geothermal power plants was studied (Unverdi & Cerci, 2018). The paper tried to review the debate over the usage of working fluids in binary cycle power plants from a broader perspective. One of these devices was a binary cycle that allowed power to be generated from geothermal energy sources. Thermal energy from geothermal sources was transferred to a second working fluid in the cycle. As a result, the choice of a second working fluid had a significant impact on cycle performance. A sample geothermal binary power cycle was modelled in the study, and 12 refrigerants were chosen as working fluids, including HFC, HC, and zoetrope refrigerant mixes. For 12 refrigerants, binary cycle energy and exergy efficiencies were computed. The examined refrigerants R 236ea, R 600 R 600a, and R 227ea have tremendous energy and exergy efficiencies in dry fluids. On the other hand, wet fluids R 143A, R 415A, R 290, and R 413A demonstrated poorer energy and exergy efficiencies.

2.2.7 Biomass Gasification Based Combined Power and Refrigeration Plant

The performance of a biomass gasification-based combined power and refrigeration system for community-scale use was investigated (Chattopadhyay & Ghosh, 2020). The study looked at the thermal performance and size of a biomass gasification-based combined power and refrigeration plant (CPR). The plant could generate 100 kW of electrical power while also creating a refrigeration impact that ranged from 28 to 68 tonnes of refrigeration (TR). The top gas turbine cycle is an all-air indirect heated cycle. A CHX unit (combustor heat exchanger duplex) burns, producing gas and transferring heat to the air. This arrangement eliminated the need for complex gas cleaning for biomass-derived producing gas. The topping GT's exhaust

air was used to power a bottoming ammonia absorption refrigeration (AAR) cycle via a heat recovery steam generator (HRSG), with steam produced by the HRSG giving heat to the refrigeration cycle's generator.

Critical operating parameters such as the topping cycle pressure ratio and turbine inlet temperature (TIT) on the plant's energy performance are investigated. Energy efficiency needs biomass consumption, and the fuel energy savings ratio is used to assess the plant's energetic performance (FESR). The FESR calculation approach was helpful in demonstrating the fuel savings of a combined power and process heat plant over separate power and process heat plants. According to the study, in the pressure ratio range of 8-10, the topping cycle achieved a maximum power efficiency of 30%. The needed air flow rate through the GT unit reduces with increasing pressure ratio up to a certain point and then increases with increasing pressure ratio. The AAR unit's refrigeration capacity drops until it reaches a particular value of topping the GT cycle pressure ratio, then increases as the pressure ratio rises. The most outstanding value of the FESR was determined to be 53 percent at a pressure ratio of 9 (when TIT was equal to 1100 ^{O}C). For more significant TIT levels, the FESR is higher. It was also discovered that the topping cycle pressure ratio has an impact on heat exchanger sizing.

2.2.8 Combined Hybrid Solar-Biomass Power System

Sahoo et al. (2017) created a groundbreaking poly producing approach that may be used in hybrid solar-biomass systems to make power, cooling, and desalination all at the same time. In a hybrid solar-biomass (HSB) system with increased energy efficiency, the poly generation process involves the simultaneous production of electricity, vapour absorption refrigeration (VAR) cooling, and a multi-effect humidification and dehumidification (MEHD) desalination system from a variety of heat sources. All of these operations are carried out in a hybrid solar-biomass (HSB) system. It is one of the possibilities for meeting energy demand from renewable sources while simultaneously helping to reduce carbon dioxide emissions.

The extracted heat from the turbine is used to power the VAR cooling system. In contrast, the desalination system uses the VAR cooling system's condenser heat to create sufficient amounts of drinkable water. Even if the heat extraction from the turbine for VAR cooling and desalination results in a reduction in power generation, the complete system can still satisfy the required energy requirements and save more primary energy (PES). A thermodynamic evaluation and optimization of the HSB system in the poly generating process for integrated power, cooling, and desalination is being done to examine the effects of the multiple operational parameters. In the HSB system, the poly production process's principal

energy savings (PES) were reduced by 50.5 percent. This method improves the quantity of energy produced by 78.12 percent compared to a standard power plant.

2.2.9 Natural Gas Micro Turbine Power Plant and Refrigeration

Other cogeneration methods, beyond solar concentration power plants, were researched and are worth considering in refrigeration systems. Yin et al. (2018) studied the experimental results and thermodynamics of a small-scale natural gas cogeneration facility for power and refrigeration. The findings of an experiment with a small-scale cogeneration plant for energy and refrigeration are presented. A natural gas microturbine and a steam-fired ammonia and water absorption chiller were installed in the facility. Different turbine loads, steam pressures, and chiller outlet temperatures were used to test the system. The first and second Laws of Thermodynamics were also used to assess the situation. The plant can provide 19 kW of saturated steam at a pressure of 5.3 bar and a temperature of 161°C at an ambient temperature of 24°C with a microturbine at full load, corresponding to 9.2 kW of refrigeration at 5°C with a COP of 0.44. It was discovered that there is an optimal chiller outlet temperature that maximizes energetic chiller efficiency from a 2nd law perspective. In order to reduce plant exergy destruction, the microturbine had the highest irreversibility, followed by the absorption chiller and the HRSG.

The research was done on the exert economic analysis and optimization of a new cogeneration system that produces both power and refrigeration (Kordlar & Mahmoudi, 2017). A unique combination of cooling and power cogeneration system powered by geothermal hot water is proposed in this study. From the standpoints of thermodynamics and economics, the design, which was a combination of an organic Rankine cycle and an absorption refrigeration cycle, was examined and optimized.

Ammonia is the working fluid of the organic Rankine cycle, and an ammonia and water solution were used in the refrigeration cycle. Before optimization, parametric studies were used to find decision parameters. Three design instances were explored to optimize system performance: designs for maximum first law efficiency (case 1), maximum second law efficiency (case 2), and minimal total product unit cost (case 3). The overall product unit cost in example 3 was roughly 20.4 percent and 24.3 percent cheaper than in cases 1 and 2, respectively. In comparison to cases 1 and 2, the reduced product unit cost in instance three was followed by a fall in first and second law efficiencies of 10.21 percent and 4.5 percent, respectively. The results also showed that the turbine, condenser, and absorber are the most

expensive components to modify in terms of capital and exergy destruction costs. The two pumps in the system are the final component in this order.

2.2.10 Solar Updraft Power Generator and Solar Thermoelectric Generators

A solar updraft power generator, or SUPG, is a facility that uses the sun's updrafts to generate renewable energy. Unlike traditional wind turbines, which rely on the natural wind blowing through the atmosphere and frequently experience intermittent airflow or even a complete loss of connection to the wind source, the SUPG generates artificial wind as a result of solar-induced convective flows. The SUPG has a naturally low overall efficiency because it converts heat energy into pressure energy.

A solar updraft power generator with radial and curved vanes was evaluated by Akbar and Curiel-Sosa (2019). Their goal was to increase the collection's overall efficiency by constructing a series of guide walls within it. They were well aware of the collector's inefficiency and its promise as a renewable energy source. Different types of guide walls were used, including radial and curved vanes. When compared to data collected without vanes, data collected with curved vanes showed a considerable increase in updraft velocity. Updraft velocity was enhanced by 18%, while mechanical power was boosted by roughly 64%. Furthermore, the configuration of the radial vanes was determined to have a more significant impact on the smoothness of the updraft velocity profile than on the overall system efficiency.

2.2.11 Solar Thermoelectric Generators

In the lab, Jurado et al. (2019) demonstrated that solar thermoelectric generators (STEGs) can achieve a sun-to-electricity efficiency of more than 10%. They also showed that STEGs could be combined with phase-change materials (PCM) for thermal storage, allowing them to function even when the sun isn't shining. In order to meet its overall objectives, the project made significant progress in a number of required activities.

A precise Thermoelectric Generator (TEG) model was built, complete with contact resistances, realistic contact materials, and radiative losses. High-performance contact materials for skitterier and thermoelectric TE segments and brazing and soldering techniques for the construction of segmented TEGs were developed for the physical manufacturing of TEGs. These advancements were made possible by the discovery of a thermoelectric TE section. Precision measurement systems for assessing device performance (rather than just TE material performance) were developed and used to characterize TEGs for this project. On the side of the optical components, a spectrally selective cermet surface with strong solar

absorption and low thermal emission was developed. The thermal stability of this surface could also be maintained at high temperatures. At high temperatures, absorbance and total hemispheric emittance were determined using a measurement technique that was also developed. This method was used to characterize the manufactured spectrally selective surfaces. A novel reflecting cavity was also set in order to reduce radiative absorber losses and achieve high receiver efficiency with low concentration ratios.

It was demonstrated using a prototype cavity that adopting this approach can significantly reduce radiative loss. Several devices were developed for the overall focusing STEG system and put to the test on a test platform built specifically for the purpose of determining their levels of effectiveness. In addition, difficulties with the integration of PCM thermal storage were conducted, and the storage time of the lab-scale system was evaluated. The most recent round of testing gave a 9.6% efficiency grade for STEGs, indicating a promising future for STEGs with high active component concentrations.

2.2.12 Solar Chimney

Large power plants typically employ solar chimneys to generate steam, which is then used to generate other energy sources. Researchers from several disciplines have conducted several studies with the goal of improving plant performance and efficiency. The solar chimney is a tall, vertical chimney that serves as a collector and is located in the centre of a large area (Khidhir & Atrooshi, 2020). There are concerns regarding the chimney's stability and economic sustainability, requiring complex engineering techniques to build a chimney of that height.

An "Inclined Solar Chimney" (ISC) was built along a mountain's slope that receives the highest solar insolation throughout the year. The building is now robust, economical, and simple to construct due to merging the chimney and collector into a single component. A mathematical model including the entire energy balance was built with the goal of determining the temperature, velocity, and kinetic power of the emerging air draught given particular values of other factors. The model also indicated the amount of solar energy converted into various forms. As a result, it anticipated the kinetic of emerging air draught's dependency on the size of the chimney and the quality of the materials utilized. Furthermore, external breezes were shown to increase the kinetic energy of the emerging air. As a result, ISC would be able to benefit from the wind power generated at the mountain's crest.

2.2.13 Solar Thermal Power Station and PowerPoint Tracking Solar Thermal System

The design and modelling of a low-temperature solar thermal power station were vital tasks completed and studied (Ahmad et al., 2018). A binary aqua–ammonia mixture transforms its state from liquid to vapour through heat recovery in a Kalina cycle, with the more volatile ammonia vaporizing first and the water following to match the temperature profile of the hot fluid. This study optimized the heat recovery from solar thermal collectors using a low temperature Kalina cycle. For power generation, hot liquid from a solar parabolic trough collector with vacuum tubes is utilized to generate ammonia-rich vapour in a boiler. The turbine inlet conditions are adjusted to meet the fluctuating hot fluid temperature with the solar radiation's intermittent nature. Intense solution concentration, temperature separator, which affected the hot fluid inlet temperature, and turbine ammonia concentration were the important parameters considered in this study. A solar parabolic collector system with vacuum tubes was built at the optimal power plant conditions. The findings can be utilised to optimise power production systems' power output and efficiency by selecting boiler, separator, and turbine conditions. According to the model, the maximum limit temperature for the separator in Indian climatic circumstances is 150°C. At 80 percent intense solution concentration and 140°C separator temperature, full specific power of 105 kW per kg/s of the working fluid can be achieved. The efficiencies of the plant and cycle were 5.25 percent and 13 percent, respectively. However, at 150°C separator temperature, maximum efficiencies of 6% and 15% were recorded for the plant and Kalina cycle, respectively.

Solar heating system maximum power point tracking control was conducted and analysed (Omairi et al., 2017). The study developed an ultimate power point tracking control (MPPT) technique to reduce the energy required for pumping at optimal heat collection. Experimentally discovered the net solar energy gain Qnet = (Qs Wp/e) cost function for MPPT with the maximum point. The feedback tracking control system was created to track the best Qnet configuration (denoted Qmax). The instantaneous tracking target Qmax was determined using a tracking filter generated from the solar heating system's thermal analytical model (t). A step response test was utilised to derive the system transfer function model of a solar heating system, which was then employed to design a tracking feedback control system. The PI controller was created for a quadratic time function tracking target Qmax(t).

A microprocessor-based controller was used to create the MPPT control system, and the test results demonstrated good tracking performance with minimal tracking errors of less than 5%. The average mass flow rate for the specific test periods on five different days was between 18.1 and 22.9 kg/min, with average pumping power of between 77 and 140 W, which

is significantly lower than the standard flow rate of 31 kg/min and pumping capacity of 450 W, which is based on the flow rate 0.02 kg/sm^2 defined in the ANSI/ASHRAE 93-1986 Standard and the total collector area of 25.9 m^2. The average net solar heat collected Qnet is between 8.62 and 14.1 kW, depending on the weather. The MPPT control of a solar heating system has been proven to reduce pumping energy consumption while maximizing solar heat collection.

2.2.14 Solar Power Generation Cost Benefits Analysis

Using traditional carbon-based fuel as a benchmark, the cost and advantages, both financial and environmental, of two prominent sources of solar power generation, grid-tied photovoltaic cells and Dish Stirling Systems, were analysed (Guerra et al., 2020). First, they established how and why these solar technologies would be implemented. Then they created a model city with its own set of characteristics to evaluate the two solar-powered electric distribution technologies.

The restricting assumptions for each technology were then established, which served as parameters for the system computations. Finally, they estimated the present value of the total cost of conventional energy required to power the model city and used this as a baseline when evaluating the benefits and costs of solar models. Grid-tied photovoltaic cells under net-metering, the most common method of distributed electricity generation, allow individual houses to achieve some level of electric self-sufficiency while still making a profit. Substantial subsidies, however, were required to complete the investment viably.

Large dish Stirling engine installations, on the other hand, had demonstrated a substantially greater potential rate of return, but they had a number of practical restrictions. The report stated that both technologies were suitable investments for customers, but considering that the dish Stirling consumer obtains 6.37 dollars per watt vs 0.9 to 1.70 dollars per watt for a house photovoltaic system, the former appeared to be the better option. The research concluded that attracting a few strong investors to build a solar farm of this scale was considerably more possible than convincing 150,000 households to install photovoltaic arrays on their roofs despite the high cost. The development of a solar farm could have environmental consequences, given the amount of land required for this undertaking. However, there are certain advantages, such as a significant reduction in CO_2 emissions.

Emerging construction technologies that concentrate on the research and development of energy-efficient equipment have the potential to help solve a wide range of environmental and natural resource-related issues. Fossil fuels, greenhouse gases, and nonrenewable energy

sources are examples of these issues (Fatima et al., 2022). Alternative energy sources such as solar, wind, geothermal, and biogas have the potential to become a more economically viable option than the electrical current sources, leading residential developers to take notice (Hou et al., 2018). Because it is one of the most sustainable and environmentally friendly sources of electricity, photovoltaic technology has attracted a broad spectrum of clients interested in various federal incentive programs and financial returns. Alternative energy technologies are gaining popularity among homeowners because, when compared to more traditional energy sources, they have the potential to save them money (Mughal et al., 2018).

Solar energy has a number of advantages as an alternative energy source, including the ability to meet a large portion of a system's electrical demand, lower operational costs, reduce the amount of electricity generated using fossil fuels, and lower energy costs (Mohamad et al., 2018). costs associated with energy consumption as fossil fuels have risen, global climate change concerns have grown, and a more comprehensive range of alternative power production methods has been introduced.

PVs, or photovoltaic cells, are one of the many technologies that could help ameliorate these climate-related challenges (Benohr & Gebremedhin, 2021). PVs are capable of absorbing solar radiation and directly converting it to electricity. The practice of putting power-generating cells near the end consumer or any power-generating station is known as distributed generation. These cells could be found anywhere. The economic returns created by a photovoltaic (PV) investment can vary from market segment to market segment, depending on the consumer's needs.

2.3 Solar Energy Photovoltaic Systems

In tropical and subtropical locations, photovoltaic solar energy has become a popular source of electricity, facilitating new business and improving economic growth in rural and pre-urban areas where grid power is unavailable (Catalbas et al., 2021).

According to Sulich and Sooducho-Pelc (2021), fossil-generated electricity dominates global electricity generation, followed by renewable and nuclear energy. However, according to Abulut and Sardemir (2021), fossil fuels are a finite energy source that emits greenhouse gases, which negatively influence the ecosystem. Nuclear energy is a greener energy source, but it faces numerous obstacles in deployment, safety, and waste management (Bersano et al., 2020). Day et al. (2018) looked at the safety, health, and environmental consequences of solar energy technologies on the long-term viability of human activities and concluded that renewable technologies based on renewable energy sources have become more appealing and

accessible in more places. Researchers have examined and proved that solar energy systems have become more competitive with inefficiency and investment cost, making them more usable (Luderer et al., 2022). Pang et al. (2020) back this up after reviewing solar electric and solar thermal systems. They compared solar electric and thermal-mechanical systems to thermal absorption systems regarding energy efficiency and economic feasibility and found that solar electric and thermal-mechanical systems are more expensive.

Thermally driven small-scale refrigeration systems such as absorption and Rankine vapour compression refrigeration systems have proven good feasibility in urban areas as the cost of solar energy components such as photovoltaic panels has decreased (Chakravarty et al., 2022).

Photovoltaic is defined as a process in which solar radiation is transformed into electricity without stimulating devices, and a photovoltaic system is defined as any system that employs these phenomena (Hassan et al., 2017). It is the most practical strategy for utilizing modern energy sources. Various systems with varying capacities (0.5 watts to several megawatts) have been installed and run around the world, and their application is growing every day due to their reliability and performance. Photovoltaic is a solid-state electrical device that uses the photoelectric effect to convert sunlight into electric current. Mono-crystalline silicon, polycrystalline silicon, amorphous silicon, cadmium telluride, and copper indium selenite/sulphides are currently utilised in photovoltaic solar cells (Thirunavukkarasu et al., 2021).

Solar applications face difficulties compared to typical energy sources, mainly due to power supply fluctuations. According to Krauter (2018), specific applications, such as ordinary refrigerators, must be adapted to work with solar energy in order for photovoltaic systems to be successful. More recent research by Sidney et al. (2021) found that adapted vapour compression refrigeration systems powered by a DC compressor were more efficient than AC compressors.

Because solar systems are expensive and inefficient, there has been a lot of research on enhancing their performance and efficiency. The efficiency of photovoltaic systems has been proven to be proportional to temperature and sun irradiation (Rangel-Heras et al., 2022). The employment of fuzzy-based sun monitoring and maximum power point tracking at the same time has been found to boost power-delivery by 24.5 percent, resulting in a reduction in solar panel size, weight, and cost in photovoltaic systems (Shenoy et al., 2021).

2.3.1 Photovoltaic Technology

Photovoltaic technology generates power by utilizing the electrical characteristics of semiconductor materials (Rajoria et al., 2018). When a semiconductor material is exposed to sunlight, it generates an electrical charge that may be passed through a circuit to anything that uses electricity. These semiconductors are made in the form of cells in a PV system, which are then integrated with a structural panel. Depending on the amount of energy required, panels can be combined into larger groups or arrays to create increasing electricity amounts. Solar arrays come in a variety of sizes to meet the needs of a home, office, or more extensive facility.

Yang et al. (2020) demonstrated that solar energy is very inexpensive compared to other energy sources, is always available, and can be obtained in large amounts in many places. Because of its dependability, cost-effectiveness, and reachability, renewable energy, specifically photovoltaic solar energy systems, is critical for rural livelihood development. A photovoltaic solar system provides an alternate source of electricity for people who cannot acquire it from the national grid due to the distance and costs involved. It is challenging to promote health, education, or poverty reduction without access to affordable energy. Brunet et al. (2018) suggested that photovoltaic solar energy (solar electricity) is cost-effective and efficient energy that has revolutionized socio-economic lives in African villages, cities, and countries. Giving poor people access to modern energy services changed their lives and helped them break the cycle of poverty.

As described, the relevance of solar energy in rural families and community development is undeniable (Shahsavari & Akbari, 2018). It is a cost-effective and economical source of energy for rural dwellers. It is a source of energy that many individuals in the community may access regardless of their economic condition. When compared to alternative sources of energy, Shahsavari and Akbari (2018) discovered that photovoltaic solar systems are significant to rural households since their electricity is cost-effective and environmentally benign. It saves money because, depending on how much electricity the household consumes, the recovery/payback period for this expenditure can be brief; once the initial investment has been recovered, solar energy is effectively free.

Photovoltaic solar energy can work as a catalyst for various activities, creating a space where education and health can be improved, assisting in poverty eradication efforts. According to studies, solar energy has been shown to be significant in bringing development to marginalized communities, mainly rural areas. It enables the use of electric illumination for evening study, electrical gadgets such as TVs, radios, cellular phone charging, and, most importantly, income-generating activities (Allen et al.,2019). Suppose the rural community's

livelihood is to be improved. Therefore, it is not only essential but also required to look at various alternative energy sources, such as renewable energy, particularly solar energy, rather than maintaining track of sources that appear to have endless obstacles.

Okaka and Odhiambo (2018) examined the importance of solar energy by reviewing the risks and dangers caused by fuel combustion, which adds to the already high levels of greenhouse gases that contribute to global warming. Photovoltaic and solar concentrator energy as a solution, with a bright future due to its ability to power the entire world. However, he stated that even engineers find harnessing this free energy at high efficiency a problematic task. In addition, according to Bohra and AnvariMoghaddam (2022), critical atmospheric energy sources such as solar and wind power should be harnessed more effectively and converted directly into electricity and heat energy to meet the growing demand for cheaper power supplies and the challenges posed by the unprecedented increase in population and industrial products, as well as the development of technology. Humans seek ways to use more and more energy while avoiding damaging or even destroying the natural environment.

2.3.2 Photovoltaic Systems Power Output Maximization

Money and space can be saved by maximizing the output power of solar panels utilizing a combination of sun-tracking and maximum power point tracking done by fuzzy controllers. This is an essential factor to consider (Bhukya & Nandiraju, 2020). When working with low energy conversion efficiency applications, increasing output power increases efficiency. The characteristics of the surrounding environment and the load profile have a significant impact on the solar panel's maximum output power.

This research aimed to develop a strategy for maximizing the amount of energy generated by a solar panel in a photovoltaic system. The names of the two fuzzy controllers employed simultaneously were fuzzy-based sun tracking and maximum power point tracking. Two DC motors with the appropriate design were used to change the horizontal and vertical alignment of the solar panels in order to perform sun tracking. An AC-to-DC converter was used to track the peak power point of the solar panels. In addition, the presented system was capable of obtaining I-V curves from solar panel data, which indicate current and voltage. Experiments demonstrated that the proposed fuzzy techniques enhanced the amount of electricity delivered by the solar panel, leading to smaller, lighter, and less expensive photovoltaic solar panels.

2.3.3 Performance of Solar Photovoltaic Modules Models

The power output of a solar photovoltaic module was investigated using several models. One of the research goals was to build an adequate model for predicting the performance of solar photovoltaic modules (Al-Waeli et al., 2020). Adjustments to the layouts of solar photovoltaic systems were performed using the model in order to provide a sustainable electricity supply. This research looked at various models, including efficiency, power, fill factor, and current-voltage characteristic curve models.

When the weather was gloomy, the models anticipated a yield of just 40% of the rated power, but they predicted a yield of up to 80% when the sky was bright. When low irradiance was taken into account, the models performed brilliantly, preserving electricity on cloudy days. The design of the better model, which included both analytical and numerical methods, resulted in an inaccuracy of +/- 2% compared to the rated power output of a solar photovoltaic module. The proposed model is more adequate in terms of the number of variables used and acceptable performance in humid environments.

2.3.4 PV Modules Power Prediction

Predicting the cost evolution based on cumulative installed capacity is the first step in growing the use of photovoltaics for electricity generation (Pahle et al., 2022). This learning curve was first published and used to create PV module predictions, followed by predictions for system cost reduction. Forecasts based on the time axis are more subject to the impact of political actions and altering market conditions than this technique. Cost reductions due to innovation, scaling effects, enhanced project management, standardized procedures, including the hunt for better sites, and project size optimization were only possible during the first construction of a project. As a result, it was suggested that a comparison be established between CAPEX and cumulative installed capacity in order to demonstrate the technology's future advancement potential to the market and political system. Despite this, it was unable to derive a learning curve from the extensive literature on the cost of CSP that it had read. It was critical to design a coherent cost structure for direct and indirect capital expenditures to conduct future evaluations.

Reference costs were generated using typical power plant layouts and then forecast future prices. The Levelized Cost of energy for solar thermal power plants should only be computed for specific projects with varied capacity factors at different locations, taking into account the cost structure and learning curve.

A unique approach for assessing solar irradiance has been created by modelling solar irradiance and solar PV power generation to develop a resource evaluation using linear multiple multivariate regression. This method was created by Kumar et al. (2020). A solar photovoltaic resource dataset was created using satellite data. These data were combined with variables from numerical weather forecast assimilation models. Furthermore, ground-to-base measurements with excellent resolution were reported. Around 152,000 geographical areas, each dataset has about 26,000 hourly time increments. The outputs of solar irradiance were diffuse horizontal irradiance (DHI), global horizontal irradiance (GHI), and direct normal irradiance (DNI). The method was developed primarily in the United States of America, with ten different locations used to train a linear multiple multivariate regression scheme. The procedure was then used to examine data from various places across the entire geographic domain. In order to calculate solar PV power within the range of estimations for a 13-kilometre-diameter grid cell, the predicted irradiance was entered into the solar PV power modelling technique. The dataset was examined, and the results were used to calculate prediction capacity factors for solar resources across the United States from 2006 to 2008. Statistics were provided to demonstrate the system's efficacy in geographic regions that were not included in the training set.

2.3.5 Photovoltaic Power Management Algorithms

Other methods for analyzing the effects of power tracking algorithms on the longevity of power electronic devices used in solar systems have been developed and implemented (Abdulrazzaq & Ali, 2018). In photovoltaic solar energy systems, power management algorithms (PMAs), also known as maximum power point tracking (MPPT) algorithms, are frequently used to gather the maximum amount of available power at any given time. However, this may restrict the number of solar energy installations available.

This is the fundamental reason for thermal stresses and disturbances imposed on the accompanying power electronic converters (PECs). The study looked into how PMA influences solar system DC-DC converter lifespan consumption, thermal stressors, and the number of breakdowns. Initially, theoretical analysis and model of photovoltaic solar systems were built, which included the electrothermal characteristics of converters. Then, utilizing two different PMAs, perturb and observe (P&O), and incremental conductance, research was conducted on photovoltaic solar systems. The research was carried out using these two PMAs (IC). Data was captured in real-time using a thermal imaging camera and d SPACE in a range of working scenarios. The thermal characteristics of the system are included in this data. Thermal cycling of converters was around 3 degrees Celsius hotter than IC techniques. The IC

reached 52.7 degrees Celsius at steady-state, whereas the P&O reached 42.6 degrees Celsius. Even though the IC technique provided a more precise power management tool, it caused more severe thermal stresses, resulting in 1.4 times the life consumption of the perturb and observe methods, according to the study's findings (P&O).

2.3.6 Photovoltaic (PV) Array

PV solar energy has the potential to be a viable alternative to fossil fuel-based generators (Hereher & El Kenawy, 2020). After examining the components and operating conditions of the refrigeration system that chills 150 litres of milk per day, this conclusion was reached. The system consisted of twenty photovoltaic modules rated at 120 watts peak each, two direct current motors rated at 650 watts and 24 volts, and two permanent magnets. It is critical to have simple solar-powered systems that give an adequate performance at a low cost in order to make more efficient use of PV solar energy generated by decentralised photovoltaic generators. Users will be able to build their economic activity without relying on third-party technologies as a result of this. Solar photovoltaic cooling research and development have mainly focused on developing chilling milk systems.

A solar photovoltaic (PV) panel, according to Khatibi et al. (2019), is made up of PV cells that individually contain a semiconducting substance and are encased in glass. These cells are then connected to a load. When sunlight shines on a semiconductor, the electrons within it are excited. Following that, the electrons are gathered into an external circuit, resulting in electricity generation. An inherent internal field within the semiconductor performs this action. An array is made up of interconnected modules, whereas a photovoltaic module is made up of several corresponding PV cells. A collection, a charge controller, a DC-to-AC converter, and a battery are components of a PV solar system.

The photovoltaic effect allows solar cells to receive photons and release electrons by including light-absorbing materials in their construction. The fundamental components and efficiency of various solar cells were examined and analysed by Mehdizadeh et al. (2018). Amorphous silicon is less efficient than crystalline silicon, and multi-crystalline silicon solar cells have efficiencies ranging from 14 to 19 percent. Other forms of solar cells are also included, as Battersby (2019) has already discovered.

2.3.7 Influence of Temperatures on PV Cells

The power output from a PV cell is essential as it determines the cell and the module power conversion efficiency. Huaulmé et al. (2020) stated that the loss of power output from a

PV cell declines with the increase of cell temperature and is expressed as output $P_o = P_r(T_A - T_{STC}) \times T_C$ Where; P_o is PV cell power output P_r rated power output, T_A ambient and Standard Test Temperatures, respectively, and T_C is the Temperature Coefficient. The influence of cell output temperature was also shown to vary with cell temperature by Tress et al. (2019).

2.3.8 Evaluation of Solar Photovoltaic Panel Driven Refrigeration System

Ratlamwala and Abid (2018) investigated the performance of a solar photovoltaic panel-powered refrigeration system. Solar photovoltaic (PV) panels are used in the refrigeration system, and they play an essential role when paired with storage batteries. The performance of a solar PV panel-driven refrigeration system was examined experimentally.

The variation in battery voltage was investigated in relation to panel size. To produce 24 V, different series and parallel combinations were applied to four 35 W solar PV panels. Depending on the solar intensity, a current of 3-5 amperes was achieved using the above mixture. The experiment employed a refrigerator with a capacity of 50 litres and power consumption of 0.80 amperes AC at 230 V. An inverter that draws around 7 amperes DC from the battery bank at 24 V provided the requisite current and voltage. The refrigerator's compressor used 110 watts, which meant a 176-watt PV panel was needed. It's worth noting that the compressor used approximately 300 W for the first 50 milliseconds, 130 W for the next five seconds, and finally 110 W in 65 seconds. As a result, the panel size should be large enough to compensate for the early load requirements.

2.4 Solar Refrigeration and Cooling of Perishable Products

The Photovoltaics for Sustainable Milk for Africa via Refrigeration Technology (PV-SMART) project, funded by USAID, is a unique and imaginative proposal to provide solar milk refrigeration on-farm to Kenyan dairy farmers. PV-SMART stands for "Photovoltaics for Sustainable Milk for Africa through Refrigeration Technology" (Sempiira, 2019). It combines a modified off-the-shelf direct-drive photovoltaic refrigerator (PVR) with unique chilling and energy storage technology to cool milk on the farm at night and transport it to dairy collecting facilities the next day. The battery-free PVR device is optimized for use in areas where there are at least four average peak sun hours per day. Farmers might earn a premium if they supply dairy processors with chilled evening milk of superior quality that would otherwise deteriorate.

The solar radiation heat gain that comes via the window and the impact of room surfaces and furnishings on how efficiently they absorb and transmit radiant heat define the Solar Cooling Load (SCL) variables (Verso et al., 2019).

Refrigeration is necessary for the preservation of perishable foods such as milk (Vrat et al., 2018). In many regions of the world, rural areas produce vast amounts of food; nevertheless, these areas often lack preservation technology, such as freezers, resulting in significant food waste. Because there is a rough correlation between energy availability and cooling demand, solar refrigeration appears to be a viable option in most areas without access to electricity. Photovoltaic cells power compression refrigerators, but solar heat powers absorption refrigerators. Both types of solar refrigerators have their own set of benefits and drawbacks. This study investigates solid adsorbents and desiccants in thermal solar refrigeration systems.

Commercial milk cooling systems are divided into extensive systems with a cooling capacity of over 20,000 litres, medium systems with a cooling capacity of 10,000 to 20,000 litres, and small systems with less than 2,000 litres. Large and medium-sized commercial milk cooling systems have a high-power usage of more than 20kW. Most renewable energy sources, such as solar, are excellent for small milk cooling systems (Edwin et al., 2022).

Sidney et al. (2022) planned, produced, and studied the operating conditions of a stand-alone solar refrigeration plant using ice for thermal storage for 150 litres of milk. To generate the requisite ice for milk cooling, the refrigeration system components were of high capacity, and the system required two refrigeration cooling circuits.

The milk temperature is around 37 degrees Celsius when it is finished being milked, and it will spoil if it is not chilled to at least 20 degrees Celsius within three to six hours (Gautam & Curtis, 2021). It is possible to reduce the amount of milk that spoils by storing it at cooler temperatures and adhering to proper hygiene standards (Zavala-Nacul & Revoredo-Giha, 2022). As a result, milk should be kept at a low temperature to prevent bacteria from growing and keep bacteria levels within permissible limits set by national standards. For example, the Kenyan standard KS EAS 67:2007, as well as other national standards, establishes quality requirements for raw cow milk1. The process of cooling milk allows for extended storage times while also protecting the quality of the milk during transit. Milk is usually kept at 4 degrees Celsius for 48 hours (Meesilp & Mesil, 2019). However, in rural regions, because of the high energy cost provided by conventional electric grids and standalone diesel generators, this cooling method is usually restricted or not employed. These variables present an opportunity to adopt renewable energy-based sustainable energy practices. Because

photovoltaic systems are now available in rural areas of many African countries, this technology has become a viable choice for energy generation. After milking, quickly reducing the temperature of the milk prevents microbial multiplication and inhibits any chemical or enzymatic reactions that could compromise the milk's quality (Odeyemi et al., 2020).

The solar milk cooling gadget freezes milk using solar energy (Sidney et al., 2022). The ice is placed in an insulated milk container's ice compartment, where sublimation is used to cool the milk. The farm's output and profitability have increased as a result of this system's ability to maintain cooler temperatures throughout transit and overnight storage. This type of chilling equipment has the potential to improve milk quality and provide value throughout the milk supply chain.

Solar panels are connected to a control panel and batteries for the freezer with an ice maker in the ice-based solar-powered cooler. The system also includes a solar-powered ice maker (Abdelwanees, 2018). Small-scale farmers who struggle to keep their milk fresh and are not connected to their country's national electrical grid would greatly benefit from a solar-powered cooler. Solar-powered ice is made in a separate container within the solar-powered cooler's highly insulated churns. The solar-powered chiller is used to store the ice. Milk can be chilled for up to 12 hours without risk of bacterial growth as a result of this. The system's ability to function in regions with limited solar radiation and high ambient temperature is due to the efficient storage of ice blocks utilised to keep the milk cooler.

2.4.1 Solar-driven refrigeration system

Solar-powered refrigeration systems get their energy from the Sun either directly as heat or indirectly through photovoltaic panels or clear photovoltaic glass (Memon et al., 2020). Solar panels that employ basic photovoltaic technology are presently the most cost-effective way to generate electricity. Photovoltaic glass, on the other hand, allows for the generation of power from previously unusable surfaces such as building windows (Cannavale et al., 2020). Many lenses or reflectors are used in concentrated solar power to collect a considerable amount of the Sun's thermal energy. Only the solar panel turns solar energy into direct current (DC) power. The direct current electricity leaves the solar panel and is transformed into alternating current by an inverter (Kim & Parkhideh, 2018). The inverter drives the compressor motor, converting the direct current (DC) power to alternating current (AC). A range of auxiliary components, such as a charge controller and a backup battery, are commonly used when building a solar-powered system (Lee & Callaway, 2018).

Ghodbane and Husse'n (2021) stated that a solar-powered refrigerator runs on solar energy instead of traditional electricity. Solar-powered refrigerators in hotter climes may be able to keep perishable commodities like meat and dairy cool. These coolers are also used to keep vaccines at the right temperature to prevent them from deteriorating (Owusu-Kwarteng et al., 2020). Solar-powered freezers are projected to become popular in less developed parts of the world to combat poverty and climate change. Vaccines can be safely stored in plug-in coolers with backup generators in wealthy countries; however, other chilled alternatives are required in developing countries with unreliable energy sources (Biswas et al., 2019). Solar freezers have been distributed throughout the developing world in an effort to lessen reliance on the two most frequent alternatives, kerosene or gas-powered absorption refrigerated coolers.

The solar-powered refrigeration system at Johnson Space Center comprises the photovoltaic panel, vapour compressor, thermal storage and reservoir, and electronic controls (Diaby et al., 2021). For the refrigeration system to work, the solar panel's capacity to convert sunlight into direct current (DC) electricity is critical (Alsayah et al., 2019). The compressor is powered by direct current electricity, which circulates the refrigerant through a vapour-compression refrigeration loop to remove heat from an insulated enclosure. The phase change material and the heat reservoir are contained in this container. This substance will begin to freeze as the heat from the container is removed. The creation of an "ice pack" as a result of this method permits the cage's temperature to remain constant despite the lack of sunshine.

The refrigerator can maintain its cool temperature all year thanks to a well-designed, well-insulated cabinet, phase change thermal storage, variable speed compressor, and solar photovoltaic panel (Abdolmaleki & Berardi, 2022). Compressor control that maximizes available energy helps to increase the efficiency with which solar electricity may be converted into stored thermal energy. Two further power-saving measures are providing extra current at the start of the compressor's startup cycle and smoothing the power voltage with a capacitor. A controller monitors the rate of change of the smoothed power voltage to determine whether the compressor is operating at a power level above or below the maximum available power level. This allows you to change the compressor's speed if necessary. The compressor's operation has been tweaked so that it now aids in the conversion of the vast majority of available solar energy into thermal energy that can be stored. A cold-side water loop or the inclusion of an evaporator within the thermal storage could be beneficial uses. Electronic controllers can also be installed to supply backup power from another source, such as the electric grid.

2.4.2 Solar Small-scale Ice Maker Plants

Solar photovoltaic (PV) systems provide a significant opportunity for ice production for cooling and refrigeration applications. Xiang et al. (2022) showed that ice might be made and used in agricultural settings without electricity, which is critical for the processing and preservation of food, pharmaceuticals, and vaccines.

Several studies on solar-powered ice production refrigeration systems have been done to improve performance, lower costs, and minimize the environmental effect. Specifically, solar ice manufacturing systems use batteries, charge controllers, and PV systems (Li et al., 2020). According to their findings, there is an urgent need to phase out the use of batteries due to their short life cycles, which make disposal difficult after their useful lives (Omariba et al., 2018).

Kasera et al. (2022) devised and tested a solar ice maker that does not require batteries. The refrigerated compressors in the system were controlled by a proprietary controller based on an innovative design that allowed for easy startup, maximum power tracking, and power management. As a result, the mission was completed successfully. They came to the conclusion that using ice to store thermal energy is acceptable not just because of ice's ability to provide power quickly but also because of ice's ability to retain a substantial amount of latent thermal energy. Because milk chilling procedures must be finished promptly in order to limit the number of germs present in milk and, as a result, retain the required quality of milk, ice thermal storage systems have been used in milk cooling (Ahrens et al., 2021).

The performance of a small on-farm milk chilling system was investigated for PV applications in order to develop a simplified model for use in solar simulations (Torres-Toledo et al., 2018). The formation of ice and the cooling of milk in traditional milk cans are done with DC refrigerators, which are the backbone of the milk cooling system. The cooling system created ice blocks, which were then placed in a 20-litre milk can containing 17 litres of milk and 3 kilograms of ice to speed up the cooling process. This was done to speed up the chilling of the milk. According to the findings, the ambient temperature significantly impacted the refrigeration system's performance. At 20°C, 30°C, and 40°C ambient temperatures, the system's specific total energy consumption per litre of milk was 30 Wh/L. This value ranged from 43 to 58 Wh/L. The findings also provide a mechanism for predicting the energy required by a chilling milk system operating at a specific ambient temperature. This further optimization of solar system sizing in particular regions, ultimately providing business models with economic data inputs.

Using ice as a thermal storage medium for solar photovoltaic systems' thermal energy could greatly reduce the gap between peak and valley power demand in power generation systems (Pokhrel et al., 2020). In addition to changing loads, ice thermal storage systems move their customers' power usage from peak to off-peak hours, lowering their energy bills (Hamzeh & Miansari, 2020). According to Sanaye and Khakpaay (2020), ice thermal storage systems can reduce power plant equipment capacity by shifting peak power demand and lowering energy costs through conventional refrigeration systems.

Li et al. (2019) compared the following thermal load and following electrical load methods to compare operation strategies for integrated cooling, heating, and power systems with thermal cooling storage. Thermal and electrical load following procedures were compared in this study. The article concludes that systems that use either of the two techniques produce environmental and energy savings. As a result, the most considerable percentage savings were achieved, including a 46.5 percent reduction in operational costs, a 37.4 percent reduction in carbon dioxide emissions, and an 18.5 percent reduction in primary energy usage. This shows that peak load in commercial operations has been steadily increasing, resulting in a significant difference between peak and valley loads over time. This increase could be due to the fact that peak load has risen over time.

According to several experts, including (Rüdisüli et al., 2019), an increase in the difference between the peak and the valley could lead to additional power plants, resulting in an increase in fossil fuel use. This would have an impact on the global effort to protect the environment. Milk must be quickly cooled to avoid the formation of microorganisms and, as a result, to maintain its quality (Odeyemi et al., 2020). The effectiveness and cost of rapid milk cooling in a PV system might be achieved by completing the method in two steps using chilled water circulation and evaporator chilling to the required temperature, as illustrated by. This would speed up the chilling of the milk while also saving money (Owusu-Kwarteng et al., 2020).

2.4.3 Solar Powered Supercapacitor

Combining energy storage and conversion of a solar-powered supercapacitor, coupled solar-powered supercapacitor with a plasmonic quantum dot solar cell (QDSC) sources as the photocurrent for charging and discharging a conjoined supercapacitor based on multiwalled carbon nanotubes (MWCNTs) was demonstrated by Kelly (2018). Gold Au fibres were integrated into a titanium dioxide/cadmium sulfide (TiO_2/CdS) electrode to yield a TiO_2/CdS/Au photoanode. The plasmonic effect of Au fibres was reflected in the higher

incident photon to current conversion efficiency (IPCE = 55%) and an improved overall power conversion efficiency (3.45%) produced by the TiO_2, CdS and Au photoanode relative to the non-plasmonic TiO_2 and CdS photoanode. A Janus type bi-functional electrode composed of MWCNTs on either face separated by the glass was prepared. It is coupled with the TiO_2, CdS, Au electrode, and another MWCNT electrode to yield the tandem solar-powered supercapacitor. By channeling the photocurrent produced by the QDSC part under 0.1 sun illumination, the capacitance of the symmetric supercapacitor, without an external bias, was 150 F g−1 which compares well with that of an external bias. Their innovative design for a photo supercapacitor offered a new paradigm for combining low-cost photovoltaics with energy storage to yield a technologically sound device that needs nothing else but solar energy to run.

2.4.4 Solar Refrigeration Systems Models

Various researchers have developed a number of models based on ice thermal storage systems for use in building air conditioning in order to optimise cost and life cycle. These models include: Raccanello et al. (2019) developed a theoretical model that can be used to run dynamic simulations of encapsulated ice storage. Micena et al. (2020) offered a thorough overview of ice storage as well as a road map for conducting economic analyses. Hinkelman et al. (2022) built an ice storage system model that used a more impressive tower, a pump, and a fan to simulate their operation.

There have been models produced for the many components of solar refrigeration systems; however, because many companies manufacture these components, it has been challenging to find a solution to the model for the numerous components currently available. According to Garcia-Torres et al. (2021), a poorly sized solar refrigeration system causes the system's functioning to be terminated, resulting in low overall reliability and efficiency.

The size of photovoltaic refrigeration systems, including PV panels, batteries, charge controllers, and height, has been predicted using general algorithm (GA) models. On the other hand, the models can only compute the size by repeatedly applying GA-based algorithms to every possible combination of systems and components in the manufacturer's component database. (Burhan et al., 2018). The PV cell and battery dimensions were incorporated into the Particle Swarm Optimization (PSO) model (Dai et al., 2019). The model outperformed the GA models, but its technical performance indicators were faulty, and due to the necessary revisions, it took a long time to provide meaningful results.

The performance of a compact milk cooler with ice storage that used DC compressors and adapters was studied by researchers (Antônio et al., 2018). Computer models were built as a result of the research to anticipate heat transmission inside the refrigerator in proportion to the volume of milk that needed to be chilled and the amount of ice that formed. In order to solve nonlinear heat transfer equations, the model used finite differences. This allowed the machine to calculate the ice temperature required for ice manufacturing. The model produced correct results when it came to calculating transient energy usage over a wide range of temperatures. However, there was little discussion on the system's modelling in terms of the volume of milk that could be refrigerated by it based on the solar insolation of a given location.

Similarly, there has been a scarcity of information about models that can anticipate the available cooling load for a convectional AC refrigeration system with adapters for milk chilling based on the quantity of solar insolation available in a given geographic location. This is critical since solar insolation received at a given site varies. So, the amount of solar insolation is likely to alter the size of the system.

2.4.5 Ejector Refrigeration Systems

According to Sleiti et al. (2020), an ejector refrigeration system is a variation of the traditional vapour compression cycle (VCC). Ejectors are used in refrigeration systems instead of compressors to pressurise the refrigerant vapour generated from the evaporator and transfer it to the condenser. While being heated in the generator, the working fluid is subjected to high pressure and temperature. A high-pressure refrigerant vapour fills the nozzle. The working fluid is then accelerated to a high velocity, where it entrains motive steam from the evaporator, cooling the system. The mixed vapour steams directed to the condenser after being emitted from the nozzle. They are cooled and turned into liquids there.

A portion of the liquid refrigerant is recirculated back to the evaporator via an expansion valve, while the remainder is pumped to the generator. Ejector cooling technology can provide air conditioning in large buildings and trains (Mao et al., 2021). On the other hand, ejector refrigeration systems always have a lower coefficient of performance (COP) than vapour compression systems. Nonetheless, when waste heat, solar energy, or exhaust heat is used to heat the generator of an ejector system, it might be more practical and cost-effective. COP stands for coefficient of performance (Hafner & Ciconkov, 2021).

2.4.6 Solar Bi-Ejector Refrigeration System

The researchers developed and evaluated a mathematical simulation of a solar bi-ejector refrigeration system (Tan et al., 2018). A bi-ejector refrigeration system was presented in the study. The dual ejector refrigeration system lowered electricity consumption by replacing the mechanical pump with a vapour liquid ejector. It was a hugely important aspect of the ejector refrigeration system, which has a lot of applications based on solar energy and low-grade heat source regeneration or reutilization. The vapour and liquid ejector entrainment ratio were investigated using a performance model. The results revealed that the vapour and liquid ejectors operated similarly to the gas ejector.

The vapour and liquid ejector continued to work at high efficiency when the discharge pressure was equal to the motive pressure. The effects of increasing the producing temperature on the gaseous, vapour, and liquid ejectors would have been different. The system COP grew as the generating temperature increased from 80°C to 95°C, but when the generated temperature exceeded 95°C, the COP declined. This was due to the vapour liquid consuming more motive vapour as the generating temperature increased. Based on the mathematical simulation model, the COP of such a bi ejector refrigeration system was anticipated to reach 0.35. The producing, condensing, and evaporating temperatures were 90°C, 32°C, and 80°C, respectively, with R123 as the refrigerant.

2.4.7 Ejector Refrigeration Cycle with Solar Collectors

Khan et al. (2018) compared the arrangement of solar collectors for an ejector type refrigeration cycle. To examine the performance of three types of solar collectors, flat plate, evacuated tube, and compound parabolic solar collectors were used. The performances included the behaviour of heat absorbed by the collectors, heat loss from the collectors, and working fluid outlet temperature at various solar collector slopes. To forecast the performance of solar collectors, a new reliable heat transfer analysis approach was used.

The analysis was based on various assumptions, such that the sky in Bandung is clear and dry from 0800 to 1700 hours and that thermal resistance at the cover and absorber plate is minimal. The numerical calculations show that the evacuated tube's solar collector performed better than the others under identical operational conditions. The most incredible heat that could be absorbed by an evacuated-tubes solar collector system with an aperture area of 3.5 m^2 with the highest sun intensity of 970 W/m^2 at 12.00 with the solar collector horizontal was 3.992 kW. The most extraordinary water temperature at the exit is 347.15 K, with a mass flow rate of 0.02 kg/s and an inlet temperature of 298 K.

2.4.8 Ejector Refrigeration Cycle

Exergy studies and parametric adjustments were carried out for various cogeneration power units in the cement sector (Sani et al., 2020). The proposed construction of an entirely new power and refrigeration cycle was based on combining the Rankine cycle and the ejector refrigeration cycle. This integrated cycle allowed for the production of energy and refrigeration simultaneously. It can also run on flue gas from a gas turbine or engine and solar, geothermal, and industrial waste heat.

An exergy study was performed in order to guide the thermodynamic increase of this cycle. After that, parametric research was conducted to see how the most critical thermodynamic parameters affected the combined cycle's performance. Furthermore, the settings were optimized using a genetic algorithm to attain the highest possible exergy efficiency. According to the data, irreversibility produced the most exergy loss in the heat addition activities, while the ejector generated the second-most exergy loss. Furthermore, the pressure at the turbine's inlet, the pressure at the turbine's outlet, the temperature of the condenser, and the temperature of the evaporator all have a major impact on the turbine's power production, refrigeration output, and combined cycle exergy efficiency. The optimal exergy efficiency was calculated to be 27.10 percent under the given circumstances.

2.4.9 Solar Combined Ejector-Vapor Compression Cycle

On the basis of the performance study, a model of a solar combined ejector-vapour compression refrigeration system was investigated (Ouelhazi et al., 2020). An internal heat exchanger was installed to improve the cycle's performance. The impacts of the working fluid and operating circumstances on system performance were explored, including entrainment ratio, COP, compression ratio RP, and exergy efficiency. R 114, R 141b, R 123ae, R 245a, R600a, R 365mfc, R 123ae, and R 1234ze were recommended working fluids. The maximum COP and exergy efficiency were found in R 114 and R 1234ze, followed by R 245fa, R 123ae, R 365mfc, R 141b, R 152a, and R 600a. For all operating conditions, the new solar ejector-vapour compression refrigeration cycle has a higher COP than the standard ejector-vapour compression refrigeration cycle with R 1234ze. Due to its superior performance and ecologically benign qualities, R 1234ze was found to be a viable refrigerant for use in solar combined ejector vapour compression refrigeration systems.

2.4.10 Combined Power and Ejector–Absorption Refrigeration Cycle

A study was done to compare the effectiveness of several ejector refrigeration methods. A parametric analysis of the combined power and ejector–absorption refrigeration cycle was carried out by Wang et al. (2019). It was suggested that the Rankine cycle and the ejector-absorption refrigeration cycle could be merged to create new combined power and ejector-absorption refrigeration cycle that could provide both energy and refrigeration concurrently. An ejector was inserted between the rectifier and the condenser in this combined cycle derived from processes previously presented by other writers. As a result, performance was improved, but the system's complexity remained relatively unaltered. A parametric study is required to determine the impact of the essential thermodynamic parameters on the cycle's performance. The temperature of the heat source, the condenser, the evaporator, the pressure at the turbine inlet, the temperature at the turbine inlet, and the concentration of the fundamental solution ammonia had a significant impact on the combined cycle's net power output, refrigeration output, and exergy efficiency, it was discovered.

2.4.11 Solar Vapor Ejector Refrigeration System

Because the solar heat supply fluctuates in reaction to changes in the amount of solar irradiation received by the system, maintaining the generator temperature of a solar vapour ejector refrigeration system is problematic (Devarajan et al., 2021). The study employed computational fluid dynamics (CFD) simulations to investigate the usefulness of a variable throat ejector (VTEJ) as a technique for increasing the performance of ejectors. The outcomes of the investigation lead to assumptions and conclusions. When enlarged, an ejector with a larger throat area and solar collector allows for a more comprehensive operating range of generating temperatures; nevertheless, when the ejector is used to its maximum capacity, the cost of the ejector rises dramatically. Limiting the generator's throat area, on the other hand, will restrict its operating temperature range. As a result, an ejector with a fixed throat area would be unsuitable for using solar radiation as a source of heat. Based on the experiment's findings, a link was established between the proper throat area ratio and operating temperatures for a VTEJ. The ejector can achieve optimal and consistent performance despite varying solar heat supply by adding this connection to modify the throat area ratio.

2.4.12 Combined Power and Ejector Refrigeration System Analysis

A zeotropic mixture was used to undertake a theoretical investigation of a combined power and ejector refrigeration cycle (Maalem et al., 2020). The effects of various combination

compositions were compared and contrasted. An exergy study was carried out on the cycle. According to the statistics, more than 40% of the exergy is lost in the ejector, where most exergy degradation occurs. The generator's heat exchange is the second-largest source of wasted exergy, accounting for more than 28% of the total. The proportionate amount of exergy eliminated by each component altered as the mass fraction of isobutane declined from one hundred percent to zero. At 7.83 percent, the blend of 50/50 isobutane and pentane had the highest exergy efficiency. For each of the mixes, the parametric analysis of the generator, condenser, and evaporator temperatures revealed that each of these three thermodynamic factors had a significant impact on the cycle's performance.

2.4.13 Exergoeconomic Analysis and Optimization of Ejector Refrigeration Cycle

The researchers conducted an exergoeconomic analysis and multi-objective optimization of an ejector refrigeration cycle powered by an internal combustion (HCCI) engine (Khaliq et al., 2021). According to several academics, ejector refrigeration systems fueled by low-grade heat sources are an intriguing area for research. This study used the waste heat generated by an HCCI (homogeneous charge compression ignition) engine's exhaust gases to power the ejector refrigeration system. A new two-dimensional model for the ejector has been devised, taking into account the effects of friction on the ejector wall. A study of the recommended system's energy, exergy, and exergoeconomic was undertaken using MATLAB software.

Furthermore, using the exergy efficiency and product unit cost as objective functions, a multi-objective optimization was performed on the system to determine the ideal values for its design variables, such as the temperatures of the generator, condenser, and evaporator. This allowed the outstanding values for those variables to be determined. We were able to reduce the unit cost while increasing the product's exergy efficiency by using the evolutionary method. The Pareto frontier was drawn using the results of multi-objective optimization as a set of optimal spots. The ejector refrigeration cycle is operating at its best in terms of product unit cost and exergy efficiency when the generator, condenser, and evaporator operate at temperatures of 94.54 °C, 33.44 °C, and 0.03 °C, respectively. This was decided based on the results of the optimization.

2.4.14 Vapor Absorption Refrigeration System

According to Ghodeshwar and Sharma (2018), the majority of a vapour absorption refrigeration system consists of a binary solution consisting of a refrigerant and an absorbent

serving as the working fluid. The evacuated vessel on the left carries liquid refrigerant, while the connected vessels on the right hold binary solutions or absorbents. Both vessels have been evacuated and are connected. The pressure within the cooling vessel falls due to the solution's ability to absorb vaporised refrigerant from the container.

The evaporation of the refrigerant contained within the cooling vessel causes the refrigeration effect. The circulating solution will progressively become diluted due to the high concentration of absorbed refrigerant. The refrigerant is circulated throughout the system via the pumps in the system. According to Li et al. (2019), Vapour absorption refrigeration technologies are inconvenient and difficult to modify to meet the needs of the milk cooling process.

The refrigerant is taken from the evaporator and compressed at high pressure by the compressor in a vapour compression system (Bilen et al., 2022). Furthermore, the compressor allows unfettered refrigerant transport throughout the refrigeration cycle. Two different devices, absorbers and generators, are responsible for suction and compression during the vapour absorption cycle. The absorber and generator replace the compressor in the vapour absorption process. The absorber allows the refrigerant to flow by absorbing its heat as it moves from the absorber to the generator. The manner by which energy is transferred into the system is another significant contrast between vapour compression and vapour absorption cycles. An electric motor operated by an electric motor is the source of energy that is input into a vapour compression system in the form of a mechanical function. The output of an energy supply in a system that uses vapour absorption is heat. This could be due to the heating process or the steam generated by hot water.

All of the processes in a vapour compression refrigeration system also occur in a vapour absorption refrigeration system. These processes include compression, condensation, expansion, and evaporation. Ammonia, water, or lithium bromide are used as refrigerants in vapour absorption refrigeration systems (McLinden et al., 2020). In the condenser, the refrigerant condenses, while in the evaporator, it evaporates. The refrigerants exert their cooling effect in the evaporator while releasing heat into the condenser's atmosphere.

2.4.15 Thermodynamic Analysis of Refrigeration Systems

The refrigerant used in the systems is an essential parameter for evaluating the performance of refrigeration systems. Yi et al. (2022) investigated the thermodynamic and heat transport properties of R1234yf and R1234ze (E) as R134a drop-in replacements in a small power refrigeration system. The study presents two independent assessments of R1234yf and

R1234ze as drop-in replacements for R134a in a modest power refrigeration system. The first study assumes that evaporation and condensation temperatures are the same before and after the refrigerant change. The second analysis was carried out under similar cooling medium conditions in the condenser, taking into account the three refrigerants' transport properties and heat transfer characteristics.

A simulation model was created to do the studies, taking into consideration the dimensions, characteristics, and specific data of the critical components of a small power refrigeration system. For R134a, the model was validated using experimental data, and it was then used to predict behaviour for R1234yf and R1234ze. The results demonstrated that if the decrease in the analysis was carried out for equal condensation temperatures or similar temperatures of the cooling medium in the condenser, various conclusions could be drawn and that these results are influenced by the condenser design. R1234yf appears to be an excellent drop-in refrigerant for R134a, although R1234ze may function better when an override compressor is used to match the cooling power of the refrigerating system.

2.4.16 Optimization Solar-Powered Adsorption Refrigeration System

The rate of heat transfers and the amount of mass delivered by the collector dictate the performance of absorbent refrigeration systems. It's critical to figure out how the two variables differ for optimization purposes. The structure of a solar-powered finned-tube adsorption refrigeration system was optimised, and performance tests were done, according to Wang et al. (2018).

A large-diameter aluminum-alloy finned-tube absorbent bed collector was designed and optimised. This was done to improve the collector's heat and mass transmission. The relatively constant temperature distribution aided the adsorption/desorption of the adsorbate in the absorbent bed in the absorbent bed. The adsorbent bed collector's collection effectiveness ranged from 31.64 to 42.7 percent, and the temperature distribution was stable. A solar-powered solid adsorption refrigeration system was created using an absorbent bed collector with finned tubes. Experiments related to the adsorption/desorption process were done with and without valve control in four different weather conditions. On this beautiful day, there was a clear sky, a partly cloudy sky, a cloudy sky, and an overcast sky. The working pair for adsorption refrigeration in the testing was activated carbon and methanol. This combination was used. A maximum COP of 0.122 and a maximum daily ice output of 6.5 kg were attained over the course of the study. Different meteorological conditions were used to observe ice-forming activities, including sunny with a clear sky, partly cloudy sky, and a foggy atmosphere.

When total solar radiation was 11.51 MJ and the sky was cloudy, the cooling effectiveness of the system was 0.039 percent. This was true even when the device was exposed to direct sunlight. In the adsorption/desorption process, the solar-powered adsorption refrigeration system with valve control has a much greater cooling efficiency than the system without valve control.

2.4.17 Solar-Powered Adsorption Cooling System

Solar-powered adsorption cooling systems have difficulty providing cold constantly throughout the day due to the intermittent nature of solar radiation. The systems will have to deal with this. A study investigated a thermodynamic analysis of a hypothetical solar-powered adsorption refrigeration system in continuous operation (Oluleye & Boukhanouf, 2019). The design and implementation of a solar-powered adsorption cooling system have been completed. The proposed system, which worked successfully around the clock, could provide the essential cold whenever needed.

The theoretical foundation for the system's thermodynamic operating cycle was the adsorption process at a constant temperature. The cooling system's operational strategy and the thermodynamic cycle have been thoroughly documented and explained. In addition, all processes and components of the newly introduced system were subjected to a steady-state differential thermodynamic analysis. The research was based on energy conservation theory and equilibrium dynamics of adsorption and desorption processes. The adsorption equilibrium equation of Dubinin and Astakhov was used in this study.

Furthermore, the refrigerant's thermodynamic properties were estimated using its equation of state as a starting point. This case study looked at a water chiller that activated carbon and methanol to cool water. The chiller was capable of producing 2.63 kg of cold water at 0°C per kilogramme of adsorbent per day from 25°C water. The suggested technology also achieved a cooling performance coefficient of 0.66.

2.4.18 Solar Adsorption Refrigerator Powered by a Parabolic Trough Collector

The authors reported a scenario in which the reactor was heated by a parabolic trough collector (PTC) and linked to a heat pipe (HP) in their investigation of the solar adsorption cooling machine (Ouagued et al., 2018). The reactor's porous media was activated carbon, which interacted with ammonia by adsorption. The refrigerant's equilibrium equations, adsorption isotherms, heat and mass transfer within the adsorbent bed, and energy balance in the hybrid system components were used to build a model. The model used actual climate data

to calculate the machine's performance. The expected results showed that the recommended system, compared to existing systems driven by flat plate or evacuated tube collectors, can reach a high level of performance due to the high efficiency of PTC and the high flux density of heat pipe. Because of PTC's effectiveness, this was conceivable.

Cavallaro et al. (2018) proposed using solar refrigerators to store vaccines in regions where daily energy is less than eight hours. The WHO specifications were more stringent. It was unable to evaluate whether solar refrigerators are advantageous in locations where power outages are less frequent. The researchers simulated solar versus electric mains-powered refrigerators (which will be referred to as "electric refrigerators" in the following paragraphs) at various supply chain locations and under varying conditions using a computational model of the Mozambique routine immunisation supply chain generated by HERMES. The annual cost of each solar refrigerator is 132 percent higher than the yearly cost of each electric refrigerator at the district level.

In comparison, the annual cost of each solar refrigerator is 241 percent higher at the health facility level. Solar refrigerators were more cost-effective than electric refrigerators when there were more than five one-day power outages per year at the district level or health institutions. This was true even when the carryover period for electric refrigerators was longer than the outage. Solar refrigerators saved money because power outages lasting two days occurred more than three times per year at the district level and more than twice per year at the health facilities. Solar refrigerators saved money when one-day outages occurred more than once per year at the facility level, when two-day outages occurred more than once per year at the district level, or when they occurred once per year at health facilities because their annual cost was only 75% higher than an electric refrigerator. Solar refrigerators become cost-effective on both levels as a result of this. The outcomes of the study matched WHO and Gavi's recommendations. Compared to refrigerators powered by electricity, solar refrigerators may have lower total expenses per dose of medication due to fewer power disruptions. Their study determined the number and duration of power interruptions required for solar refrigerators to produce a lower overall cost per dose when compared to electric refrigerators at various solar refrigerator pricing.

2.4.19 Solar-Powered Adsorption System with Activated Alumina and Activated Carbon

When activated alumina was submitted to a series of laboratory tests using a continuous radiation heat flow, it was well known that it had a higher adsorption capacity. Sugiartha (2020) used activated alumina and activated carbon as sorbents in an experimental study of a solar-

powered adsorption refrigeration cycle. In solar-powered adsorption refrigeration cycles, activated carbon is a common type of adsorbent. During this investigation, a solar-powered adsorption refrigeration cycle with a generator packed with various adsorbents was exposed to solar radiation in the Indonesian city of Medan.

The generator is heated by flat-plate solar collectors measuring 0.5 metres by 0.5 metres. Experiments on solar-powered adsorption cycles were carried out using four different types of generators: one filled with 100% activated alumina (designated as 100AA), one filled with 75% activated alumina and 25% activated carbon (designated as 75AA), and one filled with 100% activated carbon (designated as 100AC). Each case was investigated for three days in total. The performance, as well as the temperature and pressure histories, were then presented and analysed. The coefficients of performance (COP) for 100AA, 75AA, 25AA, and 100AC, respectively, were determined to be 0.054, 0.056, 0.06, and 0.074. The most important conclusion from these findings concerns Indonesian conditions and flat plates.

Employ a mixture of ammonia and water as the working fluid in a combined-power Rankine refrigeration cycle and an artificial neural network to analyse its thermodynamic properties. Zhang et al. (2019) proved that the combined cycle might generate power and refrigeration from a single external heat source. A secondary turbine was built after the boiler in order to expand the hot, weak solution that was being released. This was done in order to attain the best possible exergy efficiency. Furthermore, an artificial neural network (ANN) was used to describe the thermodynamic properties of the cycle as well as the impact of the input thermodynamic variables on the cycle's performance. This was done to ensure that the results were correct. The combined cycle's net power production, refrigeration output, and overall output were shown to be heavily influenced by energy efficiency, turbine inlet pressure, refrigeration temperatures, and heat supply. Furthermore, the ANN's conclusions are similar to those of the mathematical simulation, and they cover a more excellent range of cycle performance evaluations. The combination of activated carbon and methanol outperforms activated alumina in solar collectors.

2.4.20 Solar Adsorption Refrigeration System with Concentrated Collector

Aramesh et al. (2020) experimented with a concentrated collector and a solar adsorption refrigeration system. The adsorbent bed, condenser, evaporator, cooling subsystem, and solar collector were the system's most essential components. The vapour-saturated mattress was heated by sun radiation during the experiment's first phase. As a result, the bed's temperature and pressure increased. A switch was turned to connect the bed to the condenser after the

required bed pressure was achieved. As a result, water vapour continuously flowed from the bed to the condenser, where it was cooled and condensed into a liquid. The bed needed some time to cool down after completing the desorption process. The bed's circulating water loop became available due to the solar-shielding state produced using aluminium foil. The heat built in the bed was released due to the constant flow of water through the bed, resulting in a reduction in the pressure imposed on the bed. The valve leading to the evaporator was opened when the pressure in the bed fell below the saturation pressure at the evaporation temperature. The zeolite material did an excellent job absorbing the massive amount of water vapour that had just entered the bed. The refrigeration effect was caused by significant evaporation of the water contained within the evaporator. Regardless of the adsorption time, the SAPO-34 zeolite had a higher COP (system performance coefficient) and SCP (system-specific cooling power) than the ZSM-5 zeolite, according to the results. This was true regardless of the time gap between adsorptions. The SAPO-34 zeolite-based system achieved a maximum COP of 0.169.

Sorption systems, which include absorption and adsorption refrigeration systems, were among the most efficient solar heating and cooling technologies. Sztekler et al. (2021) investigated solar-powered air conditioning systems that can adjust to a variety of solar collector temperatures. A modular silica gel and water adsorption chiller was built and put through its paces during testing. A LiBr chiller with a single/double effect and a water absorption chiller was used and evaluated. It was conceptualised, designed, and tested a LiBr and water-based absorption chiller. We built and tested a CaCl2 and AC–ammonia adsorption refrigerator. A new ice maker that absorbs H3 and H2O and has improved internal heat recovery has been developed. A single/double effect LiBr and water adsorption chiller and a modular silica gel and water adsorption chiller are among the five systems available. The researchers exhibited a water and ammonia absorption chiller, a CaCl2/AC (activated carbon) and ammonia adsorption refrigerator, and a water and ammonia absorption ice maker with improved internal heat recovery. The five sorption chillers/refrigerators we've looked at work in a wide range of operating temperatures and can handle a wide range of refrigeration needs. A presentation on the systems' thermodynamic design and system development was followed. All of the systems were more advanced than the previous ones, and they held a lot of promise for highly efficient solar cooling in the near future.

2.4.21 Solar-Powered Closed Sorption Refrigeration Systems

Day et al. (2018) highlighted in their general reviews on solar-powered closed sorption refrigeration systems that the negative environmental consequences of burning fossil fuels had

forced the energy research community to investigate renewable sources such as naturally accessible solar energy. The energy research community has been forced to explore renewable alternatives due to the severe environmental repercussions of fossil fuel burning. For thermally powered refrigeration, two methods are used: thermo-mechanical technology and sorption technology (open systems or closed systems).

An in-depth look into closed solar sorption (absorption and adsorption) refrigeration systems with functioning pairs (fluids). A report on the evolution of solar sorption refrigeration technology and the most recent technological breakthroughs was delivered after an explanation of the underlying concepts underpinning these systems. Most of the time, the adsorption cooling temperature needed was lower than the absorption cooling temperature requirement. Absorption systems are preferred over adsorption systems based on the coefficient of performance (COP). However, solar adsorption systems might readily handle higher temperature problems if used instead. The thermodynamic properties of the majority of currently used working fluids and the use of ternary mixtures in solar-powered absorption systems were examined in this study. As a result of this research, a number of novel solutions, such as the creation of hybrid or thermal energy storage adsorption systems, have been proposed to increase the fundamental adsorption cycles' operational efficiency and long-term viability. According to the findings of this study, solar-powered closed sorption refrigeration technologies can be viable alternatives not only for air conditioning, refrigeration, ice production, thermal energy storage, or hybrid heating and cooling applications but also for energy conservation and environmental protection (Razmi et al., 2019).

2.4.22 Absorption Refrigerator Driven by Solar Cells

In areas where electricity is unavailable, solar energy could power a portable or vehicle-mounted absorption refrigerator (Du et al., 2018). A solar-powered absorption refrigerator was used for experiments and research (Erzen et al., 2019). The goal of this experiment was to see how a solar-powered absorption refrigerator worked. An energy storage battery provided power in the evenings and on days when the weather was bad. If an alternating current (AC) power supply was available, the energy storage battery might be fully charged to serve as a backup supply. The suggested system was validated by cycling between 550 and 700 W/m2 of solar irradiation as a source of solar energy and 500 cc of room-temperature water as a cooling load.

The proposed refrigerator can maintain a temperature of 5 to 8 degrees Celsius after 160 minutes, and the COP of the NH3-H2O absorption refrigeration system is around 0.25. As

a result, this system was expected to be used in isolated places for the refrigeration of food and beverages during outdoor activities in remote and desert areas, for long-distance food road transportation, or for low-temperature vaccine refrigeration to prevent food or vaccines from decaying.

2.4.23 Solar Absorption Cycle of Ammonia

The utilised couples of absorbents refrigerating fluids and the solar energy collecting and unit refrigeration using an improved, have been conceived of and explored following the completion of a bibliographic study project on absorption cycles (Al-Yasiri et al., 2022). The simulation results under a permanent regime addressed variation in performance standards based mainly on the study's retained workers. The findings showed that ammonia's improved mono-pressure absorption cycle is perfect for producing cold using solar energy. An essential plate collector may obtain a power output of 900 watts, sufficient for household use.

An investigation into the performance analysis of an independently operating solar absorption refrigerator was done (Galindo et al., 2018). Water and a Libr machine were used to keep the temperature cool during the day. The performance of the refrigerator was simulated using a dynamic model. The solar-powered absorption device could be used for two different purposes. The sun's radiated radiation provided the thermal component of valuable energy. It was required to use more power in addition to the electric energy to operate the pumps, fans, and control system.

On the other hand, the sun can provide all of the energy required. Heat concentrators and solar cells were both used in this case. The user must be aware of the geometric properties of each component, such as the exchange areas and internal volumes, in order to simulate the dynamic regime of the cycle. The applied thermodynamic research unit (ATRU) of the Engineers' National School of Gabes (Gabes) provides information on the essential qualities of a stocked refrigerator. The thermal and matter balances in each component of the cycle had to be created in order to model the performance of a solar absorption refrigerator operating with the water and LiBr couple for air cooling in the dynamic regime. This breakthrough allowed for the simulation of the cycle. The proposed model was capable of completing intermittent refrigeration cycles on its own.

2.4.24 Modified Solar Absorption Refrigeration System

Several improvements were made to improve the performance coefficient of a solar-powered absorption refrigeration system (COP). The addition of a refrigerant storage unit and

the recovery of waste heat from a dephlegmator were changing. Simulated results from Shabari et al. (2018) indicated a 10% increase in the COP of the conventional design with dephlegmator heat recovery and an 8% increase in the COP of the traditional design with refrigerant storage. The COP of the conventional design increased by 8% as a result of these two increases. According to the data, the cumulative effect of the adjustments results in an 18 percent increase in the COP compared to a traditional design. The computed coefficients of performance show excellent agreement with those obtained through measurement.

It was observed that even a slight increase in the thermal efficiency of power cycles might result in significant cost savings in the generation of energy; hence, having a tool that allowed simulation of power cycles enabled modelling of the best changes for the best results (Zare & Palideh, 2018). During this period, research on the Organic Rankine Cycle (ORC), which intended to create energy at low power through cogeneration and whose working fluid is often a refrigerant, also increased dramatically. This area of study grew in popularity. A tool for designing the components of an ORC cycle and selecting the working fluid would be helpful. This is because the heat sources from cogeneration are so variable, and each situation would require a unique design. The development of a multiplatform simulation programme for power cycles and refrigeration is part of this study. The software was written in the C++ programming language and had a graphical user interface. It was created in a multiplatform environment and is Windows and Linux compatible. The programme allowed users to create custom power cycles, choose the type of fluid (thermodynamic properties are computed using the Cool Prop library), calculate the plant's efficiency, identify flow fractions in each branch, and generate an educational report in pdf format using the LaTeX tool.

2.4.25 Hybrid Solar Cooling System

The tested and reported solar hybrid cooling architecture featured radiant cooling via absorption refrigeration and a desiccant dehumidification system. This design was created to meet a typical subtropical location's high cooling load requirements (Fong & Lee, 2020). The ventilation load (predominantly latent) is handled by desiccant dehumidification. In contrast, chilled water from absorption refrigeration and radiant cooling manages the zone cooling load (which is mainly sensible). This is the case for the typical cooling load of a building. The regeneration of the desiccant wheel and the operation of the absorption chiller are powered by solar energy in this hybrid system.

Desiccant dehumidification was used since the high chilled water temperature generated by the absorption chiller was insufficient to manage the needed latent load. Desiccant

dehumidification, radiative cooling, and absorption refrigeration were all driven by solar energy. Radiant cooling was also included in the system. Using dynamic modelling, the researchers in this study were able to assess the application potential of a solar hybrid cooling system for high-tech offices in subtropical locations. Internal sensible heat gains were quite prominent in high-tech offices due to electrical equipment. One of the offices' characteristics was this. Two of the most critical performance measures were the fraction of energy derived from the sun and the amount of primary energy consumed. Both passive and active chilled beams, both popular forms of chilled ceilings, were used in the comparative research for the solar hybrid cooling system. The solar hybrid cooling system was technically feasible for more outstanding cooling demand applications. The classic vapour compression refrigeration system consumed roughly 36.5 percent more primary energy per year than the solar hybrid cooling system. When combined with a solar hybrid cooling system in a hot and humid environment, passive chilled beams were the more energy-efficient choice. This was the case when comparing the two options for chilling ceilings. It would be beneficial to power air conditioners with solar energy to mitigate the effects of climate change and contribute to reducing carbon emissions.

Absorption refrigeration and reversible solid/gas processes can be combined to create hybrid systems with the continuous operation and excellent thermal performance of absorption systems and the energy storage efficiency of thermochemical systems. These hybrid systems can be made by combining technology. Rosato et al. (2020) proved that hybrid systems could correct the mismatch and run continuously even when the driving source is intermittent, such as solar heat. They may also be ideal for autonomous operation off the grid if adequately constructed and sized. Both absorption and thermochemical systems use natural working fluids that do not deplete the ozone layer or contribute to global warming.

2.4.26 Solar Ammonia Absorption Refrigeration system

Even in the absence of electric grid connectivity, the Solar Ammonia Absorption Cycle (SAAC) refrigeration system provides low-cost, efficient, and stable refrigeration. Garcia and Rosa (2019) used the Intermittent Solar Ammonia Absorption Cycle (ISAAC) to examine refrigeration. The study was carried out in underdeveloped countries. A compound parabolic solar collector, two pressure vessels, a condenser, a cold box or refrigerated chamber, and simple connecting pipes made up the refrigeration system. The majority of the components are simple plumbing or building supplies, which are readily available in many isolated locations. Because it includes semi-skilled labour that is reasonably easy to learn, this technology has the

potential to produce a low-cost and reliable source of ice and a source of employment for the local economy. Storage of vaccinations for use in medical clinics, fish, meat, dairy products, and personal consumption are all possible applications. Significantly, this technology improves the quality of life in impoverished countries without depleting fossil fuel supplies or increasing greenhouse gas emissions like carbon dioxide and chlorofluorocarbons. This is a significant achievement.

2.4.27 Combined Power and Absorption Refrigeration systems

The device that combined the Rankine and absorption refrigeration cycles used a binary mixture of ammonia and water as the working fluid and produced both power and refrigeration from a single heat source. The parametric optimization analysis research of Moghimi et al. (2018) focused on a combined power and refrigeration cycle. A parametric analysis was used to assess how thermodynamic factors affect combined cycle performance.

The temperature of the refrigeration system, the temperature of the turbine inlet, the temperature of the heat source, the temperature of the environment, the pressure at the turbine inlet, and the concentration of basic solution ammonia had a significant impact on the combined cycle's exergy efficiency, net power output, and refrigeration output. A genetic algorithm was used to optimise settings in order to obtain maximum possible exergy efficiency. The ideal exergy efficiency was 43.06 percent under the given conditions.

2.4.28 Solar Lithium Bromide Absorption Refrigeration Cycle

The performance of refrigeration systems based on a linear Fresnel solar thermal photovoltaic system was tested by Singh and Das (2021). The Solar Lithium Bromide Absorption Refrigeration Cycle was the name given to their research. This paper explains the operation and system components of the linear Fresnel solar lithium bromide absorption refrigeration cycle. The report also discusses several absorption refrigeration cycles, such as single-effect, two-stage, and double-effect lithium bromide absorption refrigeration cycles. A linear Fresnel solar absorption chiller system was modified by adding an absorption chiller system built utilising the optimal parameters. The field refrigerator performance test results show that, based on this heat cycle design and processing lithium bromide absorption refrigeration power up to 35,2 kW, it is capable of meeting theoretical expectations, has good flexibility and dependability, and provides guidance for solar thermal energy utilisation.

In addition to flat plate collectors and the hot water storage tank, Elsheniti et al. (2021) developed a computer programme to simulate the functioning of a two-bed silica gel and water

adsorption cooling system. This application was used to affect the operation of a solar adsorption cooling system. The programme was then used to simulate the functioning of a sample solar adsorption cooling system in order to cool a group of rooms in the Iranian city of Ahwaz with a total size of roughly 52 m2. The system was modelled using typical Ahwaz climatic data, such as the amount of solar radiation and average temperatures. The data includes adsorption/desorption bed, evaporator, condenser temperature profiles, and hot, cooling, and chilled water profiles. The impact of cycle time, switching time, and hot water temperature on COP and refrigeration capacity is also investigated. Furthermore, the effects of solar collector surface area and storage tank volume on total system cost are analysed in order to determine their optimal values for optimising the thermo-economic performance of the investigated system. This is done in order to determine their optimal values, which are capable of identifying their optimal values.

2.4.29 Optimization of Solar Absorption Refrigeration Systems

Figaj and odek (2021) used the dynamic behaviour of a solar absorption refrigeration system working under a reversible paradigm to optimise a solar-powered absorption refrigerator in the transient domain. Introductory thermodynamics, mass, and heat transfer principles were used in the research. To do this, the time spent exchanging heat was reduced in order to maximise performance. The temperature of the collector has a significant impact on the model's parameters, with effects comparable to those of thermal load and thermal conductance. The dynamic manner of theoretical examination of an absorption refrigeration system using a reversible model is the subject of this paper. Solar energy was used to power the device, which operated as a cold-producing station. A chilled room, an absorption refrigerator, and a solar collector shape made up the cycle. The fundamentals of thermodynamics, mass transmission, and heat transport were all incorporated into a mathematical model. The numerical simulation was conducted using a variety of operational and conceptual parameters. A worldwide optimization with the goal of reducing time was carried out in order to attain optimal performance. It was critical to creating appropriate dimensionless categories. The collector temperature has a much more significant impact on conceptual and functional aspects than the stagnation temperature. The thermal load in the refrigerated space and the thermal conductance of the walls, on the other hand, showed parallel impacts, showing that these factors must be considered during the actual design process. As a result, the model is a valuable tool for modelling, designing, and optimising solar collector-based energy systems.

Solar collectors can function in a wide variety of temperatures. Therefore solar-powered air conditioning systems can still be helpful. The most efficient sun cooling options are sorption systems, which include absorption and adsorption refrigeration systems. An ammonia adsorption refrigerator, a water and ammonia absorption ice maker with improved internal heat recovery, a modular silica gel and water adsorption chiller, a single/double effect LiBr water absorption chiller, a LiBr water absorption chiller with CaCl2 and AC (activated carbon), and an ammonia adsorption chiller were among the five systems demonstrated. The five sorption chillers/refrigerators we've looked at work in a wide range of operating temperatures and can handle a wide range of refrigeration needs. As illustrated, the systems were designed with thermodynamics and system development in mind. These approaches are more efficient than those currently in use and could provide extremely desirable solar cooling options in the near future.

Huang et al. (2018) developed an anti-idling system that uses a battery and an engine-driven generator to run the refrigeration system's compressor for an optimal power management system for a regenerative auxiliary power system to deliver refrigerated vehicles. In refrigerated delivery vehicles, this technique would be used. He concluded that idling could be eliminated by turning off the engine and using the battery to provide auxiliary power whenever the truck was halted for loading or unloading. Regenerative braking was also used to improve the amount of gasoline saved. For this system's power management to work correctly, it is required to meet two requirements. It needed to reduce the total gasoline used during the cycle first. Second, it had to ensure that the battery had enough power to keep the refrigeration system functioning while the engine was turned off. As a means of meeting these goals, a two-level controller was proposed. A fast-dynamic programming technique was used in the higher level of this controller to identify the suboptimal beginning and final State of Charge SOC values for any two consecutive loading/unloading stops. This strategy made use of statistical data derived from a refrigerated truck's drive and duty cycles. Based on the upper-level controller's beginning and final SOC values, the lower-level controller used an adaptive equivalent fuel consumption minimization (A-ECMS) method to calculate the split ratio of auxiliary power between the generator and the battery for each segment. According to the simulation results, the newly devised technology has the potential to eliminate the practise of refrigerator trucks idling and significantly cut their fuel consumption. As a result, the expense of replacing components could be recouped in a short amount of time.

Valencia et al. (2019) investigated an adsorption-desorption refrigeration and air conditioning system powered by the sun and using nanostructured materials as the adsorptive

medium. These nanostructure materials include aerogels, zeolites, and sol-gels. Molecules of refrigerant could be adsorbed onto the enormous surface area of the nanostructural material while it was kept at a temperature close to room temperature. It's possible that this happened at night. The refrigerant was thermally desorbed from the surface of the aerogel during daylight hours when the nanostructure components were heated by the sun. Within the aerogel-containing vessel, this resulted in the creation of a pressurised gas phase. The sun creates this pressure, which forces the heated gaseous refrigerant through a condenser and opens an expansion valve. The condenser is in charge of collecting heat from the refrigerant by cycling air or water through the system and then removing it. The cooled gaseous refrigerant expands isothermally through a throttle valve and into an evaporator, similar to traditional vapour recompression systems.

2.4.30 Solar Adsorption Chiller Using Silica Gel Water Mixture

Adsorption refrigeration systems were developed to replace conventional systems that use environmentally hazardous refrigerants and consume high-grade electrical power, according to a research project conducted by Pan and Wang (2018) to review solar adsorption chiller utilising a mixture of silica gel and water. When addressing cooling needs in remote places, such as air conditioning, ice making, water chilling, and medicinal or food preservation, solar adsorption refrigeration systems are essential. Furthermore, they did not corrode, emit noise, or negatively affect the environment.

When using adsorption refrigeration, several refrigeration pairings were discovered to be available (Chen et al., 2019). The authors of the review research looked at a number of different silica gel-water adsorption refrigeration systems. According to the study's conclusions, the bulk of the system could operate at a low generation temperature of 70 to 80 degrees Celsius, with chilled water temperatures of 10 to 20 degrees Celsius. The pressure range of the system is 1 to 12 kilopascals (kPa). The adsorption chiller's performance coefficient (COP) was between 0.3 and 0.5.

2.4.31 Solar Adsorption Refrigeration System with CPC Collector

The flat plate collector is commonly used to design and test collectors for solar adsorption cooling systems. On the other hand, concentrating collectors have gotten virtually little research in this area. CPCs, or compound parabolic concentrators, are versatile solar collectors that may be customised to a wide range of geometries and applications. Masood et al. (2022) researched the topics mentioned above. Only a piece of a CPC collector with a

tubular receiver containing the sorption bed was exposed to solar radiation in the paper. Only a portion of the receiver was exposed to sunlight to achieve this. The geometric specifications of the proposed CPC are detailed here, including the profile, length, and height of the reflecting sheet. A solar adsorption chiller prototype using this collector and the activated carbon-methanol working pair has been detailed in detail, with representative experimental results published. Solar COP has been measured to be between 0.078 percent and 0.096 percent.

2.4.32 Adsorption Reactor Solar Refrigeration System

Alvarez et al. (2021) investigated a solar refrigerating unit using an adsorption reactor and evacuated tube collectors. The principles of operation of a solar refrigerator with the following fundamental components were provided: a reactor, a set of evacuated tube solar collectors, a condenser, a heat exchanger, and an evaporator. Solar energy was captured during the heating phase and transmitted to the reactor via a vapour thermal syphon loop for desorption. A second water vapour loop released heat from the reactor to the atmosphere during the cooling phase. During the adsorption and desorption processes, ambient data was recorded on a daily basis for 18 years and then separated into hourly values for use in replicating the temperatures of the reactor, which used salt loaded with graphite and ammonia. The results showed that the refrigerator worked effectively in Fortaleza, with better results expected in the Ceara countryside. Finally, it was demonstrated that the system could use a high-efficiency collector set.

Bagheri et al. (2019) conducted an exergy analysis of a combined vapour power cycle, and boiler flue gas has driven double effect water–LiBr.This study presented a combination vapour power cycle (PC) and double effect water and LiBr absorption refrigeration system (ARS). The boiler leaving the PC's flue gas is the heat source for the dual effect ARS's high-pressure generator (HPG). An exergy study of the suggested system was carried out to show how the topping PC's performance and the bottoming ARS changed when the HPG temperature increased from 120 to 150 degrees Celsius. The performance of a double effect ARS integrated combined power, and cooling system was also compared to a single impact ARS integrated system. The HPG temperature of the dual impact ARS was $80^{O}C$, and the generator temperature of the single effect ARS was $120^{O}C$. The power and efficiency of the topping PC reduce as the HPG temperature rises due to a fall in the boiler's steam output rate. Exergy and COP efficiency of the double effect ARS decreased as HPG temperature increased. Due to increased exergy loss with HPG exiting flue gas and irreversibility of the ARS components, irreversible losses in PC components were reduced.

In contrast, the total irreversibility of the combined power and cooling system grew with HPG temperature. The replacement of the double effect ARS with the single product ARS had little impact on PC performance. In contrast, the dual effect system achieved more outstanding COP and exergy efficiency with significantly reduced irreversible losses in the HPG and ARS condenser.

2.4.33 Constant Temperature Adsorption Refrigeration System

As a result of recent advancements, CO-SAR, which stands for continuous operation solar-powered adsorption refrigeration, was born. Alahmer et al. (2020) investigated the dynamic analysis of the CTAR cycle (constant temperature adsorption refrigeration). The first SAR machine, which stood for solar-powered adsorption refrigeration, was a cold-production gadget that only worked intermittently. The continuous temperature adsorption refrigeration (CTAR) cycle provided the theoretical basis of the CO-SAR machine.

The adsorption process occurs at a constant temperature equal to the temperature of the surrounding environment in this cycle. There must be a temperature difference between the adsorption bed and the surrounding atmosphere in order to have a driving potential for heat transfer. The study's dynamic analysis of the CTAR cycle provided may be seen here. This study compared and contrasted the theoretical and practical applications of the CTAR cycle. The dynamic model was built on the basis of the adsorption equilibrium equation and the energy and mass balances in the adsorption reactor. The findings suggest that the idealisation of the constant temperature adsorption process, often known as the theoretical CTAR cycle, was not too far off the mark and might be corrected. Furthermore, increasing heat transmission between the adsorption bed and the surrounding environment during the bed pre-cooling phase speeds up heat rejection from the adsorption reactor, bringing the process closer to isothermal operation.

2.4.34 Characterization of Autonomous Solar Adsorption Refrigeration System

The construction of an autonomous solar adsorption refrigerator was documented by Wu et al. (2021). The researchers praised the refrigerator's portability and small size. The refrigerator operates continuously throughout the day and night cycles, using water as its working fluid and silica gel as its adsorbent. A collector and absorber surface area of one cubic metre was required for a cooling volume of approximately 100 litres, and the total mass of the system was around 150 kilogrammes. Lightweight materials were used in the equipment's construction to reduce its mass as much as possible. A high-performance insulation material

was used to insulate the cold storage room, which reduced heat loss while maintaining an acceptable level of cooled volume. The need for manual manipulation during normal operation has been eliminated thanks to the development of a brand-new automatic valve system. In a Sahelian climate, proper cooling system sizing allowed for a daily temperature reduction of 30 K for the equivalent of 2.5 to 3.7 kg of water. The evaporator was built to store cooling energy as ice, gradually released over three days of cloudy weather. The solar-powered refrigerator was assembled through a collaborative effort involving a number of locally owned businesses and workshops. Between May and September of 2012, the system was tested thanks to a collaboration with a non-governmental organisation. The tests were carried out in a Sub-Saharan African region where an equivalent model had been built using locally available materials. In Burkina Faso, a market study was carried out to determine the viability of solar adsorption refrigerators in the country. According to the study's findings, establishing a production workshop in Burkina Faso for the manufacture of such refrigerators would be advantageous.

According to Hayat et al. (2019), the photovoltaic effect is the most crucial factor in converting solar energy into usable electricity. Photons bombarding photovoltaic cells cause an electromotive force to be generated within the material. The Seebeck effect is a phenomenon in which an asymmetric thermal differential causes charge carrier mobility. By combining solar evacuated tube technology with commercially available Bismuth Telluride semiconductor modules, the study advances the state-of-the-art in thermoelectric system management. The primary heat source was chosen to be solar radiation, and the direct heat sink was chosen to be thermal convection into the surrounding air. The wind-aided the forced convection process. These energy sources were replicated in a controlled laboratory environment in order to maintain a thermal dipole across a thermoelectric module. Following that, the device was tested in a natural setting. Experimental confirmation of theoretical electrical characteristics in relation to a varying electrical load and a net thermoelectric power gain that can be implemented in applications in ambient environments are among the novel aspects of this work.

The energy efficiency of a sophisticated solar-powered refrigeration system was investigated. Lekbir et al. (2018) examined a solar refrigeration system incorporating the most recent and significant technological advances in training solar systems (SCS) and improved absorption units. The energy behaviour of an absorption refrigeration system with an air-cooled natural gas-solar heat exchanger was evaluated and analysed with the help of a hybrid power plant (GAX). The intended methodology called for a calculation sequence for the external currents and an iterative procedure for the internal currents due to the high degree of

nonlinearity displayed by the resulting system of occupations. Both of these processes would be carried out again. The unit's working fluids were ammonia and water, and its capacity was 10.6 kilowatts, which was equivalent to 3 tonnes of refrigeration cooling load. A GAX cycle configuration ensured a maximum of 19 percent solar input at full load, with the possibility of more at part loads. This GAX cycle configuration was recommended because internal energy integration was prioritised. Despite using air at 40 degrees Celsius and 24 to 25 percent relative humidity as a cooling medium, a coefficient of performance (COP) of 0.86 in cooling mode and 1.86 in heating mode was achieved, with an internal energy integration of 1.013 mJ/min, which is 37 percent more energy than is supplied in the generator. Compared to the flow rates of an essential cycle, the circulation rate and flow rate of the mass in the GAX cycle were 73 percent and 62 percent lower, respectively, than the flow rates of a primary cycle.

A study was conducted on the performance analysis of minimally nonlinear, irreversible refrigerators with a finite amount of cooling power (Long et al., 2018). The coefficient of performance, or COP, for universal refrigerators with a limited cooling capacity was thoroughly investigated using the least nonlinear irreversible model. The work proposes minimum and maximum values for the COP in various operating areas. Considering the tight coupling requirements, they estimated the universal COP limits for a number of distinct operating environments. When the refrigerator was utilised in a region with a lower external flux, the researchers discovered that the general boundaries of 0 contained significant values. This was in contrast to the relatively small amount of electricity lost during peak cooling capacity. When the amount of cooling power was the primary concern, it was determined that it was preferable to operate the refrigerator at a slightly lower level of cooling power than the maximum level, as even a small reduction in cooling power results in a significantly greater increase COP.

2.4.35 Solar Collector Adsorptive Refrigeration System

Using a solid adsorption cooling unit based on the binary silica gel and water couple was a promising way of harvesting solar energy for refrigeration via an adsorptive refrigeration system that incorporated a solar collector with a thermal insulating module (Entezari et al., 2018). The study led to the creation of a mathematical model for modelling the system in a range of scenarios, which was shown to be congruent with experimental findings. Several completed simulations demonstrated the need to build a regulated reactor that can cool at night.

In addition, the simulations demonstrated the advantages of using a solar collector that is easily accessible, as well as how the thermal insulating module should be positioned across

the glass near the thermal radiation once the desorption process is complete. As a result of the better nighttime cooling of the collector, the simulation results show that this arrangement has a more outstanding COP.

2.4.36 Trough Collector Solar Adsorption Refrigeration System

Bellos and Tzivanidis (2018) investigated the design and performance characteristics of a parabolic trough collector-based solar adsorption refrigeration system. The work done, which included both experimental and statistical optimization methodologies, revealed that a built model of a solar adsorption refrigeration system might be designed to match specific needs and specifications. The most modern design can function as a refrigerator and cooling unit in remote locations. Olive waste was used as the adsorbent, while methanol was used as the adsorbate in this system—a solar collector with a parabolic trough reflector powers the system (PTC). The cooling output, coefficient of performance, and COP a were used to determine the system's efficiency (gross cycle coefficient of performance).

Statistical analysis and hands-on experimentation were used to obtain the best values for the system design parameters in this study. The cooling chamber's lowest temperature was 4 degrees Celsius, while the outside temperature was 27 degrees Celsius. As the actual cooling began, the temperature gradually dropped between 20 and 30 degrees Celsius. The temperature dropped more till it hit 4 degrees Celsius at 01:30 the following day when it began to rise again. The COP value of 0.75 was discovered to be the highest.

2.4.37 Freeze Proof Solar Powered Adsorption Cooling System

The mechanical and experimental performance of a freeze-proof solar adsorption cooling tube made from activated carbon and methanol was investigated (Zhao et al., 2018). The study focuses on a freeze-proof solar-powered adsorption cooling tube through mechanical and empirical research. The testing findings showed that the most incredible adsorbent bed temperature was below 110 °C when solar radiation was between 15.3 and 17.1 MJ per m2. When the evaporation temperature was around four °C, the freeze-proof solar cooling tube had a cooling capacity of approximately 87 to 99 kJ and a coefficient of performance (COP) of more than 0.11.

2.4.38 Solar Powered Thermoacoustic Refrigeration System

De and Ganguly investigated a cold storage system's design and dynamic behaviour with a solar-powered thermoacoustic refrigerator (2019). According to the study, a heat-

powered thermoacoustic refrigerator consists of a thermoacoustic engine that generates acoustic work using heat and a thermoacoustic cooler that turns this acoustic energy into a cooling effect. These units had already proven their worth in laboratory and space cooling applications. Previous research has shown that concentrated solar energy can be used as a thermal energy source for low-power heat-driven thermoacoustic refrigerators. Even while the cooling requirement generally increased with the strength of solar radiation, like with other solar refrigeration systems, one of the primary challenges was ensuring a frigorific power supply when there was no or low solar radiation.

This research aimed to investigate a kW-scale solar thermoacoustic refrigerator capable of reaching industrial refrigeration temperatures. This refrigerator was paired with latent cold storage to ensure enough chilling capacity in the face of refrigeration loads regardless of output changes. The examined prototype was described, and the model constructed to characterise the transient behaviour of the machine's primary components was presented. The findings of a one-week simulation with fundamental solar radiation were introduced, and the behaviour and energetic performances of the complete system were investigated. Finally, the impact of cold storage system sizing was explored. With the optimal storage design, the system was capable of producing a cooling power of 400 W at a temperature of 20°C or below, with a solar thermoacoustic refrigerator average coefficient of performance of 21%.

2.4.39 Solar Electrochemical Refrigeration System

A dye-sensitized solar cell and a thermally regenerative electrochemical refrigerator were coupled to study an idea for a solar-powered electrochemical refrigerator. This made it possible to create a solar-powered electrochemical refrigerator (Zhao et al., 2020). The researchers accounted for a variety of irreversible losses that occur within the dye-sensitized solar cell, the thermally regenerative electrochemical refrigerator, and between these two devices to derive mathematical formulas for the performance parameters of the dye-sensitized solar cell, the thermally regenerative electrochemical refrigerator, and the solar-driven electrochemical refrigerator. The energy balance equation calculated the electric current relationship between the dye-sensitized solar cell and the thermally regenerating electrochemical refrigerator. The solar-powered electrochemical refrigerator has a maximum cooling rate density of 800.47 W m2 and a maximum performance coefficient of 0.80. These are their values. A tiny layer thickness was appropriate for getting the best results from the system. The performance of the solar-powered electrochemical refrigerator was greatly enhanced by increasing the photoelectron absorption coefficient, specific charge capacity,

isothermal coefficient, or regeneration efficiency. If the Schottky barrier is more considerable, the internal resistance is more excellent, and the temperature differential between the hot and cold heat reservoirs is more significant, the performance of the solar-powered electrochemical refrigerator will be reduced. The findings could have benefited the design and optimization of a refrigerator of this type in the future.

Cheekatamarla's research aimed to promote the development of liquid/gas absorption cycles by using solid/gas chemical interactions at high temperatures. The study came up with some exciting ideas for thermally integrating solid/gas thermochemical processes with liquid/gas absorption. These restrictions do not apply to solid/gas thermochemical working pairs, but they do to water/lithium bromide and ammonia/water, two well-known liquid/gas absorption working pairs. Due to their corrosiveness and thermal disintegration at high temperatures, these limitations do not apply to solid/gas thermochemical working couples. To achieve additional refrigeration effects, it is feasible to thermally combine single-effect and double-effect liquid/gas absorption with solid/gas reaction in a high-temperature area. The study offers and evaluates a number of coupling configurations that could be used with a variety of working pairs.

Furthermore, it creates a mechanism for estimating the global machine's COP. Suresh et al. (2020) discovered that hybrid systems are a viable alternative if the primary goal is to reduce CO2 emissions. This is because hybrid systems can compensate for the shortcomings of one technology by utilising the advantages. This is because hybrid systems can compensate for one system's weaknesses by using the capabilities of the other.

The "happening in these systems" phenomenon describes the transformation of thermal energy into chemical energy and vice versa that occurs as a result of thermochemical reactions (Parida et al., 2022). Depending on the design and desired outcome, these processes can produce cold or heat. If, on the other hand, a solid sorbent is used, the refrigeration unit will come to a halt. In terms of energy storage, however, thermochemical methods are preferred. The thermal energy supplied to these systems is either stored as chemical bonds or chemical potential, and the inverse process can be employed to retrieve this energy later (Mahon et al., 2021). These systems are ideal candidates for long-term energy storage, generally referred to as seasonal storage, because of the high energy density of the working pairs and the low heat losses that occur during operation. As a result, we know more about these devices' storage capacity, which bodes well for their use in solar-powered applications.

The term "thermochemical storage" refers to various techniques that may or may not include sorption (Aydin et al., 2015). Both chemical adsorption and chemical absorption are

formed in chemical sorption. As the fundamental distinguishing property between the two types of sorption, the sort of force at work distinguishes physical sorption from chemical sorption. Chemical sorption is caused by valence forces, while Van der Waals forces cause physical sorption. Another distinction between chemical and physical sorption is the process's thermodynamic unpredictability. The valence equals two in the case of physical absorption and adsorption but one in the case of chemical sorption. Mono variant processes are commonly used to describe solid-gas sorption processes. Reversible solid-gas reactions have a high energy density because they are dependent on reaction heat, which is greater than both sensible and latent heat. This reduces the required equipment's size, cost, energy density, and the energy stored (Moumin et al., 2019). The existence of a solid, which creates a constraint in heat and mass transmission and has a negative impact on the system's kinetics, is the fundamental limitation of storage systems based on reversible solid-gas processes. Because the constraint is imposed by the solid, this is the case. A variety of potential solutions to this problem have been proposed in the literature, including the usage of fluidized reactive beds.

2.5 Performance Evaluation of Solar Adsorption Refrigeration System

The effectiveness and efficiency of a solar adsorption refrigeration system using a wing-type compound parabolic concentrator were investigated by Ojha et al. (2021). Using a wing-type compound parabolic concentrator (CPC), a simulation study was conducted on a solar adsorption refrigeration system using a wing-type compound parabolic concentrator (CPC). The system includes a condenser, a refrigerator, an adsorption bed, and an angle-adjusted wing-type collector for maximum efficiency. As opposed to a linear collector, a wing collector may gather more solar energy in the morning and afternoon and maintain an adequate temperature for a more extended period. The study's purpose was to assess the system's performance, quantify the impact of wing length, and compare the performance of other linear CPC systems and wing types.

The mass and energy balance equations served as the foundation for developing a comprehensive dynamic simulation model. The simulation demonstrated that the system performance of a wing-type CPC increased by up to 6% in the summer and up to 2% in the winter when compared to a linear CPC with the same collector length. The wing-type CPC allows for a 13 percent increase in ice output during the hot summer months. This demonstrated that the wing-type CPC outperforms the linear CPC with the same collector length and without the necessity for tracking in terms of system performance.

2.5.1 Performance of Mobile Solar Adsorption Refrigeration System

Adsorption results in a decrease in pressure, which can lower the temperature to the desired level. Thiangchanta et al. (2020) investigated the design and prediction of solar adsorption cooling for mobile vaccine refrigerators. Adsorption cooling is a technique for chilling a substance that uses a pressure decrease generated by the adsorption of adsorbate onto an adsorbent. This method can transport vaccines that need to be kept at temperatures between -2 and -8 degrees Celsius to stay viable. The temperature in the primary chamber can be lowered via water adsorption into zeolites, which can also result in a decrease in pressure. The process of water absorption will become less critical until it achieves saturation. Heat is essential for the system's continuity since it starts the desorption process. The portable vaccination refrigerator can reach 2 degrees Celsius in 180 seconds and provide up to 1,530 watts of cooling electricity, according to a simulation done in MATLAB. The temperature of the vaccine compartment may remain within the permissible limit for up to 15.6795 hours due to the insulation.

The absorption vapour compression hybrid refrigeration cycle has been proposed as a possible way to reduce the amount of mechanical effort required when using low-grade heat sources like solar energy. Yang et al. (2019) researched the best refrigeration settings, behaviour switching, and thermodynamic analysis for a hybrid absorption–compression refrigeration cycle. The thermodynamic process behind the hybrid refrigeration cycle will be investigated in this study. The ultimate refrigerating temperature (also known as the maximum temperature lift) and behaviour turning are considered fundamental notions that have been improved. The interaction mechanism of raising compressor pressure with other relevant factors and the effect of increasing compressor pressure on cycle performance were explored using this data. The most critical requirements were the concentration differential, the working fluid circulation ratio, and other factors. According to the investigation, when the compressor's output pressure changed, the performance of the hybrid refrigeration cycle changed.

Furthermore, whether the absorption or compression subsystem was dominant determined the performance of the hybrid refrigeration cycle. When the parameters are changed, the behaviour switches direction and the heat-powered coefficient of performance reaches its maximum value. The performance of the hybrid refrigeration cycle was at its peak in this circumstance, as low-grade heat consumption was the most efficient. A solar hybrid refrigeration cycle with R134a and DMF as the working pair was simulated to support the theoretical analysis. The Peng–Robinson equation of state was chosen as the most suited method for obtaining the thermophysical properties of the R134a and DMF system. This

decision was taken after examining the prediction models' accuracy using data from the relevant literature. The results were very similar to the theoretical investigation.

An absorption refrigeration cycle-based automotive air cooling system was investigated and modelled by Liang et al. (2020). The waste heat-driven vapour absorption refrigeration system is a replacement for the traditional vapour compression refrigeration technique used in automotive air conditioning. To cool the vapour, this system absorbs it. A steady-state simulation model was needed to undertake a performance analysis of the vapour absorption refrigeration system and examine the limits imposed by the proposed system. When compared to the typical refrigerants commonly used in vapour compression refrigeration applications, the water lithium bromide pair was chosen as a working mixture because of its superior thermodynamic and transport qualities. The suggested vapour absorption refrigeration system's pump requires less electricity than standard vapour compression refrigeration systems' compressors. It has been claimed that vehicles might have a single absorption system layout.

2.5.2 Performance and Simulation Solar Vapor Absorption Cooling System

The performance and modelling of a solar-powered vapour adsorption cooling system were investigated by Xu et al. (2019). Saudi Arabia has three distinct climates, and the study evaluated the efficacy of a single-effect absorption cooling system in each of them. The proposed system has a capacity of 10.5 kW and will run on LiBr and water pairs. The analysis discovered that the cooling cycle's significant dynamic response increased the time required to establish steady-state operations by up to 30% and made the system more susceptible to the formation of lithium bromide precipitation. The performance dynamics were also investigated under various heat inputs.

The results showed that increasing the heat input reduced the transient's duration. In addition, the solar absorption system's effectiveness was assessed by simulating a typical summer day in each of Saudi Arabia's climate zones. If there is no alternative heat source between the hours of 9:00 a.m. and 4:00 p.m. every day, the results indicate that a combination of distinct collector zones must meet the absorber heating demand. Between midnight and nine a.m., it was concluded that external heating was required. Based on the data, the system was predicted to run more efficiently in Riyadh than in Jeddah and Dhahran. This study demonstrated that while analysing the performance of such systems, the thermal inertia of the system's components must be taken into account.

2.5.3 Performance Analysis of Solar Adsorption Cooling System

Altun and Kilic (2020) investigated the effect of heat storage tank placement on solar adsorption cooling system performance. A solar-powered adsorption cooling system was added to the design and an insulated storage tank. The storage tank was expected to play a substantial role in the chiller's overall performance, which it did. The solar-heated storage tank was connected to a single-stage, two-bed primary adsorption chiller. Two different ways to activate this chiller were silica gel and water. The solar collectors supplied hot water to the desorption bed, and the desorber's effluent was collected in a reserve tank. The reserve tank also provided water to the collector and completed the heat transfer cycle. The solar collector was in charge of sending hot water to the tank and then forwarded it to the desorber. The desorber's effluent was supplied to the collector once more. Studies comparing both systems were undertaken while they were in their steady states, in addition to the heat storage tank. The system's architecture was stable, and it was discovered that the system's performance improved after sunset due to heat storage.

Many researchers are motivated to examine its possibilities because of the economic and environmental benefits of the solar adsorption refrigeration (SAR) system in the design of cooling systems. Panda et al. (2021) used multidimensional mathematical models to forecast the value of the SAR system's coefficient of performance (COP), which was obtained as a function of the evaporator, condenser, and generator temperatures. A mathematical model based on one-dimensional data gathering was constructed using fuzzy logic and regression analysis. The model provides several correlations between the COP value and condensation, evaporation, and generation temperatures. One-dimensional data gathering was used to create this model. Observations revealed that the results of calculating COP with the two different models matched the measured values quite well. Compared to the computed COP value, however, the fuzzy logic technique significantly outperformed the regression model. This is owing to the optimal nature of the procedures involved in creating the needed model using fuzzy logic.

Halon et al. (2019) investigated the use of artificial neural networks to forecast the performance of solar adsorption refrigeration systems. The researchers suggested a method for analysing the performance of a single-stage solar adsorption refrigeration system with activated carbon R134a as the working pair. An artificial neural network was presented to calculate the system's performance parameters, including the coefficient of performance, specific cooling power, adsorbent bed discharge temperature (thermal compressor), and solar cooling coefficient of performance. The neural network toolbox in MATLAB (version 7.8) was used

to create the artificial neural network (ANN) utilised to predict performance. Temperature, pressure and sun insolation were the input layer factors. Researchers used a back-propagation technique with three different variations scaled conjugate gradient, pola-ribiere conjugate gradient, and Levenberg-Marquardt (LM) and logistic to find the optimal strategy sigmoidal transfer function. The 9-neuron LM algorithm was the most suitable for modelling a solar adsorption refrigeration system after training. R2 values for ANN performance parameter predictions are close to 1, and the maximum error rate is less than 5%. This means that the forecasts and the experimental results agree. The RMS and covariance values were found to be within the acceptable ranges.

2.5.4 Simulation of Solar Autonomous Absorption System

Because of Algeria's vast terrain and the significant number of geographically isolated rural districts, there is a high demand for solar-powered, autonomous cooling systems that do not require an auxiliary boiler. In Batna, Algeria, Ammari et al. (2018) investigated the performance of a small capacity solar autonomous absorption air-conditioning system in combination with a low-energy residential building. Using the TRNSYS-EES application, a dynamic simulation model for solar autonomous absorption air-conditioning systems was built. The model was used to explore the system's practicability and evaluate its performance using the meteorological conditions in Batna, Algeria. With a single effect, the suggested system used solar thermal flat plate collectors to power a modest-capacity LiBr water absorption chiller. This was done to suit the cooling needs of a typical low-energy residential construction with a floor area of 120 m2. A model of a 4.5 kW cooling capacity commercial absorption chiller was created using EES software. Because the prediction and experimental data had a high degree of concordance ($R^2 > 0.98$), the validation findings demonstrated that the model could accurately anticipate the chiller's performance. According to the dynamic analysis results, the proposed mechanism and size allow the chiller to operate for up to ten hours each day. This ensured a steady supply of cold water (between 8 and 18 degrees Celsius) and a comfortable temperature of 26 to 28 degrees Celsius.

Alizadeh et al. (2018) studied solar-powered perfect adsorption cooling systems, including numerical modelling and performance evaluation. In a solar-powered adsorption cooling system, the study looked at one of the environmentally beneficial approaches to reducing cooling energy requirements. To analyse the broad theoretical performance trends of a solar-powered adsorption cooling system, TRNSYS and MATLAB were used throughout the investigation. Several constant and seasonal transient models investigated the effects of a range

of cycle improvements, working pairs, operating and design circumstances, and how these affected overall performance. A normalised model was also developed to assess the effects of various system sizes, the need for a backup power system, numerical modelling, the collector area, and the adsorbent mass. The results were presented as cooling capacity values and ratios weighted by the performance coefficient (COP). Under the investigated conditions, wet cooling towers, the thermal wave cycle, high evaporation temperatures, and evacuated tube collectors had the highest COP values. For both the primary and heat recovery processes, the adsorbent bed's heat capacity and shell were lower. To attain the highest COP possible, the adsorbent bed must be cooled to condensation temperatures in all circumstances. It was discovered that the temperature of the available heat source influenced the choice of a functional pair. This was the case because each working pair had a temperature range within it could perform.

Pandya et al. (2018), from India, presented a paper that comprised the modelling and simulation of a solar absorption cooling system. The article illustrates a solar-powered, single-stage absorption cooling system that uses a flat plate collector and a water-lithium bromide solution. Computer software was built to simulate various cycle configurations for the absorption system. Several meteorological data for the village of Bahal in the Bhiwani district in the Indian state of Haryana were used to do this. The impact of hot water inlet temperatures on the absorption cooling component's performance coefficient and surface area is being examined. The surface area of several system components was affected by the temperature of the entering hot water. The impact of the reference temperature, which was the lowest allowable hot water inlet temperature, was also assessed in terms of the fraction of total load satisfied by non-purchased energy (FNP) and the performance coefficient. A higher reference temperature increased the system COP while reducing the surface area of system components, whereas a lower reference temperature gave better FNP results.

Cagnoli et al. (2018) created a detailed one-dimensional numerical model that explained the heat and fluid-dynamic behaviour inside a compound parabolic concentrator (CPC) utilised as an ammonia vapour producer. A two-phase flow model of a solar concentrator was used in this study to see if it might be used as an ammonia vapour generator in an absorption refrigerator. The governing continuity, momentum, and energy equations and the energy equation in the tube wall and the thermal analysis in the solar concentrator were solved in the CPC absorber tube. The computational methods developed and implemented aided in the design of the solar vapour generator used in absorption cooling systems. A number of analyses were carried out to see how different CPC design characteristics affected the exit temperature and vapour quality. The accepted half-angle and CPC lengths, the diameter of the

absorber tube, it is a coating, and the materials used to make the cover, reflector, and absorber tube, were among the criteria. When striving to increase ammonia-water vapour production, it has been determined that the reflector material, absorber tube diameter, selective surface, and acceptance half-angle are the most important design aspects to consider. After ranking the criteria from most important to least significant, this conclusion was reached. The direct ammonia-water vapour generation produced by a 35-meter long CPC was coupled to an absorption refrigeration system model to calculate the solar component, cooling capacity, coefficient of performance, and overall efficiency during a typical operational day. It can provide roughly 3.8 kW of cooling at a temperature of -10 OC, with solar efficiencies of up to 46.3 percent and total efficiencies of 21.2 percent.

Rashidi and Yoo (2018) looked at the thermodynamics and economics of two new high-efficiency power-cooling cogeneration systems based on the Kalina and absorption refrigeration cycles. Two innovative power and cooling cogeneration systems based on the Kalina cycle (KC) and the absorption refrigeration cycle (AC) have been explored and proposed. The Kalina Power-Cooling Cycle (KPCC) combines the Kalina Cycle (KC) with the water and ammonia absorption chiller's refrigerant loop. An evaporator and two throttle valves make up the refrigeration circuit. A portion of the KC mass flow is sent to the evaporator to generate cooling after condensation in the KPCC system. The KPCC is a flexible system that can adjust its power and cooling cogeneration to meet the needs of the situation. The Kalina lithium bromide absorption chiller cycle is the second technique that has been proposed (KLACC). It consists of a single-effect KC and a lithium bromide-water absorption chiller (AC LiBr-water). Heat is released from the KC subsystem and passed to the AC LiBr water disrober before it can condense in the condenser. Performance and cost analyses are performed on both proposed systems and the stand-alone KC, and the results are compared. The sensitivity of efficiency and the amounts of electricity and cooling generated to the essential operating factors were explored using a parametric analysis. According to the data, the KPCC system's thermal efficiency and total yearly costs were reduced by 5.6 percent and 8%, respectively, whereas the KLACC systems grew by 4.9 percent and 58 percent, respectively. Because KLACC has a 42 percent higher power-cooling efficiency than KPCC, it can be employed in situations where cooling generation is the primary goal, regardless of cost.

2.5.5 A Mathematical Model for Performance of Zeolite Water Adsorption Cooling System

A mathematical model was developed and analysed to simulate the thermal performance of a single bed zeolite water adsorption cooling system (Ahmed et al., 2018). We were able to solve a set of equations expressing the energy balance of the system's components using the application Engineering Equation Solver (EES). An experimental test loop was created to verify the model's and system's technological viability. The temperature fluctuations in the adsorption bed, condenser, and evaporator were tested and analysed. The performance coefficient of the system was discovered to vary depending on the mass concentration ratio of the water vapour present in the system. The ideal coefficient of performance (COP) was 0.39 when the minimum and maximum adsorbate concentration ratios were around 0.077 and 0.2, respectively. When the temperature was around 170 degrees Celsius, the coefficient of performance (COP) was at its highest. As a result, the model could be considered a valuable tool for researchers and engineers to use in designing, simulation, and analysing the adsorption cooling system's performance. The model's findings showed acceptable consistency with the experimental results.

Traditional steam and gas turbine cycles are powered by sun thermal producing facilities that focus on direct solar energy (also known as concentrating solar power, or CSP). They can be used with huge facilities that store heat at high temperatures to produce thermal energy. According to Srivastava and Yadav's (2018) study on CSP, in addition to wind and photovoltaic electricity, concentrating solar thermal power (CSP) contributes significantly to the availability of energy from renewable sources. CSP is a well-established technology with a proven track record of cost and performance. This is due to the roughly thirty years of multi-megawatt operational expertise in its development. It is feasible to offer power according to demand by combining thermal energy storage with electricity. There are 1.3 gigawatts (GW) of solar thermal power plants operating worldwide, with another 2.3 GW under construction and 31.7 GW in advanced planning. It is possible to reach temperatures of up to 1,000 degrees Celsius depending on the concentration factors in order to create saturated or superheated steam for use in steam turbine cycles or compressed hot gas for use in gas turbine cycles. The heat lost during these thermodynamic cycles can be reused for seawater desalination, industrial processes, and as a central source of cooled water. Even though the cost of generating power from CSP plants is now greater than from wind turbines or photovoltaic panels, the value of this method of electricity generation is higher due to its independence from daily fluctuations in wind speed and solar radiation. To compete with conventional power plants for mid-load

electricity in the next ten to fifteen years, technological advancements will need to be combined with mass production of components, increased plant capacity, and more expertise in planning and operating the plant. The DESERTEC Industry Initiative was formed on October 30, 2009, when a number of major industrial businesses banded together. By 2050, this initiative intends to create 15% of Europe's electricity from renewable energy sources in North Africa and ensure the region's energy, water, income, and employment opportunities.

The Badia region of Jordan has serious electrical challenges, according to Sharmin's (2021) findings from the first experimental demonstration of a solar updraft tower power plant in Jordan in. This aim appealed to all of us since it would safeguard the environment while enabling easy access to the refrigeration process, allowing food and medical vaccinations to be stored at reasonable prices. A solar cooling method that uses solar power instead of batteries or electrical power, for example, allows for the storage and continuing use of a power system. A solar refrigerator pilot project was put to the test to guarantee that method control tests are accurate and exact and that technological data is collected consistently. Solar refrigerators don't need electricity since they use convection and conduction to heat and chill the food within.

Furthermore, it was made with widely available resources such as sand, scrap metal, and cardboard. An inner metal cylinder is installed inside, while an exterior wooden or plastic cylinder is installed on the outside. An organic substance such as (sand, wool, or soil) is placed in the space between the two cylinders, and the space is then saturated with water. It is made up of two cylindrical halves. The sun's heat evaporates the water, while the inside chamber is cooled to keep the temperature at six degrees Celsius.

2.5.6 Economic Investigation of a Solar Thermal-Driven Two-Bed Adsorption Chiller

Alahmer et al. (2020) conducted a study investigating the dynamic and economic aspects of a solar thermal-driven two-bed adsorption chiller while it was operating in the climate of Perth. An evaluation of the efficiency of a refrigeration system powered by solar thermal energy and consisting of two beds of silica gel-water adsorption was carried out in a climate representative of Perth, Australia. Based on the actual data received from the Meteonorm programme, version 7.0 for Perth, Australia, a Fourier series was utilised to simulate solar radiation. In order to evaluate the economics of the system and optimise the demand for solar collector areas, two different economic approaches, namely Payback Period and Life-Cycle Saving, are utilised. According to the study's findings, the order of the Fourier series did not significantly impact The average cooling capacity of the chiller at peak hour 13:00 for a normal summer day is approximately 11 kW, while the cyclic chiller system

coefficient of performance COP and the solar system COP are about 0.5 and 0.3, respectively. According to the economic study results, the payback period for the solar adsorption system that was investigated was around 11 years, and the best solar collector surface area was approximately 38 m2 when employing a compound parabolic collector (CPC) panel. According to the study's findings, it is technically and economically feasible to use solar-driven adsorption cooling in environments with weather conditions similar to those seen in Perth, Australia.

A study on the most current developments in the technology of solar thermal sorption cooling systems was carried out by Hussain et al. (2018). The most recent advancements in adsorption and absorption of solar cooling systems were the primary focus of this study. There is both an in-depth thermal analysis and an economic evaluation provided. The absorption process operates in a closed cycle and makes use of a variety of liquid sorbents; however, the combination of liquid bromine and water is the most prevalent type of refrigerant. The most efficient coefficient of performance (COP) that can be attained is 0.8, but the conventional cooling system can get up to 3.

In contrast to the other solar cooling systems, absorption has the highest coefficient of performance (COP). The amount of heat and mass transfer, the number of stages, the number of beds, the kind of solar collector, the cooling load schedule, the management strategy, and the thermal storage capacity all play a role in the performance of the absorption cooling system. A vast number of studies have been prompted to find ways to solve these limitations as a result of the high initial cost and low efficiency. Utilization of a high-temperature solar receiver, double-effect chiller, sophisticated control, and better chiller efficiency are some ways the system's efficiency could be enhanced.

The adsorption method operates in a closed cycle and makes use of a variety of solid adsorption and desorption combinations. The system's performance is mostly dependent on the kind of adsorption and desorption pairs used, the temperature of the source, the design of the adsorption chiller, and the operating conditions. Significant commercial expansion is not possible due to the lengthy amount of time required for adsorption and desorption, the scale of the system, the high cost of adsorption chillers, and the poor performance of adsorption chillers. The coefficient of performance (COP) was measured to have attained 0.45, which, in comparison to the other cooling system, was regarded as a very poor result. A high COP and SCP could be attained by increasing the amount of heat and mass recovery, as well as by creating technologies with several stages and beds and by optimising the operating parameters.

Up until that point, the Pb of both the solar absorption and adsorption system had surpassed the lifespan in significant portions of the world.

As a consequence of this, it was essential to enhance the performance of these systems. The absorption system achieved the greatest commercial penetration among the several sun cooling technologies. The absorption chillers that are fitted with thermal energy storage systems have the potential to offer a solution for space cooling that is both technically and economically feasible. Based on the results of the economic analysis, it was determined that the solar cooling system is only viable for use as a double-purpose system (heating and cooling systems), which has a higher coefficient of performance (COP) than single-purpose systems. In conclusion, parabolic trough concentrators have the potential to dramatically boost the efficiency of solar cooling (Li et al., 2022).

2.5.7 Economic Assessment of Solar Absorption and Absorption Refrigeration Systems

The team explored the exergy economic assessment of solar absorption and absorption compression hybrid refrigeration systems in building cooling (Jing et al., 2018). The study's main focus was on the compatibility of solar refrigeration. Exergy-based building cooling, solar or natural gas-powered absorption chillers (SNGDAC), solar vapour compressional absorption integrated refrigeration systems (SVCAIRSPC), and solar absorption subcooled compression hybrid cooling systems were among the options (SASCHCS). The following three cooling strategies for a structure were investigated: The Type 1 category includes two- and three-story constructions. Type 2 buildings are single-story structures, while type 3 structures are multi-story structures. Turpan, as well as both Chinese cities, were also considered.

The rate at which product costs were incurred was the key variable used in the calculation. SNGDAC was shown to be a viable choice for Guangzhou type 1 buildings as a result of the investigation. This was due to the fact that it used almost no natural gas and had a lower flow rate in terms of the product cost. Because of its higher actual cooling capacity and lower fuel and product cost flow rate, SVCAIRSPC was more suitable for type 2 buildings in Turpan. These two components contributed to the system's overall cost decrease. Furthermore, SASCHCS has the highest overall cost-effectiveness; particularly, when employed in all building types in Guangzhou or type 3 structures in Turpan, its exergy destruction and product cost flow rate are the lowest.

2.6 Solar cooling technologies

The term "solar cooling" refers to the equipment and systems that use solar energy for cooling (Huang & Zheng, 2018). Solar cooling systems use operating fluids that are largely non-toxic and environmentally friendly, such as water or a salt solution. Furthermore, these systems are capable of working on their own. Solar cooling systems can often produce refrigeration while conserving conventional energy (Sun et al., 2020). Both active and passive cooling systems are potential options (Khosla et al., 2021). When the amount of solar irradiation, also known as insolation, is at its highest, solar cooling system capacity is at its highest. As a result, solar cooling systems are well suited to meet the needs of countries located in sunny regions, when cooling demand is often at its greatest around midday (Laine et al., 2019). This research attempts to review current solar cooling technologies and the businesses that can benefit from them. Solar cooling systems and methods will not be restricted to those using sunlight to cool structures. The project will also include water cooling, perishable goods refrigeration (pharmaceuticals or food), and saltwater desalination. Solar cooling employs at least four different ways that have been proven to be effective: Vapour compression, sorption-based cooling (including absorption and adsorption chilling), and evaporative cooling are all options. Vapour compression is the most common method (Singh & Das, 2021).

Solar cooling is now the most popular application for CST heat systems and a potential application for solar process heat (Eveloy & Ayou, 2019). Throughout the summer, air cooling rapidly dominates the midday to evening period of peak electricity demand in many countries. This is something that the utility business is well aware of. Because solar irradiation is at its peak right now. Any device that can convert solar energy to cold is perfectly positioned to take advantage of the perfect storm of high demand and ideal operational circumstances.

Scientists have previously examined a wide range of solar cooling approaches, including PV-driven vapour compression and other options for thermally-driven cold and dehumidification cycles (Almasri et al., 2022). The battle to develop the most powerful, reliable, or cost-effective technology is still ongoing. However, there will be no single best technique because of the many different boundary conditions. Hot and humid temperatures, for example, necessitate a different response than dry, desert-like settings.

A system's cooling capacity is the quantity of heat it can remove from a cooled region over time (Afshari et al., 2019). The refrigerant's specific enthalpy in the evaporator is the difference in the refrigeration load multiplied by the refrigerant's mass flow rate. The refrigeration load has caused this change.

Non-steady-state processes must be taken into account when estimating cooling loads. This is due to the fact that the maximum cooling demand occurs during the day, and solar radiation produces significant environmental changes throughout the day (Nguyen et al., 2020). Furthermore, all internal sources contribute considerably to cooling loads. Ignoring them would result in an overestimating necessary cooling capacity and a danger of failing to sustain acceptable interior conditions. As a result, predicting cooling demands is inherently more difficult (Fu, 2018). The sensible and latent loads induced by ventilation and leakage losses in the return air ducts and the heat created by the return air fan must all be taken into account when determining the system's needed cooling capacity.

The most popular cooling system powered by solar thermal collectors is absorption heat pumps (Huang & Zheng, 2018). The fundamental principle of thermodynamics is summarized as follows: Heat received from a collector at a high-temperature T3 is utilized to "pump" heat from a low-temperature level T1 to an intermediate temperature level T2. Low temperatures cause cooling (the thermodynamic principle of "cooling" is the elimination of heat from a system). At T1, a refrigerant is evaporated at low partial pressure, and the heat emitted is absorbed by a second working fluid (at T2). The diluted solution is heated outside to freshen it (at point T3). This indicates that the solution was boiled in order to eliminate the refrigerant (desorbed). It then passes through a second condensation process (at T2) to become liquid and given to the evaporator. Although the temperatures of absorption and condensation at T2 do not have to be identical all of the time, it is frequently preferable to do so.

Ammonia/water and water/lithium bromide are the two most common working combinations. Water is utilized as the refrigerant in the first case, while ammonia is used in the second (Mussati et al., 2019).

Figure 19.1 depicts this thermodynamic concept as well as the basic heat flux and temperature values. The heat transfers from the cold zone, Q1, to the heat driving the system is thus characterized as the so-called coefficient of performance (COP)

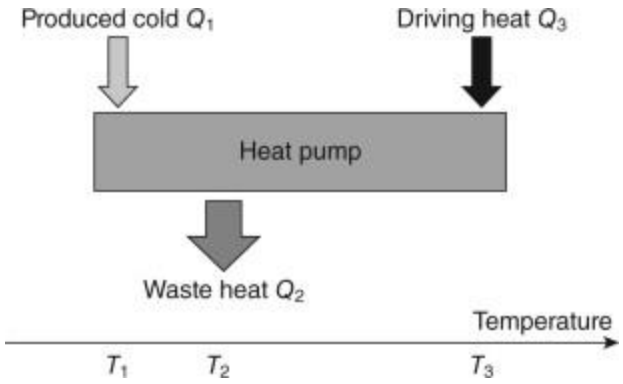

Source: Raj et al. (2019).

2.6.1 Vapor Compression Refrigeration System

A circulating liquid refrigerant is used in a vapour-compression refrigeration system to collect and convey heat from the space to be cooled before dissipating it elsewhere. "Vapor compression" is the name for this technique (Roy & Kundu, 2021). The vapour-compression refrigeration cooling system is very common to provide air conditioning and supply refrigeration. According to Chahartaghi et al. (2019), Vapor compression machines are closed-loop systems that include a mechanical compressor, condenser, expansion valve, and evaporator. These components are in charge of changing the refrigerant's thermodynamic states. The compressed and heated vaporous refrigerant is compressed and heated in the compressor. The refrigerant is prepared to be condensed into a liquid in the condenser during this phase. According to Jiménez-Garca and Rivera (2018), the condensation process discharges thermal energy from the refrigerant into the condenser. Water or air can absorb this energy and remove it from the system. The condensed refrigerant is subsequently passed via an expansion valve, which causes a significant pressure reduction. This causes some liquid refrigerant to evaporate quickly, cooling the resulting combination of liquid and vaporous refrigerant. The cooled mixture is then passed to the evaporator, using air from the cooling chamber to vaporise the refrigerant's liquid part. After that, the combination is given to the condenser. This allows the extraction of thermal energy from the air before it is cooled. The loop is complete when the vaporous refrigerant is recirculated back to the compressor. The development of vapour compression technology began in the nineteenth century (Turner, M. W.). [Bibliography is required] (2020). Even though most of the equipment used in the vapour compression process is powered by electrical or mechanical energy, solar cooling could contribute significantly to the procedure's energy supply.

Despite being a highly developed and widely used technology, vapour compression is plagued by vibration and noise issues due to the functional principle adherence of its components (Zou et al., 2020). According to Capr et al. (2020), there are alternatives to vapour compression machines in sorption-based cooling systems. These devices use processes that are different from machines that compress vapour. Furthermore, sorption-based cooling systems are appealing if the power supply is insufficient or expensive or if thermal energy, such as from solar plants or solar heat collectors, is readily available. These circumstances make sorption-based cooling systems more appealing. Sorption relies on chemicals called sorbents, which have the ability to "hold" liquids or gases as a cooling mechanism (Lee et al., 2019). Absorption cooling, in which liquids or gases are dissolved in the bulk of the sorbent and then released, and adsorption cooling, in which liquids or gases are bound to the surface of the sorbent and then released, are the two types of cooling technologies. Sorption cooling refers to these cooling processes (Almasri et al., 2022). These phase shifts are always accompanied by a release or expenditure of thermal energy.

Vapour compression refrigeration systems primarily consist of a compressor, a fixed-orifice expansion device, two heat exchangers (condenser and evaporator), and a light secondary fluid known as (refrigerant), which readily evaporates and condenses. Vapour compression refrigeration systems are frequently utilised to deliver chilled media for space heating and climate control in commercial buildings. Since then, the system has been closed, and refrigerant never escapes the system because it is closed (She et al., 2018).

Two separate refrigeration models have been applied in the chilling food business. Photovoltaic energy can power both thermoelectric and vapour compression refrigeration in these systems. Dai et al. (2003) reported that a thermoelectric refrigerator powered by solar cells has a coefficient of performance (COP) of 0.3 and can maintain a temperature between 5 and 10 degrees Celsius. A thermoelectric refrigerator can only be used for cold storage due to its ability to produce heat. It cannot freeze food due to the limitations of its operating principle. Researchers were intrigued by photovoltaic-powered vapour compression refrigeration for the reasons stated above. When Riffat et al. (2021) tested the performance of a DC-driven vapour compression refrigerator, they discovered that when a DC-driven compressor was used, the coefficient of performance (COP) rose by roughly 27%. At an ambient temperature of 42 degrees Celsius, Ekren (2020) was able to attain a coefficient of performance (COP) of 2.102 for a solar-powered alternating current (AC) refrigerator. This has a substantially higher value than other types of refrigeration systems. Variable-speed compressors supplied by either AC or DC can be used in PV-driven vapour compression refrigeration systems. To minimise future

issues, it would be smart to assess the functioning of both systems. When it comes to variable-speed compressors, Su et al. (2020) found that DC compressor operation is significantly more efficient than constant speed operation in their experiments. Variable speed DC compressors enhanced exergy efficiency by more than 4% and coefficient of performance by more than 7% compared to constant speed DC compressors.

Due to the difficulty of maintaining a consistent sun thermal system throughout the day (Muz et al., 2022), solar thermal cooling systems have a lower thermodynamic efficiency than vapour solar refrigeration systems. Commercially available solar thermal energy-powered cooling systems typically have a capacity of more than 20 TR due to the inability of solar collectors to shrink in size.

The most appealing and cost-effective economic solution is to use traditional vapour compression refrigeration systems in conjunction with PV panels, as proved by (Varvagiannis et al., 2021). According to Gado et al. (2021), PV vapour compression refrigeration systems have proven their competitiveness in terms of efficiency, investment cost, and solar collection area, thanks to a considerable drop in PV panel prices. The two most popular cooling mechanisms in milk refrigeration systems are vapour absorption and vapour compression. This is because the devices can generate temperatures below 0 degrees Celsius, and temperature profiling is simple to maintain (Mahalle et al., 2019).

An evaporator, compressor, condenser, and expansion valve make up a vapour compression refrigeration system, according to Joshi et al. (2022). The expansion valve separates the high-pressure and low-pressure sides of the system. The compressor's condenser and another component are located on the high-pressure side of the system. The evaporator and another compressor component are located on the low-pressure side of the system. When the liquid refrigerant in the evaporator boils due to low pressure, the refrigeration effect is noticeable. Figure 2.1 illustrate the basic components and the refrigerant cycle of the system.

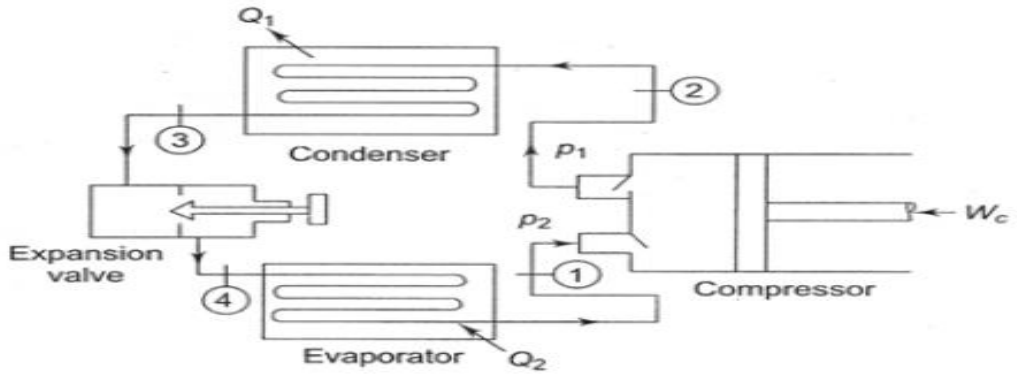

Figure 2.1: Components of VCR system *(Source: Khurmi & Gupta, 2008)*.

Zhang et al. (2018) stated that VCR has higher (COPr) than other refrigeration systems and is less bulky. Dhamneya et al. (2018) showed the evaporator cooling process in a VCR system operating on dry saturated refrigerant to the compressor. Devecioğlu and Vedat (2018) showed that the COP_r of a VCR system is expressed in terms of refrigerant enthalpies as in Equation 2.22

$$COP_r = \left(\frac{\dot{Q}_L}{W_{in}} \right) = \left(\frac{h_1 - h_4}{h_2 - h_1} \right) \qquad 2.22$$

2.6.2 Thermal Design of Evaporators

The thermal design of Refrigeration Evaporators is complicated due to the difficulty in determining the heat transfer coefficients in both the refrigerant and the fluid-cooled (Devecioğlu & Vedat, 2018). This arises due to the Heat transfer coefficient varying widely along the tubes due to refrigerant evaporation and change of flow regimes from individual bubble to stable thin-film boiling regimes, and significant pressure drop in the evaporator, which is more critical as it influences the evaporator performance.

De Blas et al. (2003) developed a correlation of refrigerant's two-phase heat transfer coefficient inside a horizontal tube as shown in Equation 2.23.

$$\alpha = 262.89 \times \frac{k_l}{D_b} \left(\frac{q_l \times D_b}{k_l \times T_{re}} \right)^{0.745} \left(\frac{\rho_v}{\rho_l} \right) \times \mathrm{Pr}_l^{0.533} \qquad 2.23$$

Where;

α is heat transfer coefficient (W/m^2 K)

k_l is the thermal conductivity of the liquid refrigerant (W/m-K), D_b is the bubble departure diameter (m), q_l is the heat flux in the liquid (W/m^2), T_{re} is the absolute temperature of refrigerant (K), ρ_v and ρ_l densities of saturated vapour and liquid refrigerant resp.(kg/m^3),

Pr_l is Prandtl number of liquid refrigerants.

The heat transfer rate in the evaporator was expressed by Dabas et al. (2014) as in Equation 2.24

$$Q_E = \dot{m}(h_i - h_o) \qquad 2.24$$

Where;

Q_E is heat transfer rate (W), $\dot{m}$ is the mass flow rate of refrigerant in the evaporator (kg/s)

h_i is specific enthalpy of the refrigerant at evaporator inlet (kJ/kg)

h_o is the particular enthalpy of the refrigerant at evaporator exit (kJ/kg).

Kashif et al. (2020) showed that the evaporator cooling is expressed as in Equation 2.25

$$Q_e = a_1 + a_2 T_e + a_3 T_e^2 + a_4 T_c + a_5 T_c^2 + a_6 T_e T_c + a_7 T_e^2 T_c + a_8 T_e T_c^2 + a_9 T..{}_e^2 T_c^2 \quad 2.25$$

Where;

T_e and T_c are evaporator and condenser temperature ^oC

a_1 to a_9 are constantly determined by curve fitting experimental data.

If the evaporator is treated as a counter-flow heat exchanger, the mean temperature difference, according to Shen and Gong (2018), is expressed as in Equation 2.26

$$LMTD = \frac{(T_{bi} - T_{bo})}{In\left[\frac{T_{bi} - T_c}{T_{bo} - T_c}\right]} \quad 2.26$$

2.6.3 Refrigeration Components Models

The four main components of a vapour compression refrigeration system are the compressor, condenser, thermal expansion valve and evaporator (Sun et al., 2020). The compressor size model involves the refrigerant mass flow rate in a high heat removal vapour compression refrigeration system as expressed in Equation 2.27 by Baakeem et al. (2018).

$$\dot{m} = \omega V_d \rho \eta_v \quad 2.27$$

Where;

ω is compressor speed, V_d is displacement volume, ρ , is inlet refrigerant density

η_v , is volumetric compressor efficiency, respectively

The volumetric efficiency was expressed as in Equation 2.28

$$\eta_v = 1 + C_v - d_r\left(\frac{p_o}{P_i}\right)^{Cv/C_p} \qquad 2.28$$

Where;

C_r, d_r is the coefficient of the compressor, P_o and P_i are compressor outlet and inlet pressures,

C_v is specific heat capacities at constant volume in compressor inlet

C_p is heat capacities at a continuous, consistent volume and constant pressure.

Work input to the compressor C_{wi} was expressed as in Equation 2.29

Herbert and Mohan (2010).

$$C_{wi} = \dot{m}(h_o - h_i) \qquad 2.29$$

Where;

h_o is the outlet specific enthalpies of the refrigerant, h_i and is the particular outlet enthalpies of the refrigerant at the compressor.

h_o is expressed as in Equation 2.30

$$h_o = h_i + (h_{is} - h_i)/\eta_s \qquad 2.30$$

Where;

h_{is} is the isentropic efficiency of the refrigerant at the compressor inlet.

Pastuszko (2018) stated that for a steady heat transfer rate, the uniform heat flux $q^{"}$ relates to the heat transfer rate of an evaporator q_E as in Equation 2.31.

$$q_E = q^{"} \times S_E \qquad 2.31$$

Where;

S_E is the evaporator surface area.

Herbert and Mohan (2010) considered condenser operating conditions in two or three zones.

A two-zone condenser has superheated and liquid refrigerant, while a three-zone consists of superheated, saturated liquid and undercooled refrigerant. The heat rejection for a zone K in the condenser $q_C K$ is as in Equation 2.32

$$q_C K = U_K \times S_K \frac{(T_o - T_{cool}) - (T_{iK} - T_{cool})}{In\left[\frac{T_{oK} - T_{cool}}{T_{iK} - T_{cool}}\right]} \quad 2.32$$

Where;

U_K is condenser overall heat transfer coefficient, S_K is surface area,

T_{cool} **A**nd T_{oK} are the second fluid temperature inlet and outlet at the K zone.

The total condenser heat q_C loss is the sum of heat losses for n number of zones, as in Equation 2.33

$$q_C = \sum_{K=1}^{n} q_C k \quad 2.33$$

Assuming an adiabatic expansion and a constant enthalpy process in the expansion valve, the pressure drops in the expansion valve, according to Knabben et al. (2020), is as Equation 2.34

$$\Delta P = \frac{\dot{m}}{K_V^2 \times A_V \times \rho_i} \quad 2.34$$

Where;

K_V Its coefficient of expansion valve obtained from the manufacturer

A_V is the percentage of the opened area of the valve, ρ_i is the refrigerant density at the inlet of the valve.

Ewert and Bergeron (2002) discovered that a solar-powered vapour compression refrigeration system could be made feasible with the help of thermal storage and inventive management tactics in their study of solar-powered refrigeration systems. In one form of the invention, the refrigeration system included a photovoltaic panel, a variable speed compressor, an insulated enclosure, and a thermal reservoir. Solar electromagnetic radiation is converted into direct current by the photovoltaic panel, also known as a PV panel (DC). A compressor is driven by DC electrical power to extract heat from the insulated container. In turn, a vapour compression refrigeration circuit feeds refrigerant through this compressor. A phase change

substance is contained in the thermal reservoir located within the insulated container. The phase change compound will freeze when heat is removed from the insulated container. Once frozen, the phase change material will act as a heat sink, allowing the temperature of the insulated enclosure to be maintained even in the absence of solar radiation. A compressor control system that maximises the compressor's consumption of available energy is used to optimise the conversion of solar electricity into thermal energy that can be stored. During the compressor's startup, a capacitor is used to help level off the voltage from the power supply and give additional current. A controller monitors the rate of change of the smoothed power voltage to assess whether the compressor is operating below or above the available power maximum. In response to this information, the controller adjusts the compressor's speed. The compressor's operation is tweaked to convert virtually all of the solar energy available into thermal energy that can be stored.

D'Isep and Sertorio (1983) investigated the non-equilibrium thermodynamic steady-state behaviour of a model system consisting of a core surrounded by an envelope that interacts with solar radiation and an external bath with a specific temperature profile. A core was wrapped in an envelope in the model system. The transmission of heat between the core and the envelope could be controlled by adjusting the thermal conductivity of the interface between the two components. This device worked like a passive heat pump by raising the core's average temperature above the typical equilibrium value associated with a constant value of the interface conductivity while reducing the oscillation it displayed over time. The system's conductivity can be changed to fluctuate over time, allowing it to serve as a refrigerator. Passive factors such as surface conductivities, heat capacities, and other comparable features were dependent on the performance constraints. The daily cycle was the sort of periodicity investigated in this study.

2.6.4 Thermal Storage Vapour Compression Solar Refrigerator

Thermal storage can be employed in applications where peak demand is limited to a few hours per day and load for the rest of the working or operational hours is substantially lower, such as milk cooling on farms. There is no load throughout the balance duration of 24 hours. Process applications, such as milk processing, are typical examples. Refrigeration requirements in milk processing are normally limited to six to eight hours per day, with no load during 24 hours (Sankar et al., 2018).

The scientific community is working hard to optimise the functioning of refrigeration plants due to the quantity of energy required by the refrigeration sector, which is estimated to be around 15% of total global energy consumption.

Compressor success in PV refrigeration systems is secured by the installation of a specific controller that allows for the simple startup, maximum power tracking, and compressor power management (Ramalingam et al., 2021). Batteries are responsible for a considerable percentage of the cost and maintenance in standalone PV vapour compression refrigeration systems. Batteries pollute the environment due to their high levels of polluting materials and short life cycle of 1500 charge/discharge cycles before being disposed of (Lai et al., 2021).

A study was undertaken by Khalifa et al. (2018) on constructing a battery-free solar refrigerator. As a result of NASA's aerospace refrigeration research, the study determined that recent technological advancements and a system engineering design approach led to the development of a feasible battery-free solar refrigerator. Suppose thermal storage is included and a direct link is built between the cooling system and the PV panel. In that case, off-grid refrigeration is a good application of solar photovoltaic (PV) power. Water was used as a phase-change medium in a well-insulated refrigerator cabinet. A microprocessor-based control system was developed to allow the direct connection of a PV panel to a variable speed compressor. This second advancement enabled peak power-point tracking from the PV panel and the removal of batteries from the system. A laboratory unit was created first to prove the concept, followed by the production of a commercial team and deployment in a field test. The laboratory unit was used to evaluate a variety of cooling systems cycles, including thermoelectric, Stirling, and vapour compression. A vapour compression cooling cycle, vacuum insulation, a passive condenser, an incorporated evaporator/thermal storage tank, two 77 watt PV panels, and the unique controller were all utilised in the final form. The variable speed BD35 compressor from Danfoss was the only moving portion in the system. With only 274 watt-hours per day of average PV power, the 365-litre cabinet stayed cool. For several months, battery-free testing was carried out with excellent results. The amount of thermal storage, compressor size, and power of PV panels linked can be modified to optimise the design for a given application and climate. The commercial unit addressed the high cost of the vacuum insulated refrigerator cabinet and the stainless-steel thermal storage tank to make the technology economically viable. This unit began with a mass-produced 142-litre chest freezer cabinet with the evaporator built into the inner walls.

Solar Chill, a solar PV refrigerator without a battery, was studied by Khalifa et al. (2018). A worldwide effort combining Greenpeace International, GTZ, UNICEF, UNEP,

WHO, industry partners, and the Danish Technological Institute resulted in the development of a solar-powered refrigerator (Solar Chill). The fridge may run entirely on solar PV panels without using battery or other electronics, making it ideal for sites where low maintenance and reliable operation are required. The Solar Chill Project's major goal is to assist in delivering vaccines and refrigeration to the rural poor. The Solar Chill Project was designed and intended to make a versatile refrigeration technology that is environmentally sound, technologically reliable, economical freely available in order to achieve this goal. Solar Chill's cooling technology and insulation do not include any fluorocarbons. Other solar refrigerators are being developed for household and small commercial purposes. This upright model is ideal for keeping food and beverages chilled in regions where grid electricity is unavailable or inconsistent. As a result, both developed and developing countries have the market potential for this type of product. Solar Chill is distinguished because energy is stored in ice rather than batteries. An ice compartment keeps the cabinet at the proper temperature during the night. The report outlined the product development process, potential Solar Chill applications, experience with the two types of solar coolers, and laboratory and field test findings.

The circulation of water through an ice bank is another method of chilling milk (IB). An insulated water tank holds a copper tube evaporator array in an IB. Ice forms a cylindrical shape around the copper tubes. Water circulates through the cooling device and back to the IB in a closed loop. Due to the lower evaporation temperature required for making ice, water circulators have greater coefficients of performance (COP) than IBs. Still, IBs are significantly more compact and less expensive to purchase and install due to the high energy density of ice (Sidney et al., 2020).

2.6.5 Rankine Cycle Vapor Compression for Power and Refrigeration Cogeneration

By analysing the performance of a combined organic Rankine cycle and vapour compression cycle for power and refrigeration cogeneration (Toujani et al., 2018). This paper presents a thermodynamic analysis of power and refrigeration cogeneration using low-grade sensible energy. The investigation included the limited situation of cold production without net electricity output using an organic Rankine cycle (ORC) for power generation and a vapour compression cycle (VCC) for refrigeration using the same working fluid. They looked at how critical characteristics, including net power production, refrigeration, and thermal and exergy efficiency, affected system performance. The total number of transfer units (NTU), size parameter (SP), and isentropic volumetric flow ratio (VFR), all of which are proportional to the cost of heat exchangers or turbines, were also investigated. The flow division ratio, turbine

intake temperature, and turbine inlet pressure were chosen as three key system parameters. The investigation was carried out on a variety of working fluids. Due to its relatively high efficiency, isobutane was selected for a sensitivity study in a few unique circumstances. The findings revealed that the device could successfully employ low-grade heat sources. Both the accepted settings and the working fluid have an impact on system performance.

Yan et al. (2020) looked at energy-efficient refrigeration and flexible power use in a smart grid. Refrigeration and heating systems use a lot of energy all over the world. However, because of the thermal capacity, the system had the potential to store 'coldness,' or heat or cooling loads. This capability allowed for various load shifting and shedding tactics to reduce energy consumption while maintaining the original cooling and indoor climate quality. They looked into the possibilities of such a method and its capacity to drastically reduce the cost of operating systems like supermarket refrigeration and heat pumps for residential homes in this study. They used weather forecasts and predictions of varying electricity prices to apply more load to the system when the thermodynamic cycle was most efficient and consume larger shares of the electricity when demand and thus prices were low, using modern Economic Model Predictive Control (MPC) methods. The capacity to regulate power use in response to power grid demands was a popular feature in a future Smart Grid. The efficient use of more renewable energy necessitates ways to control power consumption such that it increases when there is an energy surplus and lowers when there is a shortage. This should happen almost quickly to handle intermittent energy sources such as wind turbines. They hoped that their power management method would allow thermal storage devices to be used for flexible power consumption. The aggregation of numerous units then considerably contributed to the reduction in total electricity usage. They illustrated the possibility of exploiting daily changes to supply energy-efficient cooling or heating and the implementation of Virtual Power Plants in Smart Grid scenarios, using modest case studies.

Bellos and Tzivanidis investigated a solar-direct driven organic Rankine cycle vapour compression cooling ORC-VCC system with an electric motor for an air-conditioning office building (2021). This study proposed an ORC-VCC method powered by solar energy and propelled by an electric motor in a Guangzhou office building to ensure smooth operation when solar radiation was intermittent and unstable. China was chosen for this case study. The findings revealed that the beam solar radiation and generation temperature significantly impacted system performance. There was an ideal generation temperature at which the system performed at its best. In the hybrid solar cooling system design process, the cooling power per square metre collector was also considered a critical signal.

In comparison to the vapour compression cooling system, I discovered that the hybrid cooling system saved roughly 68.23% of electricity.

In conclusion, the generation temperature had a significant impact on the thermodynamic performance of the solar ORC-VCC system, which initially increased and subsequently dropped as the generation temperature climbed. More emphasis was devoted to cooling power per square metre solar collector when considering the term economic performance of the solar ORC-VCC system. With the inclusion of an electric motor, the hybrid solar cooling system was able to meet the cooling load for the target building even when solar energy was unreliable and intermittent. Electric motor electricity consumption is more affected by solar radiation intensity and cooling load. The solar ORC-VCC system saves up to 8094.87 kWh per day in electricity consumption.

2.6.6 Vapour Compression Refrigeration with Fresnel Lens and Sunlight Tracker

Chu et al. (2021) studied a solar refrigeration system that included a solar water vapour generator, a pump, a condenser, a throttling valve, an evaporator, and a liquid storage tank as a Fresnel lens and a sunshine tracker. This system also included a solar water vapour generator. The solar water vapour generator was a transparent glass pipeline positioned at the focus of the Fresnel lens, water flowed through the transparent glass pipeline, and a substance consisting of an expanded graphite layer and a carbon foam layer floated on the water's surface.

The focusing mechanism of the convex lens lowered the structure of the solar refrigeration system. The liquid water was transformed into water vapour using carbon foam and expanded graphite, which could be used for refrigeration. A solar energy absorption refrigeration system that used hot water as its heat source was compared to this technology. The structure of the solar refrigeration system was simplified, resulting in fewer potential failure points. Furthermore, the plan was corrosion-free and had a high heat consumption rate.

2.6.7 Phase Change Material Vapour Compression Refrigeration System

Siddharth et al. (2018) developed, researched, and simulated a phase change material-based vapour compression refrigeration system. The research focused on designing and manufacturing a solar-powered vapour compression refrigeration system. The impact of a phase transition material, ice, on a solar-powered vapour compression refrigeration system was examined. The battery and solar panels were chosen to allow the system to run independently for at least 12 hours. The inclusion of a phase change material in the refrigeration system produced a considerable increase in the compressor's off and on time. The ratio in which on

time increased was substantially greater than the ratio in which off time increased. The compressor on time increased by 219 percent, with the compressor off time increasing by 139 percent and compressor work increasing by 3.5 percent, with a 5.5 percent loss in COP. When there is enough load in the system to make the initial off, and on timings equivalent, the inclusion of a phase change material may lead the compressor to have a longer on period than its off period.

Sharma et al. (2020) examined the ESD capacity of several sorption refrigeration working pairs, such as absorption, adsorption, solid/gas reaction, and phase change materials (PCM). Absorption working pairs had the highest ESDs, 277 Wh/kg; stable/gas reaction working pairs had 353 Wh/kg; adsorption available pairs had 82 Wh/kg, and phase change materials had 85 Wh/kg. These figures were based on the mass of the species in question (i.e. refrigerant and its sorbent pair, except in the case of PCM, where only one specie is involved). The higher ESD of absorption thermal energy storage and thermochemical storage makes them more appealing for solar refrigeration than conventional thermal energy storage systems.

2.7 Solar Energy Radiation Models

Solar radiation is the major engine of many physical, chemical, and biological processes on the earth's surface, precise dates for specific regions are critical for solar energy technologies (Onwuka & Mang, 2018). Because records of worldwide solar radiation are sparse due to the high cost of maintaining and calibrating monitoring equipment, empirical solar models are used to estimate global radiation.

It's also worth noting that Kenya, which is on the equator, has an average of 5 sunny hours over 700 W/m^2 and receives 4 to 6 kWh/m^2 per day, which equates to 250 MTOE every year. As a result, Kenya has the world's highest homeownership of 30,000 PV modules ranging from 20 to 100 watts (Monyei et al., 2018).

A high-quality solar measurement network is essential for obtaining reliable sun irradiation estimations. Multiple commercial networks provide solar radiation mapping for a variety of locations. However, the assessments are not based on other weather-related factors and are subject to improvements such as better special resolution and temporal resolutions and removing biases on RMSE (Awan et al., 2018).

For research and technical applications, values of global and diffuse radiations for individual hours are required. Many stations have hourly global radiations on horizontal surfaces, but only a handful have hourly diffuse radiation measurements. As a result, decomposition models have been built to estimate diffuse radiation using global data

(Boussaada et al., 2018). Similarly, it has been demonstrated that predicting direct irradiance beam components is critical in designing solar-energy components such as high-intensity solar cells (Benatiallah et al., 2019). According to Heidrich et al. (2018), the two types of solar radiation perfection models are sky component-based, parametric, and decomposition models. Meteorological characteristics such as cloud distribution, sunlight, air turbidity, and precipitation are required for parametric models. Decomposition models anticipate the beam and sky components based on global radiation data.

Due to the significant attenuation of incoming solar flux on its transit through the atmosphere, both solar flux composition and cloud distribution, developing reliable solar prediction models for the ground level is difficult (Bamehr & Sabetghadam, 2021). Mousavi et al. (2017) stated that the computing methods for calculating solar radiation intensity outside the earth's atmosphere are well established. Most of the total radiation measured on a horizontal surface can be detected using a satellite. However, because meteorological measurements are site-specific, they yield more precise estimates.

Angstrom (1924) devised a regression model based on daylight hours and day length for predicting alien and incoming solar radiation, which was later updated by Prescott (1940). Several researchers have looked into and tweaked solar radiation prediction algorithms based on the Angstrom and Prescott regression models. Samanta et al. (2019) examined models for forecasting global solar radiation with different coefficients based on the Angstrom and Prescott models. They found that quadratic models were more accurate than linear models in predicting global solar radiation. Wang et al. (2022) examined quadratic models based on cloud conditions, which are difficult to establish at most local meteorological stations due to complexity, a lack of equipment, and staff. Various solar radiation models based on Angstrom and Prescott regressions with changed coefficients and environmental parameters were examined by Shrestha et al. (2021). Ren et al. (2018) used a combination of a site's mean daily temperature and daily precipitation, while Ronno (2018) used latitude and fraction of sunshine duration after conducting a study to correlate global radiation with relative sunshine duration and determine the variations of their coefficients on a geographical scale as a function of the radiation climatic area. Guermoui et al. (2018) investigated the difference between the maximum and minimum daily air temperatures and the sunshine duration fraction. Gopinathan's (1988) model based on latitude, a fraction of sunshine duration, and height above sea level, according to Otunla (2020), produced the best results.

Vincent et al. provided a global solar prediction model based on solar inclination angle and cloud coverage at Oktas-scale (2020). They created a stochastic model that can be used to

produce cloud observations for simulations. They also stated that it had a minor impact because the model is primarily interested in temporal average projections. The model had the advantage of not being geographically limited and not requiring the measurement of other associated global solar measures. This model, however, requires a long time of cloud cover observation. Vincent et al. (2020) calibrated seven current models to build one new daily solar radiation model based on extraterrestrial radiation, maximum and minimum air temperatures, mean atmospheric pressure of a site, and vapour pressure at maximum and minimum temperatures. They claimed that the new model provided the most accurate estimates for all seven areas studied. It may thus be used to estimate daily global solar radiation on a horizontal surface. Even though it featured numerous site-specific characteristics, some of them were unavailable in the most remote regions, and it performed badly in comparison to other models.

For the proper design of building energy systems, solar energy systems and a full study of the thermal environment within structures is required to understand local solar radiation (Faragallah & Ragheb, 2022). Long-term measurements from the site where the intended solar system would be installed would make up the ideal database. On the other hand, solar radiation models are an absolute necessity due to the limited coverage of radiation monitoring networks. Modelling the beam component, also known as direct irradiance, is typically prioritised in building solar energy systems, such as high-temperature heat engines and high-intensity sun cells because it plays a big part in the process. According to Lee and Callaway (2018), the scientific literature has two types of solar radiation models. These models are either parametric or decomposition models, and they predict the beam or sky component based on more easily quantifiable quantities.

Parametric models require extensive environmental data to be precise. Meteorological factors, including cloud type, number, distribution, and additional statistics like sunlight fraction, air turbidity, and precipitable water content, are widely used as predictors (Lawrence et al., 2019). The ASHRAE algorithm was simplified, and the engineering and architecture communities have now widely accepted it. According to Khan and Malik (2021), the Iqbal model is more exact than other, more traditional models. It is feasible to develop correlation models that can forecast beam or sky radiation when paired with other solar radiation measurements.

Decomposition models frequently employ only global radiation information to accurately predict the beam and sky components (Laiti et al., 2018). These interactions are usually expressed using irradiations, time integrals of the radiant flux or irradiance. Irradiance is also known as radiant flux. Models of decomposition were created using global irradiance to

estimate direct and diffuse irradiance. This post looks at a few of the most common solar radiation models used in solar energy systems. These models' projected values are compared to the actual data collected in Hong Kong.

2.7.1 Gadiwala Solar Radiation Models

In most remote regions, global solar radiation data and its components are not available in all locations due to a lack of sufficient meteorological equipment, and there is a need for global solar radiation estimation models which use Climatological parameters (Gadiwala et al., 2013). The empirical model for estimation of daily global solar radiation based on sunshine hours of a location was developed by Gadiwala et al. (2013) as in equation 2.1

$$H = H_o\left[A + B\left(\frac{n}{L_d}\right)\right] \qquad 2.1$$

H is incoming daily global solar radiation ($MJm^{-2}d^{-1}$)

Where;

H_o is daily extra-terrestrial radiation ($MJm^{-2}d^{-1}$);

A and B are Empirical constants.

n is brightness sunshine hours per day (hr)

L_d is Astronomical day length (hr)

The astronomical day length is calculated by equation 2.2

$$L_d = \frac{2}{15}\cos^{-1}[-\tan(\phi)\tan(\delta)] \qquad 2.2$$

ϕ is latitude in degrees and δ is the solar declination angle in degrees.

$$H_o = \frac{24}{\pi} I_{SC}\left[1 + 0.033\cos\left(\frac{360n}{365}\right)\right]\left[\cos(\phi)\cos(\delta)\sin(\omega_s) + \frac{2\pi\omega_s}{360}\sin(\delta)\right] \qquad 2.3$$

I_{SC} is solar constant and ω_s is sunset hours.

The regular A is considered the fraction of extraterrestrial radiation on overcast days. The Sum of A and B is regarded as the fraction of radiation received on a clear day. The coefficients A and B are estimated by;

$$A = -0.110 + \cos(\phi) + 0.323\left(n/L_d\right) \quad B = 1.449 - 0.553\cos(\phi) - 0.694\left(n/L_d\right) \qquad 2.4$$

Eftimie (2009) performed a simulation of horizontal irradiance using the model and found out that the Gadiwala et al. (2013) model had low accuracy in predicting long-term solar irradiance beyond eight months.

2.7.2 Coste Model

Coste and Serban (2011) developed monthly global radiation models based on diffuse solar radiation and sunshine duration. Table 2.1 shows the solar radiation models for a few months of the year produced by Coste and Serban (2011).

Table 2.1: Specific Models for global solar radiation

Month	Equation
January	$G_h = I_o \sin(\alpha)[(0.0457)(t\_solar)+0.0874]$
March	$G_h = I_o \sin(\alpha)[(0.0291)(t\_solar)+0.3074]$
May	$G_h = I_o \sin(\alpha)[(0.0258)(t\_solar)+0.3623]$

Source: Coste and Serban (2011).

G_h Is Global solar radiation (W/m^2), I_o is Extraterrestrial radiation (W/m^2), α is an altitude angle in degrees, and t_solar r is the solar sunshine hours (hr).

The limitation of the models was that they were inaccurate in the prediction of solar radiation above 800 W/m^2 (Kim et al., 2019).

2.7.3 Seme Models

Solar radiation models based on the global geographical location by applying an artificial neural network in order to predict half-hourly solar irradiation during the day were formulated by Seme and Štumberger (2011). They reported that the results obtained from the artificial neural network and the one from meteorological data were in agreement, especially for the clear days. The parameters used are as indicated in equation 2.5

$$H = \int_{t_0}^{t_o+\Delta t} I_o e \sin\alpha(t)dt \qquad 2.5$$

H is the solar radiation in kW/m^2, I_o is Solar constant; 1.367 kW/m^2

$$e = 1 + 0.034\left[\cos\left(\frac{2\pi n}{365}\right)\right]$$

Where; n is the number of days starting from the first day of January

α is the solar azimuth angle in degree. $sin\,\alpha = sin\,L\,.\,sin\,\delta_S + cos\,L\,.\,cos\,\delta_S\,.\,cohs\,s$

L is the latitude of the site in degrees, and h_S is the hour angle δ_S is the solar declination angle

$$\delta_S = 23.45\sin\left[\frac{360(284-n)}{365}\right] \quad h_S = \cos^{-1}(-\tan L.\tan\delta_S)$$

The models were formulated for clear days, and more improvement was needed for predicting the daily distribution of global solar irradiance on cloudy days (Mirmasoudi et al., 2018).

2.7.4 Ehnberg and Bollen Model

Ehnberg and Bollen (2005) reported that geographical parameters-based models were inaccurate in determining solar radiation. Thus they developed a Global radiation predictive model without geographical parameters but based on cloud observations. The method of generating cloud coverage was by discrete Markov model. The Global solar radiation was expressed as follows;

$$G = \left[\frac{a_0(N) + a_1(N).\sin\psi.a_3(N)\sin^3\psi - L(N)}{a(N)}\right] \qquad 2.6$$

Where;

ψ is the vector of local elevation angle over a period determined by d (rad)

N is the number of Oktas, $L, a, a_i, i = 0,1,3$ are Empirical constants (W/m^2).

G is global solar radiation over some time in (W/m^2)

d is the day for the year for the period of simulation.

δ_S is the solar declination angle over a period determined by d (rad)

ϕ_r is the tilt of the earth's surface relative to the orbital plane of the world around them sun=0.409rad

$\delta_S = \phi_r \cos\frac{[C(d-d_r)]}{d_y}$ d_r and d_y are days of the leap and non-leap year, respectively.

$\sin\psi = \sin\phi.\sin\delta_S - \cos\phi.\cos\delta_S.\cos\left[\frac{C.t_{UTC}}{t_d} - \lambda_e\right]$ ϕ Is the location's longitude positive north of the equator (rad), λ_e is the longitude of the positive location west of Greenwich (radiation). t_{UTC} is the coordinated universal time(h) and t_d is the hours of the day(h)

According to Sun and Kok (2007), the models required a longer period of cloud coverage.

2.7.5 Sendanayake Models

Gadiwala et al. (2013) stated that solar radiation could be predicted using meteorological data available in most meteorological stations. However, the most commonly available data in meteorological stations are temperature, precipitation and wind-related data. Sendanayake et al. (2014) developed a predictive model for estimating daily global solar radiation on a horizontal surface based on air dry-bulb temperature differences of any geographical location, as shown in equation 2.7

$$G_{dh} = H_o(KT)^1(TD)^{0.5} \quad 2.7$$

Where;

(TD) is the maximum daily temperature minus minimum daily temperature (^{O}C)

$$(KT)^1 = 0.0185(TD)^2 - 0.0433(TD) + 0.4023$$

Where;

G_{dh} is the daily global radiation on a horizontal surface (MJm^{-2} day^{-1})

H_o is the daily extraterrestrial radiation (MJm^{-2} day^{-1})

The model, when tested on tropical regions by Sendanayake et al. (2014), showed a coefficient of correlation of 0.81.

2.5.6 Almorox Daily Global Solar Radiation Models Analysis

Daily global solar radiation forecast models based on extraterrestrial solar radiation, maximum and minimum air temperatures, mean atmospheric pressure, and saturated vapour pressure at maximum and minimum air temperatures were investigated (Fan et al., 2018). Yari et al. (2020) modified and analysed the models, estimating solar radiation and relating it to crop evapotranspiration using minimum climatological data and reporting that the proposed modifications allow for the correction of errors related to indirect climatological parameters that affect the local temperature range.

$$H_c = H_o \times \left[Kr(T_{\max} - T_{\min})^{1/2} \right] \quad 2.8$$

Where;

H_c is the estimated solar radiation (MJ/m^{2}day),

H_o is the extraterrestrial radiation (MJ/m^{2}day),

$T_{\max}$ and $T_{\min}$ are maximum and minimum daily air temperatures ^{O}C.

Kr Is an empirical constant, 0.17, 0.16 and 0.19 for semi-arid, interior and coastal regions.

Allen (1997) modified the Kr coefficient to include a function of a site elevation effect on atmospheric pressure. The mean daily atmospheric pressure and the empirical coefficient A were equal to 0.17 and 0.2 for coastal regions. This model excluded the arid and semi-arid areas. The final model, according to Allen (1997) model was presented as follows;

$$H_c = H_o \times \left[A \times (P/1031)^{1/2} (T_{\max} - T_{\min})^{1/2}\right] \quad 2.9$$

Due to errors in the estimation of solar radiation, Valiantzas (2018) modified the empirical coefficient as:

$$Kr = A(T_{\max} - T_{\min})^2 + B(T_{\max} - T_{\min}) + C$$

The coefficient of A, B and C were 0.00185, -0.0433 and 0.4023, respectively. The final model was presented as:

$$H_c = H_o \times \left[A \times (T_{\max} - T_{\min})^{1/2} + B(T_{\max} - T_{\min}) + C\ (T_{\max} - T_{\min})^{1/2}\right] \quad 2.10$$

Rodríguez et al. (2022) reviewed the daily solar radiation model as an exponential asymptotic function of daily temperature range $\Delta T(^{o}C)$ as follows;

$$H_c = H_o A\left[1 - \exp\left(-B\Delta T^{C}\right)\right] \quad 2.11$$

Where $\Delta T = T_{\max(i)} - 0.5\left(T_{\min(i)} + T_{\min(i+1)}\right)$ i and $(i+1)$ are current day and the next day Coefficients A and C were equal to 0.7 and 2.4 $B = 0.036\exp\left(-0.154\Delta T_1\right)$.

A Represents maximum value for atmospheric transmission coefficient and characterises the site pollution and elevation. Coefficient C determined the increment of ΔT the full value of the atmospheric transmission. ΔT_1 The monthly average temperature ranges from 0.001945 to 0.007846.

Almorox et al. (2013) developed a model that included the daily temperature range and the saturated vapour pressure at maximum and minimum temperatures with the following relationship;

$$H_C = H_o A(T_{\max} - T_{\min})^{B}\left(1 - \exp\left(-C\left(es(T_{\min})/es(T_{\max})\right)^{D}\right)\right) \quad 2.12$$

There C were empirical constants and $es(T_{\max}), es(T_{\min})$ maximum and minimum vapour pressures (kPa).

2.5.7 Collares (1979) Model

A model for the prediction of hourly solar radiation on a horizontal surface base on the ratio of hourly to global radiation was developed by Collares et al. (1979) as in Equation 2.13

$$I_t = r_t . H_n \qquad 2.13$$

Where; I_t is hourly solar radiation at time t, r_t is the ratio of hourly to daily global solar radiation at time t, H_n is the daily global radiation

$$r_t = \frac{\pi}{24} x + y \cos w \frac{\cos w - \cos w_s}{\sin w_s - 2\pi / 360 \cos w_s} \qquad 2.14$$

$$x = 0.409 + 0.501 \sin w_s - 60 \quad , \qquad y = 0.6609 - 0.4767 \sin w_s - 60$$

Where; w and w_s are hour angle sunset hour angle in degree.

$$w_s = \cos^{-1}\left[-\tan(\varphi)\tan(\delta)\right]$$

Where; φ and δ are latitude and solar declination angles, respectively.

Ya'u et al. (2018) modified the ratio of a specific site by including day daily length of the day S_o latitude (φ) and solar declination (σ)

$$S_o = \frac{2}{15} \cos^{-}\left[-\tan \varphi . \tan \varphi\right]$$

2.14

$$\sigma = 23.45 \sin\left[360n + 284 / 365\right]$$

Where; n is the numerical number of the day of the year.

Al-Aboosi (2020), using the Baig et al. (1991) model to estimate the daily global solar radiation on a horizontal surface for the Himalayas region, predicted the month with the least sunshine ratio and molar ratio with an accuracy whose correlation of coefficient R^2 of 0.71.

2.5.8 Bindi and Miglietta Air Temperature and Rainfall Model

Wang et al. produced another daily solar forecast model adapted for usage with fewer environmental inputs (2018). Daily air temperature differential and precipitation measurements were used as inputs. The model first calculates the mean sky transmittance by determining which days have a high probability of clear and overcast skies. Latitude and auxiliary data were utilised to create station parameters for the model. 22 stations in 11 nations were operated to test the model, with estimated and measured irradiance data compared and used as an input to a wheat growth simulation model. They reported that the model resulted in a very minor

difference in grain yield when measured irradiance was employed. The model related daily global radiation (R) based on extraterrestrial Insolation (Q) and the mean daily sky transmittance (K), according to Equation 2.15 below.

$$R = QK \tag{2.15}$$

The parameters were given values based on whether the day was clear or overcast, determined by the daily temperature difference and rainfall amplitude. This model implies that the greater the temperature change over two days, the greater the mean sky transmittance. However, it has been found that it varies depending on the type of site, such as rural, urban, or industrial (Eikenberry & Gumel, 2018).

2.5.9 Climatological Solar Radiation (CSR) Models

Climatological Solar Radiation (CSR) models, such as the METSTAT algorithms, used monthly data provided from National Renewable Energy Laboratories (NREL) satellite products to reliably anticipate solar radiation (Salmon et al., 2021). Benkaciali et al. (2018) found that METSTAT models had a Mean Bias Difference (MBD) of -15 to 15% and a Mean Absolute Error (MAE) of 3%.

2.5.10 Solar Radiation Predictive Model Analysis

Rao et al. (2018) developed a model to estimate global solar radiation from sunshine duration using linear, quadratic, cubic, logarithmic, and exponential models based on six years of measured hourly global solar radiation data and concluded that the goodness of global solar radiation estimation should be based on measured solar radiation versus calculated solar radiation values. The correlation coefficient (R2), Root-mean-square error (RMSE), Mean Biased error (MBE), Mean absolute biassed error (MABE), Mean percentage error (MPE), Mean absolute percentage error (MAPE), and t-statistics were selected as the most often utilised statistical tools by Kaba et al. (2018). (t-stat). The correlation coefficient is used to test the relationship between the measured and the predicted values and is expressed as in Equation 2.16

$$R^2 = 1 - \frac{\sum_{i=1}^{i=n} \left(H_m - H_c\right)^2}{\sum_{i=1}^{i=2} \left(H_m - H_{mav}\right)^2} \tag{2.16}$$

Where; H_m is the measured radiation, H_c the calculated model values,the mean average, and the number of data.

MBE provides long-term performance of the correlation by allowing a comparison of actual deviation between calculated and measured values (Zhao et al., 2013). MBE and MABE were expressed in Equations 2.17 and 2.18

$$MBE = \frac{1}{n}\sum_{i=1}^{i=n}\left(H_c - H_m\right) \quad 2.17$$

$$MABE = \frac{1}{n}\sum_{i=1}^{i=n}\left(\left|H_c - H_m\right|\right) \quad 2.18$$

Diez et al. (2021) used various inclination angles to investigate the diffuse component of solar radiation on a tilted surface. They compared the measured value to the circumsolar and anisotropic model results and the isentropic of Kulcher and Hay of Lucknow and Uttar Pradesh, India. They claimed that the comparison revealed that the Kulcher model produced accurate estimates, particularly at low inclination degrees. The model showed the short-term performance information as expressed by RMSE in Equation 2.19

$$RSME = \sqrt{\left(\frac{1}{n}\right)\sum_{i=1}^{i=n}\left(H_c - H_m\right)} \quad 2.19$$

Mean Percentage Error (MPE) and Mean Absolute Percentage Error (MAPE) were used to determine the long-term performance and are expressed in Equations 2.20 and 2.21

$$MPE = \frac{1}{n}\sum_{i=1}^{l=n}\left(\frac{H_m - H_c}{H_m}\right)100\% \quad 2.20$$

$$MAPE = \frac{1}{n}\sum_{l=1}^{l=n}\left(\left|\frac{H_m - H_c}{H_m}\right|\right)100\% \quad 2.21$$

2.9 Model for predicting daily mean solar energy availability

Various solar energy models have been produced in the scientific literature, according to Tang et al. (2018), each adopting a different set of methodologies and procedures. Several initiatives have used linear mathematical functions, including Algeria, which used satellite data in sparse areas and Malaysia. Non-linear functions have also been merged with Angstrom coefficients in quadratic and unconstrained procedures to determine daily diffuse solar radiation and irradiation models. Furthermore, non-linear functions have been used in a wide range of applications (David et al., 2018). Fuzzy logic has been applied to meteorological

aspects in addition to short-term energy predictions (VanDeventer et al.,2019). Finally, genetic algorithms and artificial neural networks can be employed to create a self-sustaining pump.

Barrera et al. (2020). According to Linear, models can be simple to understand. Their linearity makes them a good tool for ensuring that optimal weights for each component (and hence a quasi-optimal solution) are found if the connection is linear. Linear also stated that models could accurately predict outcomes. Linear models, on the other hand, have low predictive performance on average. This is due to the restricted number of correlations that can be taught, which causes people to oversimplify a more complex reality. Furthermore, linear models are particularly vulnerable to outliers (anomalies); as a result, outliers must be identified and removed before applying linear functions, which is not always an easy task.

Non-linear functions, according to Akhter et al. (2019), have the advantage of being able to deal with more intricate interactions (since they are not constrained only to linear functions). However, because there are so many possible options, it is sometimes necessary to undertake research to discover which position best fits the existing data. As a result, they necessitate a substantially longer time commitment than linear models. Due to their well-defined rule basis, fuzzy logic models have the advantage of being able to deal correctly with inaccurate data. This gives fuzzy logic models a competitive advantage in the market (Okwu & Nwachukwu, 2019). Unlike other systems, fuzzy logic models have this feature, which allows for greater adaptability. On the other hand, the number of negatives considerably outnumbers the number of benefits: rule design can be quite complex, domain expertise is necessary to solve the presented problem appropriately, and defining precise values for the purpose of constructing the rule base can be difficult.

Genetic algorithms are effective in solar energy modelling when a near-optimal solution is needed (Schellenberg et al., 2018). Furthermore, when it comes to managing noisy functions, evolutionary algorithms outperform linear models. However, genetic algorithms must converge to be effective, which can take a long time and require a large population, so this method is both time-consuming and costly (Barrera et al., 2020).

Artificial neural networks (ANNs) use graphics cards to boost their computational speed (Zuo et al., 2022). As a result, these systems are ideal for making predictions in multidimensional spaces, where their high cardinality increases the likelihood of discovering non-linear functions between different magnitudes or dimensions. This makes these systems ideal for predicting multidimensional space. However, because of the neural network's ability to adapt to the distribution function, there is a risk of "overfitting." This risk emerges because the neural network will fit the training data too well (Negash & Yaw, 2020). The artificial

neural network (ANN) "remembers" the obtained data and loses its ability to make accurate predictions. This can give the impression that the model is more accurate than it is. The data must be separated into training and test models (either 80%-20% or 90%-10% for different samples). This is done to establish the level of accuracy that a model trained on completely unknown cases would achieve. ANNs have considerable use in the solar energy industry because of their appropriateness for multidimensional settings (Barrera et al., 2020).

The persistence model, also known as the smart persistence model, is the most important technique, according to Zhang et al. (2020), since it uses previous data to anticipate the amount of electricity generated in the near future (2-3 hours). This method has the potential to be used as a benchmark against which other forecasting techniques can be assessed. A prediction is usually divided into two parts. A numerical weather forecast, also known as an NWP, is first prepared for a certain period and place. Following the completion of the NWP, forecasting algorithms are used to forecast electricity generation. Alternatives include using a physical model, a statistical technique, or a machine learning-based strategy. ML algorithms are compared to the Smart Persistence (SP) technique in terms of prediction, and the results show that ML models beat SP models (Amarasinghe et al., 2020). Grid management has become more complex as solar energy penetration rates have risen due to the unpredictability of solar resources. One of the most significant barriers to integrating renewable energy sources into the grid is the unpredictability and irregularity of power transmission (Babatunde et al., 2020). As a result, solar power forecasting is becoming an increasingly important component for grid stability, unit commitment, and dispatch cost reduction. Machine learning techniques can sort through a large number of unusual solar radiation forecast models to solve the challenge (Khan et al., 2020). In order to construct accurate prediction models, various regression techniques such as linear least squares and support vector machines with a variety of kernel functions are considered.

2.10 Challenges of Solar Energy Technology Development and Application

Solar technology implementation has presented a variety of challenges as compared to traditional conventional energy sources utilised to generate power. The challenges of solar photovoltaic (PV) milk chilling systems were demonstrated by Rahman et al. (2022). These challenges are caused by variations in solar energy throughout the year and on a daily basis. These differences may reduce the systems' effectiveness and dependability. This came about as a result of the invention of an evaporative cooler and subsequent research into its effectiveness as the device was distributed to small-scale dairy farmers in western Uganda.

According to Jani et al. (2018), a number of researchers have looked into the use of solar energy technologies in refrigeration systems. These experts have identified solar energy fluctuation as a major barrier to solar technology adoption, particularly for on-farm milk chilling systems. According to Victor et al. (2016), the availability of solar-generated electrical power allows for the implementation of a conventional system. On the other hand, he observed that in order to meet the criteria of standalone systems, solar energy systems needed to be adjusted to accept the changeable characteristics.

Calise et al. (2019) published the results of an experimental thermochemical system that might provide cooling in the summer and heating in the shoulder seasons for a house application. The apparatus utilised the $H_2O/SrBr_2$ working pair as its salt component, which was contained in a 1 m3 thermochemical reactor containing expanded natural graphite in the form of consolidated material to increase heat and mass transfer. During the winter, the system provided heating at an intake temperature of Theat equal to $35^{O}C$ (external ambient temperature of Text, mid similar to $7^{O}C$) and cooling at an inlet temperature of Theat equal to $18^{O}C$ (external ambient temperature of Text, mid equal to $7^{o}C$). Flat plate solar collectors gave the source heat with a maximum temperature of Ths, max equivalent to 8 ^{O}C (external ambient temperature of Text, the sum was equal to $35^{O}C$). Based on the experimental data, the study team predicted ESD values of up to 218 kWh/m^3 using a variety of reactor and reactive solid composite combinations.

Experimental ESD values were given by Wu et al. (2020) for cooling of 42 kWh/m^3, domestic hot water output of 88 kWh/m^3, and heating of 110 kWh/m^3. Aside from the restrictions imposed by high-temperature heat sources, thermochemical processes may face challenges when seeking to generate cold at extremely low temperatures (-30 ^{O}C and below). During the synthesis phase of a single-stage thermochemical process, the reactor temperature is related to the cold production temperature; so, the lower the cold production temperature, the lower the reactor temperature. If the reactor's temperature dropped below a particular point, removing the heat generated by the reaction using cooling water would be difficult.

Tang et al. (2019) created a thermochemical technique with an internal thermal cascade to alleviate this constraint and applied it to the working pair of NH_3 and $BaCl_2$. Because of this cascade, their technology, which was designed for deep freezing with a low-grade heat source, could produce temperatures as low as -23 degrees Celsius with a heat source of around 70 degrees Celsius. This means that solar heat can power the process utilising flat-plate collectors. The system's prototype demonstrated the method's viability, achieving an experimental global COP value of 0.06. This approach comes within the typical range of practical thermochemical

refrigeration systems powered by solar heat and creates cold at a lower temperature than prior solar refrigeration systems. Exegetical material yielded about 0.06 each year on average.

Financial restrictions have been identified as the most significant impediment to the advancement of solar energy technology. It is considered that solar energy can only advance if the cost of photovoltaics is reduced. Mahama et al. (2021) found that the primary impediment to adopting renewable energy practices is often not technological capability but a lack of long-term financial resources. Solar energy technologies have helped the population segments in Sub-Saharan Africa with the highest incomes the most. The high cost of photovoltaic solar panels is the reason behind this. Due to the region's extreme poverty, solar photovoltaic systems are out of reach for the great majority of Sub-Saharan Africans (Szabó et al., 2021). Chowdhury and his colleagues investigated the use of solar energy in Bangladesh (2018). This research appears to focus on the installation and exhibition of new technology and the technology's usefulness in Bangladesh. They determined that the cost of solar panels and the technology itself were impediments to the system's flexibility. The applicability of the technology and many other technical issues were given top priority. Adwek et al. (2020) researched solar energy electrification in Sub-Saharan Africa, concentrating on the relationship between technology and society changes or benefits. The study looked at how PV solar energy could be used in a variety of urban and rural settings and residences. According to the study's findings, the rapid growth of renewable energy technologies can be attributed to the growing demand for solar photovoltaic systems in rural homes. According to the study's conclusions, a significant number of rural inhabitants have adopted the technology, and the solar sector in Sub-Saharan Africa has exploded in recent years.

According to AlMallahi et al. (2022), one of the significant technological obstacles was the high unpredictability of solar power intake and battery capacity. A variety of environmental conditions, including weather, humidity, dust, and temperature, contributed to this difference. He outlined a set of devices that might be put onboard high-power wireless sensor networks to assess battery capacity and condition and the amount of easily available solar power in the essay. These characteristics were critical for optimising, sensing, and maximising the system's reliability in order to achieve the best possible results. The results of the trials revealed that typical lithium-ion batteries degrade dramatically when used outside in a matter of weeks or months and that solar energy availability in a solar-powered wireless sensor network in an urban setting is highly variable. These findings highlight the importance of energy and power estimation approaches.

Employees in the solar energy business may be exposed to arc flashes, electric shock, falls, and thermal burns. Any one of these hazards has the potential to cause a life-threatening injury or even death to a worker. Arc flash burns and explosions are two potential risks, according to Gündüz et al. (2021).

The markets for various forms of risk transfer, such as insurance, are expected to increase with the rise of the renewable energy sector (Taghizadeh-Hesary & Yoshino, 2020). The amount spent on risk management services in the renewable energy sector is expected to increase by more than four fold by 2020, owing to a predicted increase in investments of more than 50% by 2020 (Pietzcker and colleagues, 2021). Depending on the scenario, spending on third-party risk management services in six of the world's most important renewable energy sectors might range between USD 1.5 billion and USD 2.8 billion by 2020. Traditional insurance, derivatives, and structured goods are among these offerings.

Insurance and other forms of risk transfer are becoming increasingly popular for three reasons. The sheer increase in the amount of money required for renewable energy projects would necessitate the creation of new funding channels. This is because the costs of these efforts are skyrocketing. According to Schafer (2018), institutional investors allocate 5% of their entire asset allocation to alternative investments. Renewable energy enterprises are included in this investing category.

On the other hand, Bonds typically account for around 40% of total asset allocation. It is critical to align the risk/return profile of renewable energy investments with that of bond investments in order to attract institutional investors on a bigger scale. This is a must. One way to achieve this goal is to reduce the risk associated with the shifting cash flows produced by renewable energy assets.

The third component that adds to the rise in demand for risk transfer solutions is everyone who has been affected by the increasing presence of renewable power generation on the energy market (Egli, 2020). This is owing to the fact that energy market rivalry is increasing at a rapid pace. Renewable energy sources' variable production has prompted the development of novel risk management strategies in the power markets (Alola, 2021). This upward tendency is projected to continue. Traders and grid operators must contend with significant production unpredictability and difficulty in maintaining system equilibrium in addition to low and usually negative power pricing. In markets with set feed-in tariff rates, existing electricity suppliers must cope with low electricity prices and the requirement to provide backup capacity. As a result, current power plants will become less profitable. Complex solutions for managing these

risks have the potential to lower the costs associated with changing output in locations with a significant number of renewable energy sources (Maulidia et al., 2019).

2.11 Conceptual Framework

When solar radiation levels are low, solar energy is captured and stored in batteries for subsequent use in operating refrigeration systems. However, batteries are linked to a high failure rate and pollutants due to their short cycle when thrown after usage. A cooling system can be attached to the solar panels for direct power delivery without batteries. The refrigeration system creates ice in the ITS system, which captures and stores solar energy as sensible thermal energy. When the PV system does not offer enough power to the refrigeration system compressor due to low solar radiation levels, the ice provides the thermal cooling load energy required for chilling milk. Based on the mean daily solar radiation available at a certain location, this research established mathematical models for projecting maximum cooling demands from a refrigeration system. The solar-driven refrigeration cooling load model received the mean daily solar radiation available at a certain location as input from the solar radiation forecast model. Based on the solar radiation of the location, the refrigeration cooling capacity output was the maximum cooling load for the solar-driven refrigeration system. Lastly, the refrigeration system requires power from a PV supply, calculated using the COPr and the refrigeration system's cooling load. Models for PV power delivery to the solar-driven refrigeration system have been created.

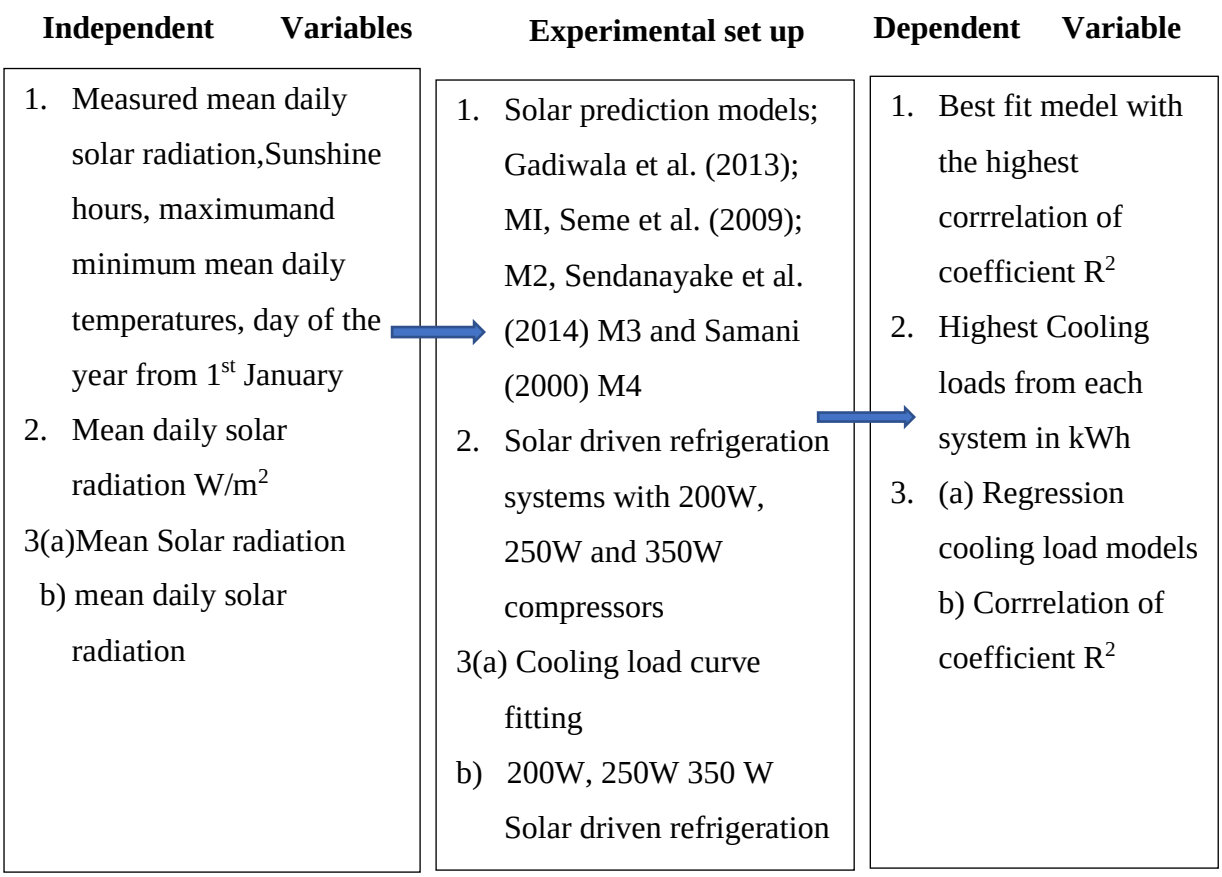
Independent Variables
1. Measured mean daily solar radiation,Sunshine hours, maximumand minimum mean daily temperatures, day of the year from 1st January
2. Mean daily solar radiation W/m2
3(a)Mean Solar radiation
b) mean daily solar radiation
Experimental set up
1. Solar prediction models; Gadiwala et al. (2013); MI, Seme et al. (2009); M2, Sendanayake et al. (2014) M3 and Samani (2000) M4
2. Solar driven refrigeration systems with 200W, 250W and 350W compressors
3(a) Cooling load curve fitting
b) 200W, 250W 350 W Solar driven refrigeration
Dependent Variable
1. Best fit medel with the highest corrrelation of coefficient R2
2. Highest Cooling loads from each system in kWh
3. (a) Regression cooling load models
b) Corrrelation of coefficient R2

CHAPTER THREE
MATERIALS AND METHODS

3.1 Study site

This research was carried out at Nakuru town in Nakuru County in Kenya at a latitude of 36.02^{O} E and a longitude of 0.284^{O} S. The research was carried out in three main sections according to the objectives.

The first section of the research was to establish a model for predicting daily mean solar energy availability for a site. The mean daily solar energy output from the established model in a specific site is used to determine the refrigeration capacity of a solar driven refrigeration system that would provide maximum cooling load based on available solar radiation. Having established the solar-driven refrigeration system with maximum cooling load based on available solar radiation, mathematical models for predicting the solar-driven refrigeration system with maximum cooling load based on solar energy available at a site was developed.

The mathematical models developed from regression analysis curve fitting were validated by variation of the solar radiation and comparing the performance of the models to the actual cooling loads obtained from the solar-driven refrigeration systems. The last section was carried out to determine the system's reliability under varying mean daily solar radiation in Nakuru. The materials and methods used are stipulated as per the outlined objectives.

3.2 Establishment the best fitting model for predicting solar radiation at varous sites in Nakuru county

Ten years of mean daily solar radiation in Nakuru town was obtained from three sources; Satellite data from National Renewable Energy Laboratories, Regional Meteorological Centre in Nairobi and the Egerton University meteorological station data. The mean daily solar radiation in W/m^2 for the ten years was computed using Excel spread sheet 2010 from the three sources, and the mean daily solar radiation was obtained from $1^{st}$of May 2008 to 30^{th} May 2019.

A Pyranometer; Kipp and zomen (Germany) model SP lite 2 with an accuracy $\pm 5\%$ manufacturer calibrated mouted on a roof top and used to measure the daily mean solar radiation at Nakuru. COMBILOG data logger connected to the pyranometer, stored the solar radiation measured at a frequency of 3 minutes, from which mean daily solar radiation was computed between July 2018 to November 2019. Using origin 2019 b application, A coefficient

of correlation test was performed between the historical and the measured data. Figure 3.1 shows the installation and moumting of the pyramometer

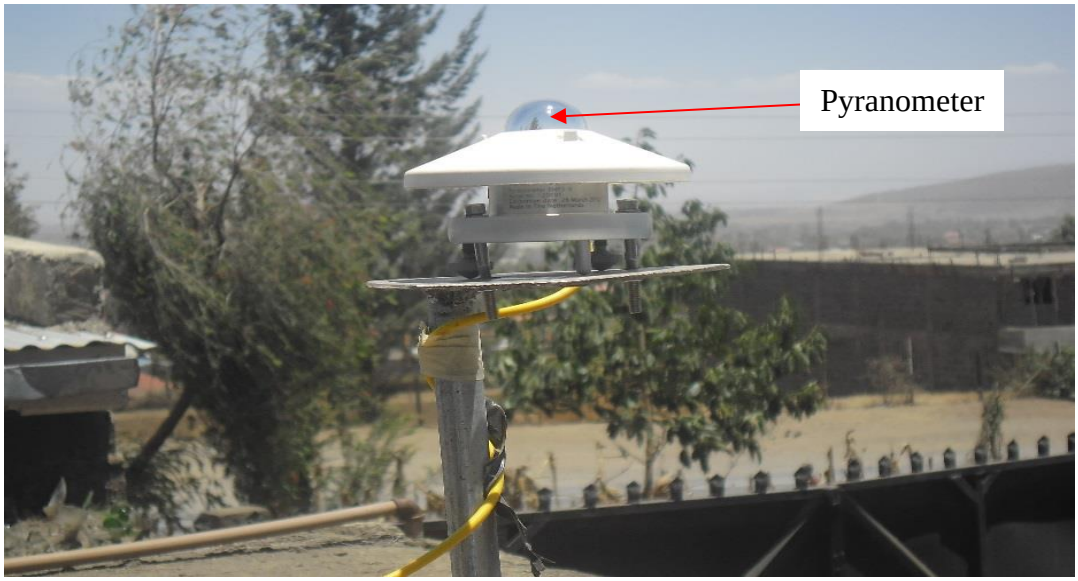

Figure.3.1: Pyranometer mounting and installation

To determine the accuracy of the measured and historical mean daily solar radiation. The correlation coefficient obtained from the measured and historical data.

3.2.1 Inputs for Solar Radiation Prediction Models

The selection and analysis for the accuracy of daily mean solar prediction models were based on the availability of input weather parameters from most meteorological stations in remote regions (meteolorogical stations that few equipment for solar radiation measurement and recording). The parameters considered readily available in remote meteorological stations within Nakuru county, that influenced the establishment of the model's analysis were; sunshine duration, day of the year, maximum and temperatures, Latitude and longitude of the site.

Four models, namely; Gadiwala et al. (2013); MI, Seme et al. (2009); M2, Sendanayake et al. (2014), M3 and Samani (2000) M4, were adopted by this study since they use readily available input parameters, namely, Latitude and longitude (^{O}), Sunshine duration (hours), Maximum temperature (^{O}C) and Minimum Temperature (^{O}C) from the remote meteorological centres. The Four models Gadiwala et al. (2013); M1, Seme et al. (2009); M2, Sendanayake et al. (2014), M3 and Samani (2000) M4 were analyzed for accuracy in the prediction of mean daily solar radiation. MATLAB 2012(b) program was used to simulate the daily mean solar radiation for each model based on the specific inputs for the model for 365 days. The data obtained were compared with the measured mean daily solar radiation by statistical performance tools. The

four models were found favorable compared to other models whose input parameters were unavailable in remote sites.

3.3 Solar Refrigeration System Cooling Loads

Solar refrigerated cooling loads is the sensible thermal energy generated by the refrigeration system in kWh. The determination of the cooling load for the solar-driven refrigeration system was based on the annual mean daily solar radiation available at the site where the solar-driven refrigeration system is to be installed.

The choice of four models for accuracy analysis in prediction of solar radiation was based on the availability of the input parameters for models within Nakuru county. Several models in the literature review such as Ehnberg and Bollen (2005), Diez et al. (2021) and Collares (1979) required input parameters that were unavailable in most meterological stations in Nakuru.

After the analysis of the four models under consideration, the correlation coefficient for the models were; Gadiwala et al. (2013) model 0.826, (Seme, 2009) 0.735, Sedanayeke, (2013) 0.809 and Samani (2000) had 0.766.

Evaluation of the annual mean daily solar radiation available at the site was predicted from the Gadiwala et al. (2013) model, as was the accurate solar radiation prediction model.

3.1 System Setup for Solar Radiation prediction and Refrigeration Cooling Loads Measurements

Three vapour compression solar driven refrigeration system were designed to cool 20 kg water with five hours, and to form ice that would preserve the milk in two cosequitive days when the systems are not operating due to insufficient solar radiation availability. Data obtained from Danfoss compressors of 200W, 250W and 350W were capable to cool up to 30kg the five hours. The sizing of the condenser, evaporator and the expansion devices was carried out by use of the Danfoss catalogue.

The refrigeration cooling loads were obtained from three refrigeration systems integrated with different AC compressor capacities of; 200 W Danfoss model TL5G Universal compressor, 250 W Danfoss model TLS5FT Tropical compressor and 350 W Danfoss model SC 12G universal compressor.

The three AC compressor systems of 200W, 250W and 350W were connected to four polycrystalline PV solar panels each of 200 Wp and an effective surface area of 1.34 m^2 each. The evaporators for each compressor system were submerged in a 15 kg brine solution in a

cooling tank for direct water cooling and ice bank formation. The 'on' and 'off' status of each compressor depended on the solar radiation available, to actuated the control unit and hence start the operation of each refrigeration system. A 30 Wp pilot solar panel was placed adjacent to the pyranometer to generate a voltage depending on the intensity of solar radiation. Using a PLC program, the voltage was converted to the corresponding solar radiation in W/m^2 and recorded by a COMBILOG data logger at 15 seconds. Figure 3.2 illustrates the layout of the solar driven refrigeration system.

The solar driven refrigeration system cooling load was determined from 3rd June to 31st September 2019. Excel spread sheet were used to determine the maximum cooling loads.

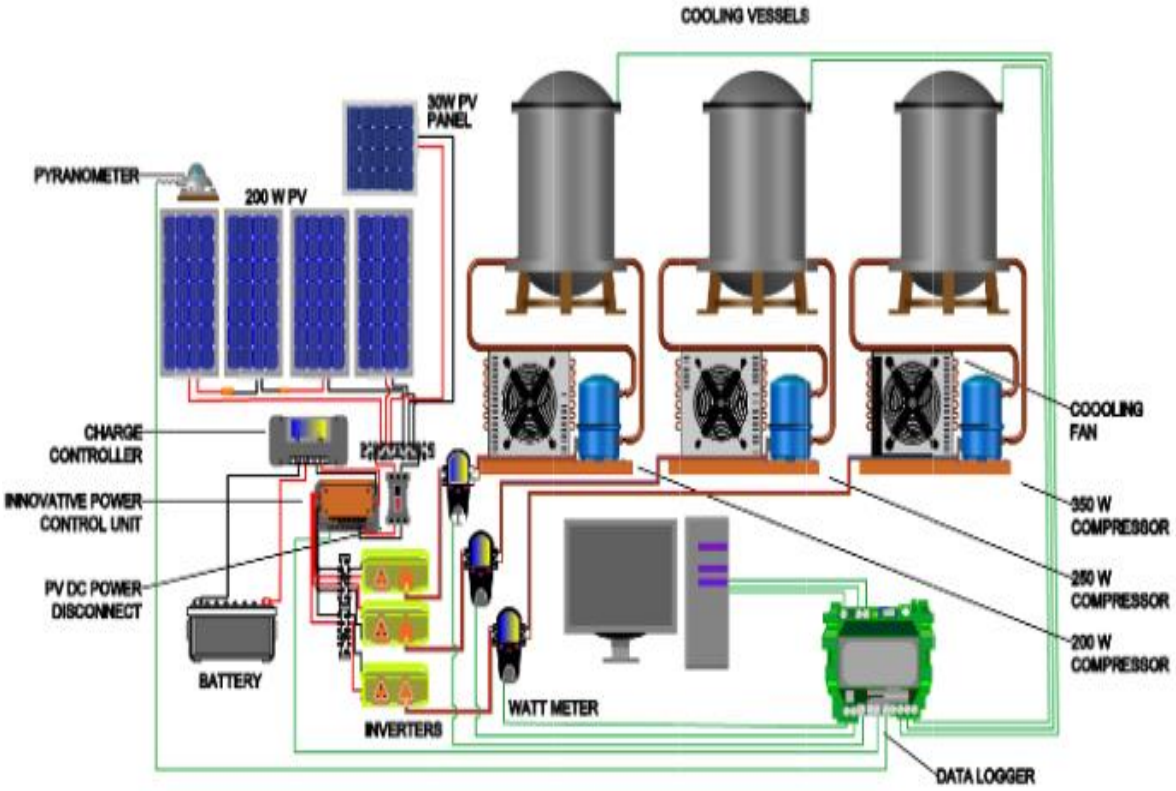

Figure 2.2: Solar driven refrigeration plant layout

3.3.2 Calibration of The Control Unit

To ensure that the control unit regulated the 'on' and 'off' status of the three solar refrigeration systems with the corresponding amount of solar radiation available and similar values obtained by the pyranometer, the unit was thus calibrated. The calibration of the control unit was done by use calibrated by use of Kipp and zomen (Germany) model SP lite 2. Pyranometer with an accuracy of $\pm 5\%$.

To determine the accuracy of the generated voltage signal, the solar radiation obtained from the pyranometer was plotted against the solar radiation from the control unit. A coefficient of correlation between the control unit and pyranometer readings was performed.

3.4 Mathematical modeling for simulating cooling load harnessed by solar driven refrigeration system

Determination of the solar refrigeration system, which provided maximum cooling loads, was based on the mean daily solar radiation W/m^2 available at a location. This was obtained by establishing the cooling loads of three different refrigeration systems integrated with the compressor of various sizes, exposed to varying solar radiation for the same time.

The three AC compressor systems of 200 W, 250 W and 350 W integrated with their corresponding evaporator were connected to the 4 PV modules, 200 Wp. An inverter was connected to the system that supplied AC power from the DC source generated by the PV modules to each refrigeration system compressor. A control unit controlled the 'on' and 'off' switching of the three compressors depending on the available solar radiation levels and the power required to operate each refrigeration system compressor. The data logger recorded the time taken by each of the refrigeration systems when each compressor was 'on' status

Water at 33^OC was drained in to each milk can of the Three refrigeration sytems at the beginning of the cooling process. The cooling process started at different time in the three compressors depending on the solar radiation level required to start each system compressor. All the refrigeration systems were switched off at 4 PM daily. The cooling Load in kWh for each of the system was obtained summation of the daily loads.

The physical properties of raw milk, skimmed raw, and pasturezed milk considered for for milk so as to replace it with water were the freezing point and the density. It was observed that the freezing point of milk range from -0.468 to -0.640. and the density ranges from1020 kg/m^3 t0 1027 kg/m^3 at 20^OC. The physical properties of water at 20^OC showed insignificant difference to water.

A cooling vessel consisting of 20 kg of water replaced milk contained in a milk can, and a container of the ice with 15 kg of water was placed adjacent to the milk can. The milk can was placed centrally in the ice container, which was surrounded by an outer jacket of a brine solution of 35% concentration as a secondary refrigerant in which the evaporator of each refrigeration system was submerged. To reduce heat influx into and out of the cooling vessel, 60 mm thick Polystyrene extruded light form insulation of density 21.5 kg/m^3 was used. Figure

3.4 shows the cross-section of the milk cooling can in each of the solar-driven refrigeration systems.

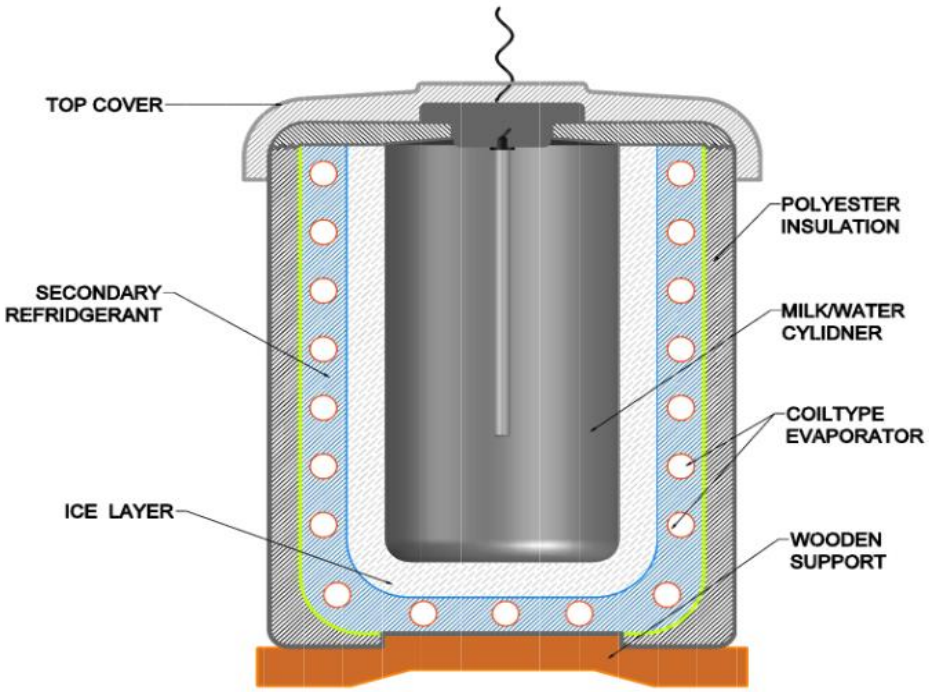

Figure 3.4: Cooling tank cross-section

Three PT-100 thermometers of accuracy$\pm 0.01^{O}C$ were used to measure the temperature profile of water can in each of the refrigeration systems from 9 am to 4 pm. A COMBI-LOG 1021 data logger recorded the temperature changes at 15 seconds for each refrigeration system. The mass of ice formed from water in the ice container was determined by draining and weighing the water that remained in the ice container at the end of each day. The difference between the water collected and the 15 kg of water initially at the beginning of the cooling process provided the mass of ice formed.

3.5 Developing Mathematical Models for Predicting Refrigeration Cooling Loads

Cooling loads mathematical models for the three refrigeration systems were established from the regression of cooling loads curves produced by each refrigeration system.

3.6 Validation of Mathematical Cooling Loads Prediction Models

The validation of the mathematical models was performed by exposing the PV panels of three solar-driven refrigeration systems to different mean daily solar radiation of between 305.824 and 695.613 W/m^2 and comparing the cooling loads generated by each of the solar

refrigeration the with the cooling loads predicted by the models developed for the three refrigeration system for the corresponding mean daily solar radiation.

3.6.1 Solar Driven Refrigeration System Power Supply Models

The power supply to each compressor from the PV panels and its inversion from DC to AC were developed from each of the refrigeration system compressor COPr and the operating temperature for the evaporator of each refrigeration system. The COPr values were obtained from the manufacturer's catalogue of each compressor at an evaporator temperature of $-5^{O}C$.

3.6.2 Validation of Power Supply Prediction Models

The validation of the power supply models was performed by exposing the PV panels of three solar-driven refrigeration systems to different mean daily solar radiation. The power supply to each refrigeration system was measured by Aposun digital watt meters model CHD900, measuring voltage 0-600 V and current 0-15 A and a current and voltage accuracy of 0.35+2 digits 0.5%+2 digits respectively. An inverter of 85 amperes pure sine wave was connected to each wattmeter. The power in kWh obtained from the watt meters was compared with the power supply from the prediction models for the three refrigeration systems and the corresponding mean daily solar radiation between 346.146 and 683.189 W/m^2.

CHAPTER FOUR

RESULTS AND DISCUSSION

4.1 Establishment of best fitting models for predicting Solar Radiation in Nakuru

The mean daily sun radiation accuracy over the past ten years was determined using satellite data from the National Renewable Energy Laboratories, the Regional Meteorological Center in Nairobi, and data from the Egerton University meteorological station. This was significant because it provided the foundation for measuring and comparing the anticipated mean daily solar radiation from known models to the actual solar radiation of a specific region. Figure 4.1 showed a coefficient of correlation of 0.971 when existing mean daily solar radiation was tested against measured mean daily solar. This accuracy compares well with some of the (Antonopoulos et al., 2019) models.

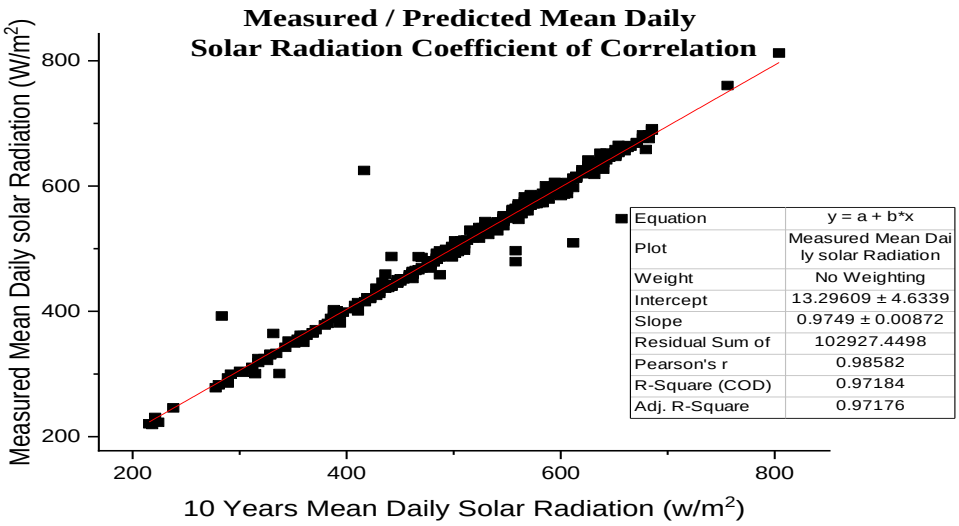

Figure 4.1: Relation between measured and 10-year mean daily solar radiation for Nakuru

Factors that determine the intensity of solar radiation largely depend on the geographical location of the earth's surface relative to the sun and the climatic condition of a location (Sreenath et al., 2021). The input parameters considered for the models were based on their availability in meteorological centres in remote regions. Table 4.1 shows the four parameters considered and the models used.

Table 4.1: Solar Radiation models and input Parameters

Parameter	Models			
	M1 (Gadiwali, 2013)	**M2 (Seme, 2009)**	**M3 (Sedanayeke, 2013)**	**M4 (Samani, 2000)**
Latitude and longitude (^{O}C)		×	×	×
Day of the year from Jan 1	×	×	×	
Sunshine duration (hours)	×	×	×	×
Maximum temperature (^{O} C)			×	×
Minimum temperature (^{O}C)			×	×

× Indicates input parameter considered

The four models, namely; Gadiwala et al. (2013); MI, Seme et al. (2009); M2, Sendanayake et al. (2014), M4 and Samani (2000) M4, which had readily available input parameters from the remote meteorological centres, were each simulated for 365 days using MATLAB 2012(b) program. The data obtained were compared with the measured mean daily solar radiation by statistical performance tools; RMSE, MBE, MABE, MPE and MAPE. The performance of the three models were tabulated in Table 3. When compared with measured data from the location, the performance of the four models M1, M2, M3 and M4 was as indicated in figures 4.2a- 4.2d.

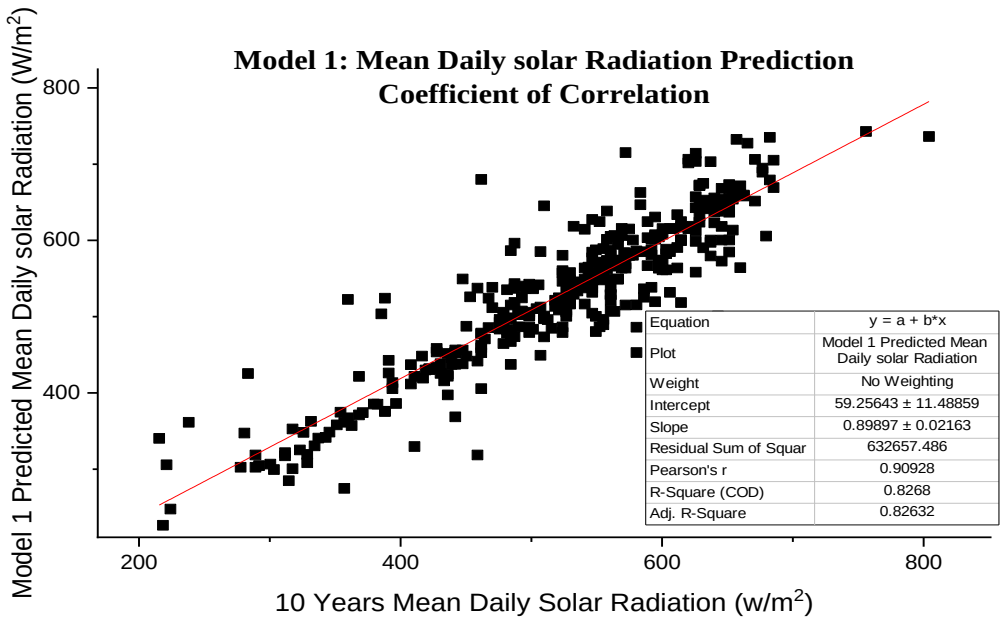

Figure 4.2a: Relation between predicted (Gadiwala et al. (2013) and measured solar radiation

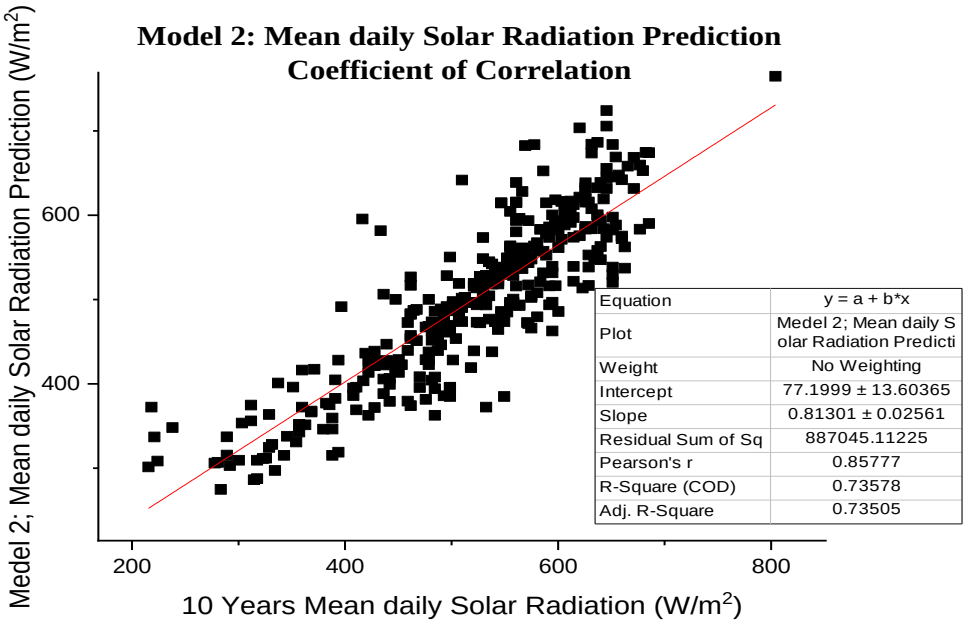

Figure 4.2b: Relation between predicted (Seme et al., 2009) and measured solar radiation

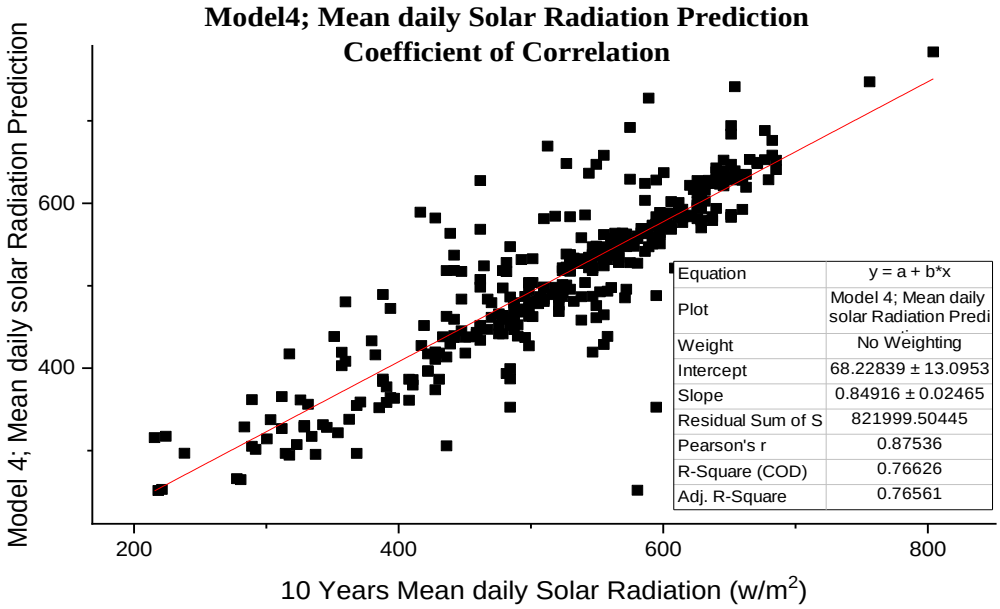

Figure 4.2c: Relation between predicted (Sendanayake et al., 2014) and measured solar radiation

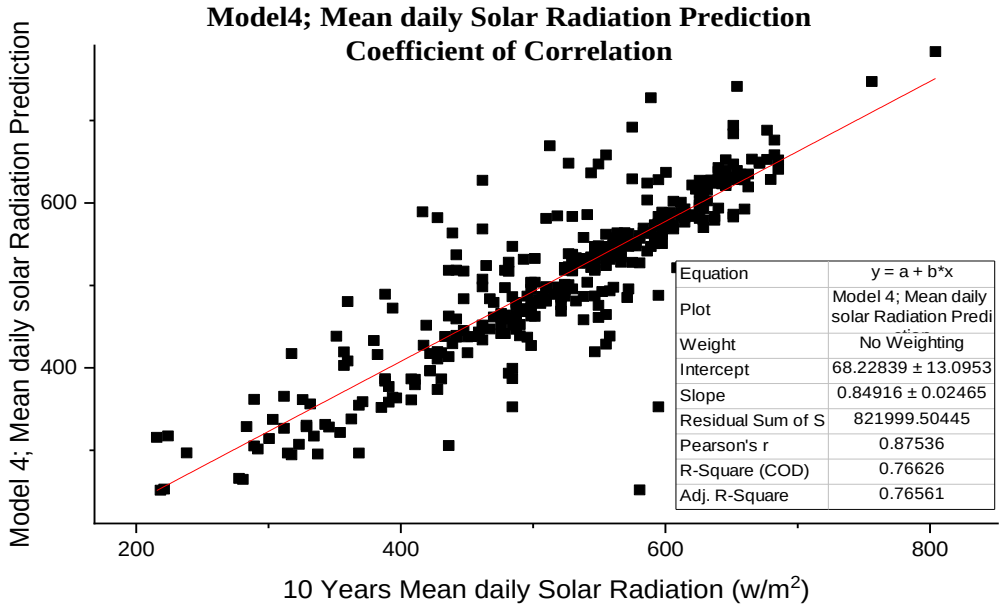

Figure 4.2d: Relation between predicted (Samani, 2000) and measured solar radiation

Table 4.2 indicate the measures of performance for the relation between predicted and measured solar radiation for various models.

Table 4.2: Measures of performance for relation between predicted and measured solar radiation for various models

Parameter	M1	M2	M3	M4
1.R^2 (unit less)	0.826	0.735	0.810	0.766
2.RMSE (W/m^2)	18.591	22.034	20.565	21.601
3.MBE (W/m^2)	-0.592	-0.571	-0.597	-0.604
4.MABE (W/m^2)	15.59	15.88	15.60	16.03
5.MPE (%)	12.31	12.88	12.83	13.08
6.MAPE (%)	18.92	21.75	20.10	20.71
Suns of Errors 2,3,4,5, and 6	**64.819**	**71.973**	**68.496**	**70.817**

The four models using MATLAB program simulations are as indicated in Figures 4.3a, 4.3b, 4.3c and 4.3d.

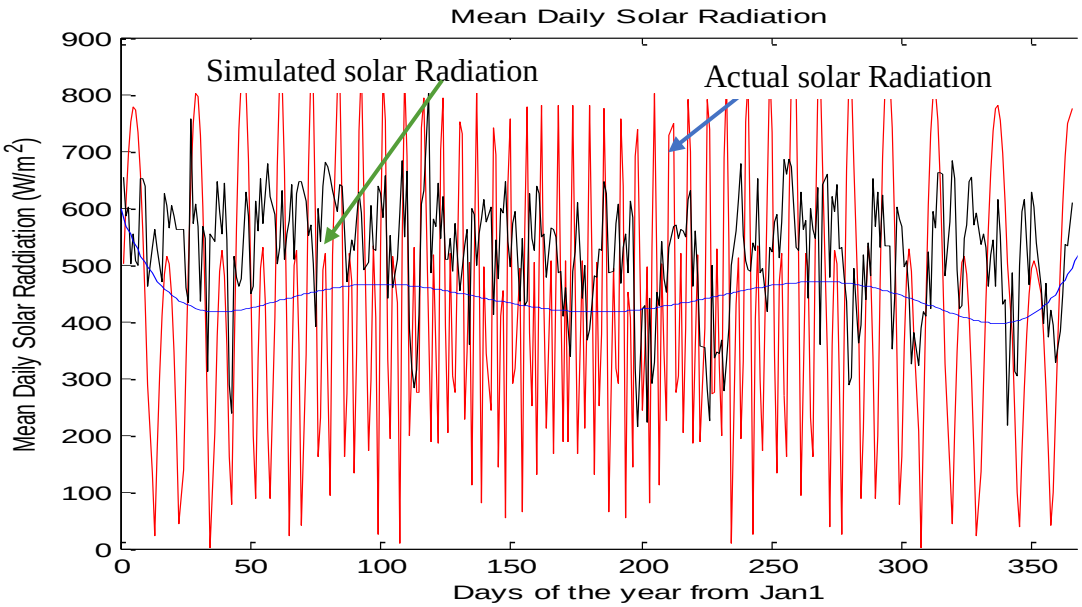

Figure 4.3a: Sendanayeke (2013) solar radiation model simulation

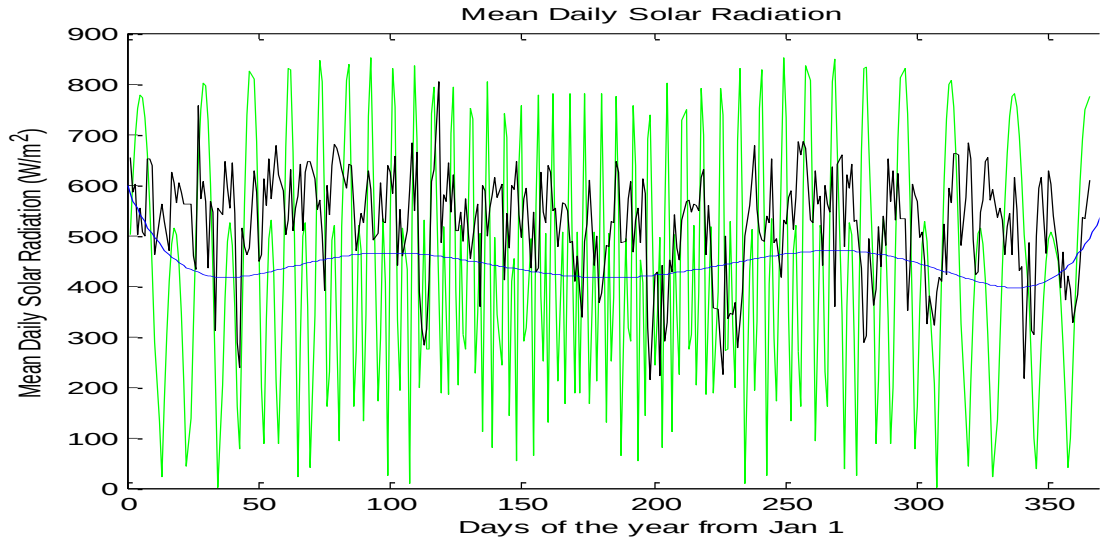

Figure 4.3b: Samani (2000) solar radiation model simulation

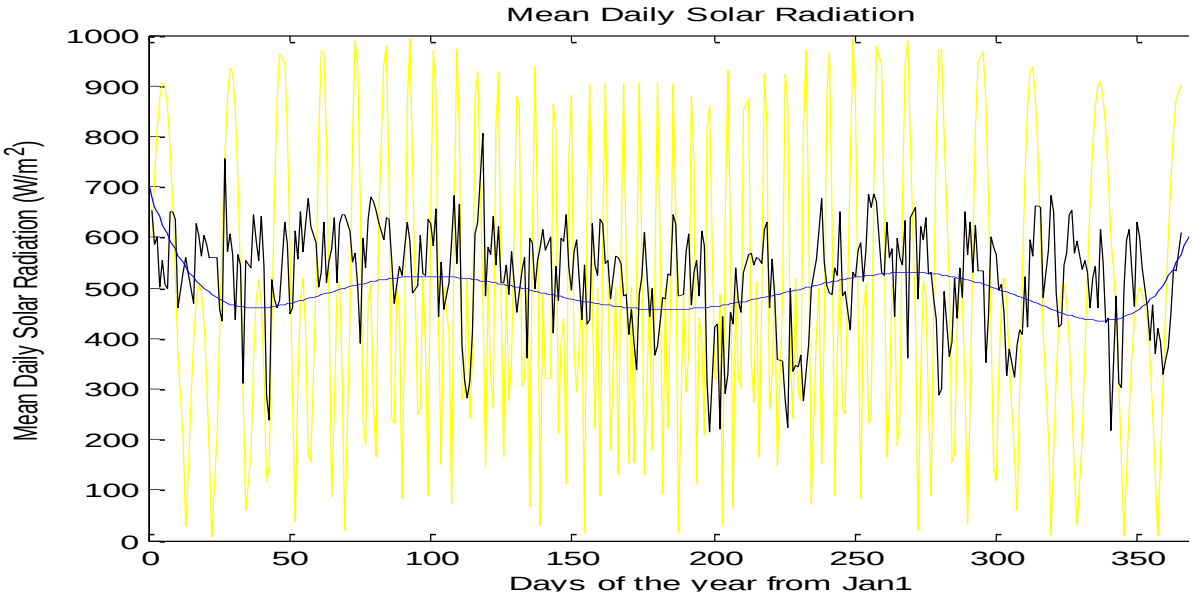

Figure 4.3c: Gadiwala (2013) solar radiation model simulation

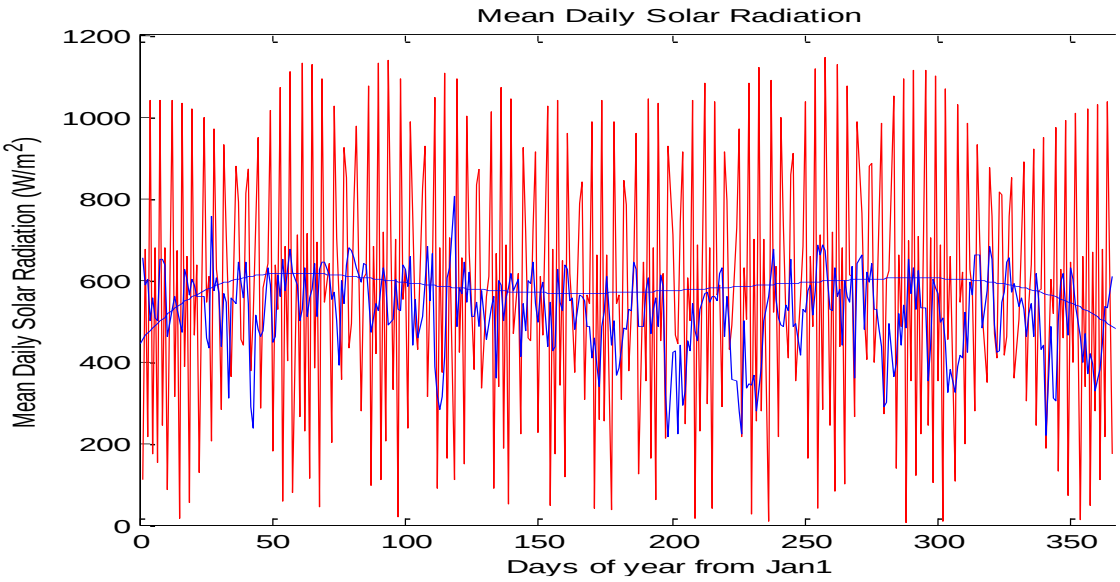

Figure 4.3d: Seme (2009) solar radiation model simulation

Results from Table 4.2 show that the most accurate model for predicting short- and long-term horizontal mean daily solar radiation is the Gadiwala (2013) model. Similarly, simulation of the four models using the MATLAB programme showed a distinct trend line in the year's seasonality as seen in the ten years' data, with the Gadiwala (2013) model as shown in figures 4.3a, 4.3b, 4.3c and 4.3d. This indicates that horizontal mean solar daily solar radiation can accurately be predicted by latitude and longitude, length of the day and sunshine duration hours. These parameters are available in remote regions. Quej et al. (2017) models based on extraterrestrial radiation, maximum and minimum air temperatures mean atmospheric pressure showed R^2 of 0.76and MPE of 12.3. Quej et al. (2017) models predicted the daily global solar radiation in a warm sub-humid environment, the month with the least sunshine ratio and solar ratio with an accuracy whose correlation of coefficient R^2 of 0.75. Gadiwala model prediction lies within the three models. Gadiwala et al. (2013) model is expressed as in Equation 4.1

$$H = H_o\left[A + B\left(\frac{n}{L_d}\right)\right] \qquad 4.1$$

$$H_0 = \frac{24}{\pi} I_{SC}\left[1 + 0.033\cos\left(\frac{360n}{365}\right)\right]\left[\cos(\phi)\cos(\delta)\sin(\omega_s) + \frac{2\pi\omega_s}{360}\sin(\delta)\right]$$

Where;

n is brightness sunshine hours per day (hr), L_d is Astronomical day length (hr)

$L_d = \frac{2}{15}\cos^{-1}[-\tan(\phi)\tan(\delta)]$, ϕ is latitude in degrees and δ solar declination angle in degrees

I_{SC} is solar constant and ω_s is sunset hours.

4.2 Capacity of Solar Refrigeration System with Maximum Cooling Load

4.2.1 Calibration of the Control Unit

The solar radiation obtained received by pyranometer was tracked by the voltage signal generated by the control unit using a 30 Wp PV panel as the power source. Figures 4.4a and 4.4b show the voltage tracking in (blue colour) of the solar radiation (in red colour) of the control unit during calibration. The COC on the 3rd January 2017 with high and low solar radiation peaks with a mean daily solar radiation of 414.37W/m^2 was found to be 0.9876. From the high performance of the control unit in generating a voltage signal equivalent to the solar radiation, the control unit was thus accurate in the 'on' and 'off' operations of the refrigeration system.

From figure 4.4a, it was observed solar radiation was tracked accurately and actuated the compressors of the refrigeration systems with fairly high accuracy as in figure 4.4b, as was also observed by (Langdon-Arms et al., 2018).

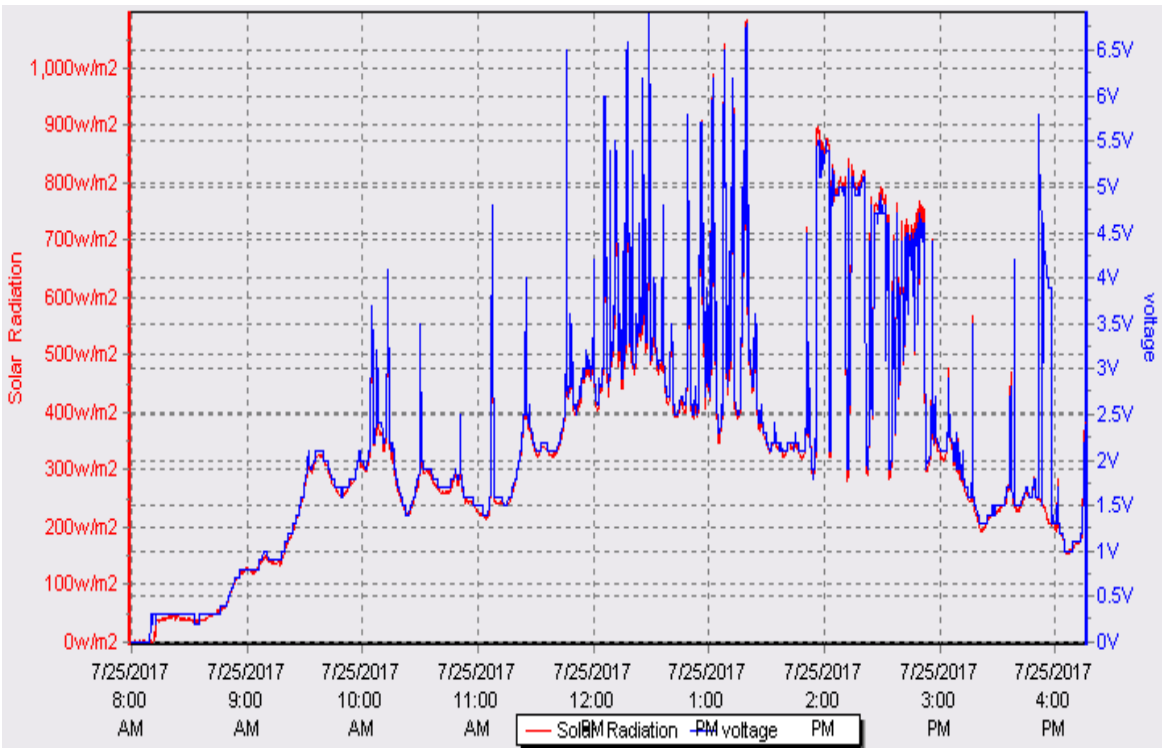

Figure 3.4a: Correlation between measured and controlled unit tracked solar radiation

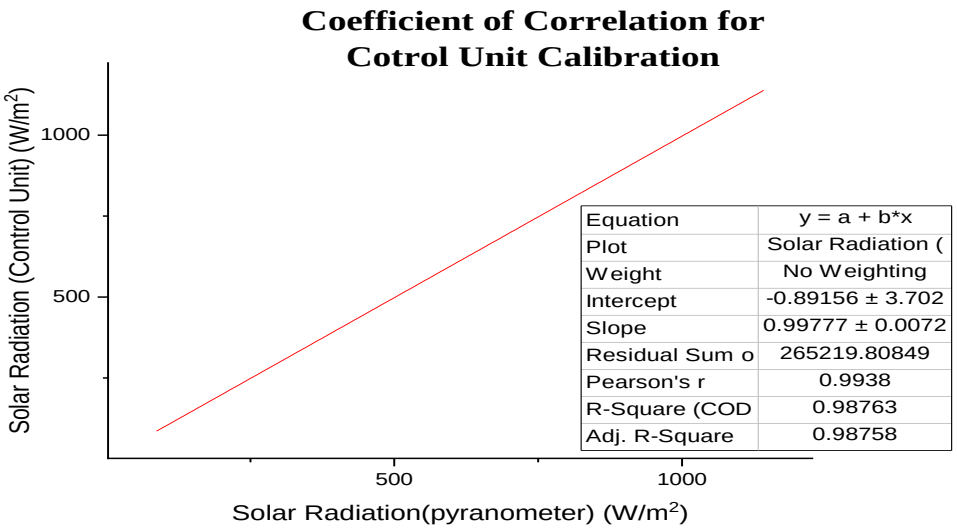

Figure 4.4b: Coefficient of Correlation for solar radiation

4.2.2 Solar Driven Refrigeration System with Maximum Cooling Load

The time required for the compressors to obtain a temperature drop of 5K of water in each milk can vary with mean daily solar radiation bands for each refrigeration system. The 200W refrigeration system indicated a mean daily solar radiation between 200.281 W/m^2 to 414.382 W/m^2. In comparison, the 250 W had a mean daily solar radiation between 420.715 W/m^2 to 580.847 W/m^{2,} and the 350 W refrigeration system was from 580.391 W/m^2 to 664.358 W/m^2. The minimum, mid and maximum solar radiation for each band, was established from the minimum temperature when the ice started forming, mid-temperature when the amount of ice was half full in the milk can, and the maximum temperature corresponding to the maximum amount of ice included as recorded by the data logger as in Table 4.3.

Table 2.3: Compressor size/refrigeration system mean daily solar operating bands

Compressor size/refrigeration system (W)	**Operating mean solar radiation band (W/m^2)**	**Mean daily solar Radiation (W/m^2)**		
		Minimum	Average	Maximum
200	100.281-420.715	213.653	350.682	414.382
250	420.715-580.391	446.988	497.548	570.847
350	580.391-670.803	580.391	623.362	664.358

Cooling loads variations with the mean daily solar radiation curves for each refrigeration system were determined. The cooling profiles for the 200W, 250W, and 350 W solar refrigeration systems are shown in Figures 4.5a-c.

The 200 W refrigeration system cooling profile shows that the cooling process of the water in the milk can of the cooling vessel started the cooling process quite early when the solar radiation was low, between 100.281 W/m^2 and 420.715 W/m^2. It is evident that the refrigeration system started running before, but the cooling process was slow, as indicated by the cooling profile gradient. This is attributed to the capacity of the 200 W compressor integrated into the system. The cooling rate was steady when the solar radiation was above 400 W/m^{2,} and the water temperature dropped from 25^{O}C to 10^{O}C. At about 10^{O}C, the cooling rate significantly dropped and resumed cooling when the temperature was about 7^{O}C. The cooling profile showed that, the water temperature dropped from 33^{O}C to 4^{O}C in 4 hour and 45 minutes.

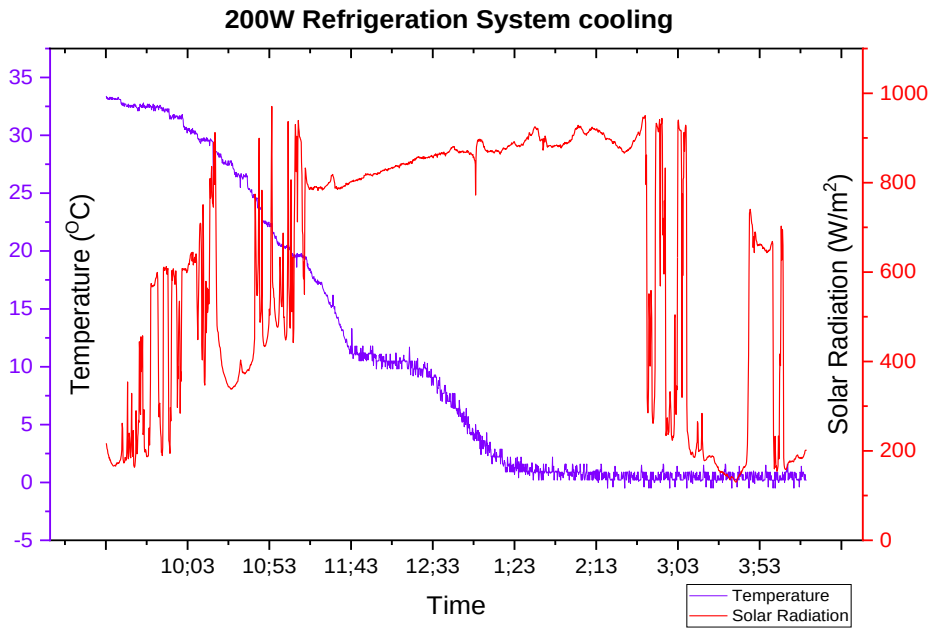

Figure 4.5a: Cooling profile for 200 W Solar driven refrigeration system

The cooling rate in the 250 W refrigeration system indicated a slow cooling rate in the early morning hours between 9 am, and 10 am. This resulted from insufficient solar radiation in the early hours needed to run the compressor of the refrigeration system, which should be a minimum of 420.715 W/m^2. The cooling rate was steady and fast between 10:30 am, and 11:50 am when the solar radiation was between 447 W/m^2 and 570 W/m^{2,} sufficient to run the refrigeration system's compressor. At 10 ^{O}C, the cooling rate dropped significantly and then resumed the cooling rate at 7.5 ^{O}C. It was observed that the milk temperature dropped from 33 ^{O}C to 4 ^{O}C.

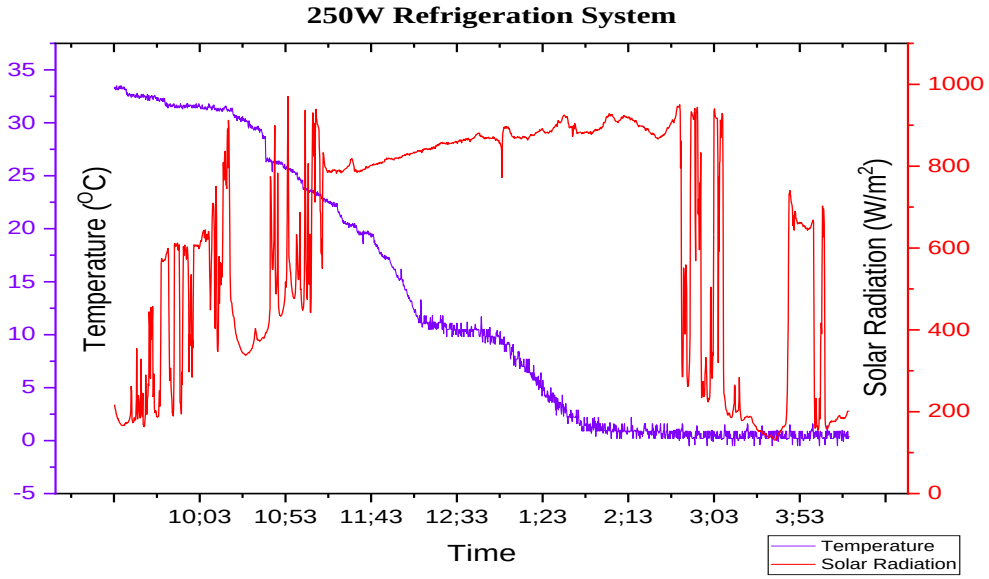

Figure 4.5b: Cooling load profile for 250 W solar-driven refrigeration system

When plotted under varying solar radiation, figures 4.6a and 4.6b show the cooling curves for the 200 W, 250 W and 350 W refrigeration systems. It was observed that the 200 W refrigeration system had the highest cooling rate in the morning hours, with a maximum cooling load of 0.245 kWh. Again, this resulted from the small capacity of the system's compressor that allowed the system to start with low solar radiation levels compared to the other higher capacity refrigeration systems

The cooling profile of the 350W refrigeration system exhibited no cooling rates between 9 am, and 10:45 am. This resulted from insufficient solar radiation in the early morning hours, below the minimum required to run the 350 W compressor of the system. The cooling rate improved between 10:50 am to 11:40 am when the solar radiation was above 500 W/m^2, and the water temperature dropped from 33 ^{O}C to 10 ^{O}C. This section of the cooling profile indicated the highest cooling rate. When the water temperature was at 10 ^{O}C, the cooling rate reduced significantly and resumed when the temperature was 8.0 ^{O}C.

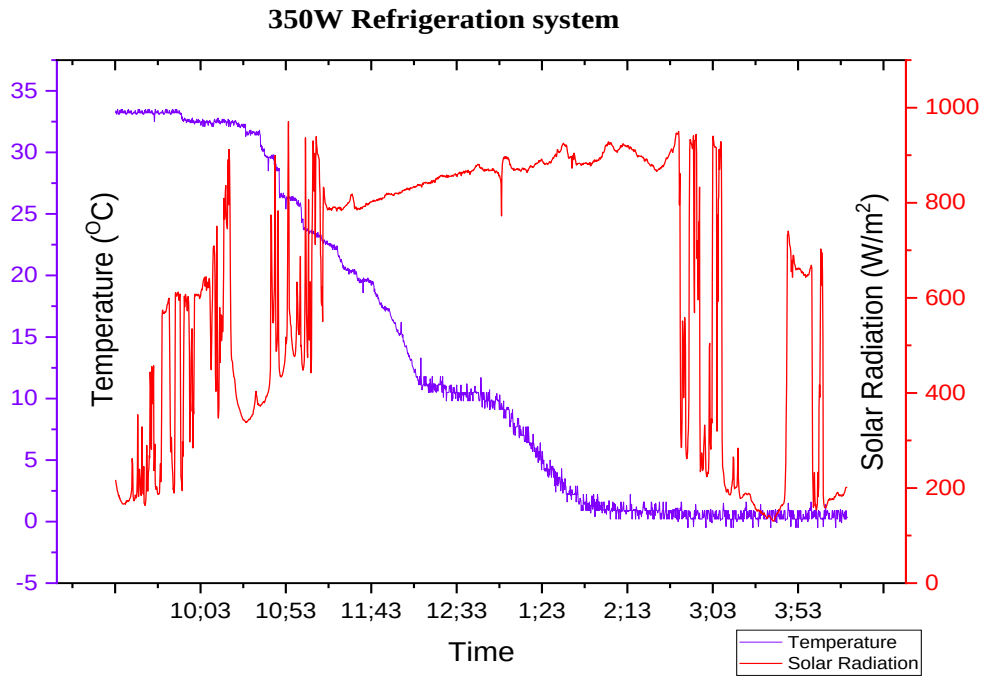

Figure 4.5c: Cooling profile for 350 W solar-driven refrigeration system

The 250 W refrigeration system had lower cooling rates than the 200W refrigeration system in the morning hours. The highest cooling rate occurred between 450 W/m^2 and 570 W/m^2. This was due to the availability of sufficient solar radiation required to start and maintain the running of the 250 W compressor. The 250W refrigeration system showed the highest cooling load of 0.262 kWh, the highest of the three refrigeration systems. The mean daily solar radiation for this particular day was 414.37 W/m^2 which meant that the larger number of hours of the day experienced solar radiation of between 420 W/m^2 to 570 W/m^2 hence providing the largest cooling load than the other refrigeration systems.

.

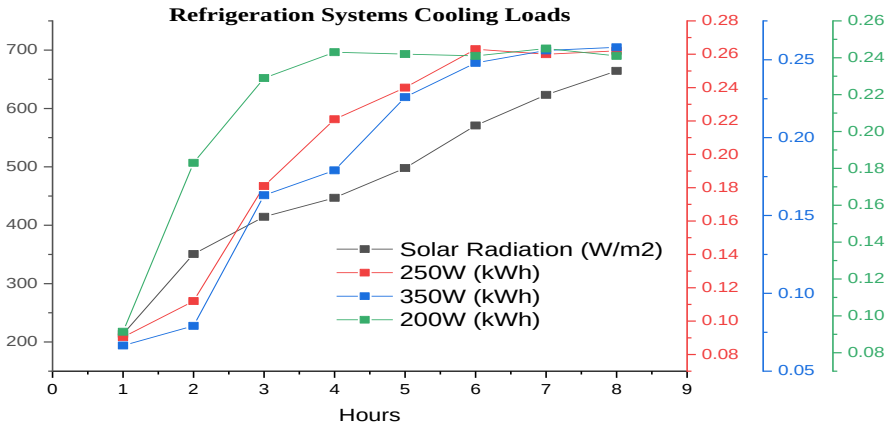

Figure 4.6a: Solar driven refrigeration systems cooling loads

Mean daily Solar Radiation (W/m^2)	System mean Cooling loads (kWh)		
	200 W	**250 W**	**350 W**
213.651	0.0914	0.0904	0.0665
350.682	0.183	0.112	0.0791
414.368	0.229	0.181	0.163
446.985	0.243	0.221	0.179
497.848	0.242	0.240	0.226
570.848	0.241	0.263	0.248
623.362	0.245	0.260	0.256
664.358	0.241	0.262	0.258
Total daily cooling Load (kWh)	**1.4744**	**1.6294**	**1.4736**

The lowest cooling rate in the morning hours was in the 350W refrigeration system for the three refrigeration systems. This was attributed to insufficient solar radiation below 570 W/m^2 in the morning to start running the 350 W compressor integrated into the refrigeration system. The highest cooling rate of this system was experienced when the solar radiation was above 580 W/m^2. The refrigeration system recorded the highest cooling load was 0.258 kWh, as indicated in table 4.4. The 250 W solar-driven refrigeration system exhibited the highest cooling load of the three refrigeration systems as indicted in 4.6a and similar the highest summation in cooling loads as in table of 1.6294kWh in. Victor Toress et al. (2016) and Petros and Michael (2009) observed a similar trend when experimenting with DC refrigeration compressors.

In determination of each refrigeration system's performance, the total cooling load was by adding the direct cooling load and the mass of ice created in each refrigeration system. Table 4.4 illustrates the average daily cooling loads for each refrigeration system. Table 4.5 shows the mass of ice created in each water container during chilling procedures as the mean daily solar radiation varies

Table 4.4: System mean cooling load

Mean daily Solar Radiation (W/m^2)	System mean Cooling loads (kWh)		
	200 W	**250 W**	**350 W**
213.651	0.0914	0.0904	0.0665
350.682	0.183	0.112	0.0791
414.368	0.229	0.181	0.163
446.985	0.243	0.221	0.179
497.848	0.242	0.240	0.226
570.848	0.241	0.263	0.248
623.362	0.245	0.260	0.256
664.358	0.241	0.262	0.258
Total daily cooling Load (kWh)	**1.4744**	**1.6294**	**1.4736**

4.2.3 Mass of Ice Formed in The Solar Driven Refrigeration Systems

Apart from direct cooling of milk when there was sufficient solar radiation, the solar-driven refrigeration system was also designed to cool milk for a minimum of 3 days when there was insufficient solar radiation occasioned to weather and seasonal changes. The thermal cooling load needed for milk cooling in the event of low solar radiation was provided by ice banks formed when there was sufficient solar radiation.

Table 4.5 shows the mass of ice formed by each of the three refrigeration systems on 3rd January 2017, when the mean daily solar radiation was 414.37 W/m^2, while figure 4.6b shows the profiles of the mass of ice formed in the three systems. From table 4.5 and figure 4.6b, the 200 W refrigeration system produced the maximum amount of ice equivalent to 5.78 kg between the solar radiation of 213.651 W/m^2 and 350 W/m^2. The 250 W refrigeration system generated the largest ice of 7.35 kg when the solar radiation band range was between 414.368 W/m^2 and 623.362 W/m^2. The largest refrigeration system with the highest compressor capacity generated 6.95kg of ice above a solar radiation band of 623.362 W/m^2. Thus, the 250 W solar-driven refrigeration system generated the largest ice, 7.35 kg, compared to the other refrigeration systems. This was due to the greater number of hours the 250 W refrigeration system was in operation and the compressor's capacity. Victor Torres et al. (2015), while experimenting on a small milk cooling system with ice storage, obtained 6 kg of ice when the system operated with mean solar radiation of about 414 W/m^2. It was observed that the three refrigeration systems received the maximum cooling loads at different solar radiation bands.

The 200W refrigeration system had a maximum cooling load of 0.243 kWh and an ice mass of 6.26 kg at a solar radiation band between 213.651 and 446.985 W/m^2. The 250 W refrigeration system had a maximum cooling load of 0.263 kWh in six hours when solar radiation band of 446.985 W/m^2 and 570.848 W/m^2. The 350 W refrigeration system showed a maximum cooling load of 0.258 kWh and ice of mass 6.95 above 664.358 W/m^2

Table 4.5: Mass of ice formed for different solar radiation and refrigeration systems

Mean daily Solar Radiation (W/m^2)	Refrigeration system and mass of ice formed (kg)		
	200 W	250 W	350 W
213.651	4.38	4.18	3.16
350.682	5.78	5.43	3.26
414.368	6.27	6.78	4.34
446.985	6.63	6.89	5.92
497.848	6.71	7.03	6.88
570.848	6.73	7.24	6.91
623.362	6.72	7.35	6.95
664.358	6.74	7.34	6.94

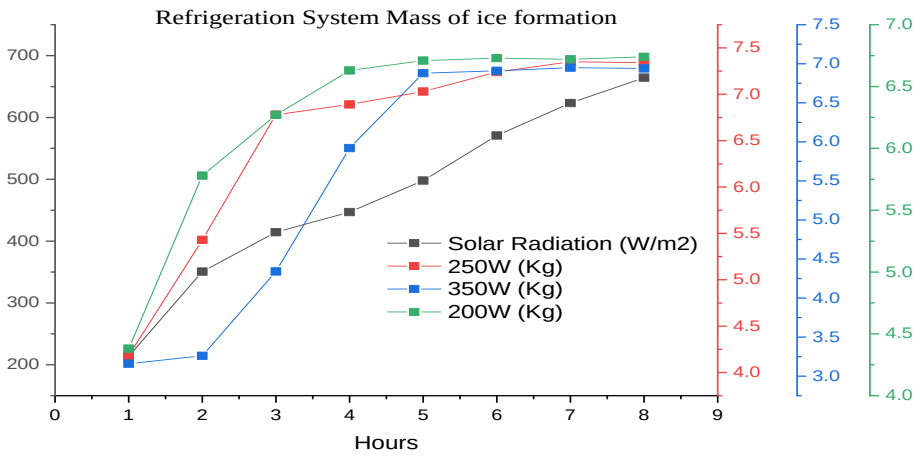

Figure 4.6b: Mass of ice formed in cooling process curves

4.3 Solar Refrigeration Cooling Load Curves

Since each solar-driven refrigeration system exhibited minimum and maximum cooling loads and a corresponding mass of ice formed at different mean daily solar radiation operating bands, the cooling load for each refrigeration system, when plotted separately, shows regression cooling loads curves as indicated in Figures. 4.7a, 4.7b and 4.7c.

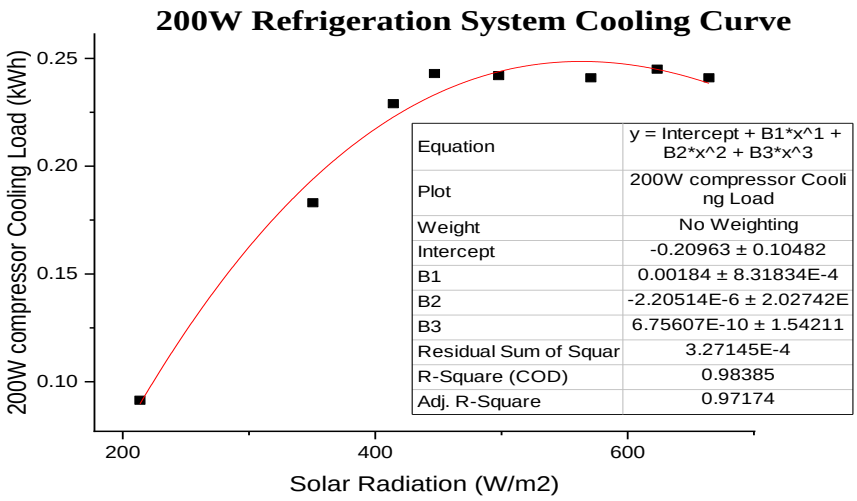

Figure 4.7a: Cooling load curve for 200 W solar-driven refrigeration system

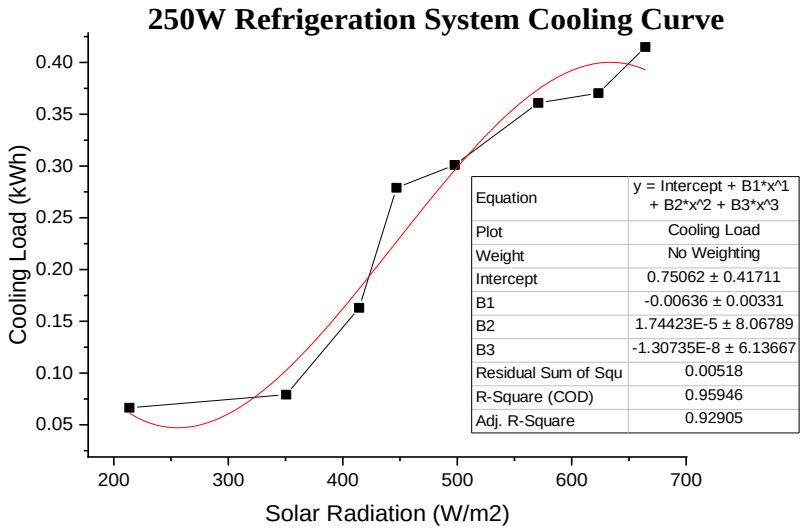

Figure 4.7b: Cooling load curve for 250 W solar-driven refrigeration system

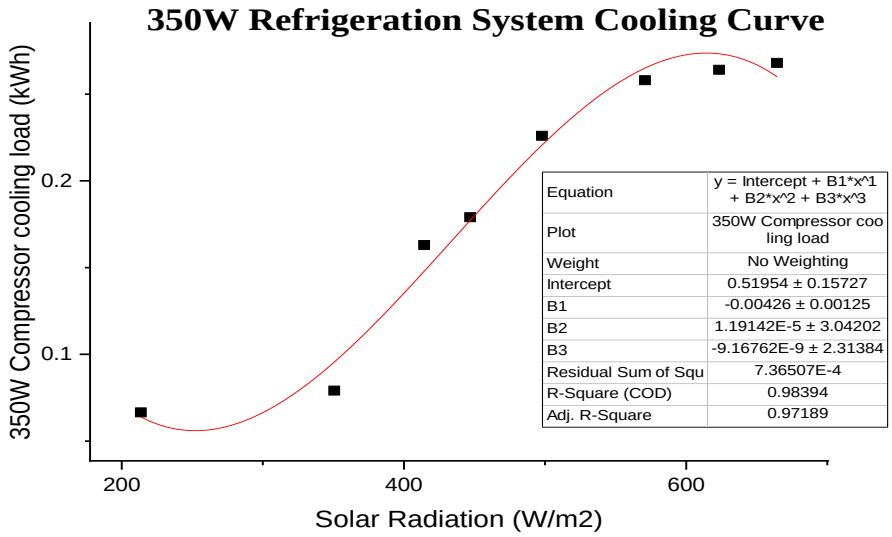

Figure 4.7c: Cooling load curve for 350 W solar-driven refrigeration system

The cooling load regression curves were used to develop the mathematical regression models for each refrigeration system based on the solar radiation between 200W/m^2 and 750W/m^2 and the best regression curve fitting. From the cooling curves in Figures 4.7a, 4.7b and 4.7c, the three refrigeration systems of 200 W, 250W and 350W generated the regression cooling models as shown in Equations 4.1, 4.2 and 4.3.

$$Q_L = -0.2096 + 0.00184S_R - 2.205E-6\left(S_R{}^2\right) + 6.756E-10\left(S_R{}^3\right) \quad 4.1$$

$$Q_L = 0.7506 - 0.00636S_R + 1.744E-5\left(S_R{}^2\right) - 1.3076E-8\left(S_R{}^3\right) \quad 4.2$$

$$Q_L = 0.5195 - 0.00426S_R + 1.1914E-5\left(S_R{}^2\right) - 9.176E-9\left(S_R{}^3\right) \quad 4.3$$

Q_L *is Cooling Load in kWh* S_R *is mean daily solar radiation in* W/m^2

Zhang et al. (2021) developed regression analysis models for estimating the refrigeration capacity of an ice storage system and obtained prediction of the cooling load R^2 of 0.951 when using gradient boosting decision tree (GBDT) model based on selection of input variables to predict the cooling load of commercial buildings. The highest COC was 0.9834.

4.3.1 Models for Predicting Power Supply to Solar Driven Refrigeration System from PV Panels

Power supply to the refrigeration systems compressors was obtained from the PV panels, which formed part of the major components of the solar-driven refrigeration system. It is important to develop power supply models for the refrigeration systems compressors to size PV panel components and equipment of the solar-driven Refrigeration systems.

The power supply to each compressor of the respective refrigeration system, from the PV panels and its inversion from DC to AC, depended on the coefficient od performance of the refrigeration COPr and the operating temperatures of the evaporator in each refrigeration system (Song et al., 2018). These two factors were stated in the manufacturer's catalogue of each compressor. Equation 4.4 relates the COPr of the refrigeration systems to the cooling load and the power supplied to the compressor from the PV panels and the accessories;

$$COPr = \frac{Cooling\ Load\ kWh}{Power\ Supplied\ kWh} \quad 4.4$$

From Equation 4.4, the power supplied to the compressor was expressed in Equation 4.5

$$Power\ supplied\ \ to\ compressor\ kWh = \frac{Cooling\ Load\ kWh}{COPr} \quad 4.5$$

An extract from the Danfoss compressor catalogue for the $COPr$ of 200W, 250W, and 350W compressors with evaporator temperatures of -5^{0}C are as indicated in Table 6.

The power supply to each of the three compressors when the solar radiation was between 200W/m^2 and 750W/m^2 from Equation 4.6 was expressed in Equations 4.7 and 4.8 for the 200 W, 250 W and 350 W compressors, respectively.

$$P_S = COP_r^{-1}[Evaporator\ cooling\ Load]\ kWh$$

$$P_s = \left[-0.1226 + 1.076^{-3}S_R - 2.377^{-3}E - 14.236\left(S_R{}^2\right) + 0.0962E - 5.848\left(S_R{}^3\right)\right] \quad 4.6$$

$$P_S = \left[0.4265 - 2.7125^{-3}S_R + 4.7306^{-3}E - 0.0237E\left(S_R{}^2\right) - 0.03093E - 0.2474\left(S_R{}^3\right)\right] \quad 4.7$$

$$P_S = \left[0.2778 - 1.1835^{-3}S_R + 1.41^{-3}E - 0.03525\left(S_R{}^2\right) - 0.3233E - 2.9094\left(S_R{}^3\right)\right] \quad 4.8$$

The above equations are applicable when the solar radiation is above 200W/m^2

Table 4.6: COPr for Danfoss compressors

Compressor size W	Model	Evaporating Temperature	COPr
200	TLS5FT tropical compressor R134a 220-240V 50/60HZ ASHRAE Low Back Pressure	-5ºC	1.71
250	SC12G Universal compressor R134a 220-240V 50/60HZ ASHRAE Low Back Pressure	-5ºC	1.76
350	TL4G Universal compressor R134a 220-240V 50/60HZ ASHRAE Low Back Pressure	-5ºC	1.87

4.4 Validation of Cooling Load Prediction Models

The validation of the mathematical models was performed by exposing the PV panels supplying power to the three solar-driven refrigeration systems to different mean daily solar radiation and comparing the cooling loads generated from each of the refrigeration systems with the cooling loads predicted by each of the three refrigeration system models at the corresponding mean daily solar radiation band. The mean daily solar radiation for the three refrigeration systems is indicated in Table 4.7. In contrast, Table 4.8 shows the corresponding cooling loads generated by the refrigeration system and the related models predicted cooling loads.

Table 4.7: Mean daily solar radiation

Compressor size (W)	Operating mean solar radiation band (W/m^2)	Mean daily solar Radiation (W/m^2)		
		Minimum	Average	Maximum
200 W	305.824 - 486.936	346.146	436.446	473.276
250 W	497.714 - 615.158	501.188	543.459	609.296
350 W	620.471- 695.613	629.678	652.791	684.189

For the purposes of comparing results obtained in this research with other similar research, statistical analysis on the performance of the cooling load predicting models, was

done using the coefficient of correlation in each refrigeration system. Figures 4.8a, 4.8b and 4.8c shows the correlation coefficients obtained for the 200 W, 250 W and 350 W refrigeration systems as 0.845, 0.9413 and 0.956, respectively.

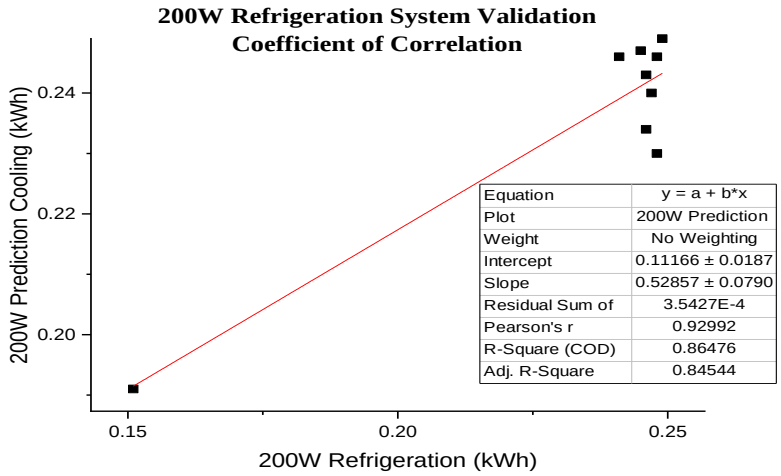

Figure 4.8a: Correlation between predicted and actual cooling load for 200 W Solar driven refrigeration system

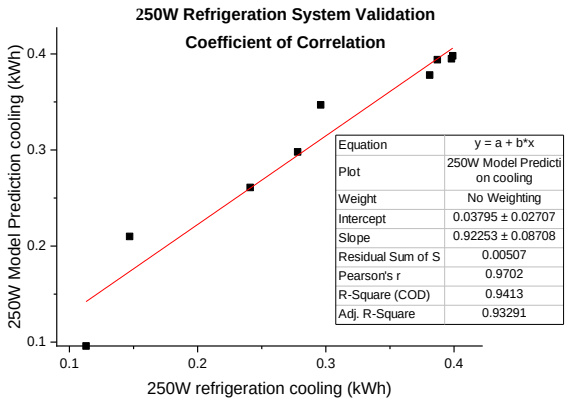

Figure 4.8b: Correlation between predicted and actual cooling load for 250 W Solar driven refrigeration system

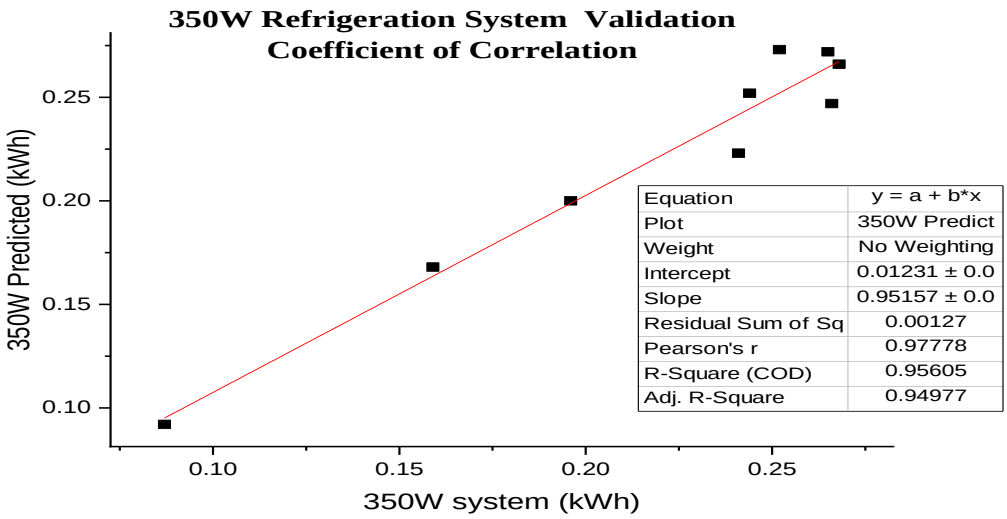

Figure 4.8c: Correlation between predicted and actual cooling load for 350 W Solar driven refrigeration system

Similarly, the power supply models to the three refrigeration systems of 200 W, 250 W and 350W, when tested for accuracy against power supply from the watt meters, showed a correlation coefficient of; 0.952, 0.958 and 0.908, respectively, as in Figures 4.9a, 4.9b and 4.9c.

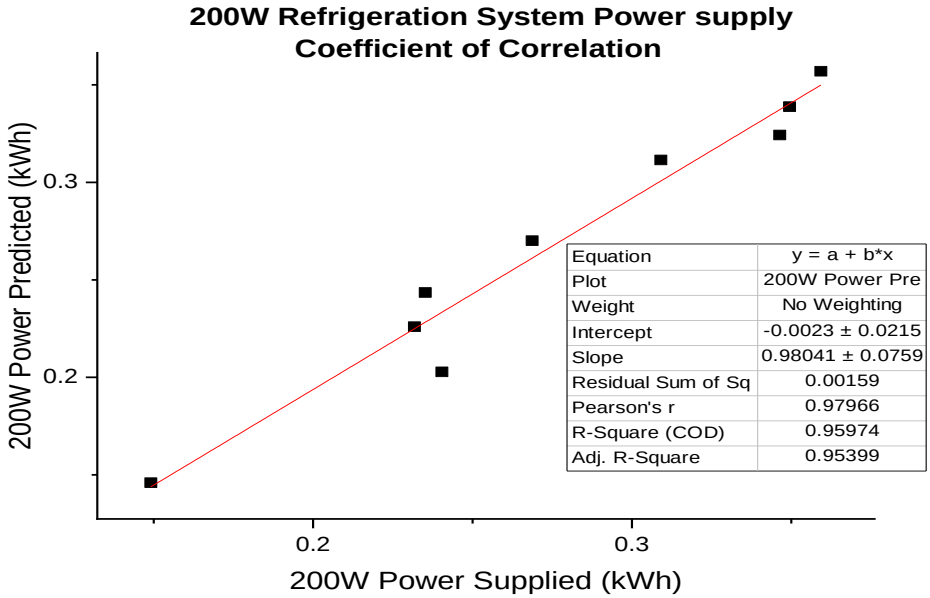

Figure 4.9a: Power supply Coefficient of correlation for 200 W Refrigeration system

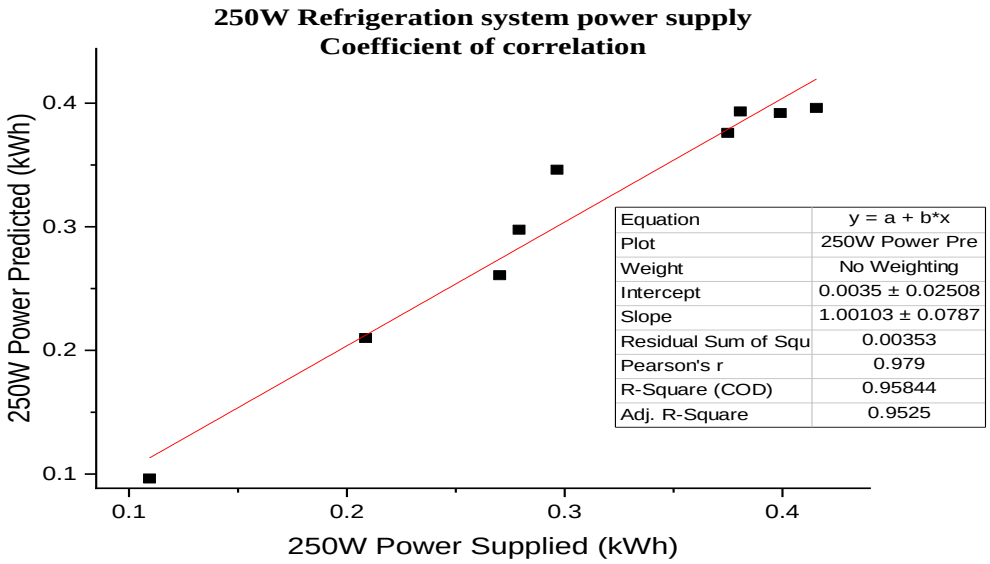

Figure 4.9b: Power supply Coefficient of correlation for 250 W Refrigeration system

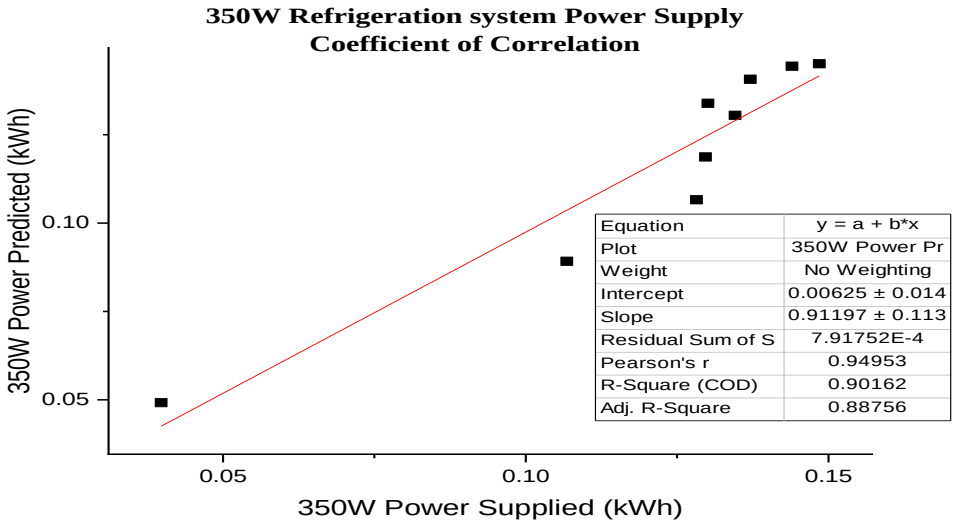

Figure 4.9c: Power supply Coefficient of correlation for 350 W Refrigeration system

CHAPTER FIVE

CONCLUSIONS AND RECOMMENDATIONS

5.1 Models for Predicting Solar Radiation

In this study four models were evaluated to determine their performance in predicting glodal mean solar radiation at different locations. The first models M1 (Gadiwali, 2013) showed a COC ($R^{2)}$ of 0.826. The other Three models: M2 (Seme, 2009), M3 (Sedanayeke, 2013) and M4 (Samani, 2000) had a COC of 0.735, 0.810 and 0.766 respectively. The most accurate of the three model from the Coefficient of Correlation was thus model M1 (Gadiwali, 2013) followed by M3 (Sedanayeke, 2013), M4 (Samani, 2000) and the least was M2 (Seme, 2009), with the corresponding values of 0.810, 0.766 and 0.735 respectively. Statically measures of errors from the deviation of the predicted and measured solar radiation RMSE, MBE, MABE, MPE and MAPE, showed a sum of errors of 64.819 for model M1 (Gadiwali, 2013). The was the least value from the other four models and thus the most accurate. From the two statistical tests mathematical model M1 (Gadiwali, 2013) was the most accurate in predicating mean daily solar radiation.

5.1.2 Capacity of solar driven refrigeration system that provide maximum cooling load

The 200W refrigeration system showed a highest cooling load of 0.229 kWh when exposed to the minimum mean solar radiation of 414W/m^2. The 250W refrigeration system showed a lower cooling load of 0.181kWh at the same mean solar radiation of 414.368W/m^2. The largest refrigeration system had the minimum cooling load of 0.163 kWh. the was the least cooling load of the three refrigeration systems. When the mean daily solar radiation increases from 414.368W/m^2 to a maximum of 570.848W/m^2, the highest cooling load was generated by the 250W refrigeration system of 0.263kWh. the 350W refrigeration system once again had a moderate cooling load of 0.248W/m^2. This cooling load values shows that the 250W refrigeration system had the maximum cooling load when the mean daily solar radiation was between 414.368W/m^2 and 570.848W/$m^{2.\ The}$ 350W refrigeration system showed a maximum cooling load of 0.258 at a solar radiation of 664.358W/m^2. The maximum cooling load for the three refrigeration systems was thus dependent on the mean daily solar radiation available. To compare among the three refrigeration systems' maximum cooling load, the total cooling load for each day was summed up to obtain the total daily cooling load. The 250W refrigeration system exhibited the maximum cooling load of 1.6294 kWh, followed by 200W and lastly by the 350W refrigeration system. From the performances the 250W refrigeration system had thus the maximum cooling rate when exposed to mean solar radiation of between 213.651W/m^2.

The maximum amount of ice formed was also a maximum of 7.34 kg from the 250W refrigeration system. The other refrigeration systems indicated 6.94 kg for the 350 W and 6.74 kg for the 200W refrigeration system. once again, the maximum cooling load was the 250W solar driven refrigeration system for mean daily solar radiation between 213.651W/m^2 and 664.358 W/m^2.

5.1.3 Mathematical Models for Predicting Solar driven Refrigeration Cooling Loads

The cooling load and volume of ice produced by the vapour compression refrigeration system were governed by the mean daily solar radiation available and the compressor capacity of the system. Because each refrigeration system's cooling load curve revealed a distinct ideal cooling load. Mathematical regression models were generated from the best regression curve fitting in each of three refrigeration systems cooling load curves produced. The maximum cooling load mathematical model was thus established as in equation 4.2. However, the other mathematical models are applicable in regions were mean daily solar radiation is between 213.651W/m^2 and 414.368W/m^2 for equation 4.1 and between mean daily solar radiation of 570.848W/m^2 and 664,358W/m^2 for equation 4.3.

5.2 Validation of the maximum solar driven refrigeration system cooling loads models

The validation in prediction of maximum cooling load for a solar driven refrigeration system that is accurate for a site depending on the mean daily solar radiation available, was carried out as follows; the three solar driven refrigeration systems; 200W, 250Wand 350W were exposed to different mean solar radiation between 346.146 W/m^2 and 683.189 W/m^2. The actual cooling load from each solar driven refrigeration system was compared with its corresponding predicted cooling load calculated from the model.

The coefficient of correlation between the actual and predicted maximum cooling loads for the 200W, 250W and the 350W solar refrigeration systems were 0.8647, 0.9413 and 0.956 respectively. Hence the maximum cooling loads predicted by the models for each system was comparable with the actual cooling loads generated the solar refrigeration system.

5.3 Recommendations

The above conclusions can be transferred with appropriate modifications for adoption in industrial design, production and operations of commercial solar driven refrigeration systems applicable in site with varying mean daily solar radiation.

Further research is recommended to determine;

i. The accuracy of the mean daily solar radiation prediction when models with parameters such as sky transmittance, albedo, relative air pressure, clearness index, and cloudiness index.

ii. The accuracy and precision of the maximum cooling load prediction models when other types of refrigeration systems are used such vapour adsorption.

iii. The effect of exposing the refrigeration system to mean solar radiation above 780W/m^2.

iv. The accuracy of the maximum cooling loads, when a combination of different compressor sizes is integrated in a single refrigeration system.

v. Test the reliability of the maximum cooling load prediction models due to variability of solar radiation caused by season of the year.

REFERENCES

Abdelwanees, E. A. (2018). *Design of Adsorption Cooling Cycle Operates by Solar Energy* (Doctoral dissertation, University of Benghazi).

Abdolmaleki, L., & Berardi, U. (2022). Single and Multi-phase Change Materials Used in Cooling Systems. *International Journal of Thermophysics*, *43*(4), 1-31.

Abdulrazzaq, A. A., & Ali, A. H. (2018). Efficiency performances of two MPPT algorithms for PV system with different solar panels irradiances. *International Journal of Power Electronics and Drive System (IJPEDS)*, *9*(4), 1755-1764.

Adenugba, F., Misra, S., Maskeliūnas, R., Damaševičius, R., & Kazanavičius, E. (2019). Smart irrigation system for environmental sustainability in Africa: An Internet of Everything (IoE) approach. *Mathematical Biosciences and Engineering*, *16*(5), 5490-5503.

Adwek, G., Boxiong, S., Ndolo, P. O., Siagi, Z. O., Chepsaigutt, C., Kemunto, C. M., & Yabo, A. C. (2020). The solar energy access in Kenya: a review focusing on Pay-As-You-Go solar home system. *Environment, Development and Sustainability*, *22*(5), 3897-3938.

Afshari, F., Karagoz, S., Comakli, O., & Ghasemi Zavaragh, H. (2019). Thermodynamic analysis of a system converted from heat pump to refrigeration device. *Heat and Mass Transfer*, *55*(2), 281-291.

Ağbulut, Ü., & Sarıdemir, S. (2021). A general view to converting fossil fuels to cleaner energy source by adding nanoparticles. *International Journal of Ambient Energy*, *42*(13), 1569-1574.

Ahmad, M. W., Reynolds, J., & Rezgui, Y. (2018). Predictive modelling for solar thermal energy systems: A comparison of support vector regression, random forest, extra trees and regression trees. *Journal of Cleaner Production*, *203*(8), 810-821.

Ahmadi, M. H., Ghazvini, M., Sadeghzadeh, M., Alhuyi Nazari, M., Kumar, R., Naeimi, A., & Ming, T. (2018). Solar power technology for electricity generation: A critical review. *Energy Science & Engineering*, *6*(5), 340-361.

Ahmadi, M. H., Ghazvini, M., Sadeghzadeh, M., Alhuyi Nazari, M., Kumar, R., Naeimi, A., & Ming, T. (2018). Solar power technology for electricity generation: A critical review. *Energy Science & Engineering*, *6*(5), 340-361.

Ahmed, M., El-Ghetany, H., Aziz, A. A., & Zohir, A. (2018). Modeling and Performance Prediction of an Adsorption Cooling System with Single Bed. *International Journal of Renewable Energy Research (IJRER)*, *8*(4), 2156-2166.

Ahrens, M. U., Foslie, S. S., Moen, O. M., Bantle, M., & Eikevik, T. M. (2021). Integrated high temperature heat pumps and thermal storage tanks for combined heating and cooling in the industry. *Applied Thermal Engineering*, *189*(1), 116-731.

Akbar, M., & Curiel-Sosa, J. L. (2019). An iterative finite element method for piezoelectric energy harvesting composite with implementation to lifting structures under gust load conditions. *Composite Structures*, *219*(3), 97-110.

Akhter, M. N., Mekhilef, S., Mokhlis, H., & Mohamed Shah, N. (2019). Review on forecasting of photovoltaic power generation based on machine learning and metaheuristic techniques. *IET Renewable Power Generation*, *13*(7), 1009-1023.

Al-Aboosi, F. Y. (2020). Models and hierarchical methodologies for evaluating solar energy availability under different sky conditions toward enhancing concentrating solar collectors use: Texas as a case study. *International Journal of Energy and Environmental Engineering*, *11*(2), 177-205.

Alahmer, A., Wang, X., & Alam, K. C. (2020). Dynamic and Economic Investigation of a Solar Thermal-Driven Two-Bed Adsorption Chiller under Perth Climatic Conditions. *Energies*, *13*(4), 1-19.

Al-Hajj, R., Assi, A., & Fouad, M. (2021). Short-term prediction of global solar radiation energy using weather data and machine learning ensembles: A comparative study. *Journal of Solar Energy Engineering*, *143*(5), 6-24

Alizadeh, H., Ghasempour, R., Shafii, M. B., Ahmadi, M. H., Yan, W. M., & Nazari, M. A. (2018). Numerical simulation of PV cooling by using single turn pulsating heat pipe. *International Journal of Heat and Mass Transfer*, *127*(1), 203-208.

Allen, E., Lyons, H., & Stephens, J. C. (2019). Women's leadership in renewable transformation, energy justice and energy democracy: Redistributing power. *Energy Research & Social Science*, *57*(10), 101-233.

Allen, R. G. (1997). Self-calibrating method for estimating solar radiation from air temperature. *Journal of Hydrologic Engineering*, *2*(2), 56-67.

AlMallahi, M. N., El Haj Assad, M., AlShihabi, S., & Alayi, R. (2022). Multi-criteria decision-making approach for the selection of cleaning method of solar PV panels in United Arab Emirates based on sustainability perspective. *International Journal of Low-Carbon Technologies*, *17*(1), 380-393.

Almasri, R. A., Abu-Hamdeh, N. H., Esmaeil, K. K., & Suyambazhahan, S. (2022). Thermal solar sorption cooling systems-A review of principle, technology, and applications. *Alexandria Engineering Journal*, *61*(1), 367-402.

Alola, A. A. (2021). Risk to investment and renewables production in the United States: An inference for environmental sustainability. *Journal of Cleaner Production*, *312*(1), 1-25.

Alsayah, A. M., Aboaltabooq, M. H. K., Majeed, M. H., & Al-Najafy, A. A. (2019). Multiple modern methods for improving photovoltaic cell efficiency by cooling: A review. *Journal of Mechanical Engineering Research and Developments*, *42*(4), 71-78.

Altun, A. F., & Kilic, M. (2020). Economic feasibility analysis with the parametric dynamic simulation of a single effect solar absorption cooling system for various climatic regions in Turkey. *Renewable Energy*, *152*(1), 75-93.

Alvarez, J. C., Bravo, L., Marçal, R. C., Hatakeyama, K., & Barrantes, E. (2021). Knowledge construction and systematization of solar adsorption refrigeration prototypes. *Energy Reports*, *7*(5), 428-440.

Álvarez-Alvarado, J. M., Ríos-Moreno, J. G., Obregón-Biosca, S. A., Ronquillo-Lomelí, G., Ventura-Ramos, E., & Trejo-Perea, M. (2021). Hybrid techniques to predict solar radiation using support vector machine and search optimization algorithms: a review. *Applied Sciences*, *11*(3), 10-44.

Al-Waeli, A. H., Kazem, H. A., Yousif, J. H., Chaichan, M. T., & Sopian, K. (2020). Mathematical and neural network modeling for predicting and analyzing of nanofluid-nano PCM photovoltaic thermal systems performance. *Renewable Energy*, *145*(3), 963-980.

Al-Yasiri, Q., Szabó, M., & Arıcı, M. (2022). A review on solar-powered cooling and air-conditioning systems for building applications. *Energy Reports*, *8*(5), 2888-2907.

Amarasinghe, P. A. G. M., Abeygunawardana, N. S., Jayasekara, T. N., Edirisinghe, E. A. J. P., & Abeygunawardane, S. K. (2020). Ensemble models for solar power forecasting—a weather classification approach. *AIMS Energy*, *8*(2), 252-271.

Ammari, E. T., Aksas, M., & Benmachiche, A. H. (2018). Performance study of small capacity solar autonomous absorption air-conditioning system coupled with a low-energy residential building under Batna (Algeria) climate. *International Journal of Air-Conditioning and Refrigeration*, *26*(1), 1-19.

Andrade, J. R., & Bessa, R. J. (2017). Improving renewable energy forecasting with a grid of numerical weather predictions. *IEEE Transactions on Sustainable Energy*, *8*(4), 1571-1580.

Angstrom, A. (1924). Solar and terrestrial radiation. Report to the international commission for solar research on actinometric investigations of solar and atmospheric radiation. *Quarterly Journal of the Royal Meteorological Society*, *50*(210), 121-126.

Antônio, A. D. S., Oliveira Filho, D., & Silva, S. C. D. (2018). OEM Original Quality Mobile Phone Touch LCD Replacement Display Screen for Alcatel Ot5008 Complete. *Engenharia Agrícola*, *38*(4), 518-525.

Antonopoulos, V. Z., Papamichail, D. M., Aschonitis, V. G., & Antonopoulos, A. V. (2019). Solar radiation estimation methods using ANN and empirical models. *Computers and Electronics in Agriculture*, *160*(1), 160-167.

Apell, J. N., & McNeill, K. (2019). Updated and validated solar irradiance reference spectra for estimating environmental photodegradation rates. *Environmental Science: Processes & Impacts*, *21*(3), 427-437.

Aramesh, M., Pourfayaz, F., Haghir, M., Kasaeian, A., & Ahmadi, M. H. (2020). Investigating the effect of using nanofluids on the performance of a double-effect absorption refrigeration cycle combined with a solar collector. *Proceedings of the Institution of Mechanical Engineers, Part A: Journal of Power and Energy*, *234*(7), 981-993.

Awan, A. B., Zubair, M., & Abokhalil, A. G. (2018). Solar energy resource analysis and evaluation of photovoltaic system performance in various regions of Saudi Arabia. *Sustainability*, *10*(4), 11-29.

Baakeem, S. S., Orfi, J., & Alabdulkarem, A. (2018). Optimization of a multistage vapor-compression refrigeration system for various refrigerants. *Applied Thermal Engineering*, *136*(1), 84-96.

Babatunde, O. M., Munda, J. L., & Hamam, Y. (2020). Power system flexibility: A review. *Energy Reports*, *6*(2), 101-106.

Babu, R., Raj, S., & Prasad, B. R. V. (2021). A Review at the Utilization of Renewable Energy in an Agricultural Operation. *Biophysical Economics and Sustainability*, *6*(4), 1-13.

Bagheri, B. S., Shirmohammadi, R., Mahmoudi, S. S., & Rosen, M. A. (2019). Optimization and comprehensive exergy-based analyses of a parallel flow double-effect water-lithium bromide absorption refrigeration system. *Applied Thermal Engineering*, *152*(2), 643-653.

Bailek, N., Bouchouicha, K., Abdel-Hadi, Y. A., El-Shimy, M., Slimani, A., Jamil, B., & Djaafari, A. (2020). Developing a new model for predicting global solar radiation on a horizontal surface located in Southwest Region of Algeria. *NRIAG Journal of Astronomy and Geophysics*, *9*(1), 341-349.

Baloch, Z. A., Tan, Q., Kamran, H. W., Nawaz, M. A., Albashar, G., & Hameed, J. (2022). A multi-perspective assessment approach of renewable energy production: policy perspective analysis. *Environment, Development and Sustainability*, *24*(2), 2164-2192.

Bamehr, S., & Sabetghadam, S. (2021). Estimation of global solar radiation data based on satellite-derived atmospheric parameters over the urban area of Mashhad, Iran. *Environmental Science and Pollution Research*, *28*(6), 7167-7179.

Barrera, J. M., Reina, A., Maté, A., & Trujillo, J. C. (2020). Solar Energy Prediction Model Based on Artificial Neural Networks and Open Data. *Sustainability*, *12*(17), 1-20.

Battersby, S. (2019). News Feature: The solar cell of the future. *Proceedings of the National Academy of Sciences*, *116*(1), 7-10.

Belgasim, B., Aldali, Y., Abdunnabi, M. J., Hashem, G., & Hossin, K. (2018). The potential of concentrating solar power (CSP) for electricity generation in Libya. *Renewable and Sustainable Energy Reviews*, *90*(1), 1-15.

Bellos, E., & Tzivanidis, C. (2018). Parametric analysis and optimization of a cooling system with ejector-absorption chiller powered by solar parabolic trough collectors. *Energy Conversion and Management*, *168*(1), 329-342.

Bellos, E., & Tzivanidis, C. (2021). Parametric analysis of a solar-driven trigeneration system with an organic Rankine cycle and a vapor compression cycle. *Energy and Built Environment*, *2*(3), 278-289.

Benatiallah, D., Bouchouicha, K., Benatiallah, A., Harrouz, A., & Nasri, B. (2019). Forecasting of solar radiation using an empirical model. *Algerian Journal of Renewable Energy and Sustainable Development*, *1*(2), 212-219.

Benedek, J., Sebestyén, T. T., & Bartók, B. (2018). Evaluation of renewable energy sources in peripheral areas and renewable energy-based rural development. *Renewable and Sustainable Energy Reviews*, *90*(2), 516-535.

Benkaciali, S., Haddadi, M., & Khellaf, A. (2018). Evaluation of direct solar irradiance from 18 broadband parametric models: Case of Algeria. *Renewable Energy*, *125* (2), 694-711.

Benöhr, M., & Gebremedhin, A. (2021). Photovoltaic systems for road networks. *International Journal of Innovative Technology and Interdisciplinary Sciences*, *4*(2), 672-684.

Bersano, A., Segantin, S., Falcone, N., Panella, B., & Testoni, R. (2020). Evaluation of a potential reintroduction of nuclear energy in Italy to accelerate the energy transition. *The Electricity Journal*, *33*(7), 106-813.

Bhukya, L., & Nandiraju, S. (2020). A novel photovoltaic maximum power point tracking technique based on grasshopper optimized fuzzy logic approach. *International Journal of Hydrogen Energy*, *45*(16), 9416-9427.

Bilen, K., Dağidir, K., & Arcaklioğlu, E. (2022). The effect of nanorefrigerants on performance of the vapor compression refrigeration system: a comprehensive review. *Energy Sources, Part A: Recovery, Utilization, and Environmental Effects*, *44*(2), 3177-3203.

Biswas, S., Banerjee, R., Bhattacharyya, D., Patra, G., Das, A. K., & Das, S. K. (2019). Technological investigation into duck meat and its products-a potential alternative to chicken. *World's Poultry Science Journal*, *75*(4), 609-620.

Bohra, S. S., & Anvari-Moghaddam, A. (2022). A comprehensive review on applications of multicriteria decision-making methods in power and energy systems. *International Journal of Energy Research*, *46*(4), 4088-4118.

Boussaada, Z., Curea, O., Remaci, A., Camblong, H., & Mrabet Bellaaj, N. (2018). A nonlinear autoregressive exogenous (NARX) neural network model for the prediction of the daily direct solar radiation. *Energies*, *11*(3), 30-620.

Brunet, C., Savadogo, O., Baptiste, P., & Bouchard, M. A. (2018). Shedding some light on photovoltaic solar energy in Africa–A literature review. *Renewable and Sustainable Energy Reviews*, *96*(8), 325-342.

Burhan, M., Shahzad, M. W., & Ng, K. C. (2018). Sustainable cooling with hybrid concentrated photovoltaic thermal (CPVT) system and hydrogen energy storage. *International Journal of Computational Physics Series*, *1*(2), 40-51.

Cagnoli, M., Mazzei, D., Procopio, M., Russo, V., Savoldi, L., & Zanino, R. (2018). Analysis of the performance of linear Fresnel collectors: Encapsulated vs. evacuated tubes. *Solar Energy*, *164*(1), 119-138.

Calise, F., Vicidomini, M., Costa, M., Wang, Q., Østergaard, P. A., & Duić, N. (2019). Toward an efficient and sustainable use of energy in industries and cities. *Energies*, *12*(16), 1-28.

Cannavale, A., Martellotta, F., Fiorito, F., & Ayr, U. (2020). The Challenge for Building Integration of Highly Transparent Photovoltaics and Photoelectrochromic Devices. *Energies*, *13*(8), 1-24.

Caprì, A., Frazzica, A., & Calabrese, L. (2020). Recent developments in coating technologies for adsorption heat pumps: A Review. *Coatings*, *10*(9), 855.

Catalbas, M. C., Kocak, B., & Yenipınar, B. (2021). Analysis of photovoltaic-green roofs in OSTIM industrial zone. *International Journal of Hydrogen Energy*, *46*(27), 14844-14856.

Cavallaro, K. F., Francois, J., Jacques, R., Mentor, D., Yalcouye, I., Wilkins, K., ... & Tohme, R. A. (2018). Demonstration of the use of remote temperature monitoring devices in vaccine refrigerators in Haiti. *Public Health Reports*, *133*(1), 39-44.

Chahartaghi, M., Kalami, M., Ahmadi, M. H., Kumar, R., & Jilte, R. (2019). Energy and exergy analyses and thermo-economic optimization of geothermal heat pump for domestic water heating. *International Journal of Low-Carbon Technologies*, *14*(2), 108-121.

Chakravarty, K. H., Sadi, M., Chakravarty, H., Alsagri, A. S., Howard, T. J., & Arabkoohsar, A. (2022). A review on integration of renewable energy processes in vapor absorption chiller for sustainable cooling. *Sustainable Energy Technologies and Assessments*, *50*(10), 18-22.

Chattopadhyay, S., & Ghosh, S. (2020). Techno-economic assessment of a biomass-based combined power and cooling plant for rural application. *Clean Technologies and Environmental Policy*, *22*(4), 907-922.

Cheekatamarla, P. (2021). Opportunities for Catalytic Reactions and Materials in Buildings. *Encyclopedia*, *2*(1), 36-55.

Chen, H., Chen, Z., Zhang, L., Li, P., Liu, J., Redfern, L. R., ... & Farha, O. K. (2019). Toward Design Rules of Metal–Organic Frameworks for Adsorption Cooling: Effect of Topology on the Ethanol Working Capacity. *Chemistry of Materials*, *31*(8), 2702-2706.

Chowdhury, N., Hossain, C. A., Longo, M., & Yaïci, W. (2018). Optimization of solar energy system for the electric vehicle at university campus in Dhaka, Bangladesh. *Energies*, *11*(9), 1-10.

Chu, P., Wang, H., Chen, J., Sun, H., Wang, H., & Dai, Y. (2021). Experiment investigation on a LiBr-H2O concentration difference cold storage system driven by vapor compression heat pump. *Solar Energy*, *214*(1), 294-309.

Collares-Pereira, M., & Rabl, A. (1979). The average distribution of solar radiation-correlations between diffuse and hemispherical and between daily and hourly insolation values. *Solar energy*, *22*(2), 155-164.

Coste, A. L., & Serban, C. (2011). Solar and wind power for brasov urban area. *Environmental Engineering and Management Journal*, *10*(2), 257-262.

Dai, Q., Liu, J., & Wei, Q. (2019). Optimal photovoltaic/battery energy storage/electric vehicle charging station design based on multi-agent particle swarm optimization algorithm. *Sustainability*, *11*(7), 1107-1973.

David, A., Joseph, E., Ngwa, N. R., & Arreyndip, N. A. (2018). Global Solar Radiation of some Regions of Cameroon using the Linear Angstrom Model and Non-linear Polynomial Relations: Part 2, Sun-path Diagrams, Energy Potential Predictions and Statistical Validation. *International Journal of Renewable Energy Research (IJRER)*, *8*(1), 649-660.

Day, J. W., D'Elia, C. F., Wiegman, A. R., Rutherford, J. S., Hall, C. A., Lane, R. R., & Dismukes, D. E. (2018). The energy pillars of society: Perverse interactions of human resource use, the economy, and environmental degradation. *Biophysical Economics and Resource Quality*, *3*(1), 1-16.

De Fazio, R., Al-Hinnawi, A. R., De Vittorio, M., & Visconti, P. (2022). An Energy-Autonomous Smart Shirt Employing Wearable Sensors for Users' Safety and Protection in Hazardous Workplaces. *Applied Sciences*, *12*(6), 1206-2926.

De, R. K., & Ganguly, A. (2019). Energy, exergy and economic analysis of a solar hybrid power system integrated double-effect vapor absorption system-based cold storage. *International Journal of Air-Conditioning and Refrigeration*, *27*(02), 1-13.

Devarajan, Y., Nagappan, B., Subbiah, G., & Kariappan, E. (2021). Experimental investigation on solar-powered ejector refrigeration system integrated with different concentrators. *Environmental Science and Pollution Research*, *28*(13), 16298-16307.

Devecioğlu, A., & Vedat, O. R. U. Ç. (2018). A comparative energetic analysis for some low-gwp refrigerants as r134a replacements in various vapor. *Isı Bilimi ve Tekniği Dergisi*, *38*(2), 51-61.

Dhamneya, A. K., Rajput, S. P. S., & Singh, A. (2018). Comparative performance analysis of ice plant test rig with TiO2-R-134a nano refrigerant and evaporative cooled condenser. *Case Studies in Thermal Engineering*, *11*(1), 55-61.

Dhraief, M. Z., Bedhiaf-Romdhania, S., Dhehibib, B., Oueslati-Zlaouia, M., Jebali, O., & Ben Youssef, S. (2018). Factors affecting the adoption of innovative technologies by livestock farmers in arid area of Tunisia. *FARA Research. Rep*, *3*(5), 1-22.

Diaby, A. T., Byrne, P., Loulergue, P., Sow, O., & Maré, T. (2021). Experimental Study of a Heat Pump for Simultaneous Cooling and Desalination by Membrane Distillation. *Membranes*, *11*(10), 7-25.

Diez, F. J., Martínez-Rodríguez, A., Navas-Gracia, L. M., Chico-Santamarta, L., Correa-Guimaraes, A., & Andara, R. (2021). Estimation of the hourly global solar irradiation on the tilted and oriented plane of photovoltaic solar panels applied to greenhouse production. *Agronomy*, *11*(3), 30-495.

Ding, W., & Bauer, T. (2021). Progress in research and development of molten chloride salt technology for next generation concentrated solar power plants. *Engineering*, *7*(3), 334-347.

D'Isep, F., & Sertorio, L. (1983). A passive solar heater-refrigerator. *Il Nuovo Cimento C*, *6*(6), 653-667.

Do, H. Q., Luther, M. B., Amirkhani, M., Wang, Z., & Martek, I. (2022). Radiant Conditioning Retrofitting for Residential Buildings. *Energies*, *15*(2), 4-49.

Du, K., Calautit, J., Wang, Z., Wu, Y., & Liu, H. (2018). A review of the applications of phase change materials in cooling, heating and power generation in different temperature ranges. *Applied Energy*, *220* (1), 242-273.

Echarri-Iribarren, V., Wong, N. H., & Sánchez-Ostiz, A. (2021). Radiant floors versus radiant walls using ceramic thermal panels in mediterranean dwellings: Annual energy demand and cost-effective analysis. *Sustainability*, *13*(2), 1-28.

Edwin, M., Nair, M. S., & Joseph Sekhar, S. (2022). A comprehensive review for power production and economic feasibility on hybrid energy systems for remote communities. *International Journal of Ambient Energy*, *43*(1), 1456-1468.

Egli, F. (2020). Renewable energy investment risk: an investigation of changes over time and the underlying drivers. *Energy Policy*, *140*(1), 1-24.

Ehnberg, J. S., & Bollen, M. H. (2005). Simulation of global solar radiation based on cloud observations. *Solar Energy*, *78*(2), 157-162.

Eikenberry, S. E., & Gumel, A. B. (2018). Mathematical modeling of climate change and malaria transmission dynamics: a historical review. *Journal of Mathematical Biology*, *77*(4), 857-933.

Ekren, O. (2020). Analysis of a Direct Current Compressor for Solar Cooler. *Journal of Solar Energy Research Updates*, *7*(1), 12-16.

Elbeh, M. B., & Sleiti, A. K. (2021). Analysis and optimization of concentrated solar power plant for application in arid climate. *Energy Science & Engineering*, *9*(6), 784-797.

Elmi, M. D. (2018). *Design of a Solar PV Energy System for Wajir Town, Wajir County, Kenya* (Doctoral dissertation, JKUAT-IEET).

Elsayed, M., Attia, A., & Tawfeek, S. (2022). Steady state numerical simulation and studying performance of a modified diffusion absorption refrigeration cycle. *Alexandria Engineering Journal*, *61*(4), 2591-2600.

Elsheniti, M. B., Abd El-Hamid, A. T., El-Samni, O. A., Elsherbiny, S. M., & Elsayed, E. (2021). Experimental evaluation of a solar two-bed lab-scale adsorption cooling system. *Alexandria Engineering Journal*, *60*(3), 2747-2757.

Entezari, A., Ge, T. S., & Wang, R. Z. (2018). Water adsorption on the coated aluminum sheets by composite materials (LiCl+ LiBr)/silica gel. *Energy*, *160*(1), 64-71.

Erzen, S., Açıkkalp, E., & Hepbasli, A. (2019). Performance assessment of a biogas fuelled molten carbonate fuel cell-thermophotovoltaic cell-thermally regenerative electrochemical cycle-absorption refrigerator-alkaline electrolyzer for multigenerational applications. *International Journal of Hydrogen Energy*, *44*(42), 23741-23749.

Eveloy, V. & Ayou, D. S. (2019). Sustainable District Cooling Systems: Status, Challenges, and Future Opportunities, with Emphasis on Cooling-Dominated Regions. *Energies*, *12*(2), 1-64.

Fan, J., Chen, B., Wu, L., Zhang, F., Lu, X., & Xiang, Y. (2018). Evaluation and development of temperature-based empirical models for estimating daily global solar radiation in humid regions. *Energy*, *144*(C), 903-914.

Fan, X., Liu, X., Hu, W., Zhong, C., & Lu, J. (2019). Advances in the development of power supplies for the internet of everything. *Information of Materials*, *1*(2), 130-139.

Faragallah, R. N., & Ragheb, R. A. (2022). Evaluation of thermal comfort and urban heat island through cool paving materials using ENVI-Met. *Ain Shams Engineering Journal*, *13*(3), 101-609.

Fashina, A., Mundu, M., Akiyode, O., Abdullah, L., Sanni, D., & Ounyesiga, L. (2018). The drivers and barriers of renewable energy applications and development in Uganda: a review. *Clean Technologies*, *1*(1), 9-39.

Fatima, T., Mentel, G., Doğan, B., Hashim, Z., & Shahzad, U. (2022). Investigating the role of export product diversification for renewable, and non-renewable energy consumption in GCC (gulf cooperation council) countries: does the Kuznets hypothesis exist?. *Environment, Development and Sustainability*, *24*(6), 8397-8417.

Figaj, R., & Żołądek, M. (2021). Operation and Performance Assessment of a Hybrid Solar Heating and Cooling System for Different Configurations and Climatic Conditions. *Energies*, *14*(4), 1-23.

Fong, K. F., & Lee, C. K. (2020). Solar desiccant cooling system for hot and humid region–A new perspective and investigation. *Solar Energy*, *195*(5), 677-684.

Fu, G. (2018). Deep belief network-based ensemble approach for cooling load forecasting of air-conditioning system. *Energy*, *148*(1), 269-282.

Gadiwala, M. S., Usman, A., Akhtar, M., & Jamil, K. (2013). Empirical models for the estimation of global solar radiation with sunshine hours on horizontal surface in various cities of Pakistan. *Pakistan Journal of Meteorology, 9*(18), 43-55.

Gado, M. G., Megahed, T. F., Ookawara, S., Nada, S., & El-Sharkawy, I. I. (2021). Performance and economic analysis of solar-powered adsorption-based hybrid cooling systems. *Energy Conversion and Management*, *238*(1), 1-15.

Galindo Luna, Y. R., Gómez Franco, W. R., Dehesa Carrasco, U., Romero Domínguez, R. J., & Jiménez García, J. C. (2018). Integration of the experimental results of a parabolic trough collector (PTC) solar plant to an absorption air-conditioning system. *Applied Sciences*, *8*(11), 1-24.

Garcia, J. M., & Rosa, A. (2019). Theoretical Study of an Intermittent Water-Ammonia Absorption Solar System for Small Power Ice Production. *Sustainability*, *11*(12), 1-18.

Garcia-Torres, F., Zafra-Cabeza, A., Silva, C., Grieu, S., Darure, T., & Estanqueiro, A. (2021). Model predictive control for microgrid functionalities: Review and future challenges. *Energies*, *14*(5), 5-1296.

Gautam, O. P., & Curtis, V. (2021). Food Hygiene Practices of Rural Women and Microbial Risk for Children: Formative Research in Nepal. *The American Journal of Tropical Medicine and Hygiene*, *105*(5), 1383.

Ghodbane, M., & HUSSEİN, A. K. (2021). Performance analysis of a solar-driven ejector air conditioning system under El-Oued climatic conditions, Algeria. *Journal of Thermal Engineering*, *7*(1), 172-189.

Ghodeshwar, A., & Sharma, P. (2018). Thermodynamic analysis of lithium bromide-water (LiBr-H2O) vapor absorption refrigeration system based on solar energy. *International Research Journal of Engineering and Technology (IRJET)*, *5*(01), 1365-1371.

Girma, Z. (2020). Success, Gaps and Challenges of Power Sector Reform in Ethiopia. *American Journal of Modern Energy*, *6*(1), 33-42.

Gopinathan, P. M., Pichan, G., & Sharma, V. M. (1988). Role of dehydration in heat stress-induced variations in mental performance. *Archives of Environmental Health: An International Journal*, *43*(1), 15-17.

Guasp, M., Laredo, C., & Urra, X. (2020). Higher solar irradiance is associated with a lower incidence of coronavirus disease 2019. *Clinical Infectious Diseases*, *71*(16), 2269-2271.

Guermoui, M., Gairaa, K., Rabehi, A., Djafer, D., & Benkaciali, S. (2018). Estimation of the daily global solar radiation based on the Gaussian process regression methodology in the Saharan climate. *The European Physical Journal Plus*, *133*(6), 1-17.

Guerra, O. J., Zhang, J., Eichman, J., Denholm, P., Kurtz, J., & Hodge, B. M. (2020). The value of seasonal energy storage technologies for the integration of wind and solar power. *Energy & Environmental Science*, *13*(7), 1909-1922.

Gündüz, B., Dindar, B., & Gül, Ö. (2021). Arc-flash hazard calculations in a electrical distribution system with distributed generation for electrical safety audit. *International Journal of Safety and Security Engineering*, *11*(5), 1-25.

Gupta, S., & Sharma, V. K. (2021). Design and analysis of metal hydride reactor embedded with internal copper fins and external water cooling. *International Journal of Energy Research*, *45*(2), 1836-1856.

Hafez, A. A., Nassar, Y. F., Hammdan, M. I., & Alsadi, S. Y. (2020). Technical and economic feasibility of utility-scale solar energy conversion systems in Saudi Arabia. *Iranian Journal of Science and Technology, Transactions of Electrical Engineering*, *44*(1), 213-225.

Hafner, A., & Ciconkov, R. (2021). Natural refrigerants in all applications. Is it possible. *Zbornik Međunarodnog Kongresa o KGH*, *52*(1), 11-20.

Halon, T., Pelinska-Olko, E., Szyc, M., & Zajaczkowski, B. (2019). Predicting performance of a district heat powered adsorption chiller by means of an artificial neural network. *Energies*, *12*(17), 1-11.

Hamzeh, H. A., & Miansari, M. (2020). Numerical study of tube arrangement and fin effects on improving the ice formation in ice-on-coil thermal storage systems. *International Communications in Heat and Mass Transfer*, *113*(1), 104-520.

Hassan, G., Khan, F., Hassan, A., Ali, S., Bae, J., & Lee, C. H. (2017). A flat-panel-shaped hybrid piezo/triboelectric nanogenerator for ambient energy harvesting. *Nanotechnology*, *28*(17), 175-402.

Hayat, M. B., Ali, D., Monyake, K. C., Alagha, L., & Ahmed, N. (2019). Solar energy—A look into power generation, challenges, and a solar-powered future. *International Journal of Energy Research*, *43*(3), 1049-1067.

Heidrich, L., Friess, N., Fiedler, K., Brändle, M., Hausmann, A., Brandl, R., & Zeuss, D. (2018). The dark side of Lepidoptera: colour lightness of geometrid moths decreases with increasing latitude. *Global Ecology and Biogeography*, *27*(4), 407-416.

Herbert Raj, M., & Mohan Lal, D. (2010). Boiling heat transfer coefficient of R22 and an HFC/HC refrigerant mixture in a fin-and-tube evaporator of a window air conditioner. *Heat Transfer—Asian Research*, *39*(6), 410-439.

Hereher, M., & El Kenawy, A. M. (2020). Exploring the potential of solar, tidal, and wind energy resources in Oman using an integrated climatic-socioeconomic approach. *Renewable Energy*, *161* (7), 662-675.

Hernández Moris, C., Cerda Guevara, M. T., Salmon, A., & Lorca, Á. G. (2021). Comparison between concentrated solar power and gas-based generation in terms of economic and flexibility-related aspects in Chile. *Energies*, *14*(4), 1063.

Hinkelman, K., Wang, J., Zuo, W., Gautier, A., Wetter, M., Fan, C., & Long, N. (2022). Modelica-based modeling and simulation of district cooling systems: A case study. *Applied Energy*, *311*(16), 118-654.

Hojjatian, M., Heravi, A., & Asad Poor, J. (2021). An overview of the use of solar energy in building construction projects. *Creative City Design*, *4*(2), 33-39.

Hou, J., Cao, M., & Liu, P. (2018). Development and utilization of geothermal energy in China: Current practices and future strategies. *Renewable energy*, *125*, 401-412.

Huang, L., & Zheng, R. (2018). Energy and economic performance of solar cooling systems in the hot-summer and cold-winter zone. *Buildings*, *8*(3), 1-37.

Huang, Y., Khazeraee, M., Wang, H., Fard, S. M., Zhu, T., & Khajepour, A. (2018). Design of a regenerative auxiliary power system for service vehicles. *Automotive Innovation*, *1*(1), 62-69.

Huaulmé, Q., Mwalukuku, V. M., Joly, D., Liotier, J., Kervella, Y., Maldivi, P., ... & Demadrille, R. (2020). Photochromic dye-sensitized solar cells with light-driven adjustable optical transmission and power conversion efficiency. *Nature Energy*, *5*(6), 468-477.

Hussain, M. I., Ménézo, C., & Kim, J. T. (2018). Advances in solar thermal harvesting technology based on surface solar absorption collectors: A review. *Solar Energy Materials and Solar Cells*, *187*(1), 123-139.

Imran, M., Özçatalbaş, O., & Bashir, M. K. (2020). Estimation of energy efficiency and greenhouse gas emission of cotton crop in South Punjab, Pakistan. *Journal of the Saudi Society of Agricultural Sciences*, *19*(3), 216-224.

Inderwildi, O., Zhang, C., Wang, X., & Kraft, M. (2020). The impact of intelligent cyber-physical systems on the decarbonization of energy. *Energy and Environmental Science*, *13*(3), 744-771.

Islam, M. T., Huda, N., Abdullah, A. B., & Saidur, R. (2018). A comprehensive review of state-of-the-art concentrating solar power (CSP) technologies: Current status and research trends. *Renewable and Sustainable Energy Reviews*, *91*(3), 987-1018.

Jani, D. B., Mishra, M., & Sahoo, P. K. (2018). A critical review on application of solar energy as renewable regeneration heat source in solid desiccant–vapor compression hybrid cooling system. *Journal of Building Engineering*, *18*(2), 107-124.

Jiang, L., Lu, H., Wang, R., Wang, L., Gong, L., Lu, Y., & Roskilly, A. P. (2017). Investigation on an innovative cascading cycle for power and refrigeration cogeneration. *Energy Conversion and Management*, *145*(2), 20-29.

Jiménez-García, J. C., & Rivera, W. (2018). Parametric analysis on the performance of an experimental ammonia/lithium nitrate absorption cooling system. *International Journal of Energy Research*, *42*(14), 4402-4416.

Jing, Y., Li, Z., Liu, L., & Lu, S. (2018). Exergoeconomic assessment of solar absorption and absorption–compression hybrid refrigeration in building cooling. *Entropy*, *20*(2), 1-22.

Joshi, Y. G., Zanwar, D. R., Joshi, S. S., & Bhave, N. A. (2022). Experimental investigation of Al2O3 nanosuspension in vapor compression refrigeration system using tetrafluoroethane and iso-butane refrigerants. *Materials Today: Proceedings*, *50*(1), 1804-1813.

Jurado, J. P., Dörling, B., Zapata-Arteaga, O., Roig, A., Mihi, A., & Campoy-Quiles, M. (2019). Solar harvesting: a unique opportunity for organic thermoelectrics?. *Advanced Energy Materials*, *9*(45), 23-85.

Kaba, K., Sarıgül, M., Avcı, M., & Kandırmaz, H. M. (2018). Estimation of daily global solar radiation using deep learning model. *Energy*, *162*(7), 126-135.

Karunathilake, H., Hewage, K., Mérida, W., & Sadiq, R. (2019). Renewable energy selection for net-zero energy communities: Life cycle based decision making under uncertainty. *Renewable Energy*, *130*(3), 558-573.

Kasera, S., Nayak, R., & Bhaduri, S. C. (2022). A Review of Performance of Solar Photovoltaic Refrigeration System. *Advances in Energy Technology*, *766*(7), 641-651.

Kashif, M., Niaz, H., Sultan, M., Miyazaki, T., Feng, Y., Usman, M., ... & Ali, I. (2020). Study on desiccant and evaporative cooling systems for livestock thermal comfort: Theory and experiments. *Energies*, *13*(11), 1-18.

Kelly, A. G. (2018). *Printed Electronics from Solution-Processed 2D Materials* (Doctoral dissertation, Trinity College Dublin).

Khalifa, A. H. N., Mohammed, A. A., & Toma, R. R. (2018). Experimental study on thermal energy storage produced by solar energy for driving domestic freezer. *Journal of Engineering Science and Technology*, *13*(9), 2827-40.

Khaliq, A., Almohammadi, B. A., Alharthi, M. A., Siddiqui, M. A., & Kumar, R. (2021). Investigation of a combined refrigeration and air conditioning system based on two-phase ejector driven by exhaust gases of natural gas fueled homogeneous charge compression ignition engine. *Journal of Energy Resources Technology*, *143*(12), 405-2248.

Khan, F., & Malik, K. (2021). Tarbiyat-e-Khudi: A Model of Self-Development from Poems of Muhammad Iqbal in Asrar-i-Khudi. *Bahria Journal of Professional Psychology*, *20*(1), 14-26.

Khan, M. S. A., Badar, A. W., Talha, T., Khan, M. W., & Butt, F. S. (2018). Configuration based modeling and performance analysis of single effect solar absorption cooling system in TRNSYS. *Energy Conversion and Management*, *157*(1), 351-363.

Khan, P. W., Byun, Y. C., Lee, S. J., Kang, D. H., Kang, J. Y., & Park, H. S. (2020). Machine learning-based approach to predict energy consumption of renewable and nonrenewable power sources. *Energies*, *13*(18), 48-70.

Khatibi, A., Razi Astaraei, F., & Ahmadi, M. H. (2019). Generation and combination of the solar cells: A current model review. *Energy Science & Engineering*, *7*(2), 305-322.

Khatoon, S., Almefreji, N. M. A., & Kim, M. H. (2021). Thermodynamic study of a combined power and refrigeration system for low-grade heat energy source. *Energies*, *14*(2), 410.

Khidhir, D. K., & Atrooshi, S. A. (2020). Investigation of thermal concentration effect in a modified solar chimney. *Solar Energy*, *206*(1), 799-815.

Khosla, R., Miranda, N. D., Trotter, P. A., Mazzone, A., Renaldi, R., McElroy, C., ... & McCulloch, M. (2021). Cooling for sustainable development. *Nature Sustainability*, *4*(3), 201-208.

Khurmi, R. S., & Gupta, J. K. (2008). *Textbook of refrigeration and air conditioning*. S. Chand Publishing.

Kim, G. G., Choi, J. H., Park, S. Y., Bhang, B. G., Nam, W. J., Cha, H. L., ... & Ahn, H. K. (2019). Prediction model for PV performance with correlation analysis of environmental variables. *IEEE Journal of Photovoltaics*, *9*(3), 832-841.

Kim, N., & Parkhideh, B. (2018). PV-battery series inverter architecture: A solar inverter for seamless battery integration with partial-power DC–DC optimizer. *IEEE Transactions on Energy Conversion*, *34*(1), 478-485.

Kim, S. G., Jung, J. Y., & Sim, M. K. (2019). A Two-Step Approach to Solar Power Generation Prediction Based on Weather Data Using Machine Learning. *Sustainability*, *11*(5), 1-16.

Knabben, F. T., Ronzoni, A. F., & Hermes, C. J. (2020). Application of electronic expansion valves in domestic refrigerators. *International Journal of Refrigeration*, *119*(1), 227-237.

Kordlar, M. A., & Mahmoudi, S. M. S. (2017). Exergeoconomic analysis and optimization of a novel cogeneration system producing power and refrigeration. *Energy Conversion and Management*, *100*(134), 208-220.

Korkmaz, D., Acikgoz, H., & Yildiz, C. (2021). A novel short-term photovoltaic power forecasting approach based on deep convolutional neural network. *International Journal of Green Energy*, *18*(5), 525-539.

Krauter, S. (2018). Simple and effective methods to match photovoltaic power generation to the grid load profile for a PV based energy system. *Solar Energy*, *159*(11), 768-776.

Kumar, D. S., Yagli, G. M., Kashyap, M., & Srinivasan, D. (2020). Solar irradiance resource and forecasting: a comprehensive review. *IET Renewable Power Generation*, *14*(10), 1641-1656.

Lai, X., Huang, Y., Gu, H., Deng, C., Han, X., Feng, X., & Zheng, Y. (2021). Turning waste into wealth: A systematic review on echelon utilization and material recycling of retired lithium-ion batteries. *Energy Storage Materials*, *40*(1), 96-123.

Laine, H. S., Salpakari, J., Looney, E. E., Savin, H., Peters, I. M., & Buonassisi, T. (2019). Meeting global cooling demand with photovoltaics during the 21st century. *Energy & Environmental Science*, *12*(9), 2706-2716.

Laiti, L., Giovannini, L., Zardi, D., Belluardo, G., & Moser, D. (2018). Estimating Hourly Beam and Diffuse Solar Radiation in an Alpine Valley: A Critical Assessment of Decomposition Models. *Atmosphere*, *9*(117), 1-20.

Langdon-Arms, S., Gschwendtner, M., & Neumaier, M. (2018). A novel solar-powered liquid piston Stirling refrigerator. *Applied energy*, *229*(3), 603-613.

Lawrence, D. M., Fisher, R. A., Koven, C. D., Oleson, K. W., Swenson, S. C., Bonan, G., ... & Zeng, X. (2019). The Community Land Model version 5: Description of new features,

benchmarking, and impact of forcing uncertainty. *Journal of Advances in Modeling Earth Systems*, *11*(12), 4245-4287.

Lee, J. S., Yoon, J. W., Mileo, P. G., Cho, K. H., Park, J., Kim, K., ... & Chang, J. S. (2019). Porous metal–organic framework CUK-1 for adsorption heat allocation toward green applications of natural refrigerant water. *ACS Applied Materials and Interfaces*, *11*(29), 25778-25789.

Lee, J. T., & Callaway, D. S. (2018). The cost of reliability in decentralized solar power systems in sub-Saharan Africa. *Nature Energy*, *3*(11), 960-968.

Lekbir, A., Hassani, S., Ab Ghani, M. R., Gan, C. K., Mekhilef, S., & Saidur, R. (2018). Improved energy conversion performance of a novel design of concentrated photovoltaic system combined with thermoelectric generator with advance cooling system. *Energy Conversion and Management*, *177*(1), 19-29.

Li, B., Hua, L., Tu, Y., & Wang, R. (2019). A full-solid-state humidity pump for localized humidity control. *Joule*, *3*(6), 1427-1436.

Li, F., Sun, B., Zhang, C., & Liu, C. (2019). A hybrid optimization-based scheduling strategy for combined cooling, heating, and power system with thermal energy storage. *Energy*, *188*(1), 115-948.

Li, J. F., Guo, H., Wu, Y. T., Lei, B., Ye, F., Ma, C. F., ... & Jiao, X. L. (2022). Experimental investigation of solar organic Rankine cycle with parabolic trough concentrator using nitrate salt as heat transfer and storage fluid. *International Journal of Energy Research*, *46*(5), 6847-6865.

Li, S., Voigt, A., Schäfer, A. I., & Richards, B. S. (2020). Renewable energy powered membrane technology: Energy buffering control system for improved resilience to periodic fluctuations of solar irradiance. *Renewable Energy*, *149*(C), 877-889.

Li, W., & Fan, S. (2019). Radiative cooling: harvesting the coldness of the universe. *Optics and Photonics News*, *30*(11), 32-39.

Liang, Y., Sun, Z., Dong, M., Lu, J., & Yu, Z. (2020). Investigation of a refrigeration system based on combined supercritical CO2 power and transcritical CO2 refrigeration cycles by waste heat recovery of engine. *International Journal of Refrigeration*, *118*(1), 470-482.

Lima, A. A., de NP Leite, G., Ochoa, A. A., dos Santos, C. A., da Costa, J. A., Michima, P. S., & Caldas, A. (2020). Absorption Refrigeration Systems Based on Ammonia as Refrigerant Using Different Absorbents: Review and Applications. *Energies*, *14*(1), 1-1.

Luderer, G., Madeddu, S., Merfort, L., Ueckerdt, F., Pehl, M., Pietzcker, R., ... & Kriegler, E. (2022). Impact of declining renewable energy costs on electrification in low-emission scenarios. *Nature Energy*, *7*(1), 32-42.

Maalem, Y., Fedali, S., Madani, H., & Tamene, Y. (2020). Performance analysis of ternary azeotropic mixtures in different vapor compression refrigeration cycles. *International Journal of Refrigeration*, *119*(1), 139-151.

Mahalle, K., Parab, P., & Bhagwat, S. (2019). Optimization of cooling load in the combined vapour absorption–vapour compression refrigeration cycle using exergy analysis. *Indian Chemical Engineer*, *61*(1), 52-66.

Mahama, M., Derkyi, N. S. A., & Nwabue, C. M. (2021). Challenges of renewable energy development and deployment in Ghana: Perspectives from developers. *GeoJournal*, *86*(3), 1425-1439.

Mahon, D., Claudio, G., & Eames, P. (2021). An experimental study of the decomposition and carbonation of magnesium carbonate for medium temperature thermochemical energy storage. *Energies*, *14*(5), 1-23.

Manoharan, P., Subramaniam, U., Babu, T. S., Padmanaban, S., Holm-Nielsen, J. B., Mitolo, M., & Ravichandran, S. (2020). Improved perturb and observation maximum power point tracking technique for solar photovoltaic power generation systems. *IEEE Systems Journal*, *15*(2), 3024-3035.

Mao, J., Chen, G., & Ren, Z. (2021). Thermoelectric cooling materials. *Nature Materials*, *20*(4), 454-461.

Mariya, D., Usman, J., Mathew, E. N., & Aa, P. H. H. (2020). Reverse vending machine for plastic bottle recycling. *International Journal of Computer Science and Technology*, *8*(2), 65-70.

Masood, F., Nor, N. B. M., Nallagownden, P., Elamvazuthi, I., Saidur, R., Alam, M. A., ... & Ali, M. (2022). A Review of Recent Developments and Applications of Compound Parabolic Concentrator-Based Hybrid Solar Photovoltaic/Thermal Collectors. *Sustainability*, *14*(9), 1-30.

Maulidia, M., Dargusch, P., Ashworth, P., & Ardiansyah, F. (2019). Rethinking renewable energy targets and electricity sector reform in Indonesia: A private sector perspective. *Renewable and Sustainable Energy Reviews*, *101*(3), 231-247.

McLinden, M. O., Seeton, C. J., & Pearson, A. (2020). New refrigerants and system configurations for vapor-compression refrigeration. *Science*, *370*(6518), 791-796.

Meesilp, N., & Mesil, N. (2019). Effect of microbial sanitizers for reducing biofilm formation of Staphylococcus aureus and Pseudomonas aeruginosa on stainless steel by cultivation with UHT milk. *Food Science and Biotechnology*, *28*(1), 289-296.

Mehdizadeh Rad, H., Zhu, F., & Singh, J. (2018). Profiling exciton generation and recombination in conventional and inverted bulk heterojunction organic solar cells. *Journal of Applied Physics*, *124*(8), 83-103.

Mehellou, S., Rehouma, F., Hamrouni, N., & Bouras, L. (2018). Thermal loading effects on Nd: YAG solar-laser performance in end-pumping and side-pumping configurations: a review. *Optical Engineering*, *57*(12), 120-902.

Memon, S., Katsura, T., Radwan, A., Zhang, S., Serageldin, A. A., Abo-Zahhad, E. M., ... & Kiani, A. (2020). Modern eminence and concise critique of solar thermal energy and vacuum insulation technologies for sustainable low-carbon infrastructure. *International Journal of Solar Thermal Vacuum Engineering*, *1*(1), 52-71.

Micena, R. P., Llerena-Pizarro, O. R., de Souza, T. M., & Silveira, J. L. (2020). Solar-powered hydrogen refueling stations: a techno-economic analysis. *International Journal of Hydrogen Energy*, *45*(3), 2308-2318.

Mirmasoudi, S., Byrne, J., Kroebel, R., Johnson, D., & MacDonald, R. (2018). A novel time-effective model for daily distributed solar radiation estimates across variable terrain. *International Journal of Energy and Environmental Engineering*, *9*(4), 383-398.

Modenese, A., Korpinen, L., & Gobba, F. (2018). Solar radiation exposure and outdoor work: an underestimated occupational risk. *International Journal of Environmental Research and Public Health*, *15*(10), 20-63.

Moghimi, M., Emadi, M., Ahmadi, P., & Moghadasi, H. (2018). 4E analysis and multi-objective optimization of a CCHP cycle based on gas turbine and ejector refrigeration. *Applied Thermal Engineering*, *141*(1), 516-530.

Mohamad, F., Teh, J., Lai, C. M., & Chen, L. R. (2018). Development of Energy Storage Systems for Power Network Reliability: A Review. *Energies*, *11*(9), 1-19.

Monyei, C. G., Adewumi, A. O., Obolo, M. O., & Sajou, B. (2018). Nigeria's energy poverty: Insights and implications for smart policies and framework towards a smart Nigeria electricity network. *Renewable and Sustainable Energy Reviews*, *81*(19), 1582-1601.

Moumin, G., Tescari, S., Sundarraj, P., de Oliveira, L., Roeb, M., & Sattler, C. (2019). Solar treatment of cohesive particles in a directly irradiated rotary kiln. *Solar Energy*, *182*(1), 480-490.

Mousavi Maleki, S. A., Hizam, H., & Gomes, C. (2017). Estimation of hourly, daily and monthly global solar radiation on inclined surfaces: Models re-visited. *Energies*, *10*(1), 10-134.

Mughal, S., Sood, Y. R., & Jarial, R. K. (2018). A review on solar photovoltaic technology and future trends. *International Journal of Scientific Research in Computer Science, Engineering and Information Technology*, *4*(1), 227-235.

Muñoz, M., Rovira, A., & Montes, M. J. (2022). Thermodynamic cycles for solar thermal power plants: A review. *Wiley Interdisciplinary Reviews: Energy and Environment*, *11*(2), 1-19.

Mussati, S. F., Mansouri, S. S., Gernaey, K. V., Morosuk, T., & Mussati, M. C. (2019). Model-based cost optimization of double-effect water-lithium bromide absorption refrigeration systems. *Processes*, *7*(1), 1-50.

Nardell, E. A. (2021). Air Disinfection for Airborne Infection Control with a Focus on COVID-19: Why Germicidal UV is Essential. *Photochemistry and Photobiology*, *97*(3), 493-497.

Nazari, M. A., Aslani, A., & Ghasempour, R. (2018). Analysis of solar farm site selection based on TOPSIS approach. *International Journal of Social Ecology and Sustainable Development (IJSESD)*, *9*(1), 12-25.

Negash, B. M., & Yaw, A. D. (2020). Artificial neural network based production forecasting for a hydrocarbon reservoir under water injection. *Petroleum Exploration and Development*, *47*(2), 383-392.

Nguyen, H., Moayedi, H., Jusoh, W. A. W., & Sharifi, A. (2020). Proposing a novel predictive technique using M5Rules-PSO model estimating cooling load in energy-efficient building system. *Engineering with Computers*, *36*(3), 857-866.

Nishiyama, H., Yamada, T., Nakabayashi, M., Maehara, Y., Yamaguchi, M., Kuromiya, Y., ... & Domen, K. (2021). Photocatalytic solar hydrogen production from water on a 100-m2 scale. *Nature*, *598*(7880), 304-307.

Nwaigwe, K. N., Mutabilwa, P., & Dintwa, E. (2019). An overview of solar power (PV systems) integration into electricity grids. *Materials Science for Energy Technologies*, *2*(3), 629-633.

Nwaigwe, K. N., Mutabilwa, P., & Dintwa, E. (2019). An overview of solar power (PV systems) integration into electricity grids. *Materials Science for Energy Technologies*, *2*(3), 629-633.

Odeyemi, O. A., Alegbeleye, O. O., Strateva, M., & Stratev, D. (2020). Understanding spoilage microbial community and spoilage mechanisms in foods of animal origin. *Comprehensive Reviews in Food Science and Food Safety*, *19*(2), 311-331.

Ojha, M. K., Shukla, A. K., Verma, P., & Kannojiya, R. (2021). Recent progress and outlook of solar adsorption refrigeration systems. *Materials Today: Proceedings*, *46*(1), 5639-5646.

Okaka, F. O., & Odhiambo, B. D. (2018). Urban residents' awareness of climate change and their autonomous adaptive behaviour and mitigation measures in the coastal city of Mombasa, Kenya. *South African Geographical Journal= Suid-Afrikaanse Geografiese Tydskrif*, *100*(3), 378-393.

Okwu, M. O., & Nwachukwu, A. N. (2019). A review of fuzzy logic applications in petroleum exploration, production and distribution operations. *Journal of Petroleum Exploration and Production Technology*, *9*(2), 1555-1568.

Oluleye, M. A., & Boukhanouf, R. (2019). Development Trend of Solar-powered Adsorption Refrigeration Systems: A Review of Technologies, Cycles, Applications, Challenges and Future Research Directions. *Development*, *6*(8), 10491-10504.

Omairi, A., Ismail, Z. H., Danapalasingam, K. A., & Ibrahim, M. (2017). Power harvesting in wireless sensor networks and its adaptation with maximum power point tracking: Current technology and future directions. *IEEE Internet of Things Journal*, *4*(6), 2104-2115.

Omariba, Z. B., Zhang, L., & Sun, D. (2018). Review on health management system for lithium-ion batteries of electric vehicles. *Electronics*, *7*(5), 1-72.

Onwuka, B., & Mang, B. (2018). Effects of soil temperature on some soil properties and plant growth. *Advances of Plants ib Agricuture. Resesrch*, *8*(1), 34-7.

Orwa, J. D., Muliro, P. S., & Matofari, J. W. (2021). Microbiological quality of crude milk along the rural and peri-urban dairy systems of Nakuru county. *African Journal of Dairy Farming and Milk Production ISSN*, *9*(1), 001-009.

Otunla, T. A. (2020). Estimation of daily solar radiation at equatorial region of West Africa using a more generalized Ångström-based broadband hybrid model. *Meteorology and Atmospheric Physics*, *132*(3), 341-351.

Ouagued, M., Khellaf, A., & Loukarfi, L. (2018). Performance analyses of Cu–Cl hydrogen production integrated solar parabolic trough collector system under Algerian climate. *International Journal of Hydrogen Energy*, *43*(6), 3451-3465.

Ouelhazi, I., Ezzaalouni, Y., & Kairouani, L. (2020). Parametric analysis of a combined ejector-vapor compression refrigeration cycle. *International Journal of Low-Carbon Technologies*, *15*(3), 398-408.

Owusu-Kwarteng, J., Akabanda, F., Agyei, D., & Jespersen, L. (2020). Microbial safety of milk production and fermented dairy products in Africa. *Microorganisms*, *8*(5), 7-52.

Pahle, M., Tietjen, O., Osorio, S., Egli, F., Steffen, B., Schmidt, T. S., & Edenhofer, O. (2022). Safeguarding the energy transition against political backlash to carbon markets. *Nature Energy*, *7*(3), 290-296.

Palacios, A., Barreneche, C., Navarro, M. E., & Ding, Y. (2020). Thermal energy storage technologies for concentrated solar power–A review from a materials perspective. *Renewable Energy*, *156*(10), 1244-1265.

Pan, Q. W., & Wang, R. Z. (2018). Study on operation strategy of a silica gel-water adsorption chiller in solar cooling application. *Solar Energy*, *172*(1), 24-31.

Panchal, H., Patel, R., & Parmar, K. D. (2020). Application of solar energy for milk pasteurisation: a comprehensive review for sustainable development. *International Journal of Ambient Energy*, *41*(1), 117-120.

Panda, D., Kumar, M., Satapathy, A. K., & Sarangi, S. K. (2021). Optimal design of thermal performance of an orifice pulse tube refrigerator. *Journal of Thermal Analysis and Calorimetry*, *143*(5), 3589-3609.

Pandya, B., Kumar, V., Matawala, V., & Patel, J. (2018). Thermal comparison and multi-objective optimization of single-stage aqua-ammonia absorption cooling system powered by different solar collectors. *Journal of Thermal Analysis and Calorimetry*, *133*(3), 1635-1648.

Pang, Y., Zhang, J., Ma, R., Qu, Z., Lee, E., & Luo, T. (2020). Solar–thermal water evaporation: a review. *ACS Energy Letters*, *5*(2), 437-456.

Parida, D. R., Advaith, S., Dani, N., & Basu, S. (2022). Assessing the impact of a novel hemispherical diffuser on a single-tank sensible thermal energy storage system. *Renewable Energy*, *183*(1), 202-218.

Pastuszko, R. (2018). Pool boiling heat transfer on micro-fins with wire mesh–Experiments and heat flux prediction. *International Journal of Thermal Sciences*, *125*(1), 197-209.

Pelay, U., Luo, L., Fan, Y., Stitou, D., & Rood, M. (2017). Thermal energy storage systems for concentrated solar power plants. *Renewable and Sustainable Energy Reviews*, *79*(3), 82-100.

Pietzcker, R. C., Osorio, S., & Rodrigues, R. (2021). Tightening EU ETS targets in line with the European Green Deal: Impacts on the decarbonization of the EU power sector. *Applied Energy*, *293*(1), 1-24.

Pokhrel, S., Kuyuk, A. F., Kalantari, H., & Ghoreishi-Madiseh, S. A. (2020). Techno-economic trade-off between battery storage and ice thermal energy storage for application in renewable mine cooling system. *Applied Sciences*, *10*(17), 1017-6022.

Prescott, J. A. (1940). Evaporation from a water surface in relation to solar radiation. *Trans. Royal Society South. Australia.*, *46*(4), 114-118.

Quej, V. H., Almorox, J., Arnaldo, J. A., & Saito, L. (2017). ANFIS, SVM and ANN soft-computing techniques to estimate daily global solar radiation in a warm sub-humid environment. *Journal of Atmospheric and Solar-Terrestrial Physics*, *155*(6), 62-70.

Raccanello, J., Rech, S., & Lazzaretto, A. (2019). Simplified dynamic modeling of single-tank thermal energy storage systems. *Energy*, *182*(1), 1154-1172.

Radwan, N. A., Moustafaa, M. M., Biomy, M. A., & Elattar, M. Z. (2020). Design, set-up control unit system to evaluate the performance of solar energy system for warming poultry house. *Arab Universities Journal of Agricultural Sciences*, *28*(1), 177-190.

Radzai, M. H. M., Lim, C. W., Yaw, C. T., Koh, S. P., Ahmad, N. A., Shakeri, M., & Pasupuleti, J. (2022). A Brief Review on Radiant Cooling Panel with Different Chilled Water Pipe Configurations. *Journal of Advanced Research in Fluid Mechanics and Thermal Sciences*, *89*(2), 1-14.

Rahman, M. M., Khan, I., Field, D. L., Techato, K., & Alameh, K. (2022). Powering agriculture: Present status, future potential, and challenges of renewable energy applications. *Renewable Energy*, *188*(1), 731-749.

Raj, A. K., Kunal, G., Srinivas, M., & Jayaraj, S. (2019). Performance analysis of a double-pass solar air heater system with asymmetric channel flow passages. *Journal of Thermal Analysis and Calorimetry*, *136*(1), 21-38.

Ramalingam, V., Vellaichamy, P., Venkataramani, G., & Narayanasamy, R. (2021). Experimental Investigation on Solar Photovoltaic Driven Cool Thermal Storage System for the Development of Sustainable Micro Grid in Building Sectors. *Journal of Electrical Engineering*, *21*(3), 92-102.

Rangel-Heras, E., Angeles-Camacho, C., Cadenas-Calderón, E., & Campos-Amezcua, R. (2022). Short-Term Forecasting of Energy Production for a Photovoltaic System Using a NARX-CVM Hybrid Model. *Energies*, *15*(8), 28-42.

Rao K, D. V., Premalatha, M., & Naveen, C. (2018). Analysis of different combinations of meteorological parameters in predicting the horizontal global solar radiation with ANN approach: A case study. *Renewable and Sustainable Energy Reviews*, *91*(10), 248-258.

Rapisarda, R., Nocera, F., Costanzo, V., Sciuto, G., & Caponetto, R. (2022). Hydroponic Green Roof Systems as an Alternative to Traditional Pond and Green Roofs: A Literature Review. *Energies*, *15*(6), 1-27.

Rashidi, J., & Yoo, C. (2018). A novel Kalina power-cooling cycle with an ejector absorption refrigeration cycle: Thermodynamic modelling and pinch analysis. *Energy Conversion and Management*, *162*(3), 225-238.

Ratlamwala, T. A., & Abid, M. (2018). Performance analysis of solar assisted multi-effect absorption cooling systems using nanofluids: a comparative analysis. *International Journal of Energy Research, 42*(9), 2901-2915.

Razmi, A., Soltani, M., Aghanajafi, C., & Torabi, M. (2019). Thermodynamic and economic investigation of a novel integration of the absorption-recompression refrigeration system with compressed air energy storage (CAES). *Energy Conversion and Management*, *187*(1), 262-273.

Ren, P., Rossi, S., Camarero, J. J., Ellison, A. M., Liang, E., & Peñuelas, J. (2018). Critical temperature and precipitation thresholds for the onset of xylogenesis of Juniperus przewalskii in a semi-arid area of the north-eastern Tibetan Plateau. *Annals of Botany*, *121*(4), 617-624.

Riffat, J., Kutlu, C., Tapia-Brito, E., Tekpetey, S., Agyenim, F. B., Su, Y., & Riffat, S. (2021). Development and testing of a PCM enhanced domestic refrigerator with use of miniature DC compressor for weak/off grid locations. *International Journal of Green Energy*, *10*(1), 1-14.

Rodríguez, E., Cardemil, J. M., Starke, A. R., & Escobar, R. (2022). Modelling the Exergy of Solar Radiation: A Review. *Energies*, *15*(4), 1477.

Ronno, C. K. (2018). Testing the Altitude and Latitude Based Solar Irradiance Models in Kenya. *African Journal of Education, Science and Technology*, *5*(1), 135-139.

Rosato, A., Ciervo, A., Ciampi, G., Scorpio, M., Guarino, F., & Sibilio, S. (2020). Impact of solar field design and back-up technology on dynamic performance of a solar hybrid heating network integrated with a seasonal borehole thermal energy storage serving a small-scale residential district including plug-in electric vehicles. *Renewable Energy*, *154*(1), 684-703.

Roy, R., & Kundu, B. (2021). Energy and exergy analyses of LiBr/H2O absorption cooling system having recto-trapezoidal profile absorber plate. *Proceedings of the Institution of Mechanical Engineers, Part C: Journal of Mechanical Engineering Science*, *235*(15), 2851-2873.

Rüdisüli, M., Teske, S. L., & Elber, U. (2019). Impacts of an increased substitution of fossil energy carriers with electricity-based technologies on the Swiss electricity system. *Energies*, *12*(12), 23-99.

Safari, A., Das, N., Langhelle, O., Roy, J., & Assadi, M. (2019). Natural gas: A transition fuel for sustainable energy system transformation? *Energy Science & Engineering*, *7*(4), 1075-1094.

Sahoo, U., Kumar, R., Pant, P. C., & Chaudhary, R. (2017). Development of an innovative polygeneration process in hybrid solar-biomass system for combined power, cooling and desalination. *Applied Thermal Engineering*, *120*(10), 560-567.

Salmon, A., Quiñones, G., Soto, G., Polo, J., Gueymard, C., Ibarra, M., ... & Marzo, A. (2021). Advances in aerosol optical depth evaluation from broadband direct normal irradiance measurements. *Solar Energy*, *221*(4), 206-217.

Samani, Z. (2000). Estimating solar radiation and evapotranspiration using minimum climatological data. *Journal of irrigation and drainage engineering*, *126*(4), 265-267.

Samanta, S., Patra, P. K., Banerjee, S., Narsimhaiah, L., Chandran, S., Vijaya Kumar, P., & Bandyopadhyay, S. (2019). Generation of common coefficients to estimate global solar radiation over different locations of India. *Theoretical and Applied Climatology*, *136*(3), 943-953.

Sanaye, S., & Khakpaay, N. (2020). Thermo-economic multi-objective optimization of an innovative cascaded organic Rankine cycle heat recovery and power generation system integrated with gas engine and ice thermal energy storage. *Journal of Energy Storage*, *32* (1), 101-697.

Sani, M. M., Noorpoor, A., & Motlagh, M. S. (2020). Multi objective optimization of waste heat recovery in cement industry (a case study). *Journal of Thermal Engineering*, *6*(4), 604-618.

Sankar, V. R., Chandran, S., & Pandiyan, D. P. (2018). Performance assessment, kinetics and modelling of biofilm membrane bio-reactor for the treatment of dairy wastewater. *Journal of Environmental Biology*, *39*(5), 565-574.

Schäfer, H. (2018). Germany: the 'greenhorn'in the green finance revolution. *Environment: Science and Policy for Sustainable Development*, *60*(1), 18-27.

Schellenberg, C., Lohan, J., & Dimache, L. (2018). Operational optimisation of a heat pump system with sensible thermal energy storage using genetic algorithm. *Thermal Science*, *22*(5), 2189-2202.

Selvaraj, D. A., & Victor, K. (2021). Vapour absorption refrigeration system for rural cold storage: a comparative study. *Environmental Science and Pollution Research*, *28*(26), 34248-34258.

Seme, S., & Štumberger, G. (2011). A novel prediction algorithm for solar angles using solar radiation and differential evolution for dual-axis sun tracking purposes. *Solar Energy*, *85*(11), 2757-2770.

Sempiira, E. J. (2019). *Evaporative Cooling Computational Analysis: Towards Off-Grid Milk Freshness Preservation* (Doctoral dissertation, University of Georgia).

Sendanayake, S., Miguntanna, N. P., & Jayasinghe, M. T. R. (2014). Estimating incident solar radiation in tropical islands with short term weather data. *European Scientific Journal*, *10*(3), 160-167.

Shabari Girish, K. V. S., Praveen, R., & Dipesh Nair, D. S. (2018). A case study on Solar Vapour absorption refrigeration system. *International Journal of Engineering and Technology*, *7*(5), 44-47.

Shahsavari, A., & Akbari, M. (2018). Potential of solar energy in developing countries for reducing energy-related emissions. *Renewable and Sustainable Energy Reviews*, *90* (10), 275-291.

Shahsavari, A., & Akbari, M. (2018). Potential of solar energy in developing countries for reducing energy-related emissions. *Renewable and Sustainable Energy Reviews*, *90*(1), 275-291.

Sharafati, A., Khosravi, K., Khosravinia, P., Ahmed, K., Salman, S. A., Yaseen, Z. M., & Shahid, S. (2019). The potential of novel data mining models for global solar radiation prediction. *International Journal of Environmental Science and Technology*, *16*(11), 7147-7164.

Sharma, D. K., Sharma, D., & Ali, A. H. H. (2020). A state of the art on solar-powered vapor absorption cooling systems integrated with thermal energy storage. *Environmental Science and Pollution Research*, *27*(1), 158-189.

Sharmin, F. (2021). *Life Cycle Greenhouse Gas Emissions of Electricity Generated from Solar Updraft Towers* (Doctoral dissertation, University of California, Merced).

She, X., Cong, L., Nie, B., Leng, G., Peng, H., Chen, Y., ... & Luo, Y. (2018). Energy-efficient and-economic technologies for air conditioning with vapor compression refrigeration: A comprehensive review. *Applied Energy*, *232*(1), 157-186.

Shen, S., Guo, Y., & Gong, L. (2018). Analysis of heat transfer critical point in LT-MEE desalination plant. *Desalination*, *432*(1), 64-71.

Shenoy, K. L., Nayak, C. G., & Mandi, R. P. (2021). Effect of partial shading in grid connected solar pv system with fl controller. *International Journal of Power Electronics and Drive Systems*, *12*(1), 4-31.

Shrestha, G. K., Pandey, B., Joshi, U., & Poudyal, K. N. (2021). Empirical model for estimation of global solar radiation at lowland region Biratnagar using satellite data. *BIBECHANA*, *18*(1), 193-200.

Shu, H., Wang, H., & Cao, G. (2020). Thermal and flow resistance characteristics of a parallel-pipe type natural heat transfer air-conditioning terminal device for nearly zero energy buildings. *Indoor and Built Environment*, *29*(9), 1227-1237.

Siddharth, K., Chan, Y., Wang, L., & Shao, M. (2018). Ammonia electro-oxidation reaction: Recent development in mechanistic understanding and electrocatalyst design. *Current Opinion in Electrochemistry*, *9*(7)151-157.

Sidney, S., Prabakaran, R., & Dhasan, M. L. (2021). Charge optimisation of a solar milk chiller with direct current compressors. *Proceedings of the Institution of Mechanical Engineers, Part E: Journal of Process Mechanical Engineering*, *235*(3), 679-693.

Sidney, S., Prabakaran, R., Kim, S. C., & Dhasan, M. L. (2022). A novel solar-powered milk cooling refrigeration unit with cold thermal energy storage for rural application. *Environmental Science and Pollution Research*, *29*(11), 16346-16370.

Sidney, S., Prabakaran, R., Kim, S. C., & Dhasan, M. L. (2022). A novel solar-powered milk cooling refrigeration unit with cold thermal energy storage for rural application. *Environmental Science and Pollution Research*, *29*(11), 16346-16370.

Sidney, S., Thomas, J., & Dhasan, M. L. (2020). A standalone PV operated DC milk chiller for Indian climate zones. *Sādhanā*, *45*(1), 1-11.

Singh, G., & Das, R. (2021). Experimental study of a combined biomass and solar energy-based fully grid-independent air-conditioning system. *Clean Technologies and Environmental Policy*, *23*(6), 1889-1912.

Singh, M., Kele, V. D., Chavan, B., Ranvir, S., & Dhotre, A. V. (2019). A review on solar water heating systems and its use in dairy industry. *Internation Journal of Current Microbiology and Applied Science*, *8*(4), 1975-1986.

Sleiti, A. K., Al-Ammari, W. A., & Al-Khawaja, M. (2020). Review of innovative approaches of thermo-mechanical refrigeration systems using low grade heat. *International Journal of Energy Research*, *44*(13), 9808-9838.

Sreenath, S., Sudhakar, K., & Yusop, A. F. (2021). Solar PV in the airport environment: A review of glare assessment approaches & metrics. *Solar Energy*, *216*(1), 439-451.

Srivastava, S., & Yadav, A. (2018). Water generation from atmospheric air by using composite desiccant material through fixed focus concentrating solar thermal power. *Solar Energy*, *169*(1), 302-315.

Su, P., Ji, J., Cai, J., Gao, Y., & Han, K. (2020). Dynamic simulation and experimental study of a variable speed photovoltaic DC refrigerator. *Renewable Energy*, *152*(2), 155-164.

Sugiartha, N. (2020). Experimentation of an activated carbon/methanol solar refrigerator. *Logic: Jurnal Rancang Bangun dan Teknologi*, *20*(2), 129-134.

Sulich, A., & Sołoducho-Pelc, L. (2021). Renewable energy producers' strategies in the Visegrád group countries. *Energies*, *14*(11), 3048.

Sun, J., Li, W., & Cui, B. (2020). Energy and exergy analyses of R513a as a R134a drop-in replacement in a vapor compression refrigeration system. *International Journal of Refrigeration*, *112*(3), 348-356.

Sun, X., Liu, L., Dong, Y., Zhuang, Y., Zhang, L., & Du, J. (2020). Superstructure-based simultaneous optimization of a heat exchanger network and a compression–absorption cascade refrigeration system for heat recovery. *Industrial & Engineering Chemistry Research*, *59*(36), 16017-16028.

Suresh, V., Muralidhar, M., & Kiranmayi, R. (2020). Modelling and optimization of an off-grid hybrid renewable energy system for electrification in a rural areas. *Energy Reports*, *6*(1), 594-604.

Surrya Prakash, D., Logesh, K., Venkatasudhahar, M., Vignesh, H. R., Viganeshwaran, K., & Siva Haris, V. S. (2019). Study of performance parameter optimisation of resorption cogeneration utilising heat and mass recovery. *International Journal of Ambient Energy*, *40*(2), 111-115.

Szabó, S., Pinedo Pascua, I., Puig, D., Moner-Girona, M., Negre, M., Huld, T., ... & Kammen, D. (2021). Mapping of affordability levels for photovoltaic-based electricity generation in the solar belt of sub-Saharan Africa, East Asia and South Asia. *Scientific reports*, *11*(1), 1-14.

Sztekler, K., Kalawa, W., Mika, Ł., Mlonka-Medrala, A., Sowa, M., & Nowak, W. (2021). Effect of additives on the sorption kinetics of a silica gel bed in adsorption chiller. *Energies*, *14*(4), 1-13.

Taghizadeh-Hesary, F., & Yoshino, N. (2020). Sustainable solutions for green financing and investment in renewable energy projects. *Energies*, *13*(4), 1-18.

Tan, Y., Chen, Y., & Wang, L. (2018). Thermodynamic analysis of a mixed refrigerant ejector refrigeration cycle operating with two vapor-liquid separators. *Journal of Thermal Science*, *27*(3), 230-240.

Tang, K., Dong, K., Li, J., Gordon, M. P., Reichertz, F. G., Kim, H., ... & Wu, J. (2021). Temperature-adaptive radiative coating for all-season household thermal regulation. *Science*, *374*(6574), 1504-1509.

Tang, N., Mao, S., Wang, Y., & Nelms, R. M. (2018). Solar power generation forecasting with a LASSO-based approach. *IEEE Internet of Things Journal*, *5*(2), 1090-1099.

Tang, S., Hong, H., Jin, H., & Xuan, Y. (2019). A cascading solar hybrid system for co-producing electricity and solar syngas with nanofluid spectrum selector. *Applied Energy*, *248*(1), 231-240.

Tazvinga, H., Dzobo, O., & Mapako, M. (2020). Towards sustainable energy system options for improving energy access in Southern Africa. *Journal of Energy in Southern Africa*, *31*(2), 59-72.

Teitelbaum, E., Chen, K. W., Aviv, D., Bradford, K., Ruefenacht, L., Sheppard, D., ... & Rysanek, A. (2020). Membrane-assisted radiant cooling for expanding thermal comfort zones globally without air conditioning. *Proceedings of the National Academy of Sciences*, *117*(35), 21162-21169.

Teitelbaum, E., Rysanek, A., Pantelic, J., Aviv, D., Obelz, S., Buff, A., ... & Meggers, F. (2019). Revisiting radiant cooling: condensation-free heat rejection using infrared-transparent enclosures of chilled panels. *Architectural Science Review*, *62*(2), 152-159.

Thiangchanta, S., Do, T. A., Tachajapong, W., & Mona, Y. (2020). Experimental investigation of the thermoelectric cooling with vacuum wall system. *Energy Reports*, *6*(1), 1244-1248.

Thirunavukkarasu, G. S., Seyedmahmoudian, M., Chandran, J., Stojcevski, A., Subramanian, M., Marnadu, R., ... & Shkir, M. (2021). Optimization of Mono-Crystalline Silicon Solar Cell Devices Using PC1D Simulation. *Energies*, *14*(16), 49-86.

Torres-Toledo, V., Hack, A., Mrabet, F., Salvatierra-Rojas, A., & Müller, J. (2016). On-farm milk cooling solution based on insulated cans with integrated ice compartment. *International Journal of Refrigeration*, *90*(1), 22-31.

Toujani, N., Bouaziz, N., Chrigui, M., & Kairouani, L. (2018). Performance analysis of a new combined organic Rankine cycle and vapor compression cycle for power and refrigeration cogeneration. *Transactions of the Institute of Fluid-Flow Machinery*, *160*(140), 39-81.

Tress, W., Domanski, K., Carlsen, B., Agarwalla, A., Alharbi, E. A., Graetzel, M., & Hagfeldt, A. (2019). Performance of perovskite solar cells under simulated temperature-illumination real-world operating conditions. *Nature energy*, *4*(7), 568-574.

Turner, M. W. (2020). Seriality, Miscellaneity, and Compression in Nineteenth-Century Print. *Victorian Studies*, *62*(2), 283-294.

Ulsrud, K. (2020). Access to electricity for all and the role of decentralized solar power in sub-Saharan Africa. *Norsk Geografisk Tidsskrift-Norwegian Journal of Geography*, *74*(1), 54-63.

Unverdi, M., & Cerci, Y. (2018). Thermodynamic analysis and performance improvement of Irem geothermal power plant in Turkey: A case study of organic Rankine cycle. *Environmental Progress & Sustainable Energy*, *37*(4), 1523-1539.

Vaishnav, R., Jacobi, C., Berdermann, J., Schmölter, E., & Codrescu, M. (2018). Ionospheric response to solar EUV variations: Preliminary results. *Advances in Radio Science*, *16*(1), 157-165.

Valencia, L., Rosas, W., Aguilar-Sanchez, A., Mathew, A. P., & Palmqvist, A. E. (2019). Bio-based micro-/meso-/macroporous hybrid foams with ultrahigh zeolite loadings for selective capture of carbon dioxide. *ACS applied materials & interfaces*, *11*(43), 40424-40431.

Valiantzas, J. D. (2018). Modification of the Hargreaves–Samani model for estimating solar radiation from temperature and humidity data. *Journal of Irrigation and Drainage Engineering*, *144*(1), 12-75.

VanDeventer, W., Jamei, E., Thirunavukkarasu, G. S., Seyedmahmoudian, M., Soon, T. K., Horan, B., ... & Stojcevski, A. (2019). Short-term PV power forecasting using hybrid GASVM technique. *Renewable energy*, *5*(6), 367-379.

Varvagiannis, E., Charalampidis, A., Zsembinszki, G., Karellas, S., & Cabeza, L. F. (2021). Energy assessment based on semi-dynamic modelling of a photovoltaic driven vapour

compression chiller using phase change materials for cold energy storage. *Renewable Energy*, *163*(1), 198-212.

Verso, V. R. L., Javadi, M. H., Pagliolico, S., Carbonaro, C., & Sassi, G. (2019). Photobioreactors as a Dynamic Shading System Conceived for an Outdoor Workspace of the State Library of Queensland in Brisbane: Study of Daylighting Performances. *Journal of Daylighting*, *6*(2), 148-168.

Vincent, R., Houari, A., Ait-Ahmed, M., & Benkhoris, M. F. (2020). Influence of different time horizon-based battery energy management strategies on residential microgrid profitability. *Journal of Energy Storage*, *29*(10), 13-40.

Vrat, P., Gupta, R., Bhatnagar, A., Pathak, D. K., & Fulzele, V. (2018). Literature review analytics (LRA) on sustainable cold-chain for perishable food products: research trends and future directions. *Opsearch*, *55*(3), 601-627.

Waite, M., Cohen, E., Torbey, H., Piccirilli, M., Tian, Y., & Modi, V. (2017). Global trends in urban electricity demands for cooling and heating. *Energy*, *100*(127), 786-802.

Wang, J., Li, P., Ran, R., Che, Y., & Zhou, Y. (2018). A short-term photovoltaic power prediction model based on the gradient boost decision tree. *Applied Sciences*, *8*(5), 6-89.

Wang, L., Wu, B., Elnashar, A., Zhu, W., Yan, N., Ma, Z., ... & Niu, X. (2022). Incorporation of Net Radiation Model Considering Complex Terrain in Evapotranspiration Determination with Sentinel-2 Data. *Remote Sensing*, *14*(5), 11-91.

Wang, Y., Li, M., Du, W., Yu, Q., Ji, X., & Ma, X. (2018). Performance comparative study of a solar-powered adsorption refrigerator with a CPC collector/adsorbent bed. *Energy Conversion and Management*, *173*(7), 499-507.

Wu, W., You, T., & Leung, M. (2020). Screening of novel water/ionic liquid working fluids for absorption thermal energy storage in cooling systems. *International Journal of Energy Research*, *44*(12), 9367-9381.

Wu, W., Zhai, C., Sui, Z., Sui, Y., & Luo, X. (2021). Proton exchange membrane fuel cell integrated with microchannel membrane-based absorption cooling for hydrogen vehicles. *Renewable Energy*, *178*(1), 560-573.

Xiang, Q., Fan, L., Li, Y., Dong, S., Li, K., & Bai, Y. (2022). A review on recent advances in plasma-activated water for food safety: Current applications and future trends. *Critical Reviews in Food Science and Nutrition*, *62*(8), 2250-2268.

Xu, F., Bian, Z. F., Ge, T. S., Dai, Y. J., Wang, C. H., & Kawi, S. (2019). Analysis on solar energy powered cooling system based on desiccant coated heat exchanger using metal-organic framework. *Energy*, *177*(1), 211-221.

Ya'u, M. J., Gele, M. A., Ali, Y. Y., & Alhaji, A. M. I. (2018). Global solar radiation models: A review. *Journal of Photonic Materials and Technology*, *4*(1), 26-32.

Yahaya, S. M., & Mardiyya, A. Y. (2019). Review of post-harvest losses of fruits and vegetables. *Biomed. Journal of Science and Technology Research*, *13*(4), 10192-10200.

Yan, C., Wang, F., Pan, Y., Shan, K., & Kosonen, R. (2020). A multi-timescale cold storage system within energy flexible buildings for power balance management of smart grids. *Renewable Energy*, *161*(1), 626-634.

Yang, S., Liu, Z., & Fu, B. (2019). Simulation and evaluation on the dynamic performance of a cryogenic turbo-based reverse Brayton refrigerator. *Applied Sciences*, *9*(3), 1-15.

Yang, W., Feng, Y., Si, Q., Yan, Q., Long, P., Dong, L., ... & Feng, W. (2019). Efficient cycling utilization of solar-thermal energy for thermochromic displays with controllable heat output. *Journal of Materials Chemistry A*, *7*(1), 97-106.

Yang, Y., Yang, Y., Pei, Z., Wu, K. H., Tan, C., Wang, H., ... & Chen, Y. (2020). Recent progress of carbon-supported single-atom catalysts for energy conversion and storage. *Matter*, *3*(5), 1442-1476.

Yari, R., Darzi-Naftchali, A., Dehghanisanij, H., & Qi, Z. (2020). Effect of meteorological data quality control and data adjustment on the reference evapotranspiration: a case study in Jafariye, Iran. *Theoretical and Applied Climatology*, *141*(1), 331-342.

Yi, K., Zhao, Y., Liu, G., Yang, Q., Yu, G., & Li, L. (2022). Performance Evaluation of Centrifugal Refrigeration Compressor Using R1234yf and R1234ze (E) as Drop-In Replacements for R134a Refrigerant. *Energies*, *15*(7), 1507-2552.

Yin, J., Molini, A., & Porporato, A. (2020). Impacts of solar intermittency on future photovoltaic reliability. *Nature Communications*, *11*(1), 1-9.

Yin, J., Yu, Z., Zhang, C., Tian, M., & Han, J. (2018). Thermodynamic analysis and multi-objective optimization of a novel power/cooling cogeneration system for low-grade heat sources. *Energy Conversion and Management*, *166* (10), 64-73.

Yu, L., Yang, Z., He, Q., Zeng, R. J., Bai, Y., & Zhou, S. (2018). Novel gas diffusion cloth bioanodes for high-performance methane-powered microbial fuel cells. *Environmental Science & Technology*, *53*(1), 530-538.

Zare, V., & Palideh, V. (2018). Employing thermoelectric generator for power generation enhancement in a Kalina cycle driven by low-grade geothermal energy. *Applied Thermal Engineering*, *130*(2), 418-428.

Zavala Nacul, H., & Revoredo-Giha, C. (2022). Food safety and the informal milk supply chain in Kenya. *Agriculture & Food Security*, *11*(1), 1-14.

Zeng, Z., Wang, Z., Ding, M., Zheng, X., Sun, X., Zhu, W., ... & Zhang, B. (2021). Estimation and Long-term Trend Analysis of Surface Solar Radiation in Antarctica: A Case Study of Zhongshan Station. *Advances in Atmospheric Sciences*, *38*(9), 1497-1509.

Zhang, H., Zhao, H., & Li, Z. (2019). Waste heat recovery and water-saving modification for a water-cooled gas-steam combined cycle cogeneration system with absorption heat pump. *Energy Conversion and Management*, *180*(1), 1129-1138.

Zhang, W., Yu, J., Zhao, A., & Zhou, X. (2021). Predictive model of cooling load for ice storage air-conditioning system by using GBDT. *Energy Reports*, *7*(1), 1588-1597.

Zhang, Y., Qin, C., Srivastava, A. K., Jin, C., & Sharma, R. K. (2020). Data-driven day-ahead PV estimation using autoencoder-LSTM and persistence model. *IEEE Transactions on Industry Applications*, *56*(6), 7185-7192.

Zhang, Z., Wang, J., Feng, X., Chang, L., Chen, Y., & Wang, X. (2018). The solutions to electric vehicle air conditioning systems: A review. *Renewable and Sustainable Energy Reviews*, *91*(1), 443-463.

Zhao, N., Zhang, Y., Li, B., Hao, J., Chen, D., Zhou, Y., & Dong, R. (2019). Natural gas and electricity: Two perspective technologies of substituting coal-burning stoves for rural heating and cooking in Hebei Province of China. *Energy Science & Engineering*, *7*(1), 120-131.

Zhu, T., Guo, Y., Li, Z., & Wang, C. (2021). Solar Radiation Prediction Based on Convolution Neural Network and Long Short-Term Memory. *Energies*, *14*(24), 84-98.

Zou, J., Han, N., Yan, J., Feng, Q., Wang, Y., Zhao, Z., ... & Wang, H. (2020). Electrochemical compression technologies for high-pressure hydrogen: current status, challenges and perspective. *Electrochemical Energy Reviews*, *3*(4), 690-729.

Zuo, C., Qian, J., Feng, S., Yin, W., Li, Y., Fan, P., ... & Chen, Q. (2022). Deep learning in optical metrology: a review. *Light: Science & Applications*, *11*(1), 1-54.

APPENDICES

APPENDIX A

Appendix A 1; Objective number One Publication

ISSN (Print) : 2319-8613
ISSN (Online) : 0975-4024

Solar Radiation Prediction Models Analysis for Varying Climatic Conditions

Patrick M. Wainaina[#1], George. O. Owino[*2], Musa.R.Njue[#3]

[#1]Department of Industrial and Energy Engineering, Faculty of Engineering and Technology

(Egerton University, Kenya.)

[*2] Department of Industrial and Energy Engineering, Faculty of Engineering and Technology

(Egerton University, Kenya.)

[#3] Department of Agricultural Engineering, Faculty of Engineering and Technology

(Egerton University, Kenya).

Corresponding author E-mail address; wainainapatrick13@gmail.com

Abstract:

This study has investigated global solar predictive models, modified, validated and compared five models, for prediction of monthly daily mean solar radiation in four different locations of Kenya that represents the four major climatic conditions. The input variables to the models were; latitude, day length, sunshine hours, relative sunshine hours, temperature, and precipitation. Solar radiation data from 2000 to 2013 was used to obtain the monthly daily mean global solar radiation, to analyze, validate and compare the performance of the models. The predicted and measured data was simulated using MATLAB. Statistical indicators, MBE, RMSE, t-test and R, were performed to determine the models performance. The results showed that sunshine hours based models predicted global solar radiation with higher accuracy in wet and cold, wet and warm climatic conditions, while the temperature and precipitation models were accurate in solar radiation prediction in hot and dry climatic conditions.

Key words: Global solar radiation1, Sunshine hours2, Day length3

Appendix A 2; Objective number two and three Publication

IOSR Journal of Mechanical and Civil Engineering (IOSR-JMCE)
e-ISSN: 2278-1684,p-ISSN: 2320-334X, Volume 17, Issue 5 Ser. I (Sep. –Oct. 2020), PP 11-17
www.iosrjournals.org

Mathematical Models for Predicting Maximum Cooling Load ofAC Vapour CompressionMilkSolar Refrigeration Systems

Patrick Mbuthia Wainaina[1], Musa R. Njue[2],George Owino[3]
[1,3] *Department of Industrial and Energy Engineering, Egerton University Kenya*
[2]*Department of Agricultural Engineering, Egerton University Kenya*

Abstract: *The mismatch between solar energy availability and the cooling load energy demands for AC solar refrigeration systems in different geographical locations complicates the design and sizing of milk solar refrigeration systems components. This is caused by variation seasonal solar insolation and different levels of global solar insolation. In this study, three different sizes AC milk solar refrigeration systems, have been investigated for maximum cooling loads developed from the refrigeration systems when exposed to varying levels of solar insolation in Nakuru Kenya.Regression models were developed for predicting maximum cooling loads delivered from the milk solar refrigeration systems based on available mean daily solar insolation of the location. The predictive models developed is useful tools in the design and sizing of milk solar refrigeration componentsbased on solar insolation available at any global location. Three Solar refrigeration systems were fitted with AC reciprocating compressors of capacities'; 350W, 250W,200W and were investigated for maximum cooling loads under varying mean daily solar insolation. Four PV panels each of 200 Wp connected via an inverter provided the power required to operate the compressors in each of the refrigeration system.An innovative control unit operated the refrigeration systems dependent on the solar insolation level available in the day.Temperature profilesof water placed in the centralwater can, and the amount of ice formed were used to determine the maximum cooling load of each refrigeration system with, based on solar radiation available. The regression cooling curve generated by each system was used in developing the mathematical cooling load prediction models based on available solar insolation of Nakuru*

Conclusion:*The results showed that the maximum cooling loads obtained from the solar refrigeration systemsis dependent on the annual mean daily solar insolation of a specific location and the capacity of the refrigeration system compressor.The mathematical models showed a strong correction ofcoefficient of between 0.958 and 0.908when validated with actual solar refrigeration cooling loads.*

Key Words: *Cooling loads; Solar insolation; AC solar refrigeration system*

APPENDIX B

Appendix B 1: Properties of saturated R134a

Table C-3: Properties of Superheated R134a: Pressures from 80 kPa to 400 kPa

P (kPa)		Temperature, T (°C)										
		-30	-20	-10	0	10	20	30	40	50	60	70
80	v (m³/kg)	0.2388	0.2501	0.2611	0.2720	0.2828	0.2935	0.3041	0.3147	0.3252	0.3357	0.3462
	u (kJ/kg)	213.2	220.2	227.2	234.3	241.6	249.1	256.7	264.5	272.4	280.6	288.8
	h (kJ/kg)	232.4	240.2	248.1	256.1	264.3	272.6	281.0	289.7	298.5	307.4	316.5
	s (kJ/kg-K)	0.9608	0.9922	1.023	1.053	1.082	1.111	1.139	1.167	1.195	1.222	1.249
100	v (m³/kg)		0.1984	0.2074	0.2163	0.2251	0.2337	0.2423	0.2509	0.2594	0.2678	0.2763
	u (kJ/kg)		219.7	226.8	234.0	241.3	248.8	256.5	264.3	272.2	280.4	288.7
	h (kJ/kg)		239.5	247.5	255.6	263.8	272.2	280.7	289.4	298.2	307.1	316.3
	s (kJ/kg-K)		0.9721	1.003	1.033	1.063	1.092	1.12	1.149	1.176	1.204	1.231
120	v (m³/kg)		0.1639	0.1716	0.1792	0.1866	0.1939	0.2011	0.2083	0.2155	0.2226	0.2296
	u (kJ/kg)		219.2	226.4	233.6	241.0	248.5	256.2	264.0	272.0	280.2	288.5
	h (kJ/kg)		238.9	246.9	255.1	263.4	271.8	280.3	289.0	297.9	306.9	316.0
	s (kJ/kg-K)		0.9553	0.9866	1.017	1.047	1.076	1.105	1.133	1.161	1.188	1.215
140	v (m³/kg)			0.1461	0.1526	0.1591	0.1654	0.1717	0.1779	0.1841	0.1903	0.1964
	u (kJ/kg)			225.9	233.2	240.7	248.2	255.9	263.8	271.8	280	288.3
	h (kJ/kg)			246.4	254.6	262.9	271.4	280	288.7	297.6	306.6	315.8
	s (kJ/kg-K)			0.9724	1.003	1.033	1.062	1.091	1.12	1.147	1.175	1.202
160	v (m³/kg)			0.1268	0.1327	0.1385	0.1441	0.1496	0.1551	0.1606	0.1660	0.1714
	u (kJ/kg)			225.5	232.9	240.4	248.0	255.7	263.6	271.6	279.8	288.1
	h (kJ/kg)			245.8	254.1	262.5	271.0	279.6	288.4	297.3	306.3	315.5
	s (kJ/kg-K)			0.9599	0.9909	1.021	1.051	1.08	1.108	1.136	1.164	1.191
180	v (m³/kg)			0.1119	0.1172	0.1224	0.1275	0.1325	0.1374	0.1423	0.1471	0.152
	u (kJ/kg)			225.0	232.5	240.0	247.7	255.4	263.3	271.4	279.6	287.9
	h (kJ/kg)			245.2	253.6	262.1	270.6	279.3	288.1	297.0	306.1	315.3
	s (kJ/kg-K)			0.9485	0.9799	1.010	1.040	1.069	1.098	1.126	1.153	1.181
200	v (m³/kg)			0.09991	0.1048	0.1096	0.1142	0.1187	0.1232	0.1277	0.1321	0.1364
	u (kJ/kg)			224.6	232.1	239.7	247.4	255.2	263.1	271.2	279.4	287.7
	h (kJ/kg)			244.6	253.1	261.6	270.2	278.9	287.7	296.7	305.8	315.0
	s (kJ/kg-K)			0.9381	0.9699	1.001	1.030	1.060	1.088	1.116	1.144	1.171
300	v (m³/kg)					0.0709	0.0742	0.0775	0.0806	0.0837	0.0868	0.0898
	u (kJ/kg)					237.9	245.8	253.8	261.9	270.1	278.4	286.8
	h (kJ/kg)					259.2	268.1	277.0	286.1	295.2	304.4	313.8
	s (kJ/kg-K)					0.9611	0.9920	1.022	1.051	1.080	1.108	1.136
400	v (m³/kg)					0.0515	0.0542	0.0568	0.0593	0.0617	0.0641	0.0664
	u (kJ/kg)					236.0	244.2	252.4	260.6	268.9	277.3	285.9
	h (kJ/kg)					256.6	265.9	275.1	284.3	293.6	303.0	312.5
	s (kJ/kg-K)					0.9306	0.9628	0.9937	1.024	1.053	1.081	1.109
P (kPa)		-30	-20	-10	0	10	20	30	4 0	50	60	70
		Temperature, T (°C)										

Appendix B 2: KCC Milk Cooling Loads

24-Month Production & Energy data

PERIOD (MONTHS)		Electrical Energy Consumption			Electrical Energy Costs		TOTAL ENERGY	Indices			Normalized to one Calendar Month Period		
PERIOD (MONTHS)	Production Milk Ltrs	High Peak Rate (kWh)	Off Peak Rate (kWh)	Total (kWh)	Electricity KWH	KVA Demand (kva)	Cost (KSh)	Energy KWH/M3	Cost KSH/Litre	KWH / day	Normalized Electricity consumption	consoli - dated cost/kwh	Normalized Electricity cost KSH
Jan-11	273,241.72	5,385	15,062	20,447	328,026.60	72,000	400,026.60	74.83	1.46	619.61	19,651.30	19.56	388,662.56
Feb-11	163,506.00	4,347	15,459	19,806	334,698.50	70,200	404,898.50	121.13	2.48	682.97	17,968.67	20.44	380,161.17
Mar-11	87,269.27	5,429	8,307	13,736	271,051.70	69,600	340,651.70	157.40	3.90	490.57	15,619.10	24.80	382,327.84
Apr-11	98,740.74	12,374	4,109	16,483	326,001.10	67,200	393,201.10	166.93	3.98	531.71	17,040.10	23.85	406,641.91
May-11	179,982.85	11,901	6,309	18,210	365,267.60	69,600	434,867.60	101.18	2.42	587.42	19,627.67	23.88	451,930.45
Jun-11	332,672.46	19,806	10,364	30,170	574,716.30	70,200	644,916.30	90.69	1.94	838.06	25,233.89	21.38	543,252.53
Jul-11	472,581.67	16,339	4,881	21,220	428,411.50	71,400	499,811.50	44.90	1.06	884.17	24,263.94	23.55	586,763.04
Aug-11	430,073.98	11,235	6,410	17,645	392,942.50	78,600	471,542.50	41.03	1.10	534.70	22,591.89	26.72	553,969.07
Sep-11	457,412.62	21,782	20,043	41,825	829,410.30	75,000	904,410.30	91.44	1.98	1,394.17	42,659.77	21.62	937,855.82
Oct-11	461,934.15	24,597	22,319	46,916	1,002,273.20	80,400	1,082,673.20	101.56	2.34	1,513.42	41,686.26	23.08	975,150.21
Nov-11	409610.0 .03	13,022	13,799	26,821	615,158.00	69,600	684,758.00	21.05	0.54	894.03	27,212.97	25.53	688,650.72
Dec-11	300,732.43	12,107	11,740	23,847	512,697.90	70,800	583,497.90	79.30	1.94	822.31	22,110.55	24.47	541,830.63
Jan-12	64,255.26	8,296	6,443	14,739	294,649.20	69,000	363,649.20	229.38	5.66	446.64	13,794.45	24.67	344,558.76
Feb-12	32,108.85	5,605	7,135	12,740	264,587.40	67,200	331,787.40	396.78	10.33	439.31	11,911.10	26.04	321,423.88
Mar-12	24,540.64	5,784	3,522	9,306	225,852.80	63,000	288,852.80	379.21	11.77	320.90	9,734.41	31.04	305,855.85
Apr-12	23,305.96	5,432	4,078	9,510	238,759.60	69,600	308,359.60	408.05	13.23	297.19	10,906.28	32.42	319,983.18
May-12	86,552.46	8,655	8,792	17,447	351,898.80	69,600	421,498.80	201.58	4.87	581.57	20,683.73	24.16	461,311.93
Jun-12	105,282.78	12,238	23,387	35,625	609,943.90	63,600	673,543.90	338.37	6.40	913.46	27,179.08	18.91	512,207.33
Jul-12	203,668.07	7,188	17,853	25,041	434,221.80	75,600	509,821.80	122.95	2.50	1,138.23	27,619.98	20.36	594,692.77
Aug-12	276,994.56	2,832	2,931	5,763	173,589.00	73,200	246,789.00	20.81	0.89	180.09	10,360.41	42.82	312,177.78
Sep-12	182,573.32	10,015	17,588	27,603	507,764.70	73,200	580,964.70	151.19	3.18	862.59	24,093.88	21.05	521,039.27
Oct-12	178,306.96	6,948	8,732	15,680	344,395.70	72,000	416,395.70	87.94	2.34	505.81	18,431.66	26.56	454,437.81
Nov-12	168,060.09	13,997	16,631	30,628	535,775.70	74,400	610,175.70	182.24	3.63	1,056.14	31,061.11	19.92	620,485.79
Dec-12	204,826.57	18,092	10,477	28,569	501,964.00	75,600	577,564.00	139.48	2.82	952.30	29,521.30	20.22	462,051.20
Grand Total	6,082,622.43	263,406	266,371	529,777	10,464,057.80	1,710,600	12,174,657.80				530,963.49		12,067,421.49

Appendix B 3: Danfoss Evaporator specifications extracts

EN 12900 Household (CECOMAF) 220V, 50Hz, fan cooling F_2

Evap. temp. in °C	-45	-40	-35	-30	-25	-23.3	-20	-15	-10	-6.7	-5	0	5	7.2	10	15	20
Capacity in W			64.6	113	175	199	252	348	464	553	603	768	960	1054	1182	1437	
Power cons. in W			148	187	227	241	268	311	355	385	400	446	493	514	541	589	
Current cons. in A			1.63	1.72	1.83	1.87	1.95	2.09	2.24	2.34	2.40	2.57	2.76	2.85	2.96	3.17	
COP in W/W			0.44	0.61	0.77	0.83	0.94	1.12	1.31	1.44	1.51	1.72	1.95	2.05	2.19	2.44	

Appendix B 4: Cooling load prediction data for 200W refrigeration system

Linear Fit (6/15/2020 11:52:05)

Notes

Input Data

Masked Data - Values Excluded from Computations

Bad Data (missing values) -- Values that are invalid and thus not used in computations

Parameters

		Value	Standard Error	t-Value	Prob>|t|
200W Prediction Cooling	Intercept	0.11166	0.01877	5.94875	5.70779E-4
	Slope	0.52857	0.07901	6.69027	2.79932E-4

Slope is significantly different from zero (See ANOVA Table).

Standard Error was scaled with square root of reduced Chi-Sqr.

Statistics

	200W Prediction Cooling
Number of Points	9
Degrees of Freedom	7
Residual Sum of Squares	3.5427E-4
Pearson's r	0.92992
R-Square (COD)	0.86476
Adj. R-Square	0.84544

Summary

	Intercept		Slope		Statistics
	Value	Standard Error	Value	Standard Error	Adj. R-Square
200W Prediction Cooling	0.11166	0.01877	0.52857	0.07901	0.84544

ANOVA

		DF	Sum of Squares	Mean Square	F Value	Prob>F
200W Prediction Cooling	Model	1	0.00227	0.00227	44.75971	2.79932E-4
	Error	7	3.5427E-4	5.06099E-5		
	Total	8	0.00262			

Appendix B 5: Cooling load prediction data for 250W refrigeration system

Linear Fit (6/15/2020 11:28:40)

Notes

Input Data

Masked Data - Values Excluded from Computations

Bad Data (missing values) -- Values that are invalid and thus not used in computations

Parameters

		Value	Standard Error	t-Value	Prob>|t|
250W Model Prediction cooling	Intercept	0.03795	0.02707	1.40169	0.20376
	Slope	0.92253	0.08708	10.59449	1.46024E-5

Slope is significantly different from zero (See ANOVA Table).

Standard Error was scaled with square root of reduced Chi-Sqr.

Statistics

	250W Model Prediction cooling
Number of Points	9
Degrees of Freedom	7
Residual Sum of Squares	0.00507
Pearson's r	0.9702
R-Square (COD)	0.9413
Adj. R-Square	0.93291

Summary

	Intercept		Slope		Statistics
	Value	Standard Error	Value	Standard Error	Adj. R-Square
250W Model Prediction cooling	0.03795	0.02707	0.92253	0.08708	0.93291

ANOVA

		DF	Sum of Squares	Mean Square	F Value	Prob>F
250W Model Prediction cooling	Model	1	0.08127	0.08127	112.2432	1.46024E-5
	Error	7	0.00507	7.24068E-4		
	Total	8	0.08634			

Appendix B 6: Cooling load prediction data for 350W refrigeration system

Linear Fit (6/15/2020 11:13:11)

Notes

Input Data

Masked Data - Values Excluded from Computations

Bad Data (missing values) -- Values that are invalid and thus not used in computations

Parameters

		Value	Standard Error	t-Value	Prob>|t|
350W Prediction	Intercept	0.01231	0.01753	0.70211	0.50528
	Slope	0.95157	0.07712	12.33919	5.2724E-6

Slope is significantly different from zero (See ANOVA Table).

Standard Error was scaled with square root of reduced Chi-Sqr.

Statistics

	350W Prediction
Number of Points	9
Degrees of Freedom	7
Residual Sum of Squares	0.00127
Pearson's r	0.97778
R-Square (COD)	0.95605
Adj. R-Square	0.94977

Appendix B 6: Table 4.8: Cooling loads for refrigeration system and models

Mean Solar Radiation. W/m^2	Cooling Loads(kWh) for system and models					
	200 W system	200 W Predicted	250 W system	250 W Predicted	350 W system	350 W Predicted
346.146	0.181	0.191	0.113	0.096	0.087	0.092
436.446	0.248	0.23	0.147	0.21	0.159	0.168
473.276	0.246	0.249	0.241	0.261	0.196	0.2
501.188	0.257	0.246	0.278	0.298	0.241	0.223
543.459	0.251	0.247	0.296	0.347	0.244	0.252
609.296	0.237	0.246	0.387	0.394	0.252	0.273
629.678	0.253	0.243	0.399	0.398	0.265	0.272
652.791	0.248	0.24	0.398	0.395	0.268	0.266
683.189	0.246	0.234	0.381	0.378	0.266	0.247

Appendix B 7; Research License

REPUBLIC OF KENYA

NATIONAL COMMISSION FOR SCIENCE,TECHNOLOGY & INNOVATION

Ref No: **762615**

Date of Issue: **22/June/2021**

RESEARCH LICENSE

This is to Certify that Mr.. Patrick Mbuthia Wainaina of Egerton University, has been licensed to conduct research in Kericho, Mombasa, Nakuru on the topic: Mathematical Prediction of solar Driven Refrigeration System capacity; A case study of Milk Cooling for the period ending : 22/June/2022.

License No: **NACOSTI/P/21/11361**

762615

Applicant Identification Number

Director General
NATIONAL COMMISSION FOR SCIENCE,TECHNOLOGY & INNOVATION

Verification QR Code

NOTE: This is a computer generated License. To verify the authenticity of this document, Scan the QR Code using QR scanner application.

APPENDIX C

PHOTOS

Appendix C 1: Solar Refrigeration system PV power supply equipment

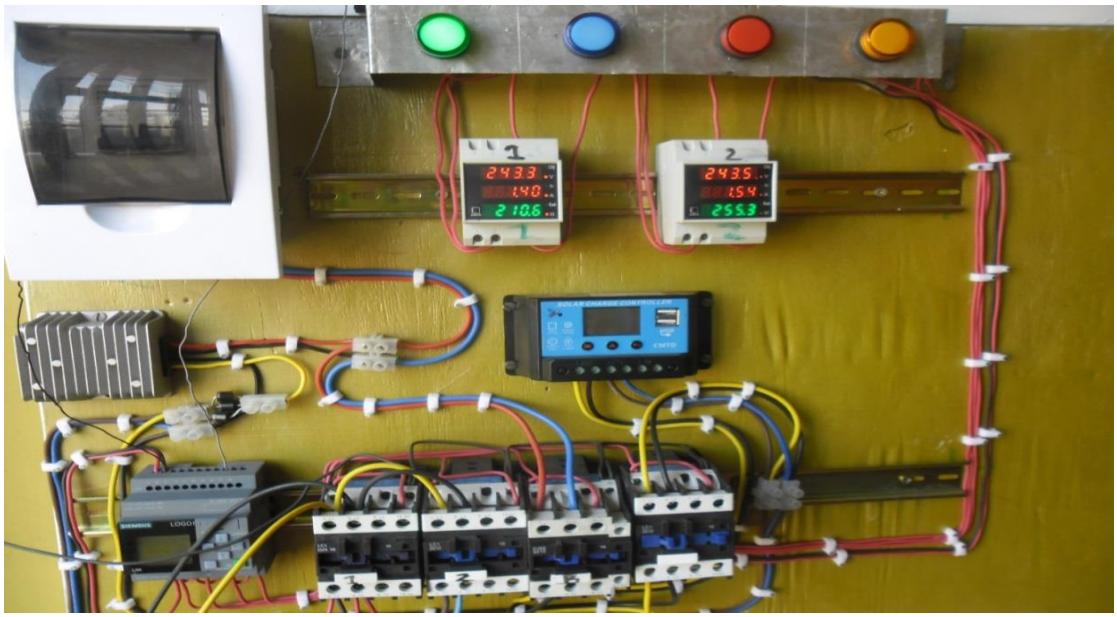

Appendix C 2: Cooling vessels setups

Appendix C 3: 200W Solar Panels Setup

Appendix C 4: Cooling vessels and Refrigeration system setups